Optimal Delivery of Therapeutic Genes to Pancreatic Islets

Amy Hughes

Thesis submitted in fulfilment for the degree of
Doctor of Philosophy

In

The Department of Medicine
Faculty of Health Sciences
The University of Adelaide

September 2012

Table of Contents

Thesis Abstract

Islet transplantation is a promising therapeutic option for Type 1 Diabetic (T1D) patients, with the ability to improve glycometabolic control and in select cases achieve insulin independence. Intraportally transplanted islets must reside in the hostile environment of the liver, where they are exposed to the instant blood mediated inflammatory reaction (IBMIR), alloimmunity, recurrence of islet specific autoimmunity, a highly toxic pro-inflammatory cytokine storm (e.g. IL-1β, IFN-α, IFN-γ and TNF-α) and hypoxia due to inadequate revascularization post-transplantation. The early loss of functional islet mass (50-70%) due to apoptosis following clinical transplantation contributes to islet allograft failure. Strategies to prevent apoptosis are therefore highly desirable to enhance islet survival for transplantation.

In **Chapter 3**, the ability of Adenoviral (Ad) and Adeno-Associated Viral (AAV)-based vectors expressing a green fluorescent protein (GFP) reporter gene to transduce isolated human and rat pancreatic islets was investigated. Specific interest was placed on tyrosine mutant AAV-based vector types, which have not been previously explored in human and rodent pancreatic islets. Ad efficiently transduced isolated human and rat pancreatic islets while AAV failed to transduce human islets and showed a varied ability to transduce rat islets. The results in this chapter demonstrate that Ad vectors are more efficient at transducing isolated islets than AAV-based vector types.

Chapter 4 aimed to characterise an Ad-based vector encoding an anti-apoptotic molecule termed Insulin-like Growth Factor-II (Ad-IGF-II). Ad-IGF-II effectively transduced rat pancreatic islets without affecting islet viability or function and did not induce uncontrolled islet cell proliferation. The results in this chapter suggest that Ad-IGF-II is an effective and non-toxic vector type for use in an islet gene therapy setting.

In **Chapter 5** and **Chapter 6**, the influence of local human IGF-II over expression on rat pancreatic islet cell survival *in vitro* and *in vivo* was examined, respectively. Over expression of IGF-II in islets resulted in enhanced islet survival *in vitro* and in an *in vivo* marginal mass islet transplant model. Transplantation of IGF-II over expressing islets under the kidney capsule of diabetic NOD-SCID mice restored euglycemia in 78% of recipients, compared to 46% and 18% of untransduced and Ad-GFP transduced control islet recipients, respectively.

In summary, this thesis demonstrated that compared to AAV, Ad is currently the optimal vector for use in an islet gene therapy setting. Moreover, over expression of IGF-II did not affect the viability or insulin secreting capacity of islets. Finally, the induced expression of anti-apoptotic IGF-II led to enhanced islet survival *in vitro* and improved transplant outcomes in an *in vivo* marginal mass islet transplant model, indicating that IGF-II gene transfer is a potentially powerful tool to improve islet survival post-transplantation.

Thesis Declaration

I certify that this work contains no material which has been accepted for the award of any other degree or diploma in any university or other tertiary institution to Amy Hughes and, to the best of my knowledge and belief, contains no material previously published or written by another person, except where due reference has been made in the text. In addition, I certify that no part of this work will, in the future, be used in a submission for any other degree or diploma in any university or other tertiary institution without the prior approval of the University of Adelaide and where applicable, any partner institution responsible for the joint-award of this degree. I give consent to this copy of my thesis when deposited in the University Library, being made available for loan and photocopying, subject to the provisions of the Copyright Act 1968. The author acknowledges that copyright of published works contained within this thesis (as listed below*) resides with the copyright holder(s) of those works. I also give permission for the digital version of my thesis to be made available on the web, via the University's digital research repository, the Library catalogue and also through web search engines, unless permission has been granted by the University to restrict access for a period of time.

***Hughes A**, Jessup C, Drogemuller C, Mohanasundaram D, Milner C, Rojas D, Russ GR, Coates PT. Gene therapy to improve pancreatic islet transplantation for Type 1 diabetes mellitus. Curr Diabetes Rev. 2010 Sep;6(5):274-84.

Signed Amy Hughes

Publications, Presentations and Awards

Publications

Invited Reviews

1. **Hughes, A**, Jessup, C, Drogemuller, C, Mohanasundaram, D, Milner, C, Rojas, D, Russ, G.R and Coates, P.T, Gene Therapy to Improve Pancreatic Islet Transplantation for Type 1 Diabetes Mellitus, 2010 Curr Diabetes Rev, 6, 274-84

Published Manuscripts (1) and Manuscripts in Preparation (2)

1. **Hughes A**, Mohanasundaram D, Kireta S, Jessup C, Drogemuller C, Coates PTH. Insulin-like Growth Factor-II Prevents Proinflammatory Cytokine-Induced Apoptosis and Significantly Improves Islet Survival After Transplantation. *Transplantation*. 2013;95: 00-00.

2. **Hughes, A,** Jessup CF, Drogemuller, CJ, and Coates PTH, Tyrosine mutations in AAV2 and AAV8 Capsids is Insufficient to Enhance Gene Delivery to Isolated Human Pancreatic Islets

Published Abstracts

1. **Hughes, A**, Mohanasundaram, D, Drogemuller, CJ, Jessup, CF, Coates PTH, Anti-Apoptotic Insulin-like Growth Factor-II Gene Therapy Protects Islets from Cytokine Induced Cell Death, American Journal of Transplantation, Volume 12, Issue Supplement s3, pages 27 – 542, May 2012
2. **Hughes, A**, Jessup, CF, Drogemuller, Mohanasundaram, D, Milner, CR, Rojas, D, Russ, GR, Coates, PTH, Transduction of Rat Pancreatic Islets with Wildtype Adeno-Associated Virus (AAV) Serotype 2, Pseudotype AAV2/8. AAV2/1 and Surface-Exposed Tyrosine Mutant AAV Vectors – A comparative study, American Journal of Transplantation, Volume 90-Supplement, pp:1-1078, July 2010
3. **Hughes, A**, Jessup, CF, Drogemuller, Mohanasundaram, D, Milner, CR, Rojas, D, Russ, GR, Coates, PTH, Adenovirus-Mediated Transduction of Isolated Pancreatic Islets Using Insulin-Like Growth Factor-II to Promote Islet Survival Post-Transplantation, American Journal of Transplantation, Volume 90-Supplement, pp:1-1078, July 2010

4. **Hughes, A**, Jessup, CF, Drogemuller, Mohanasundaram, D, Milner, CR, Rojas, D, Russ, GR, Coates, PTH, Transgenic Expression of Insulin-like Growth Factor-II (IGF-II) in Pancreatic Islets to Prevent Apoptosis, Xenotransplantation, Vol. 16, Issue 6, page 553 December 2009

Presentations

A. Hughes, A.J. Kupke, C.J. Drogemuller, D.M. Mohanasundaram, C. Mee, C.R. Milner, C.F. Jessup, P.T.H. Coates. Adenovirus-Mediated Transduction of Pancreatic Islets using Insulin-like Growth Factor-II (IGF-II) to Prevent Apoptosis. Oral presentation. Australian Society for Medical Research, Annual Scientific Conference, 2009

A. Hughes, A.J. Kupke, C.J. Drogemuller, D.M. Mohanasundaram, C. Mee, C.R. Milner, C.F. Jessup, P.T.H. Coates. Adenoviral-Mediated Transduction of Pancreatic Islets using Insulin-like Growth Factor-II (IGF-II) to Prevent Apoptosis. Oral presentation. Transplantation Society of Australia and New Zealand Annual Scientific Meeting, Canberra, 2009

A. Hughes, A.J. Kupke, C.J. Drogemuller, D.M. Mohanasundaram, C. Mee, C.R. Milner, C.F. Jessup, P.T.H. Coates. Transgenic expression of Insulin-like Growth Factor-II in pancreatic islets to prevent apoptosis. Oral Presentation. Australian Diabetes Society (ADS) and the Australian Diabetes Educators Association (ADEA) Annual Scientific Meeting, Adelaide, 2009

A. Hughes, A.J. Kupke, C.J. Drogemuller, D.M. Mohanasundaram, C. Mee, C.R. Milner, C.F. Jessup, P.T.H. Coates. Investigation of cytokine-induced early apoptosis in isolated islets of langerhans. Oral Presentation. Annual Immunology Retreat, Australasian Society for Immunology, Adelaide, 2009

A. Hughes, C.J. Drogemuller, C.J. Jessup, P.T.H. Coates. Optimal Delivery of Therapeutic Genes to Pancreatic Islets. Invited Oral Presentation, T cell Laboratory, Weatherall Institute of Molecular Medicine, Oxford, UK, 2009

A. Hughes, C.F. Jessup, C.J. Drogemuller, D. Mohanasundaram, C.R. Milner, D. Rojas, G.R. Russ, P.T.H. Coates. Transgenic expression of insulin-like growth factor-II (IGF-II) in pancreatic islets to prevent apoptosis. Poster Presentation. Joint International Pancreas and Islet Transplantation Association (IPITA) and International Xenotransplantation Association (IXA) Meeting, Venice, Italy, 2009

A. Hughes, C.F. Jessup, C.J. Drogemuller, D. Mohanasundaram, C.R. Milner, D. Rojas, G.R. Russ, P.T.H. Coates. Investigation of cytokine-induced early apoptosis in isolated islets of langerhans. Oral Presentation. The Queen Elizabeth Hospital Annual Research Day, Adelaide, 2009

A. Hughes, C.F. Jessup, C.J. Drogemuller, D. Mohanasundaram, C.R. Milner, D. Rojas, G.R. Russ, P.T.H. Coates. Comparison of wildtype adeno-associated virus (AAV) serotype 2 vectors to pseudotyped AAV vectors for the transduction of rat pancreatic islets. Oral Presentation. Transplantation Society of Australia and New Zealand Annual Scientific Meeting, Canberra, 2010

A. Hughes, C.F. Jessup, C.J. Drogemuller, D. Mohanasundaram, C.R. Milner, D. Rojas, G.R. Russ, P.T.H. Coates. Transduction of Rat Pancreatic Islets with Wildtype Adeno-Associated Virus (AAV) Serotype 2, Pseudotype AAV2/8, AAV2/1 and Surface-Exposed Tyrosine Mutant AAV Vectors – A Comparative Study. Poster Presentation. XXIII International Congress of the Transplantation Society (TTS), Vancouver, Canada, 2010

A. Hughes, C.F. Jessup, C.J. Drogemuller, D. Mohanasundaram, C.R. Milner, D. Rojas, G.R. Russ, P.T.H. Coates. Adenovirus-Mediated Transduction of Isolated Pancreatic Islets Using Insulin-Like Growth Factor-II to Promote Islet Survival Post-Transplantation. Poster Presentation. XXIII International Congress of the Transplantation Society (TTS), Vancouver, Canada, 2010

A. Hughes, C.F. Jessup, C.J. Drogemuller, D. Mohanasundaram, C.R. Milner, D. Rojas, G.R. Russ, P.T.H. Coates. Introduction to the Renal and Transplantation Immunobiology Laboratory. Invited Oral Presentation. Diabetes Research Institute (DRI), University of Miami, Florida, 2010

A. Hughes, C.F. Jessup, C.J. Drogemuller, D. Mohanasundaram, C.R. Milner, D. Rojas, G.R. Russ, P.T.H. Coates. Evaluation of wildtype adeno-associated virus (AAV) serotype 2, pseudotype AAV2/8, AAV2/1 and surface-exposed tyrosine mutant AAV vectors and their ability to transduce isolated rat pancreatic islets. Oral Presentation. The Queen Elizabeth Hospital Annual Research Day, Adelaide, 2010

A. Hughes, C.F. Jessup, C.J. Drogemuller, D. Mohanasundaram, C.R. Milner, D. Rojas, G.R. Russ, P.T.H. Coates. Adenovirus-Mediated Transduction of Pancreatic Islets using Insulin-like Growth Factor-II (IGF-II) to Prevent Apoptosis. Oral presentation. Australian Society for Medical Research, Annual Scientific Conference, 2011

A. Hughes, C.F. Jessup, C.J. Drogemuller, D. Mohanasundaram, C.R. Milner, D. Rojas, G.R. Russ, P.T.H. Coates. Optimal Delivery of Insulin-Like Growth Factor-II to Rat Pancreatic Islets using a Replication Deficient Adenoviral Construct. Poster Presentation. Faculty of Health Sciences, Postgraduate Research Conference, Adelaide, 2011

A. Hughes, C.F. Jessup, C.J. Drogemuller, D. Mohanasundaram, P.T.H. Coates. Adenoviral Overexpression of Insulin-like growth factor II Protects Pancreatic Islets from Pro-Inflammatory Cytokine Induced Apoptosis and Necrosis. Poster Presentation. Australasian Society of Immunology, Adelaide, 2011

A. Hughes, D. Mohanasundaram, C. J. Drogemuller, C. F. Jessup P.T.H. Coates. Anti Apoptotic Insulin-Like Growth Factor-II Gene Therapy Protects Islets from Cytokine Induced Cell Death. Poster Presentation. American Transplant Congress 2012, Boston, USA, 2012

A. Hughes, D. Mohanasundaram, C. J. Drogemuller, C. F. Jessup P.T.H. Coates. Transgenic Expression of Insulin-Like Growth Factor-II (IGF-II) in Pancreatic Islets Offers a Novel Therapeutic Strategy to Improve Islet Cell Survival Post-Transplantation. Oral Presentation. Australian Society for Medical Research, Annual Scientific Conference, 2012

A. Hughes, D. Mohanasundaram, C. J. Drogemuller, C. F. Jessup P.T.H. Coates. Anti-Apoptotic Insulin-Like Growth Factor-II (IGF-II) Gene Transfer Offers a Novel Therapeutic Strategy to Improve Islet Cell Survival Post-Transplantation. Oral Presentation. Transplantation Society of Australia and New Zealand Annual Scientific Meeting, Canberra, 2012

A. Hughes, D. Mohanasundaram, C. J. Drogemuller, C. F. Jessup P.T.H. Coates. Insulin-Like Growth Factor-II Decreases Islet Apoptosis *In Vitro* and Improves Islet Transplant Function in a Minimal Mass Model. Poster Presentation. 24th International Congress of The Transplantation Society, Berlin, Germany, 2012

Awards

2012 Pfizer Young Investigator Award, Transplantation Society of Australia and New Zealand, Annual Scientific Meeting, Canberra

2012 Medical Staff Society Research Prize, Medical Grand Round, Royal Adelaide Hospital

2012 Faculty of Health Sciences Postgraduate Travelling Fellowship, University of Adelaide

2010 International Travel Grant, The Transplantation Society of Australia and New Zealand

2009 Trevor Prescott Memorial Scholarship, The Freemasons Foundation, Adelaide

2009 Amgen Young Investigator Award, The Transplantation Society of Australia and New Zealand, Annual Scientific Meeting, Canberra

2009 Faculty of Health Sciences Postgraduate Divisional Scholarship, University of Adelaide

2008 The Queen Elizabeth Research Foundation Honours Scholarship, Adelaide

Acknowledgements

Firstly, I would like to thank my supervisors Associate Professor Toby Coates, Dr. Claire Jessup and Chris Drogemuller for their time, guidance and support. Thank you for reviewing all my abstracts, all my thesis drafts and all my manuscript drafts. In particular I would like to give my sincere gratitude to Dr. Coates. Toby I thank you for giving me the opportunity to complete my PhD in the laboratory. Three years ago my life became richer and more fulfilling, and then it became "amazing" simply because I was given the opportunity to work day in and day out in the field of islet transplantation, working with a remarkable endocrine cell that so elegantly exists within the pancreas to release different hormones in response to blood nutrient levels. Toby I also cannot forget Brunello di Montalcino as a wine first experienced in Venice, but to the end of time, it will remain in my heart as a reminder of your generosity.

Thank you to all the past and present members of the lab. Tim Searcy (LF), thank you for every minute I was blessed to be in your presence. Our friendship has been witness to laughter, happiness, adventures, tears and frustrations and for this I will be eternally grateful. Chris Hope, my dear friendly friend, thank you for being by my side as we hold on tight and ride the PhD roller coaster together. You are the epitome of what a good scientist represents and have never been anything but a truly exceptional friend to me. The beautiful Jodie Nitschke, from the moment I met you I have been mesmerized by your soul which at every given moment radiates nothing but pure "amazing-ness". Thank you for all your help in the lab, thanks for - saturday morning 'agarose gel master class', for your guidance with all things sequencing and PCR, for your help with preparing buffers and reagents (the list could go on and on). Julie Johnston (Jules), there has never been a question that you cannot answer. Your scientific knowledge and understanding truly rivals that of a senior post-doc. I have never been anything but in awe of you, and thankful for our friendship. Dr. Darling Rojas-Canales, thank you for your friendship, for your mentorship, patience and advice. I hold close to my heart over four years of "TIL/ITF/RTIL/TQEH/RAH" memories. Darling, I am so excited to watch your post-doctoral career because you are destined for great things. Plinio Hurtado (Plin), your love of life is contagious and I thank you for allowing me to share that passion with you. Ernesto Hurtado (E), I have enjoyed our conversations (mainly about desert and wine bars). The field of science gained an exceptional advocate when you entered the realm of medical research and I wish you the best of luck in all your future endeavors.

I thank Dr. Daisy Mohanasundaram for her patience in teaching me how to perform rat islet isolations. Daisy, I thank you for your help with the islet transplants performed in this thesis, of which Chapter 6 would not have been possible without your help. Finally, I would like to give my special thanks to Svjetlana Kireta, Clyde Milner, Dr. Michael Collins, Matthew Stephenson, Dr. Natasha Rogers, Daniella Penko and Kisha Sivanathan for their friendship and help in the laboratory.

Thank you to the donors and donor families, whom without their generosity, this research would not have been possible. I am also greatly appreciative of the support given by The Australian Islet Consortium, The University of Adelaide, CNARTS and The Transplantation Society of Australia and New Zealand. I would like to extend my sincere gratitude to the Trevor Prescott/Freemasons foundation for their commitment to health, their community involvement and awarding me the prestigious Trevor Prescott Memorial Scholarship for my PhD studies in 2009.

I want to thank my parents, Lynn and Greg Hughes from the bottom of my heart for their endless love and support throughout my academic education. You will be in my heart forever and always. Thank you to my siblings Sarah, Michelle, Matt, Joe, Hannah and Finlay. There is no other love like the love I feel for all of you. Special thanks to my niece Isabella, you are still my angel sent from god to brighten all our lives, and my nephew Callum, you might not even realize it yet, but every day you remind me that life is “amazing”.

Lauren and Erin, I have had the honor of knowing you since our very first day in undergraduate biotechnology. Thank you for the unrelenting support, laughter and fun times. You have both witnessed my countdown, for three years now. Finally, the countdown is over. Dr. Helena Ward, thank you for your support, friendship and advice. I am looking forward to our purple-themed dinner to celebrate ‘the PhD’.

To my PhD, you have been my friend, my every day, my early mornings, and my weekend accomplice (eating far too much take away laksa from Rundle Street) while running ELISAs late into the evening. For the last three years you have been the first thing on my mind in the morning and the last thing on my mind in the evening. I will miss you, but without you I would not know the true meaning of dedication, the meaning of determination and the meaning of strength.

Abbreviations

°C - Degrees celcius

1x PBS - 1 x Phosphate Buffered Saline

1xHBSS - 1x Hanks Buffered Salt Solution

4E-BP1 - Eukaryotic initiation factor binding protein

4E-eIF4E - Eukaryotic initiation factor

AAV - Adeno-associated viruses

Ad - Adenovirus

Ad-GFP - Adenoviral-Green Fluorescent Protein

Ad-IGF-II - Adenoviral-Insulin like Growth Factor-II

ALS - Acid-labile subunit

Apaf-1 - Apoptosis-protease activating factor-1

APC - Antigen presenting cell

BAD - Bcl-associated death promoter

Bcl-2 - B-cell lymphoma 2

BGL - Blood glucose levels

BLAST - Basic local alignment search tool

bp - Base pairs

CAR - Coxsackie Adenovirus Receptor

CITR - Collaborative Islet Transplant Registry

cm - Centimeter

CPE - Cytopathic effects

DAPI - 4',6-diamidino-2-phenylindole

DISC - death-inducing signaling complex

ELISA - Enzyme linked immunosorbent assay

Expect-value - E-value

FADD - Fas-associated death domain

FasL - Fas-Fas ligand

FCS - Foetal calf serum

FOXO - Forkhead transcription factor

GAD65 - Glutamic acid decarboxylase

GFP - Green fluorescent protein

GLUT2 - Glucose transporter 2

GSIS - Glucose stimulated insulin secretion

GSK-3β - Glycogen synthase kinase 3β

HEK - Human Embryonic Kidney

hIL-1Ra - Human Interleukin-1 Receptor Antagonist

h - Hour

HPRT-1 - Hypoxanthinephosphoribosyltransferase 1

HSPG - Heparan sulphate proteoglycan

HSV - Herpes Simplex Virus

i.p - Intra peritoneal

IBMIR - Instant blood mediated inflammatory reaction

IEQ - Islet equivalents

IFN-γ - Interferon-gamma

IGF - Insulin-like Growth Factor

IGF-1R - Insulin-like Growth Factor-I receptor

IGF-1R/IR - Insulin-like Growth Factor-I receptor/Insulin receptor

IGFBP - Insulin-like Growth Factor binding protein

IGF-I - Insulin-like Growth Factor-I

IGF-II - Insulin-like Growth Factor-II

IGF-IIR - Insulin-like Growth Factor-II receptor

IL-10 - Interleukin-10

IL-1β - Interleukin-1β

IL-4 - Interleukin-4

iNOS - Inducible nitric oxide synthase

IR - Insulin receptor

IRS-2 - insulin receptor substrate 2

kbp - Kilo base pairs

kDa - kilo dalton

lamR - Laminin receptor

M - Molar

MAPK - Mitogen activated kinase

ml - Millilitre

mm - Millimeter

mM - Millimolar

MOI - Multiplicity of infection

mRNA - messenger RNA

mTOR - Mammalian target of rapamycin

NF-κB - nuclear factor kappa B

nm - Nanometer

NO - Nitric oxide

NOD - Non-Obese Diabetic

NOD-SCID - Non-Obese Diabetic Severe combined immune deficiency

p70S6K - ribososmal protein S6 kinase

pAkt - Phospho-Akt

PCR - Polymerase Chain Reaction

PDK - phosphoinositol dependent kinase-1

Pfu - Plaque forming units

PI - Propidium Iodide

PI3K - Phosphoinositide-3-kinase

PKB - Protein kinase B

Post-tx - Post-transplant

Pre-tx - Pre-transplant

PS - Phosphatidyl serine

PVDF - Polyvinyl difluoride

rIGF-II - Recombinant IGF-II

RIP - Receptor-interacting protein

RT - Room temperature

RT-PCR - Real-time PCR

SCID - Severe combined immune deficiency

SDS-PAGE - Sulfate polyacrylamide gel electrophoresis

SEM - Standard error of the mean

SFA - Sulphation factor activity

SI - Stimulation index

STAT-1 - Signal transducer and activator of transcription-1

STZ - Streptozotocin

SW - Starting weight

T1D - Type 1 Diabetes

T2D - Type 2 diabetes

TNF - Tumour necrosis factor

TRADD - TNF receptor-associated death domain

TRAF2 - TNF-R-associated factor 2

TSC - Tuberous sclerosis gene product

TUNEL - Terminal deoxynucleotidyl transferase dUTP nick end labelling

VEGF - Vascular endothelial growth factor

vg - Vector genome

μg - Microgram

μl - Microliters

CHAPTER 1

LITERATURE REVIEW

1.1 Introduction

Type 1 Diabetes (T1D) is an autoimmune disease that results from destruction of insulin-producing β-cells of the pancreas. β-cell loss leads to a progressive failure in the production of insulin, the hormone that regulates glucose cellular uptake (1). Intensive insulin therapy is the current treatment of choice for T1D patients as it leads to a reduction in the occurrence of diabetic complications such as retinopathy, neuropathy and kidney damage, however it is unable to control against debilitating hypoglycaemic unawareness (2).

Islet transplantation is a promising therapeutic approach aimed at restoring β-cell function and obtaining optimal metabolic control above that offered by exogenous insulin therapy in T1D patients. However, due to substantial islet cell death (50 – 70%) in the immediate post-transplant period, islet function declines over time and the majority of patients resume insulin therapy within five years (3).

Therefore the use of gene transfer to deliver an anti-apoptotic molecule to islets prior to their transplantation may protect against islet apoptosis in the immediate post-transplant period and lead to an improvement in insulin independence rates. Based on this, the aim of this thesis is to study the optimal vector for gene transfer to islets, with specific emphasis on the ability of the anti-apoptotic molecule Insulin-like Growth Factor-II (IGF-II) to promote islet survival *in vitro* and in an *in vivo* islet transplant setting.

1.2 The pancreas

The pancreas is a gland which plays an integral role in the exocrine digestive system and the endocrine system (4). The pancreas develops through budlike structures on the primitive gut tube into a highly branched organ containing many specialised cell types (5). The pancreas is connected to the small intestine via the pancreatic duct, through which it empties pancreatic fluid, to aid in the digestion of food (6, 7). The endocrine pancreas is responsible for producing insulin which helps to control the amount of glucose in the blood. Whereas the exocrine pancreas secretes digestive enzymes to breakdown carbohydrates, proteins and fats and bicarbonates that neutralize acidic stomach acid (6).

1.3 Islet of Langerhans

The Islet of Langerhans are highly vascularized micro-organs which constitute 1 – 2% of the total pancreas mass (8, 9). Pancreatic islets are composed of multiple cell types, including insulin-producing β-cells, glucagon-producing α-cells, somatostatin-producing δ-cells and pancreatic-polypeptide producing PP-cells (7, 10). The predominant role of β-cells is to produce the endocrine hormone insulin, which is required for glucose uptake and glycogen synthesis (11).

There are reported differences in islet architecture and composition among mammalian species (12). For example, islets in the adult guinea pig are primarily composed of β-cells that are distributed throughout the islet (13, 14), with α-cells located in the periphery. Rodent islets have a highly ordered structure that is composed primarily of β-cells (60 – 80%) clustered in a central core, surrounded by α (15 – 20%), δ (<10%) and PP cells (<1%) in the periphery (15-17). Human islets display a more scattered organization of endocrine cells and a higher percentage of α-cells (50%) compared to rat islets (15 – 20%) (18, 19) **(Figure 1.3)**.

1.3.1 The β-cell and glucose homeostasis

Within the body, blood glucose levels (BGL) are tightly controlled as to ensure homeostasis is maintained within the cells and tissues of the body. In the normal physiological state, the level of glucose in the blood exists within a range of 3.6 – 5.8 mmol/l. Insulin secretion from the β-cell occurs in response to rapid increases in BGL, usually occurring following a meal (20-22). The first phase of insulin secretion consists of a sharp peak that results from the uptake of glucose into the β-cell via the glucose transporter 2 (GLUT2) receptor (23). Upon entering the β-cell, glucose is phosphorylated, leading to a rise in the ATP:ADP ratio and the opening of calcium channels (24). This promotes an influx of calcium ions, leading to insulin release and the subsequent release of c-peptide, a by-product of insulin secretion into the blood stream (25). The second phase, is characterised by sustained elevation of insulin secretion, which rises over a period of several minutes (26).

1.4 Diabetes Mellitus

Diabetes Mellitus is a group of metabolic diseases in which the pancreas does not produce enough insulin (type 1) or there is too much glucose in the blood (type 2). Approximately 346 million people worldwide have diabetes and the world health organization predict that diabetes deaths will double between 2005 and 2030. Diabetes is a major health problem that significantly affects the health of ~898,000 Australians (http://www.aihw.gov.au/diabetes).

Figure 1.3. Diagrammatical representation of a rat and human islet endocrine cell. Human and rat pancreatic islets differ in their cellular composition. Human islets display a random distribution of β-cells, α-cells, γ-cells, somatostatin- and grehlin-producing cells. In contrast, rat islets contain a β-cell rich core, with all other endocrine cells located in the periphery. Figure adapted from Suckale et al (27).

1.4.1 Type 1 Diabetes

T1D is an autoimmune disease, characterised by the progressive immune-mediated destruction of insulin producing β-cells within the pancreas (28). β-cell death in T1D occurs via apoptosis induced by infiltrating immune cells such as macrophages and T cells (29, 30). The immune cells secrete pro-inflammatory cytokines such as IL-1β, TNF-α, and IFN-γ (31, 32), leading to the production of cytotoxic nitric oxide (NO) and the up-regulation of various pro-inflammatory mediators (33, 34). One such mediator is the transcription factor nuclear factor kappa B (NF-κB) which is responsible for the activation of autoreactive T cells (35).

The onset of T1D generally occurs in the first two decades of life, with a peak incidence between 10 – 13 years of age. However, T1D may occur at any age, and approximately one quarter of all T1D cases develop later in life (36). Prior to the first clinical symptoms of T1D, the β-cell mass has already been reduced by 70 – 80% (37). The incidence of T1D is increasing worldwide (38, 39). In Australia, the incidence of T1D is rising at an average rate of 2.8% per year (40), if this continues there will be 2.5 – 3 million people with diabetes by 2025 and approximately 3.5 million by 2033 (41).

Diabetes is associated with a number of complications, which can occur from the onset of diagnosis, or many years after the diabetic disease has developed. Diabetes is the leading cause of lower limb amputation, retinopathy, neuropathy and end stage kidney failure (42, 43).

1.4.2 Immunology of Type 1 Diabetes

Lymphocytic infiltration of pancreatic islets, termed 'insulinitis', is considered a hallmark clinical feature of T1D. Cytotoxic $CD8^+$ T cells can directly kill β-cells, whereas $CD4^+$ T cells activate B cells and thus, promote autoantibody production (44). While the exact trigger for the onset of T1D is unknown, once the immune system is activated it presents self antigens to T cells, leading to autoimmune destruction of the insulin-producing β-cells (45).

Over 40 genes and regions have been found to be associated with risk of T1D (46). Genes located within the human leukocyte antigen class II region on chromosome 6p21 account for approximately 50% of genetic risk of T1D (47, 48). A region in the regulatory domain of the insulin gene has also been shown to provide approximately 10% of the genetic susceptibility to T1D (49). In addition to genetic factors, various environmental factors have been linked to

the development of T1D. Causative environmental triggers include viral infections, immunizations, diet, early exposure to cow's milk, maternal age, history of pre-eclampsia, neonatal jaundice, among others (50). However, it may take multiple environmental insults, in genetically predisposed individuals, to trigger destruction of β-cells and individual patients may experience them in differing combinations (51). Autoantibodies to several pancreatic islet auto-antigens serve as biomarkers for T1D. The primary autoantibody detected is against glutamic acid decarboxylase (GAD65). Other autoantibodies include protein tyrosine phosphatase-like molecule IA-2 and insulin (52, 53).

1.4.3 Type 2 Diabetes

Type 2 diabetes (T2D) is the most common form of diabetes, accounting for 85 – 90% of all cases (54). T2D results from the progressive failure of pancreatic β-cells in the presence of chronic insulin resistance and inadequate insulin secretion (55). Insulin resistance is characterised by the inability of cells to respond appropriately to insulin, a hormone that clasically acts to control glucose release (56).

T2D was formerly called non-insulin dependent or adult-onset diabetes, although it is now increasingly reported in younger individuals (57, 58). Long-term complications of T2D include retinopathy, kidney failure and amputation due to poor circulation. In addition, T2D patients have a 2 – 6 times increased risk of death from cardiovascular disease compared to the general population (59).

The aetiology of T2D is associated with genetic and environmental risk factors, which include unhealthy eating and lack of physical activity in individuals that are genetically predisposed. The pathogenesis of T2D involves abnormalities in insulin action, secretion and endogenous glucose output (60). T2D is initially managed with a program of increased exercise and change in diet or patients are treated with oral anti-diabetic agents. As the disease progresses, patients must begin to use insulin therapy as a way to maintain glucose control (61).

1.4.4 Current treatments for Type 1 Diabetes

Insulin therapy is the most effective treatment currently available for managing T1D, administered in the form of multiple daily injections or via an insulin pump (62). Insulin was discovered in 1921 by Canadian scientists Banting, Best, Macleod and Collip. Early after its discovery, animal insulin (porcine and bovine) was manufactured and administered to humans by injection to treat their diabetes (63). The use of human insulin, namely Humilin® rapid and Humilin N, was FDA approved in 1982. Since this time a number of biosynthetic recombinant "human" insulin or insulin analogues have been developed for clinical use worldwide. New insulin analogues more closely mimic the kinetic profile of endogenous insulin compared to past formulations, however insulin injections are not a cure for diabetes and diabetic complications can develop over time.

Continuous subcutaneous insulin infusion also known as an insulin pump is considered to be the most physiologic way to deliver insulin, as it is able to stimulate the normal pattern of insulin secretion (64). Studies have shown that insulin pump therapy leads to lower average glycated haemoglobin levels in diabetic patients versus patients with multiple daily injections (65, 66). The disadvantages to using a pump include possible weight gain, high cost and inconvenience as patients must remain continually attached to the pump.

The replacement of β-cells by whole pancreas transplantation represents an alternative therapy for diabetic patients. However, a pancreas transplant is generally only performed in combination with a kidney transplant in patients with end stage renal disease (67). Complications that can occur following whole pancreas transplantation include rejection, thrombosis, pancreatitis and infection (68). Whole pancreas transplantation is associated with significant cost and surgical risk which can lead to morbidity and mortality and is therefore not a viable option for most T1D patients. Since the endocrine tissue only comprises 1 – 1.5% of the total pancreatic mass, pancreatic islet transplantation arises as a logical alternative (69).

1.4.5 Islet Transplantation

In clinical islet transplantation, islets are isolated from a deceased donor. The pancreas is digested within a 'Ricordi Chamber' using an enzyme blend of collagenase and neutral protease (70). The pancreatic islets are subsequently purified using density centrifugation to reduce the amount of acinar tissue and then transplanted into the liver via the portal vein **(Figure 1.4.5)**.

In 1967 Paul Lacy developed a enzymatic collagenase based method to isolate islets (71). Subsequent studies showed that transplantation of isolated islets can cure chemically induced diabetes in rodents and non-human primates (72, 73). The true clinical potential of islet transplantation for treatment of T1D was demonstrated in 2000, with the introduction of the 'Edmonton Protocol'. The study showed an initial 100% insulin independence success rate in seven out of seven transplanted patients, less frequent hyperglycaemia and overall improved blood glucose control (74). The Edmonton Protocol utilised a steroid free immunosuppressive regimen in addition to a large number of islets, often from multiple donors to achieve transplant success. More than 750 islet transplants have been performed to date worldwide, with two-thirds of recipients achieving insulin independence and maintaining it out to one year, following their transplant (75). However, long term follow up reveals a marked reduction in islet graft function over time, leading to the majority of islet transplant patients needing to resume insulin therapy within five years (3).

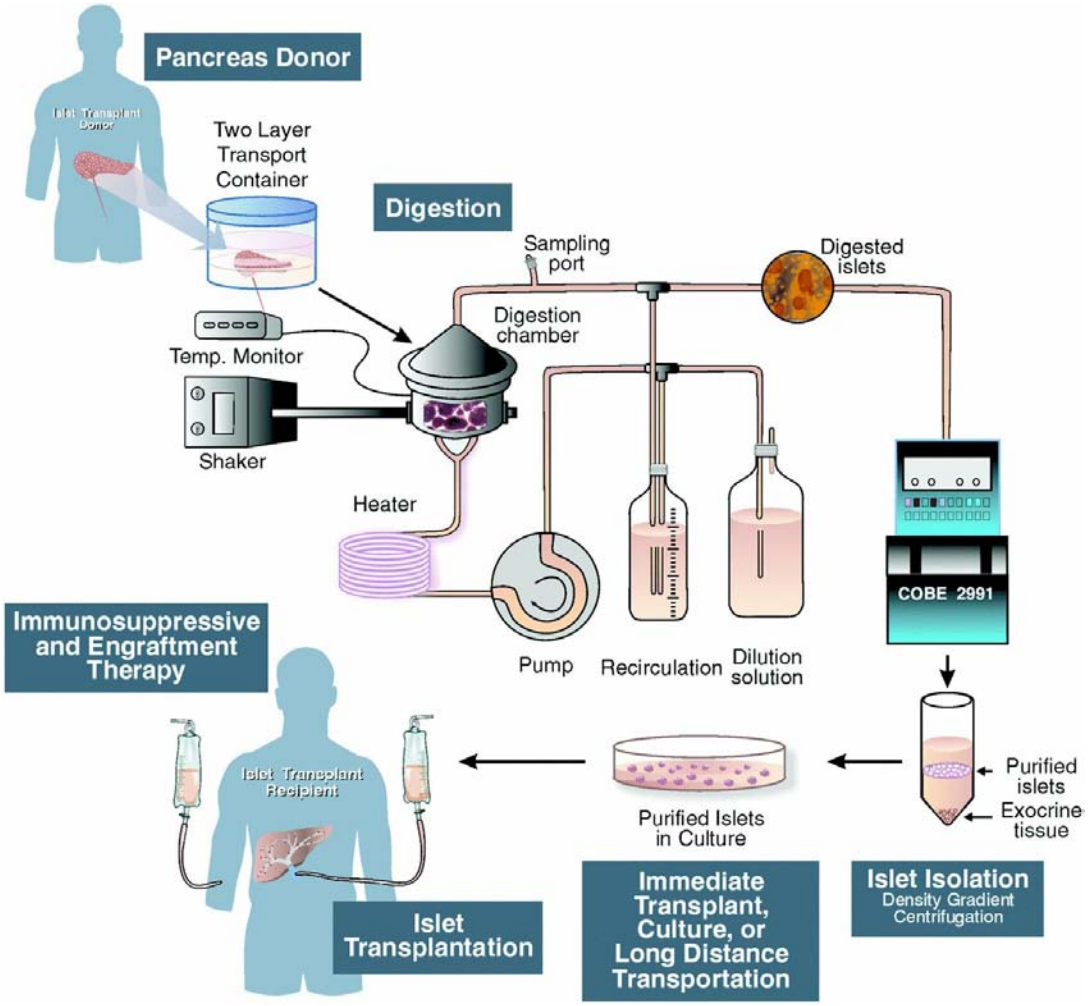

Figure 1.4.5. Islet isolation and transplantation. Islets are isolated from a donor pancreas using a semi-automated digestion method designed by Professor Camillio Ricordi, termed the 'Ricordi Chamber'. The chamber mechanically breaks down the islet tissue which is then purified by density gradient centrifugation. Purified islets of high quality and yield are then infused into the portal vein of the recipient's liver. The figure was adapted from Merani et al (76).

1.5 Barriers to successful islet transplantation

A major limitation to the success of clinical islet transplantation is the early loss of up to 70% of the islet mass 24 – 48 hours post-transplantation (77, 78), which contributes significantly to declining islet function following transplantation **(Figure 1.5)**. Eriksson et al (79) suggest a large proportion of the transplanted islet mass is lost within the first few minutes to hours following transplantation. Approximately 70% of islets are hypoxic 24 hours (h) following transplantation, as evaluated by Olsson and colleagues (80) using the hypoxia marker pimonidazole.

Many factors contribute to islet cell death including the initial instant blood mediated inflammatory reaction (IBMIR). IBMIR occurs following the exposure of pancreatic islets to recipient blood and subsequently leads to platlet activation, clot formation, lymphocyte recruitment and islet destruction (81). Destruction of the islet microenvironment and loss of trophic support occurs as a consequence of the human islet isolation process and leads to local inflammation and ischemic islet cell death (82, 83).

Native pancreatic islets are highly vascularized, a characteristic which ensures that the islets can adequately secrete insulin in response to glucose (84). However, the islet isolation process severs the connection between the islet vasculature and the systemic circulation, and subsequently renders the islets avascular for several days following transplantation (84). Moreover, prior to revascularization, islet survival is dependent on the diffusion of oxygen and nutrients, which is difficult to achieve within the liver micro environment (85, 86). The aggressive islet isolation process activates resident islet macrophages and leukocytes to release pro-inflammatory cytokines such as TNF-α, IL-1β and IFN-γ which induce the production of cytotoxic NO (87). NO is produced by the oxidation of L-arginine to L-citrulline by NO synthase, and regulated by the transcription factor NF-κB (88). Generation of excess NO inhibits mitochondrial metabolism, promotes protein modification and DNA cleavage, leading to impaired insulin secretion and β-cell death (89, 90).

Allogeneic islets trigger immune-mediated rejection that must be controlled with immunosuppressive drugs (91). Therefore, transplanted islets are continuously exposed to immunosuppressive drugs, which adversely impact β-cell survival and function (92). More widely, immunosuppressive drugs can be neprotoxic and induce other associated side effects such as ulcers, peripheral edema, anemia, weight loss, hypertension, hyperlipidemia and are associated with an increased risk of malignancies (93).

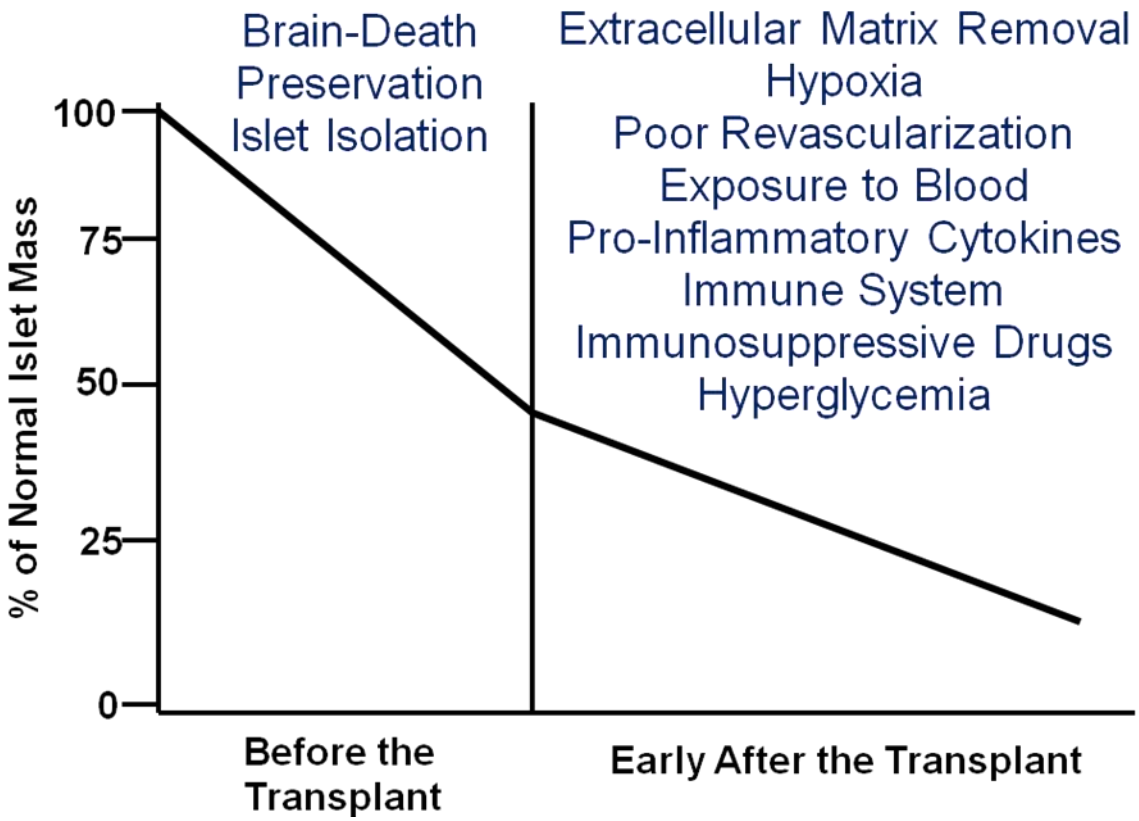

Figure 1.5. Islet transplantation is associated with a marked reduction in islet graft function over time. While short term glucose stabilization and insulin independence rates continue to improve in allogeneic islet transplant recipients, long-term follow up reveals a marked reduction in islet graft function over time. The reasons for the decline in insulin independence rates following islet transplantation are complex, beginning before pancreas procurement as brain death is associated with the production of pro-inflammatory cytokines such as TNF-α, IL-1β and IL-6. Once transplanted, islets must reside in the hostile environment of the liver, where they are exposed to a multitude of apoptotic stresses that contribute to early failure of the islet allograft. Figure adapted from Contreras et al (94).

1.6 Concepts and methods of gene therapy

Section(s) 1.6 – 1.7 are adapted and modified from the published article **(Appendix C)**:

Hughes A, Jessup C, Drogemuller C, Mohanasundaram D, Milner C, Rojas D, Russ GR, Coates PT. Gene therapy to improve pancreatic islet transplantation for Type 1 diabetes mellitus. Curr Diabetes Rev. 2010 Sep;6(5):274-84.

The development of highly efficient viral vectors capable of transferring useful genes to human cells has led to the concept of gene therapy (95). Early transplant stresses such as apoptosis may be overcome through the use of *ex vivo* gene therapy strategies to deliver anti-apoptotic genes to the islets to improve post-transplant islet viability (96).

Gene therapy can be defined as a set of approaches for the treatment of human diseases based on the transfer of genetic material (DNA) into cells, either outside the body (*ex vivo*) or by direct administration (*in vivo*) with the aim of preventing or correcting various types of disorders (97). Viral vectors are modified to carry a gene of interest (or 'transgene') into a specific target cell (98), such as islets. Compared to *in vivo* gene transfer, *ex vivo* gene transfer provides an important safety feature, whereby only the target cells express the gene of interest, avoiding unpredictable systemic side effects (97). *Ex vivo* gene therapy requires the harvest of cells from the patient. The cells are then infected or 'transduced' with the vector and returned to the patient at the time of their transplant. Successful *ex vivo* gene therapy has already been achieved for treatment of severe combined immune deficiency (SCID) (99, 100) and more recently, Parkinson's disease and Haemophilia B (101, 102).

1.6.1 Viral-mediated gene transfer to pancreatic islets

There are four major classes of viral vectors utilized in gene therapy, adenoviruses (Ad), adeno-associated viruses (AAV), herpes simplex viruses (HSV) and retroviruses (including lentiviruses) as described in **Table 1.6.1** and **Figure 1.6.1**. A number of studies have demonstrated the ability of these vectors to infect pancreatic islets of both human and animal origin (103-106).

Table 1.6.1 Commonly used gene delivery viral vectors

Type	Adenovirus	Adeno-associated virus	Herpes Simplex Virus	Retrovirus	Lentivirus
Packaging Capacity	Medium (≤7.5 kilo base pairs)	Low (≤4.5 kilo base pairs)	Large (≥30 kilo base pairs)	Medium (≤7 kilo base pairs)	Medium (≤8 kilo base pairs)
Duration of expression	Transient	Stable, long-term	Stable, long-term	Transient, however stability of expression from newer generation vectors is markedly improved to produce sustained expression	Stable, long-term
Immunogenicity	High	Low	Low	Low	Low
Repeated dosing	Not possible	Possible	Possible	Possible	Possible
Clinical Trials	Yes	Yes	Yes	Yes	Yes
Advantages	Infects both dividing and non-dividing cells, provides transient expression, particularly high short term expression, generates high titer viral stocks	Infects both dividing and non-dividing cells, integrates into host genome, provides long-term expression *in vivo*, elicits minimal immune response, generates high viral titers	Large genome, non-pathogenic, unable to reactivate, broad host range, persists long-term.	Integrates into host genome, provides long-term expression and stable transduction	Infects both dividing and non-dividing cells, genome integration, long-term expression
Disadvantages	Immunogenic, cause mild respiratory disease in humans	Requires helper virus, slow expression onset, inefficient large-scale virus production, small genome limiting the viruses packaging capacity	Potentially provoke antiviral responses against HSV-infected cells	Low efficiency *in vivo*, risk of insertional mutagenesis, low titer, host range restricted to dividing cells only	Safety concerns, production inefficient

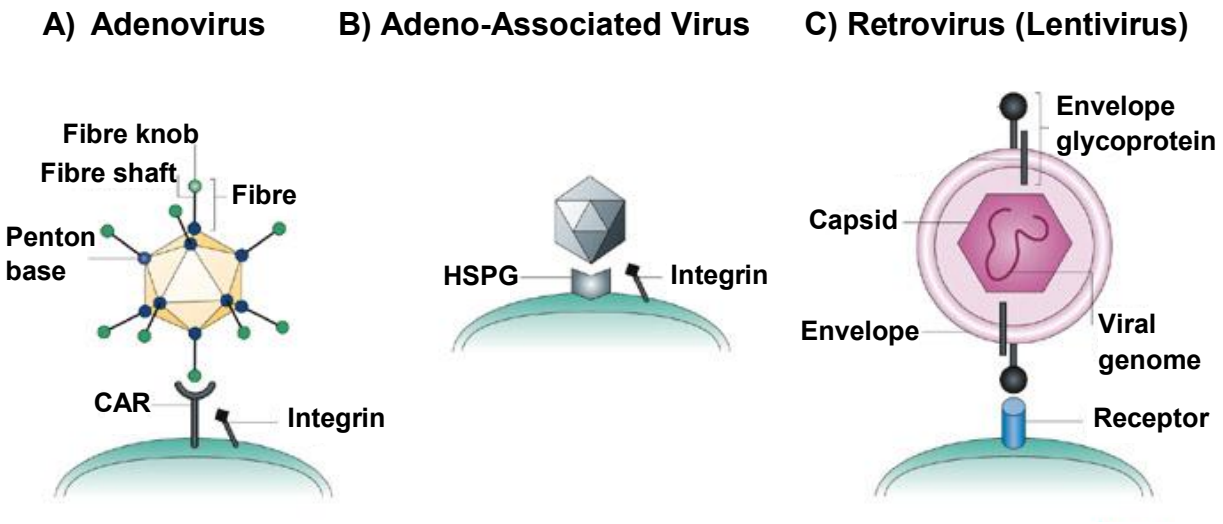

Figure 1.6.1. Entry mechanisms of viral vectors. **(A)** Ad binds to its receptor CAR through its fibre knob and integrin co-receptors facilitate entry into the cell via endocytosis. **(B)** AAV2 binds to heparan sulphate proteoglycan (HSPG) on the target cell and then to its integrin co-receptor. The virus is internalized via endocytosis. **(C)** Retrovirus (lentivirus): The virus adheres non-specifically to the cell surface, where the viral attachment glycoproteins bind irreversibly to their cognate receptors. Subsequent steps in the viral entry process vary between virus types but always result in release of the viral nucleocapsid into the cytoplasm. Figure adapted from Harrison et al (107).

1.6.1.1 Adenoviral Vectors

Ad is a non-enveloped, icosahedral virus, 60 – 90 nanometer (nm) in diameter with a linear, double-stranded DNA genome and total molecular weight of 150 kilo dalton (kDa) (108). Ad was isolated from adenoid tissue in 1953, however the use of Ad for gene transfer into islet cells was first demonstrated in the early 1990s (109, 110). Studies have shown that Ad can transduce intact pancreatic islets and fetal insulin-secreting islet cell clusters (109, 111-114). However, Barbu et al (114) have demonstrated that Ad-mediated transduction is limited to the islet periphery and as such transduction effiency is approximately 30% of the total islet mass.

Ad requires the Coxsackie Adenovirus Receptor (CAR) and an integrin co-receptor for infection (115, 116). CAR has been identified on murine islets and β-cell lines, which may explain the relatively high efficacy of Ad transduction in islets (117). Successful Ad infection of rodent pancreatic islets has been described by many research groups (109, 112, 113, 118, 119). Safety studies in human islets demonstrated that Ad infection does not diminish β-cell viability or function *in vitro* (112, 118, 119).

A major advantage of Ad vectors is that they can infect dividing and non-dividing cells, unlike lentiviral vectors, which integrate into the genome and as such are utilized for chronic transgene expression (120). The Ad genome is extra chromosomal, which significantly minimizes the risk of insertional mutagenesis that can result from insertion of exogenous DNA into the genome (115). Moreover, Ad vectors can be produced to high titer viral stocks (10^{12} – 10^{13} virus particles/ml) and offer high transduction efficiency of target cells (121, 122).

Ex vivo Ad gene therapy provides a significant advantage over *in vivo* gene therapy, which is often associated with induction of host immune response when using high viral load. This advantage also exists within an islet transplant setting, where the islets are transduced *in vitro* and washed of any unbound viral particles prior to transplantation. This important step reduces the risk of vector dissemination and off target infection of organ systems (98).

One of the first barriers that gene therapy vectors have to circumvent *in vivo* is the immune response, in particular the complement system and other components of innate immunity as well as pre existing antibody-mediated immunity. An extreme example of immune response to viral vectors occurred in a patient with ornithine transcarbamylase deficiency who died of systemic inflammatory response syndrome after hepatic arterial injection of an Ad vector (123).The toxicity associated with the use of Ad is complex as it is dose dependent, related to the route of administration, dependent on the tissue and cell type targeted and varies with

species (124). One of the most important factors of toxicity is the ability of Ad to trigger both the innate and adaptive immune responses, which reduces the efficacy of gene transfer (125, 126). However, the engineering of new generation 'gutted' or 'helper-dependent' vectors which are stripped of all viral genes, decreases the possibility of vector-mediated immune activation (98).

1.6.1.2 Adeno-Associated Viral Vectors

AAV are small, non-enveloped single-stranded DNA viruses. AAV fulfills many of the requirements of an ideal vector for gene transfer, it is non pathogenic, non toxic, poorly immunogenic, can infect both dividing and non dividing cells and can persist in the infected cells as an integrated provirus or in episomal forms, resulting in stable long term gene expression (127, 128). However, a major restriction to the use of AAV is their low packaging capacity of 4.5 kb (smaller then Ad) which limits the potential for inserting large or multiple transgenes (129). It is possible to package the AAV2 derived vector genome in capsids from different AAV serotypes, increasing the diversity of reachable target tissues and the viral transduction efficiency (130, 131). AAV2 is the most widely studied AAV serotype. The ability of AAV2 to transduce a given cell type depends on the presence of membrane-associated heparan sulphate proteoglycan (HSPG) receptors (132) and co-receptors including αvβ5 integrin (116, 133, 134).

Transduction of islets with AAV has been shown by a number of groups (135-139). Wang and colleagues (135) revealed distinct AAV islet transduction efficiency and gene transfer patterns between different vector serotypes and administration routes. Local intra pancreatic ductal administration of AAV6 showed the most efficient transduction efficiency in β-cells. Intraductal and intraperitoneal administration of AAV8 revealed transduction of both exocrine acinar cells and endocrine β-cells. The transduction efficiency of AAV8 is attributable to the distinct properties of this viral serotype, including its receptor, laminin, which is highly expressed in the pancreas and facilitates viral entry into the pancreatic cells (136).

AAV vectors have been identified as the current most promising gene delivery candidate for serious non-lethal diseases that need life-long treatment (140). As such, AAV has been tested in over 60 clinical trials for the treatment of Alzheimer's disease, arthritis, cystic fibrosis, hemophilia B, HIV infection, parkinson's disease, muscular dystrophy, and malignant melanoma, among others (Gene Therapy Clinical Trials Worldwide Gene Therapy Clinical Trials Worldwide, provided by the Journal of Gene Medicine).

1.6.1.3 Herpes Simplex Viral Vectors

Herpes Simplex Virus (HSV) is a double-stranded linear DNA virus, 152 kb in size with a virion structure consisting of an envelope, tegument, capsid and core. HSV-1 forms part of the larger *Herpesviridae* family, and is the most frequently used herpes virus for gene transfer. HSV-1 infection is common in the general population, manifesting itself as cold-sores however in rare cases it can cause encephalitis (141).

HSV-1 possesses a broad host range with the ability to infect many cell types. In particular, HSV-1 vectors provide efficient transduction and gene expression within the nervous system (142-144). Therefore, most of the research utilizing HSV-1 vectors has focused on therapies to target neurological diseases. The large genome of HSV-1 (≥30 kb pairs) allows the vector to accommodate large or multiple transgenes or regions including regulatory elements or promoters (145). In addition, the HSV-1 vector remains as an extrachromosomal episome, which decreases the likelihood of insertional mutagenesis within the host's genome (146). These properties combined with the ability of HSV-1 to infect non-dividing cells makes it a suitable vector system for use in islet gene therapy (145).

To date, there have been a limited number of studies demonstrating the ability of HSV-1 to infect pancreatic islets (147, 148). Liu and colleagues (147) have shown that murine islets and a β-cell line were efficiently transduced by a HSV vector, and that cytokine-mediated β-cell apoptosis was blocked by transduction with an anti-apoptotic B-cell lymphoma 2 (Bcl-2) expressing HSV-1 vector.

1.6.1.4 Retroviral vectors

The first human gene therapy clinical trial was based on a retroviral vector, for correction of adenosine deaminase deficiency. In this study, both integrated retroviral vector and adenosine deaminase gene expression persisted for several years (149). Retroviral vectors possess many advantages over other viral vectors for long-term treatment or correction of gene defects. Retroviral vectors allow for an insert size of up to 7 kb pairs and they integrate into the target cell genome, resulting in sustained gene expression.

There are over 250 currently approved retroviral gene therapy clinical trials, accounting for nearly 30% of the total clinical trials approved worldwide (150). However, retroviral vectors are unable to infect non-dividing cells, such as islets, severely limiting their potential for use in islet gene therapy. Lentiviruses however are a subset of retroviruses with the ability to infect non-dividing cells and are therefore a logical retroviral candidate for use in islet gene therapy (151-153). The first successful transduction of adult human pancreatic β-cells was performed using lentivirus, by Ju and colleagues in 1998 (106). One study comparing infection of intact islets found that while no infection was achieved using other retroviral vectors, up to 25% of the β-cells could be infected with lentivirus (111).

Lentiviral vectors have been shown to efficiently transduce dispersed islets (106), monolayer cultures of islets (111) and intact islets (105, 154-157) from different species including human. Giannoukakis and colleagues (105) demonstrated the ability of lentiviral vectors to transduce islets at a comparable efficiency to Ad without the drawbacks of immunogenicity. Furthermore, lentiviral vectors can efficiently transduce whole islets (104) and lentivirus transduced rat islets display no changes in islet morphology or function (158), further supporting their use in islet gene therapy.

1.6.2 Non-viral mediated gene transfer to pancreatic islets

Various non-viral islet transduction strategies such as bacterial plasmids, cationic lipid- and polymer-based carriers, gene gun technology and calcium phosphate precipitation have been considered (159-167), with low transduction efficiency being the major obstacle reported to date. Electroporation creates permeable membranes for gene transfer by applying high voltages to cells. However, Electroporation is only associated with gene transfer efficiencies in the order of 10-20% in isolated islets, which might prove inadequate for preventing apoptosis (168). To ensure efficient transduction, pancreatic islets would need to be dissociated into single cells, a process which may render them non-functional without the maintenance of their morphology (169).

A number of research groups (165, 170, 171) have investigated the use of protein transduction technology in islet gene therapy. This is a novel technique which allows delivery of specific proteins or peptides fused to small cell-penetrating peptides known as protein transduction domains to cells or tissues (172). Delivery of a c-Jun N-terminal kinase inhibitory peptide via this system prevented islet apoptosis following isolation and improved islet graft function.

Furthermore, an NF-κB inhibitor infused into the mouse pancreatic duct prior to isolation yielded islets with enhanced viability (173).

Non-viral vectors offer several advantages over their viral vector counterparts, including high clinical safety, no immunogenicity and ease of production. Despite this, non-viral vectors provide low islet transduction efficiency, owing to both the large size of the islets (167) and the diffusive barrier created by the islet nuclear membrane (166). In addition, non-viral vectors offer only transient gene expression and require high doses (160, 163, 164) when compared to viral vectors. At present, despite extensive investigation of non-viral approaches for use in islet gene therapy, no studies have progressed to clinical trials.

1.7 Alternative strategies towards islet survival

The portal vein is the current site for clinical islet transplantation, a process in which the isolated islets are implanted within the well-perfused liver sinuses of a diabetic patient (167). However, the transplantation of islets at this intravascular site can lead to diminished islet function and survival in the early post-transplant period (see section **1.5**). To this end, a variety of alternative islet transplant sites, such as the pancreas, gastrointestinal tract , muscle, omentum, bone marrow, kidney capsule, peritoneum, anterior chamber of the eye, thymus, cerebral ventricles and spleen have been investigated as to identify the ideal anatomical location to promote long-term islet survival (174).

Of those studies, Carlsson et al (85) syngenically transplanted islets to the kidney cortex, liver and spleen of diabetic rats but found that the oxygen tension of the grafts did not differ among the transplantation sites. Interestingly, the partial pressure of oxygen levels was decreased at all three transplant sites, compared to native islets, suggesting insufficient oxygenation of transplanted islets, irrespective of graft location. The major advantage of the omentum as an islet transplant site is the ease of access to the transplanted islets should the need for biopsy arise and the lack of exposure to elevated levels of immunosupression (175). Moreover, the omentum offers drainage of produced insulin into the portal vein for direct utilization in the liver (176).

Extravascular transplantation of islets by methods such as encapsulation can prevent immunogenic reactions and abate the thrombotic and inflammatory events elicited when islets are transplanted via the hepatic portal vein (177). Macro and microencapsulation are two approaches that have been introduced to prevent immune mediated islet destruction and overcome the shortfalls associated with current clinical islet transplant practice. Macroencapsulation involves the encapsulation of large numbers of islets together in one

device or capsule consisting of a semi-permeable membrane, while microencapsulation can be defined as the encapsulation of single or small groups of islets. The major distinction between intravascular and extravascular islet transplantation is that the encapsulated islets do not require anastomosis to host vasculature and they can be implanted with minimal surgical risks to different sites such as the peritoneal cavity, subcutaneously or under the kidney capsule (178).

Meyer et al (179) demonstrated long-term normoglycemia without immunosupression following the transplantation of porcine islets microencapsulated with highly purified barium-alginate under the kidney capsule or into the peritoneal cavity of chemically diabetic Wistar rats. Others (180) have demonstrated the utility of alginate macroencapsulated porcine islets to normalize the diabetic state of non-immunosupressed primates for up to six months. Calafiore and colleagues (181) successfully transplanted microencapsulated human islets into the central abdominal region of non-immunosupressed T1D patients, leading to an improvement in glycated haemoglobin levels and frequency of hypoglycaemic episodes.

Despite these promising results, xenotransplantation of porcine islets into humans is complicated by safety issues related to xenosis and xenorejection, however the former can be controlled by selection of a disease-free source herd (182). Moreover, encapsulated islets are disadvantaged by their inability to revascularize following transplantation, exacerbating islet hypoxia and subsequent β-cell death (183, 184). In addition, transplanted islets remain vulnerable to highly toxic chemokines, cytokines and nitric oxide (NO), which are small enough to pass through the capsule membrane (185-187).

1.8 Gene therapy towards islet survival

There are a number of cellular processes that may be targeted by gene therapy to improve the outcome of islet transplantation. Effective therapy may result from the over expression of an active protein, or the inhibition of a deleterious gene. Genes that are likely to be useful for islet transplantation fall into three main categories: immunomodulatory, anti-apoptotic and angiogenic (summarised in **Figure 1.8**). A number of studies have investigated the potential of gene therapy for islet transplantation in animal models (**Table 1.8**).

The clinical success of islet transplantation is currently limited by the substantial islet cell death and dysfunction occurring within the first few hours and days after islet transplantation (188). The major factors contributing to islet apoptosis include lack of islet oxygenation and re-innervation following transplantation, disruption of the islet extracellular matrix, a highly toxic pro-inflammatory cytokine storm, recurrence of anti-islet autoimmunity and allogeneic recognition (189-193). The outcomes of clinical islet transplantation could be improved by inhibiting the apoptotic damage sustained by pancreatic islets immediately after their transplantation. To this end, islet gene transfer using viral vectors to deliver an anti-apoptotic gene to the islets prior to their transplantation provides a method to improve islet viability and function.

The clinical protocol of most transplant centers involves 24 – 48 h culture of isolated human islet preparations before transplantation (194-196). Therefore, this gives an excellent 'window of opportunity' to transduce islets with viral vectors expressing a therapeutic gene, prior to their transplantation. Depending on the therapeutic strategy designed to improve islet engraftment, transient or long-term transgene expression will be required (97). The duration of gene expression is mainly dependent on transgene DNA stability and promoter choice. In general, episomal vector systems such as Ad are associated with transient DNA stability. Whereas integrating vectors such as AAV are associated with persistent transgene DNA expression (97). To achieve maximal benefit, the anti-apoptotic gene expression would be required during the initial period of islet engraftment, a process that takes approximately 14 days. This provides additional safety benefit, by circumventing the concerns of long-term apoptosis inhibition, on increased risk of malignancy or systemic toxicity.

Figure 1.8. Gene transfer strategies to improve islet transplantation. Three areas of islet cell biology that are currently being targeted by gene therapy are depicted. Immunomodulatory strategies (upper left panel) include co-stimulation blockade with CTLA4Ig and production of immunomodulatory interleukin-10 (IL-10) and interleukin-4 (IL-4). Anti-apoptotic approaches (upper right panel) target extrinsic (via stimulation of death receptors) and intrinsic (release of apoptotic factors by mitochondria) apoptosis pathways in the β-cell. Bcl-XL and Bcl-2 (blue box) block pro-apoptotic proteins while XIAP (white box) directly inhibits caspases 3 and 9. Angiogenic (lower panel) factors VEGF, HGF, FGF and matrix metalloproteinases are induced during hypoxia and can be therapeutically overexpressed to enhance revascularization. Antisense blockade of angiostatic TSP-1 (white hexagons) improves the potency of proangiogenic factors. Figure represents a whole islet, with constituent α- (blue; glucagon-producing), β- (green; insulin-producing) and PP-(white; pancreatic polypeptide-producing) cells depicted in the upper left panel. Enlarged representations of infiltrating immune cells are shown (APC = antigen presenting cell; Ag = islet-specific antigen). Figure adapted from Hughes et al (96).

Table 1.8. Genes delivered to pancreatic islets using viral vectors

Pathway	Transgene	Vector	Comment
Immunomodulation	CTLA4Ig	Adenovirus	Expression of CTLA4Ig in islets can prolong islet graft survival (197-200).
		Lentivirus	Islets transduced with CTLA4Ig prolong graft survival in a rat to mouse transplantation model (157)
	Interleukin-10	Adeno-associated virus	IL-4 transduced islets resulted in impaired metabolic function in recipient mice and normoglycaemia in only 1/7 mice (201). Viral IL-10 introduced systemically sustained suppression of autoimmune responses and prolonged islet allograft survival (202)
	Interleukin-4	Adeno-associated virus	AAV-8 mediated IL-4 gene transfer to islets prevented the onset of diabetes in NOD mice (203)
	CTLA4Ig/CD40Ig	Adenovirus	Results in simultaneous blockade of co-stimulation pathways (204)
Anti-Apoptotic	Bcl-2	Adenovirus	Over expression of Bcl-2 in islet cells failed to prevent cytokine induced toxicity (205) and reduce inflammation in porcine islets (206)
		Lentivirus	Bcl-2 transduction of pancreatic β-cell line provided protection against apoptosis induced by various stimuli including hypoxia and pro-inflammatory cytokines and corrected hyperglycaemia for several months when transplanted under the kidney capsule of diabetic C3H mice (205)
		Herpes Simplex Virus-1	Cytokine-mediated β-cell apoptosis was blocked by transduction with an Bcl-2 expressing HSV-1 vector (147)
	Bcl-XL	Adenovirus	Bcl-XL transduction of a rat insulinoma cell line blocked cytokine induced apoptosis (207)
	XIAP	Adenovirus	Adenoviral-XIAP transduced βTC-Tet cells and human islets are highly resistant to hypoxia and cytokine induced apoptosis *in vitro* and βTC-Tet cells transplanted into SCID mice successfully reverse diabetes in 3 days compared to 21 days for control cells (208-210)

Angiogenic	VEGF	Adenovirus	Rat islet grafts with elevated VEGF production exhibited significantly increased microvasculature, insulin content and reversed hyperglycaemia in diabetic mice (211)
	HGF	Adenovirus	Co-expression of hHGF and hIL-1Ra led to significant decrease in caspase-3 induced in human islets by cytokine challenge *in vitro*. Transduction of human islets improved the outcome of islet transplantation (212). Pre-transplant islet gene therapy with HGF markedly improved islet transplant outcomes even in the setting of immunosuppressant-induced insulin resistance and β-cell toxicity (213)

1.9 Insulin-like growth factor-axis

The Insulin-like Growth Factor (IGF) family consists of two IGF peptides (IGF-I and IGF-II), three cell surface receptors (IGF-1R, IGF-IIR and insulin receptor (IR)), six binding proteins (IGFBP-1 – 6) and a glycoprotein termed the acid-labile subunit (ALS). The IGFBPs regulate the actions of IGF-I and IGF-II by inhibiting or promoting their interactions with cell surface membrane receptors. The acid labile subunit protein is essential for maintaining the integrity of the circulating IGF/IGFBP system (214).

The IGFs were first discovered in 1975 when Salmon et al (215) identified a growth hormone dependent serum factor, termed 'sulphation factor activity (SFA)' that stimulated cartilage sulphation. Several laboratories also observed the ability of SFA to induce DNA replication, proteoglycan synthesis, glucosamine synthesis, protein synthesis and protein accumulation (216). Amino acid sequencing of SFA revealed the presence of two peptides, these were subsequently renamed to IGF-I and IGF-II because of their structural and functional homology with insulin (217).

IGF-I and IGF-II are single chain polypeptides of approximately 7.5 kDa, which share 63% structural homology with each other and 50% with insulin (218). Most IGF-I and IGF-II is produced locally within tissues where either peptide exerts their actions (219), with the majority of circulating IGF-II produced in the liver. The IGFs exert a broad range of metabolic, mitogenic and anti-apoptotic functions on cells *in vitro* and *in vivo*, mediated via association with the type I IGF receptor (IGF-1R) **(Figure 1.9)**.

Figure 1.9. Schematic representation of the IGF axis. IGFs are present in the circulation complexed to IGFBPs and/or a glycoprotein termed the acid-labile subunit (ALS). Cell response to IGFs depends on IGFBPs, which act to modulate the effects of IGF actions **(A)**. These binding proteins undergo proteolysis by specific proteases to release free IGF **(B)** which can interact with surface receptors to exert cell growth responses and metabolic functions **(C)**. This figure was adapted from Bayes-Genis et al (220).

1.9.1 Insulin-like Growth Factor-I

IGF-I, also called Somatomedin C, is encoded by the IGF-I gene, which is located on chromosome 12. The IGF-I peptide is 70 amino acids in length and is a integral growth factor involved in embryonic and postnatal growth (221). IGF-I plays a pivotal role in brain development (222) and a preliminary link exists between increased serum levels of IGF-I and higher IQ in normal children (223). IGF-I is a survival factor for sensory and motor neurons (224) and has the potential to influence recovery from stroke through its effects on proliferation and differentiation (225).

IGF-I binds to two receptors, the IGF-1R and the IR to mediate its effects. The physiological roles of IGF-I are considered to be mediated via the IGF-1R, which binds IGF-I at a significantly higher affinity than the IR. Moreover, the biological actions of IGF-I are regulated through association with high affinity IGFBPs, with IGFBP-3 being the predominant serum IGF binding protein (226).

1.9.2 Insulin-like growth factor-II

IGF-II is a potent growth factor made up of 67 amino acids with a molecular weight of 7.5 kDa. The IGF-II gene is transcribed from four promoters (p1 – p4), located on chromosome 11. IGF-II expression occurs from the paternal allele only. Loss of imprinting leads to Beckwith-Wiedemann syndrome whereby excess IGF-II is associated with foetal overgrowth (227).

The IGF-II gene consists of nine exons, of which exons 7, 8 and 9 encode a single transcript, which is translated into proIGF-II, a 156 amino acid protein expressed during foetal development (228). ProIGF-II becomes glycosylated and undergoes cleavage to yield mature IGF-II. IGF-II exerts the majority of its effects via the IGF-1R, including cell proliferation, survival, differentiation and migration (229). IGF-II is a major β-cell growth factor, as transgenic mice over expressing IGF-II have a 5-fold increase in mean islet size at birth, without an increase in islet number (230). During neonatal development, IGF-II knock out animals are smaller than control animals, but subsequent post-natal growth proceeds at a normal rate (231). Similarly, IGF-1R knockout mice die at birth with organ hypoplasia, delayed bone development and abnormal central nervous system development (231).

IGF-II has been shown to promote pancreatic β-cell survival (232) and proliferation in a growth-arrested mouse β-cell line (βTC-tet) (233). IGF-II up-regulates hypoxia-induced vascular endothelial growth factor (VEGF) production in hepatocellular carcinoma cells,

suggesting it may also function as an angiogenic factor (234). Human and rat pancreatic islets are capable of secreting IGF-II (235, 236) and isolated α and β-cells express the IGF-1R (237). IGF-II inhibits apoptosis acting via the IGF-1R to stimulate the anti-apoptotic molecules Bcl-2 and Bcl-XL (238).

1.9.3 Insulin-like growth factor-II expression

IGF-II is expressed at high levels during embryonic development, but decreases in mice and rats post-natally. In contrast to this, in humans IGF-II remains the most abundant IGF in circulation throughout life (239). The expression of which is detected in many tissues including the central nervous system and adrenal medulla, pancreas, purified β-cells and insulin-producing cell lines (235, 240-246). The post-natal decline in IGF-II expression may be a result of differences in the IGF-II gene promoter structure between humans and rodents (247).

The major role of IGF-II during embryonic development is the regulation of islet growth and differentiation (248). IGF-II is more highly expressed than IGF-I during development in rodents, ruminants and humans (249, 250), suggesting that it may be a more important IGF during development (251).

1.9.4 Insulin-like growth factor-II signaling

The phosphoinositide-3-kinase (PI3K)/Akt pathway plays a central role in preventing apoptotic cell death. Akt is activated following the binding of specific PI3K-generated phospholipids to Akt (252). Upon activation, Akt induces phosphorylation of BAD, a pro-apoptotic member of the Bcl-2 family of proteins. When BAD is not phosphorylated, it will inhibit Bcl-2 and various members of the Bcl-2 family by direct binding (253). Phosphorylation of BAD changes its affinity for Bcl-2 molecules, and localizes BAD to the cytosol where its pro-apoptotic activity is neutralized.

In the context of IGF-II function, binding of IGF-II to the IGF-1R leads to phosphorylation of insulin receptor substrate 2 (IRS-2), which recruits and activates down stream signaling molecules PI3K, phospho-inositide-dependent protein kinase (PDK), Akt, forkhead transcription factor (FOXO), glycogen synthase kinase 3β (GSK-3β), bcl-associated death promoter (BAD) and mammalian target of rapamycin (mTOR), among others (219). These pathways mediate gene expression, glucose metabolism, cell survival and growth signals **(Figure 1.9.4)** (219).

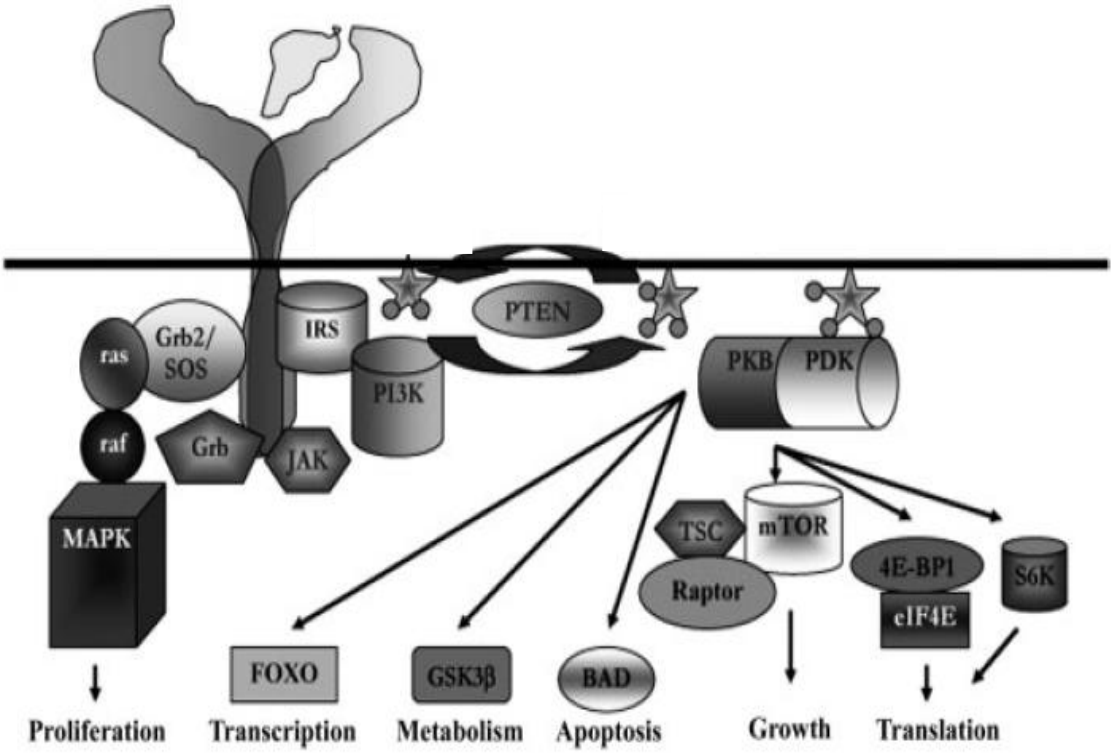

Figure 1.9.4 Intra-cellular components of the insulin-like growth factor system. Interactions with insulin receptor substrates (IRS) leads to activation of phospho-inositide-dependent protein kinase (PDK), protein kinase B (PKB), and downstream substrates that control transcription (forkhead transcription factors (FOXO)), metabolism (glycogen synthase kinase 3β (GSK-3β)), apoptosis (bcl-associated death promoter (BAD)), cell growth and translation (mammalian target of rapamycin (mTOR), tuberous sclerosis gene product (TSC), Raptor, eukaryotic initiation factor (4E - eIF4E) and its binding protein 4E-BP1 and ribososmal protein S6 kinase (p70S6K)). Via similar protein–receptor interactions, activation of proliferation is mediated via the mitogen activated kinase family (MAPK) pathway. Figure adapted from Foulstone et al (254).

1.9.5 Insulin-like growth factor receptors

IGF-I and IGF-II may bind to multiple signaling receptors, the IGF-1R, IGF-IIR, insulin receptor (IR) and IGF-1R/IR hybrid receptor, to mediate their cellular effects. The IGF-1R/IR hybrid receptor controls biological effects similar to those of the IGF-1R. The IGF-1R exhibits tyrosine kinase activity and can bind at least three different ligands, IGF-I, IGF-II and insulin (weakly). The IGF-1R is a dimer, which consists of an extracellular ligand binding α subunit and a transmembrane β subunit, linked by disulfide bonds (255). The IR has low affinity binding for IGFs, it binds IGF-II with an affinity $1/10^{th}$ that of insulin (256).

The IGF-IIR (also called the Mannose-6-phosphate receptor) is a single transmembrane domain glycoprotein (257) that can only bind IGF-II, lysosomal enzymes or Mannose-6-phosphate. The IGF-IIR functions to regulate the bioavailability and activity of IGF-II (258) and does not possess any intrinsic signaling capability. The IGF-IIR binds IGF-II with 700 fold greater affinity then IGF-1R (216) and internalizes IGF-II for degradation within the pre-lysosomal compartment so as to control the extracellular IGF-II concentration (247). IGF-IIR mutants have increased circulating and serum levels of IGF-II, increased birth weight and organomegaly (259).

Most of the biological actions of IGF-II, including its anti-apoptotic effects are mediated via the IGF-1R (260, 261). All endocrine pancreas cell types express both the IGF-1R and IGF-IIR (237, 262), providing support for an IGF-II mediated anti-apoptotic strategy to promote islet survival post-transplantation.

1.9.6 Insulin-like growth factor binding proteins

The insulin-like growth factor binding proteins (IGFBPs) are a family of six proteins that bind to IGF-I and IGF-II with high-affinity. The IGFBPs circulate in the blood complexed to IGF-I or IGF-II and in doing so, act to regulate their action, bioavailability and tissue distribution (216). Approximately 99% of IGF-I and IGF-II is bound to binding proteins, of which IGFBP-3 is the most abundant circulatory form (247). IGFBPs can either inhibit or potentiate IGF action, achieved by controlling the interactions of the IGFs with their cognate receptors (263).

1.10 Apoptosis

Apoptosis, also called programmed cell death, refers to a set of events within multicellular organisms which leads to the breakdown of chromosomal DNA and the cessation of metabolic activity (264). Apoptosis can occur as a defence mechanism such as in immune reactions or when cells are damaged by disease or toxic agents (265). Apoptosis was first described by Karl Vogt in 1842 during normal development in toads and again in 1885 by Walther Flemming, however it was initially referred to as chromatolysis to describe dying cells whose chromatin had disintegrated. Today, DNA fragmentation is one of the hallmark characteristics of apoptosis (266).

1.10.1 Necrosis

Apoptosis and necrosis are two distinct forms of cell death, the latter begining only and exclusively when the cell dies and is an irreversible process (267). Necrosis is often called 'accidental' cell death, as it usually occurs as a result of unintentional traumatic injury, which can include thermal, chemical or anoxic inducers (268). The injury sustained by the cell causes it to swell, rupture and release its intracellular contents, promoting inflammation and damage to surrounding tissue.

Cell swelling is a defining feature of necrosis, in contrast to apoptosis which is associated with cell shrinkage (268). The underlying mechanism promoting cell swelling may result from ATP unavailability, which leads to sodium accumulation in the cell, creating an uneven osmotic gradient with concomitant cell swelling and rupture (269, 270). As with apoptosis, phagocytosis of necrotic cells occurs by exposure of a phosphatidyl serine (PS) signal. However, unlike apoptotic cells who externalise PS to the outer leaflet of the cell membrane to signal their removal, necrotic cells display PS only after the cell membrane has ruptured (271).

1.10.2 Morphology of Apoptosis

Early morphological studies described the visual changes of cells undergoing apoptosis both *in vitro* and *in vivo*. These changes together with the 'disappearance' of cells were historically the only indication of cell death (272). During apoptosis, a dying cell starts to sever its attachments to other cells and the extracellular matrix and the cell begins to round up and show protrusions from the plasma membrane, commonly referred to as 'blebs' (273). Cells dying by apoptosis in most situations undergo similar morphological changes, namely cell shrinkage and pyknosis. Following cell shrinkage, the cells are smaller in size, the cytoplasm is dense and the organelles are more tightly packed. Pyknosis is the result of chromatin condensation and this is the most characteristic feature of apoptosis (274). Once the chromatin condenses, the cell will break into small fragments called apoptotic bodies during a process called "budding" (275). These bodies are subsequently phagocytosed by macrophages, parenchymal cells or neoplastic cells and degraded within phagolysosomes (274) **(Figure 1.10.2)**.

1.10.3 Mechanisms of Apoptosis

Apoptosis is caused by caspases, also known as cysteine aspartyl-specific proteases, which reside within a cell as inactive procaspases (zymogens), but can be phosphorylated to assume an active state (276). Once activated, caspases activate other caspases leading to amplification of the apoptotic signaling pathway followed by cell death. There are fourteen members of the caspase family (caspase1 – 14), ten of which have been classified as initiator, effector or executioner caspases (274). Initiator caspases act upstream of executioner caspases and cleave other substrates within the cell to trigger apoptosis.

Three pathways for activating caspases exist in mammalian cells. These pathways are described as the extrinsic or death receptor pathway, the intrinsic or mitochondrial pathway and the perforin/granzyme B pathway **(Figure 1.9.3)**. The extrinsic, intrinsic and granzyme B pathways converge on the same execution pathway, which is activated by the cleavage of caspase-3 and results in the morphological consequences of apoptosis.

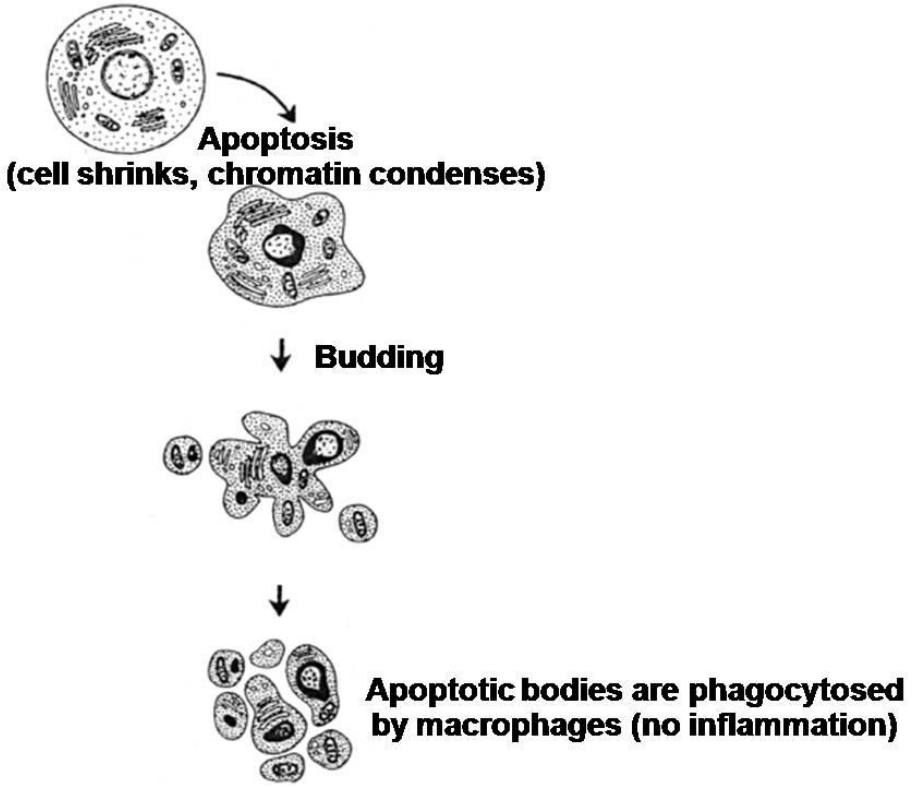

Figure 1.10.2. Morphological changes during apoptosis. Apoptosis is characterised by cell shrinkage and chromatin condensation. Apoptotic cells will undergo 'budding' whereby they divide into apoptotic bodies. The apoptotic bodies are phagocytosed by macrophages and neighbouring cells, and subsequently degraded within phagolysosomes. Figure was adapted from Van Cruchten et al (277).

Figure 1.10.3. Caspase activation pathways. Caspase activation by the extrinsic pathway **(1)** involves the binding of extracellular ligands to transmembrane death receptors. Engagement of death receptors with their cognate ligands provokes the recruitment of FADD, which in turn promotes the activation of caspase-8. Caspase-8 activates caspase-3 and caspase-7, which culminates in cell death. In some situations, extrinsic death signals can crosstalk with the intrinsic pathway to promote cytochrome c release and assembly of the apoptosome. In the intrinsic pathway **(2)** noxious stimuli provoke cell stress leading to activation of one or more members of the BH3-only protein family, which promotes the assembly of BAK–BAX oligomers. These oligomers permit the release of cytochrome c into the cytosol. The granzyme B/perforin apoptosis pathway **(3)** involves the delivery of granzyme B and perforin into the target cell through granules that are released from cytotoxic T lymphocytes or natural killer cells. Granzyme B can process BID as well as caspase-3 and -7 to initiate apoptosis. Figure adapted from Taylor et al (278).

1.10.3.1 Extrinsic (death receptor) pathway

Initiation of apoptosis via the extrinsic signaling pathway has been described using two models: the tumour necrosis factor (TNF) model and the Fas-Fas ligand (FasL)-mediated model. Both involve stimulation of transmembrane death receptors that are members of the TNF receptor gene superfamily (279).

TNF is a major mediator of apoptosis as well as inducer of inflammation and immunity. TNF signals through two cell surface receptors, TNF-R1 and TNF-R2 (280). When TNF binds to TNF-R1, this is recognized by the adaptor protein TNF receptor-associated death domain (TRADD), which recruits Fas-associated death domain (FADD), receptor-interacting protein (RIP) and TNF-R-associated factor 2 (TRAF2) (281). FADD recruits caspase-8 to the TNF-R1 complex, where it becomes activated, triggering the execution phase of apoptosis (280).

Within the Fas pathway, the Fas receptor binds FasL causing formation of the death-inducing signaling complex (DISC) which contains FADD, activated caspase-8 and caspase-10 (282). Active caspase-8 is an initiator caspases, which activates downstream caspases (3 and 7), committing the cell to apoptosis.

1.10.3.2 Intrinsic (mitochondrial) pathway

The intrinsic apoptosis pathway is triggered by cellular stress caused by growth factor withdrawal, ultraviolet radiation, DNA damage, toxins, viral infections and heat shock, among others (283). The mitochondrial pathway begins with the permeabilization of the mitochondrial outer membrane by pro-apoptotic molecules of the Bcl-2 family, resulting in release of cytochrome c which binds to apoptosis-protease activating factor-1 (Apaf-1) (284).

Pro-apoptotic molecules BAX, BID and BAK promote the release of cytochrome c and the intramembrane contents from the mitochondria (285). Cytosolic cytochrome c forms an essential part of the apoptosome, which is composed of cytochrome c, Apaf-1 and caspase-9 (286). The clustering of caspase-9 in this manner leads to caspase-9 activation and this in turn recruits and activates the executioner caspase-3 and other death effector caspases which ultimately culminates in apoptotic cell death.

1.10.3.3 Perforin/Granzyme Pathway

Perforin/granzyme-induced apoptosis is the main pathway used by cytotoxic lymphocytes ($CD8^+$ T cells) to eliminate virus-infected or tumour cells (287). $CD8^+$ T cells kill target cells through granule-mediated cytotoxicity, a process in which cytolytic granules containing the pore-forming molecule perforin are released following target cell recognition (287, 288).

Granzyme A and granzyme B are the most important components within this cascade (289). Granzyme B activates caspase-3 and the pro-apoptotic molecule Bid, which leads to cytochrome c release (290). In addition, activation of caspase-3 leads to initiation of the execution phase of apoptosis. This method of granzyme B-induced cytotoxicity serves as a control mechanism for T cell expansion of type 2 helper T cells (291). Granzyme A also plays a pivotal role in T cell induced apoptosis, its activity resulting in apoptotic DNA degradation (274).

1.10.3.4 Execution Pathway

The extrinsic, intrinsic and granzyme B signaling pathways converge to a final common execution pathway, to induce the activation of caspases. Caspase-3, caspase-6 and caspase-7 function as executioner caspases which are responsible for the controlled destruction of the cell during apoptosis, whereas caspase-8, caspase-9 and caspase-10 function as initiator caspases to activate the executioner caspases, leading to the collapse and death of the cell (292).

Caspase 3 is encoded by the CASP3 gene, the CASP3 protein is formed from a 32 kDa zymogen that is cleaved into 17 kDa and 12 kDa fragments. The caspase-3 zymogen is a necessary checkpoint in regulation of the apoptotic cascade, because if it became unregulated caspase would kill cells indiscriminately (293). Caspase-3 cleaves gelsolin, an actin binding protein, this results in disruption of the cytoskeleton, intracellular transport, cell division and signal transduction (294).

Phagocytic uptake of apoptotic cells is the final component of apoptosis (274). The apoptotic cell presents a variety of intracellular molecules on the cell surface, one of the most important being PS, which acts a signal for removal of apoptotic cells. PS, is normally located on the internal leaflet of the lipid bilayer, however PS is externalised to the outer leaflet under certain physiological conditions such as during platelet activation and in cells undergoing apoptosis (295-297).

In apoptotic cells, macrophages recognise PS externalised on cells via a specific PS receptor, resulting in engulfment (298, 299). Macrophage mediated uptake of apoptotic cells is a very efficient process, with no release of their cellular contents into the extracellular space. These processes avoid unwanted immune responses such as inflammation that may be generated following membrane breakdown (264).

1.10.4 Apoptosis in Type 1 Diabetes

Apoptosis mediated by the engagement of death receptors with their respective ligands contributes to T1D development (264). A failure in the clearance of cellular contents during apoptosis is suggested to play a role in the pathogenesis of autoimmune diseases, such as systemic lupus erythematosus (300). To this end, a failure in the clearance of apoptotic β-cells may promote adverse immune responses during the process of β-cell destruction (264).

Fas is not expressed on islets of normal subjects, but its expression is up-regulated in patients with recent onset T1D (301, 302) and *in vitro* following islet exposure to pro-inflammatory cytokines IL-1α and IFN-γ (301-303). Pro-inflammatory cytokines released by infiltrating macrophages and autoreactive $CD4^+$ and $CD8^+$ T cells drive β-cells to produce increased levels of iNOS, which up-regulates their Fas expression (303). Other apoptotic stimuli are involved in the development of T1D, including perforin and granzymes secreted from $CD8^+$ T cells (304). Perforin is required for the release of cytolytic granule contents from the cytotoxic T lymphocyte and subsequent target cell apoptosis (305).

1.10.5 Apoptosis in islet transplantation

The clinical applicability of human islet transplantation is currently limited to only a small sub-set of diabetic patients, specifically, those with severe or uncontrolled diabetes symptoms such as hypoglycemia unawareness. The success of islet transplantation is currently limited by technical, biological and immunological obstacles (306). In the immediate post-transplant period between 50 – 70% of islets are lost to apoptosis and necrosis (307). Before and during isolation, islets are exposed to a number of stresses that can lead to apoptosis and in the long term, graft failure. These include exposure to drugs and hypoxia in the donor before harvest of the pancreas and enzymatic and mechanical stress placed on the islets during their detachment from surrounding exocrine tissue (308).

Islets experience IBMIR that involves activation of coagulation pathways and complement and infiltration of pro-inflammatory cytokines, such as Interleukin-1β (IL-1β) and interferon (IFN-γ) following their transplantation (81, 309). Allogeneic rejection of islet grafts involves

activation of the adaptive immune system, in addition perforin and granzyme are primary mediators of β-cell death following transplantation (310). Despite the use of 'islet-friendly' immunosuppressive drugs that include the glucocorticoid-free regimen of sirolimus (rapamycin), low-dose tacrolimus and anti-IL2 receptor monoclonal antibody dacluzimab (74) the long-term toxicity of these drugs to islets has been observed (311).

1.11 Thesis summary

Successful islet transplantation is currently limited by the loss of up to 70% of the transplanted islet cell mass due to apoptosis and necrosis in the immediate post-transplant period. *Ex vivo* gene therapy provides a promising anti-apoptotic strategy to promote islet survival post-transplantation, by over expression of an anti-apoptotic gene in islets prior to their transplantation. Isolated islets are ideal candidates for local gene therapy, where the tissue is treated *ex vivo* prior to transplantation.

Gene therapy is a powerful therapeutic technique, allowing modulation of the processes that are occurring in the local islet micro environment, thus avoiding potential systemic side effects. With the expanding state of gene vector technology, including the development of AAV tyrosine mutant vectors with improved transduction and safety profiles, further research is required to determine the optimal vector type for use in an islet gene therapy setting. To date, Ad-based vectors have been the most commonly used vectors in preclinical studies however the increased tropism of AAV vectors, makes them another vector type worth investigating for islet transplantation.

Once the appropriate gene therapy vector has been selected, it must be paired with the optimal gene to be delivered. The pro-survival molecule IGF-II represents a promising candidate gene for over expression in pancreatic islets. The ideal anti-apoptotic strategy would improve islet graft survival and thereby improve the long-term function of transplanted islets. Based on this, the work presented in this thesis aimed to investigate the utility of a novel IGF-II gene therapy strategy to promote islet graft survival following transplantation.

1.12 Thesis aims and hypothesis

The specific aims and hypothesis of this thesis are:

1. Aim: To compare the ability of Ad and AAV-based vectors expressing a green fluorescent protein (GFP) reporter gene to efficiently transduce isolated human and rat pancreatic islets **(Chapter 3)**

   Hypothesis: Ad and AAV-based vectors would display differing levels of transduction efficiency in isolated human and rat pancreatic islets, and due to this the optimal vector type for use in an islet gene therapy setting may be identified

2. Aim: To evaluate the Ad-mediated transgenic expression of IGF-II in pancreatic islets and investigate the influence of local Ad human IGF-II over expression on pancreatic islet cell survival *in vitro* **(Chapters 4 and 5)**

   Hypothesis: Ad-IGF-II will efficiently transduce rat pancreatic islets without affecting islet viability or function. The induced expression of human IGF-II will inhibit pro-inflammatory cytokine induced cell death *in vitro*, working via the IGF-1R to mediate its anti-apoptotic effects.

3. Aim: To assess the ability of Ad-IGF-II transduced rat islets to improve islet transplant outcomes in an *in vivo* marginal mass model of islet transplantation **(Chapter 6)**

   Hypothesis: The transplantation of diabetic NOD-SCID mice with Ad-IGF-II transduced islets will lead to improved islet transplant outcomes *in vivo*

CHAPTER 2

MATERIALS AND METHODS

2.1 MATERIALS

2.1.1 Replication deficient Adenoviral-based vectors

Adenoviral-Green Fluorescent Protein (Ad-GFP)

Adenoviral-Insulin like Growth Factor-II (Ad-IGF-II)

A recombinant Ad construct containing GFP was produced previously in the laboratory and purified for use in **Chapter 3 (Appendix A)**. A commercial biotechnology company (Welgen, Inc., USA) was employed to construct, amplify and purify a customized recombinant Ad construct expressing human IGF-II **(Appendix B)**. A similarly generated Ad-GFP construct was used as a control in all Ad-IGF-II transduction experiments **(Chapter(s) 4, 5 and 6)**. Ad-IGF-II and Ad-GFP vectors were supplied as 3 ml aliquots at a viral concentration of $2x10^{10}$ pfu/ml. Gene expression in both Ad vector types was driven by the cytomegalovirus (CMV) promoter.

2.1.2 Adeno-Associated Viral (AAV)-based vectors

AAV2, is a serotype AAV2

AAV2/1, is a pseudtoype AAV2 with type 1 capsid

AAV2/8, is a pseudotype AAV2 with type 8 capsid

AAV8mutY733F, has a tyrosine to phenylalanine mutation in the type 8 capsid

AAV2mutY444F, has a tyrosine to phenylalanine mutation in the type 2 capsid

AAV2muttriple, has three tyrosine to phenylalanine mutations in the type 2 capsid

Highly purified stocks of AAV vectors, containing the GFP gene driven by the chicken β actin promoter were generated and purified as previously described (312). Vectors were titered by quantitative real-time PCR and re-suspended in a balanced salt solution. The AAV vectors were a kind gift from from Professor William Hauswirth, University of Florida, Gainesville, USA.

2.1.3 Animals

Albino Wistar rats were housed in an approved animal house facility (Institute of Medical and Veterinary Services (IMVS), SA Pathology, Adelaide). NOD-SCID mice were housed in a pathogen-free environment. Animals were purchased from the Animal Resources Centre (Perth, Australia) and were used in accordance with and overseen by the animal ethics committees of the University of Adelaide and the IMVS (approval numbers M-2009-089 and 64/10 respectively).

2.1.4 Cytokines

Rat Interleukin-1β (IL-1β) (ProSpec, Israel), 10 µg

Rat Interferon-gamma (IFN-γ) (Sigma, USA), 1 mg

Human IL-1β (ProSpec, Israel), 10 µg

Human IFN-γ (Sigma, USA), 20 µg

2.1.5 Antibodies

2.1.5.1 Primary antibodies

Insulin (polyclonal) (Millipore, USA)

Rabbit polyclonal phospho-Akt (pAkt) (Ser 437) antibody (Cell Signaling Technology, Inc., USA)

Rabbit polyclonal Akt antibody (Cell Signaling Technology, Inc., USA)

Human/Mouse IGF-1R antibody, antigen affinity-purified Polyclonal Goat IgG (R&D Systems, Inc., USA)

Anti-heparan sulphate proteoglycan (perlecan), clone AL76 (Human) (Millipore, USA)

Anti-integrin αvβ5 antibody (Abcam, Australia)

2.1.5.2 Secondary antibodies

Anti-guinea pig rhodamine IgG (Jackson Laboratories, USA)

Anti-rabbit IgG, HRP-linked secondary antibody (Cell Signaling Technology, Inc., USA)

Anti rat IgG Alexa Fluor 488 (Invitrogen, USA)

Goat anti Mouse IgG PE (Millipore, USA)

2.1.6 FACS reagents

FACS lysing solution (BD Bioscience, USA)

Annexin V (Invitrogen, USA)

Annexin V Binding Buffer (Invitrogen, USA)

7-AAD (Invitrogen, USA)

Propidium Iodide (Invitrogen, USA)

Alexa fluor 647 mouse anti-human ki67 (BD Pharmingen)

2.1.7 Molecular biology reagents

Agarose – DNA grade (Progen, Australia)

Custom Oligo-nuceleotides (Geneworks, Australia)

Oligo dT (Amersham, Australia)

RNAsin (Promega, USA)

GelRed™ Nucleic Acid Gel Stain (Biotium, USA)

RNase-Free DNase set (Qiagen, USA)

Nuclease-free Water (Qiagen, USA)

Omniscript® Reverse Transcriptase (Qiagen, USA)

AmpliTaq Gold PCR Master Mix (Applied Biosystems, USA)

DNA Marker: Ready-to-use™ 100 bp DNA Ladder (GenScript, USA)

20X TaqMan® Gene Expression Assay Mix (Applied Biosystems, USA)

2.1.8 Tissue culture reagents

Accutase (Sigma-Aldrich, USA)

RPMI-1640 (Invitrogen, USA)

RPMI-1640 (glucose-free) (Invitrogen, USA)

DMEM + glutamax (Invitrogen, USA)

Albumex 20 (Australian Red Cross, Australia)

CMRL-1066 (Invitrogen, USA)

Foetal Calf Serum (Gibbco, USA)

Penicillin (Gibbco, USA)

Gentamicin (Gibbco, USA)

L-glutamine (Gibbco, USA)

1 x Phosphate Buffered Saline (Gibbco, USA)

1 x Phosphate Buffered Saline, without calcium chloride and magnesium chloride (Gibbco, USA)

1x Hanks Buffered Salt Solution (Invitrogen, USA)

HEPES (Invitrogen, USA)

2.1.9 Kits

Rat Insulin ELISA (Mercodia, Uppsala, Sweden)

Human Insulin ELISA (Mercodia, Uppsala, Sweden)

Rat C-peptide ELISA (Mercodia, Uppsala, Sweden)

Human IGF-II ELISA kit (Life Research, USA)

Viva Pure AdenoPACK 20 (Sartorius Stedim, USA)

RNAspin mini kit (Qiagen, USA)

Griess Reagent System (Promega, USA)

In Situ Cell Death Detection Kit, fluorescein (Roche, USA)

In Situ Cell Death Detection Kit, TMR red (Roche, USA)

Novex® ECL Chemiluminescent Substrate Reagent Kit (Invitrogen, USA)

QIAamp MinElute Virus Spin Kit (Qiagen, USA)

2.1.10 Miscellaneous reagents

Dimethyl sulphoxide (Ajax Chemicals, Australia)

Trypan blue (BDH, Australia)

Dithizone (Sigma-Aldrich, USA)

Streptozotocin (Sigma-Aldrich, USA)

Cryovial (NUNC, USA)

Haemocytometer (Thermo Fisher Scientific, USA)

25 ml polypropylene tube (Sarstedt, USA)

25cm^2 tissue culture flask (Sarstedt, USA)

75cm^2 tissue culture flask (Sarstedt, USA)

175cm^2 tissue culture flask (Sarstedt, USA)

24-well non-adherent suspension plate (Sarstedt, USA)

96-well flat bottom plate (Sarstedt, USA)

Ultra-low attachment petri dish 100 mm (Corning, USA)

Coverslip (Asis, China)

β-mercaptoethanol (Sigma-Aldrich, USA)

Cell scraper (Corning, USA)

50 ml falcon (BD Falcon^{TM}, USA)

FACS tubes (BD Falcon^{TM}, USA)

FACS tubes filter top (BD Falcon™, USA)

Microscope slide (Menzel Glaser, Holland)

Isoflourane (VCA, Australia)

Sterile tubing (Dural Plastics and Engineering, Australia)

Sterile gauze (Multigate, Australia)

Collagenase X1 (Sigma-Aldrich, USA)

600 µm filter (Endecotts, England)

Histopaque-1066 (Invitrogen, USA)

Humilin® (Lilly, USA)

Chloromycetin (Pfizer, USA)

Scalpel, size 11 (Smith and Nephew, Australia)

Insulin Syringe (BD Biosciences, USA)

Ethanol AR grade (Sigma-Aldrich, USA)

Pressure cooker (Nordic Ware, USA)

Goat serum (Sigma-Aldrich, USA)

Recombinant Human-IGF-II (R&D Systems, Inc., USA)

Wortmannin (Sigma-Aldrich, USA)

Tri-sodium Citrate (AnalaR®, Australia)

Polyvinyl difluoride Membrane (Millipore, USA)

Benzonase® Nuclease (Sigma-Aldrich, USA)

ProLong® Gold Antifade Reagent with DAPI (Invitrogen, USA)

0.45 µm filter (Sartorius Stedim, USA)

5 µm filter (Sartorius Stedim, USA)

1.2 µm filter (Sartorius Stedim, USA)

5 ml polyehtylene tube (Sarstedt, USA)

Ketamine Injection 100mg/ml (Parnell Laboratories, New Zealand)

Temgesic (Reckitt Benckiser Healthcare, UK)

Xylazil-20 20mg/ml (Troy Laboratories, Australia)

0.1 ml PCR tubes (Corbett Life Science, USA)

2.1.11 Equipment

Cytospin II Shandon (Thermo scientific, USA)

NanoDrop 1000 (Thermo scientific, USA)

Perkin Elmer DNA thermal cycler (USA)

FACS CANTO II (BD Bioscience, San Jose, California, USA)

Bio-Rad Minigel Apparatus (Bio-Rad, USA)

CoolCell (Biocision, USA)

CO_2 Incubator (Sanyo, Australia)

Water bath (Julabo, USA)

Cyberscan 1000 pH meter (AdeLab, Adelaide)

Light microscope (Olympus, USA)

Model 680 microplate reader (Bio-Rad, USA)

Scales (Sartorius, USA)

Heraeus 3S-R Centrifuge (Thermo Electron Corporation, USA)

Heraeus Pico17 Centrifuge (Thermo Electron Corporation, USA)

Centrifuge 5415 R (Eppendorf, USA)

RotorGene 3000 thermocycler (Corbett Life Science, USA)

Nikon C1-Z Confocal Microscope (Nikon Instruments, USA)

Typhoon FLA 9500 Scanner (GE Life Sciences, Australia)

Orbital Mixer Incubator (Ratek, Australia)

2.2 CELLULAR TECHNIQUES

2.2.1 Maintenance of cell lines

Tissue culture foetal calf serum (FCS) was heat inactivated at 56°C for 30 minutes (min) and stored at -20 degrees celcius (°C) until required. Unless otherwise indicated, tissue culture media was supplemented with 10% FCS, penicillin (100 IU/millilitre (ml)), gentamicin (50 microgram (µg)/ml) and L-glutamine (2 millimolar (mM)) and subsequently referred to as complete medium. L-glutamine was replenished every 14 days.

2.2.2 Description of cell lines

Human Embryonic Kidney (HEK) 293 cells were grown in complete DMEM + glutamax. HepG2 and Huh7 cells were grown in complete RPMI-1640. All cells were cultured to 70% – 80% confluence in a humidified incubator at 37°C, 5% CO_2 unless otherwise stated. See **Table 2.2.2** for a description of the cell lines.

2.2.3 Cell quantitation

Cells were detached from their culture surface using Accutase and centrifuged at 400g for 10 min. Pelleted cells were resuspended in 5 ml culture medium, of which 10 µl was removed and added to an equal volume of trypan blue. 10 µl of the cell suspension was added to both sides of a haemocytometer. The cell suspension was viewed under a light microscope using 10 x magnification. The total number of cells was determined by counting the 1 mm^2 centre square and the four corner squares of the haemocytometer. The cell concentration per ml and the total number of cells was determined using the following calculations:

Cells per ml = the average number of cells per 5 squares counted x 5 x the dilution factor x 10^4

Total cell number = cells per ml x the original volume of growth medium from which cell sample was removed

Table 2.2.2. Description of cell lines

Designation	Source	Characteristics	Culture medium	Source
HEK 293	Human Embryonic Kidney	Express E1-region of adenovirus 5, Adherent	Complete DMEM + glutamax	ATCC
HepG2	Human	Liver carcinoma cell line	Complete RPMI-1640	ATCC
Huh7	Human	Hepatocyte derived cellular carcinoma	Complete RPMI-1640	ATCC

2.2.4 Cryopreservation and storage of cell lines

Adherent cells were detached from their culture surface using Accutase (a cell detachment solution of proteolytic and collagenolytic enzymes) and the number of cells counted **(see section 2.2.3)**. The cells were pelleted by centrifugation at 400g for 10 min. The supernatant was then removed and the cells resuspended at a concentration of $2x10^6$ – $4x10^6$ cells per ml in freezing medium. Aliquots (1.8 ml) of the cells were transferred into cryovials and placed inside a cell freezing chamber (CoolCell) and frozen at -80°C overnight. Frozen cells were subsequently transferred to a liquid nitrogen storage vessel.

2.2.5 Thawing frozen cell lines

Frozen cells were placed in a 37°C water bath until the contents were completely thawed. Cells were transferred to a 25 ml polypropylene tube containing 5 ml of appropriate growth medium. An additional 10 ml of growth medium was added drop-wise to the cells over a period of 10 min. The cells were centrifuged at 400g for 10 min. The cells were resuspended in appropriate growth medium. The volume of growth medium added to the cells was based on the size of the tissue culture flask required to culture the cells **(Table 2.2.5)**.

Table 2.2.5. Volume of growth medium to add to tissue culture flasks

Size of Tissue Culture Flask	Volume of Growth Medium
T-25cm^2	5 ml
T-75cm^2	10 ml
T-175cm^2	20 ml

2.2.6 Subculture of cell lines

Adherent cell lines were cultured until they had reached appropriate confluence at which point they were sub-cultured. Briefly, the medium was removed and the cell monolayer was washed twice with warm 1 x phosphate buffered saline (PBS) using a volume equivalent to half the volume of the culture medium. Accutase was added to the cell monolayer at a volume of 500 microliters (µl) per 25cm^2 of surface area. The flask was placed in a humidified incubator at 37°C, 5% CO_2 for 5 min. The cells were examined using a light microscope to ensure that all the cells were detached and floating. The cells were resuspended in 5 ml of appropriate complete growth medium (containing FCS) to inactivate the enzymatic activity of accutase. The cells were counted **(see section 2.2.3)** and the required number of cells were subsequently transferred to new labelled flasks containing pre-warmed growth medium.

2.2.7 Changing cell culture medium

If cells had been in culture for 1 – 2 days, but were not yet confluent, then a media exchange was performed to replenish nutrients and maintain the appropriate pH for optimal cell growth. The growth medium in the flask was replaced with fresh pre-warmed culture medium and the flask was then returned to a humidified incubator at 37°C, 5% CO_2 for further culturing.

2.3 MOLECULAR METHODS

2.3.1 RNA extraction

Purification of total RNA was performed using RNeasy Mini Kit according to the manufacturer's instructions. Briefly, adherent cells were harvested and centrifuged at 400g for 10 min. To lyse the cells, an appropriate volume of lysis buffer RLT and β-mercaptoethanol was added **(Table 2.3.1)**.

Table 2.3.1. Preparation of lysis buffer RLT and β-mercaptoethanol to lyse pelleted cells

Number of pelleted cells	Volume of buffer (RLT)	Volume of β-mercaptoethanol
>5 x 10^6	350 µl	3.5 µl
5 x 10^6 – 1 x 10^7	600 µl	6.5 µl

Cell lysate was homogenized using a QIAshredder spin column and then 1 volume of 70% ethanol was added to the homogenised lysate. The membrane containing bound RNA was washed two times with buffer RW1 and once with buffer RPE. After the first RW1 wash, on-column DNase digestion was performed by aliquoting 10 µl of DNase I stock solution to 70 µl of provided buffer RDD. The DNase I incubation mix (80 µl) was added directly to the RNeasy spin column membrane, which was then incubated at room temperature (RT) for 15 min. To elute the RNA, 35 µl of nuclease-free water was added directly to the spin column membrane. The purified RNA was quantified by absorbance at 260 nanometer (nm) using NanoDrop 1000 and stored at -80°C until required for further analysis.

2.3.2 Reverse transcription using Oligo dT

One µg of RNA was reverse transcribed using Omniscript® Reverse Transcriptase. Briefly, template RNA was thawed on ice. Oligo-dT's, 10 x Buffer RT, dNTP Mix and RNase inhibitor was thawed at RT (15-25°C) then stored on ice. A fresh master mix was prepared (**Table 2.3.2)** and then mixed by vortexing for 5 seconds before being centrifuged. RNA was added to each sample tube. The sample was then incubated for 60 min at 37°C. The reaction volume was made up to 100 µl by adding 80 µl of nuclease-free water. The reaction was stored at -80°C until required.

Table 2.3.2. Reverse-transcription reaction components

Component	Volume/reaction	Final Concentration
10 x Buffer RT	2 µl	1x
dNTP Mix (5 mM each dNTP)	2 µl	0.5 mM each dNTP
Oligo-dT primer (10 uM)	2 µl	1 µM
RNase inhibitor (10 units/uL)	1 µl	10 units (per 20 µl reaction)
Omniscript Reverse Transcriptase	1 µl	4 units (per 20 µl reaction)
RNase-free water	Variable	
Template RNA	Variable	1 µg (per 20 µl reaction)
Total Volume	20 µl	-

2.3.3 Polymerase Chain Reaction

Polymerase Chain Reaction (PCR) master mix was prepared in a PCR restricted area as outlined below **(Table 2.3.3A)**:

Table 2.3.3A. PCR Reaction Components

Component	**Vol (50 µl)**
Nuclease-free water	23 µl
Amplitaq gold (2x)	25 µl
Forward primer	0.5 µl
Reverse primer	0.5 µl

The PCR master mix was vortexed and pulse spun then 47.5 µl was aliquoted per PCR reaction into 0.2 ml PCR tubes on ice. Template cDNA (2.5 µl) was added to appropriate tubes. Negative controls with 2.5 µl of water instead of cDNA were included with each experiment. Details of the primers and their conditions used in these reactions are outlined in **Table 2.3.3B**.

Table 2.3.3B. PCR primers

Designation	Sequence (5'-3')	Amplicon size (bp)	Conditions
Insulin-like Growth Factor-II (genomic) (Forward)	TCG ATT AGC TAG CCT ACT TCC GAT T	580	1. Pre- denaturation hot start 94°C, 5 min 2. Denaturation 94°C, 30 seconds 3. Annealing 64°C, 60 seconds 4. Elongation 72°C, 30 seconds 5. Extension 72°C, 7 min
Insulin-like Growth Factor-II (genomic) (Reverse)	GCG GCC GCG AAT TCA CTA	580	
Insulin-like Growth Factor-II (mRNA) (Forward)	AAG TCG ATG CTG GTG CTT CT	480	6. Pre- denaturation hot start 94°C, 5 min 7. Denaturation 94°C, 30 seconds 8. Annealing 60°C, 60 seconds 9. Elongation 72°C, 30 seconds 10. Extension 72°C, 7 min
Insulin-like Growth Factor-II (mRNA) (Reverse)	GTC TTG GGT GGG TAG AGC AA	480	

2.3.4 Agarose gel electrophoresis

A 2% gel was prepared by weighing 2 grams of DNA grade agarose and mixing with 100 ml 1x TAE buffer. The mixture was dissolved by heating in a microwave. The gel was pre-stained by adding 10 µl of GelRed™ solution before being poured. The gel was subsequently covered with1x TAE buffer. DNA size markers (2 µl) were mixed with 2 µl of 6x loading buffer and 10 µl of water. For PCR products, 2 µl of 6 x loading buffer was mixed with 10 µl of the PCR product and 4 µl of water. 15 µl of each sample was loaded onto the gel and all samples were run at 120 V for 18 min. Gels were visualised using a Typhoon scanner.

2.3.5 Quantitative real-time PCR using TaqMan® primers

Real-time PCR was carried out using a RotorGene 3000 thermocycler. Hypoxanthinephosphoribosyltransferase 1 (HPRT-1) was used as a house keeping gene based on its consistent and abundant expression in HEK 293 cells. HPRT-1 was used as a basis for normalization using the ΔΔCt method of quantitation, as per (313). Untransduced islets were compared with the Ad-IGF-II samples to evaluate fold change IGF-II gene expression. All real time runs had a negative control of water containing no cDNA template. All samples were run in triplicate.

Reaction components were prepared for a single 15 µl reaction **(Table 2.3.5A)**

Table 2.3.5A. Real-time PCR TaqMan® Reaction Components

Components	Volume/reaction
TaqMan® Master Mix (20X)	5 µl
TaqMan® Primers	0.5 µl
Nuclease-free water	3.7 µl
Total Volume	9.2 µl

The master mix totaling 9.2 µl/reaction was aliquoted into 0.1 ml Corbett PCR Tubes. Following this, cDNA (0.8 µl/reaction) was added to appropriate sample tubes. The samples were run per TaqMan® primer manufacturer instructions **(Table 2.3.5B)**.

Table 2.3.5B. RotorGene 3000 thermocycler Reaction Conditions

Times and Temperatures		
Initial Setup	Each of 40 cycles	
	Denature	Anneal/Extend
HOLD	CYCLE	
10 min 95°C	15 s 95°C	1 min 60°C

2.3.6 Viral DNA purification

Purification of viral DNA was performed using QIAamp® MinElute® Virus Spin kit according to the manufacturer's instructions. Briefly, 25 µl of protease was pipetted into a 1.5 ml eppendorf tube and mixed with 200 µl of the viral lysate sample and 200 µl buffer AL, before heating for 15 min at 56°C. 250 µl of ethanol was added to the sample and incubated for 5 min at RT. The lysate was transferred to a QIAamp MinElute column. The membrane containing bound DNA was washed once with buffer AW1 and once with buffer AW2, then once with ethanol. To elute the DNA, 30 µl of nuclease-free water was added directly to the spin column membrane. The purified DNA was stored at -80°C until required for further analysis.

2.4 ADENOVIRAL METHODS

2.4.1 Large-scale Adenoviral production

First round of Adenoviral (Ad) production

HEK 293 cells were plated in 25-cm^2 tissue culture flasks (~$3x10^6$ cells/flask in 6 ml complete DMEM) to reach 80% - 90% confluence at 12 to 15 hours (h). Each tissue culture flask was infected with 100 µl of primary transfection viral supernantant (purified Ad-GFP) and 300 µl of serum free DMEM. The flasks were incubated for 4 h at 37°C, 5% CO_2 in a humidified incubator. When 30 – 50% of the infected cells were detached (3 to 5 days post-infection) they were scraped using a cell scraper and transferred to a 50 ml falcon tube prior to being centrifuged at 400g for 10 min. the supernatant was removed and 5 ml of 1x PBS was added to the cells, which then underwent four cycles of freezing in a dry ice bath and thawing at 37°C to release the virus from the cells.

Second round of Ad production

HEK 293 cells were plated in 75-cm^2 tissue culture flasks (~5–7 x 10^6 cells/flask in 16 ml complete DMEM) to reach 80% - 90% confluence at 12 to 15 h. Approximately 2 – 4 ml of the viral lysate prepared in round one was added to one 75-cm^2 tissue culture flask of cells. When 50% of the infected cells were detached, the cells were scraped and transferred to a 50 ml falcon tube and processed as outlined in the first round of Ad production

Final round of Ad production

HEK 293 cells were plated into five 175-cm^2 tissue culture flasks (~1 x 10^7 cells/flask in 16 ml complete DMEM) to reach 100% confluence at 12 to 15 h. The cells were infected with viral supernatant at a multiplicity of infection (MOI) of 10 plaque forming units (pfu) per cell. Cells were infected for 4 h at 37°C, 5% CO_2. After this incubation cells were supplemented with complete DMEM. When all cells were rounded up and detached, they were scraped and collected into 50 ml falcon tubes. The cells were centrifuged at 400 g for 10 min and then subjected to four rounds of freeze-thawing before freezing at -80°C until purification.

2.4.2 Virus purification

Viral lysate **(see section 2.4.1)** was filtered through 5 micron (μm) and 1.2 μm filters prior to purification. Virus was purified using Viva Pure AdenoPACK 20 from Sartorius Stedim as per manufacturer's instructions. Briefly, filtered lysate was treated with 12.5 U/ml of benzonase nuclease and incubated for 30 min at 37°C. The lysate was then loaded onto a VivaClear maxi column and centrifuged at 500g for 5 min. An appropriately calculated volume of 10 x loading buffer was added to the lysate. The AdenoPACK 20 Maxi spin column was equilibrated with 5 ml of diluted 1 x washing buffer. The lysate was then transferred to the equilibrated column and centrifuged at 500g for 5 min to allow viral binding to the membrane. The column was washed twice with 18 ml of washing buffer and centrifuged after each wash at 500g for 5 min. The column was then transferred to a clean column holder. The Ad was eluted off the AdenoPACK maxi membrane by aliquoting 1 ml of elution buffer to the column membrane. The column was briefly centrifuged at 500g for 30 seconds and then incubated for 10 min. The column was then centrifuged at 500g for 5 min to collect the Ad-containing eluate. The eluate was transferred to a Vivaspin 20 centrifugal concentrator and storage (physiological) buffer was added to bring the total volume up to 20 ml. The column was centrifuged at 800g for 30 min and the concentrated virus was collected from the top chamber. The virus was stored at -80°C.

2.4.3 Adenoviral titre determination by flow cytometry

Serial dilutions of purified virus (10^{-2} to 10^{-6}) **(see section 2.4.2)** were prepared in 500 μl of serum-free DMEM + glutamax medium. HEK 293 cells (80 – 90% confluent) in T-25cm^2 tissue culture flasks were infected with the viral dilutions for 4 h in a humidified incubator at 37°C, 5% CO_2. Cells were then supplemented with complete DMEM + glutamax and incubated for 24 h. Cells were then harvested and approximately $1x10^6$ cells were transferred into FACS tubes and fixed with 1 ml FACS lysing solution. Samples were analysed on FACS canto II for GFP expression. Viral titre was determined according to the following calculation (314):

$$\text{Titre (pfu/ml)} = \frac{\%\ \text{GFP positive cells} \times \text{initial number of cells infected} \times \text{dilution factor}}{\text{initial infection volume}}$$

2.5 ISLET METHODS

2.5.1 Culture conditions

Rat pancreatic islets were cultured in complete RPMI-1640 medium. Human islets were used when available and were procured as part of the laboratory's involvement in the Australian Clinical Islet Transplant Consortium through the Juvenile Diabetes Research Foundation. Human islets were maintained in complete CMRL-1066 medium. Media exchange was performed daily, unless otherwise indicated. All use of human islet tissue was approved by the Royal Adelaide Human Ethics Committee and was kindly given research consent by the donor families. All human islets were sourced from isolating centres in Sydney and Melbourne that form the 'Australian Islet Consortium'. All cells were cultured in a humidified incubator at 37°C, 5% CO_2.

2.5.2 Islet dissociation

Islets were washed with PBS to remove serum and centrifuged at 300g for 2 min. Islets were resuspended with 500 µl of Accutase and incubated in a water bath at 37°C for 10 min in order to dissociate the islet cell clusters to single cells. The islets were agitated every 3-4 min and then further dissociated with gentle pipetting. The Accutase was inactivated with the addition of 2 ml complete media and the islets were then centrifuged to remove the Accutase at 300g for 5 min, 4°C. The cells were passed through filter top FACS tubes.

2.5.3 Islet quantification

Islets were resuspended in 10 ml of media and 200 µl of the islet preparation was transferred to a 1.5 ml eppendorf tube. An equal volume of dithizone (200 µl) was mixed with the islets, which were then incubated at RT for 5 min. The eppendorf tube was mixed several times to ensure the islets were completely resuspended, then 200 µl was removed and transferred to a glass slide for counting. Islets (stained red from dithizone) were counted at 10 x magnification using a light microscope. Islet quantity is expressed as the number of islet equivalents (IEQ), which is based on the number and diameter of the islets present in the preparation, mathematically corrected for islet volume.

2.5.4 Viral transduction

Islets were transduced in a minimal volume of serum free cell culture medium in a humidified incubator for 4 h at 37°C, 5% CO_2. After incubation islets were supplemented with an appropriate volume of cell culture media **(Table 2.5.4)**.

Culture vessels were infected with AAV constructs at various vector genome (vg) concentrations as indicated in **Chapter 3**. Culture vessels were infected with Ad viral constructs at various multiplicity of infection (MOI) according to the following calculation (unless otherwise stated):

Multiplicity of infection = total number Ad particles / total number cells

MOI was calculated based on the assumption that one IEQ contains on average 2000 cells (138, 315).

Table 2.5.4. Minimal and final volumes of culture medium for islet transduction

Transduction culture vessel	Minimal volume	Final volume
24-well suspension plate	250 µl	750 µl
6-well suspension plate	500 µl	1 ml
T-25cm^2 flask	500 µl	3 ml
T-75cm^2 flask	700 µl	10 ml

HEK 293 cells (~2x10^6) were plated in 25-cm^2 tissue culture flasks and incubated at 37°C, 5% CO_2 for 12 to 15 hours prior to transduction. Residual cell culture medium was removed from the flask by washing twice with warm PBS. The cells were incubated in a minimal volume (250 µl) of serum free culture medium and viral dilution for 4 h at 37°C, 5% CO_2. An additional volume of 6 ml complete medium was added for the specified time point.

2.5.5 Cytokine treatment of islets

Islets were aliquoted (50 IEQ/well) into 24-well suspension culture plates. Islets were treated with pro-inflammatory cytokines IL-1β and IFN-γ at various concentrations, as indicated, for 24 h. Islets were cultured in a minimal volume of 500 µl cell culture medium unless otherwise specified.

2.5.6 Glucose stimulated insulin release assay of islets

Islets were transferred to 3 ml low glucose RPMI in a FACS tube. The islets were left to settle for 10 min. Approximately 2.7 ml of RPMI was removed and either 1.2 ml low (2.8 mM) or high (25 mM) glucose RPMI was added to the appropriate tubes. The islets were incubated at 37°C for 2 h. Supernatant (1 ml) was carefully removed and stored at -80°C prior to analysis.

2.5.7 Insulin-like growth factor-1 receptor blocking

Rat islets (50 IEQ) were untransduced, transduced with Ad-GFP, Ad-IGF-II or pre-treated for 30 min with Insulin-like Growth Factor-I Receptor (IGF-1R) blocking antibody (10 µg) then transduced with Ad-IGF-II for 48 h and treated for 30 min with IGF-1R blocking antibody before addition of rat pro-inflammatory cytokines IL-1β (35ng/ml) and interferon-γ (IFN-γ) (40ng/ml) for 24 h.

2.5.8 Western blotting analysis

Rat islets (50 IEQ) were untransduced, transduced with Ad-GFP, Ad-IGF-II or pre-treated for 1 h with 200 mM wortmannin prior to Ad-IGF-II transduction for 48 h. Following transduction, all experimental groups were treated with rat pro-inflammatory cytokines interleukin-1β (IL-1β) (35ng/ml) and interferon-γ (IFN-γ) (40ng/ml) for 24 h. Islets were harvested for western blotting analysis. The protein extracts were separated by sodium dodecyl sulfate polyacrylamide gel electrophoresis (SDS-PAGE) and transferred to a polyvinyl difluoride (PVDF) membrane. The blots were incubated with rabbit polyclonal phospho-Akt (pAkt) (Ser473) antibody (1:1000) and rabbit polyclonal Akt antibody (1:1000). Blots were then incubated in anti-rabbit IgG, HRP-linked secondary antibody (1:2000). The bands were detected using a Novex® ECL Chemiluminescent Substrate Reagent Kit.

2.6 FLOW CYTOMETRY

2.6.1 Annexin V/Propidium Iodide staining

Islets were harvested at their appropriate time points and transferred to a 25 ml polypropylene tube before centrifugation at 200g for 2 min, RT. The islets were dissociated using 500 µl Accutase and incubated at 37°C for 10 min **(see section 2.5.2)**. Complete RPMI-1640 (5 ml) was added to inactivate the enzymatic activity of Accutase and then the islets were centrifuged at 200g for 2 min, RT. The islets were resuspended in 2 ml Annexin V binding buffer and then transferred to filter top FACS tubes, before being centrifuged at 300g for 3 min, 4°C. The islets were stained with 5 µl of Annexin V for 15 min in the dark, RT. Following this, the islets were stained with 2 µl Propidium Iodide (PI) for 15 min on ice and then immediately analysed using a FACS CANTO II.

2.6.2 GFP detection

Islets were harvested at their appropriate time points and dissociated as per **section 2.5.2**. The islets were resuspended in 200 µl islet FACS wash and transferred to filter top FACS tubes before being immediately analysed using a FACS CANTO II.

2.6.3 7-AAD staining

Dissociated islets were resuspended in 200 µl islet FACS wash and transferred to filter top FACS tubes. The islets were then centrifuged at 200g for 2 min and then stained with 200 µl 7-AAD (5 µg/ml) for 15 min on ice before being immediately analysed using a FACS CANTO II.

2.6.4 Ki67 staining

Islets were harvested at their appropriate time points and dissociated as per **section 2.5.2** and then fixed with 1 ml of 70% ice-cold ethanol and then stored at -20°C for 2 h. The islets were washed twice in FACS wash and resuspended at $1x10^5$ cells/50 µl FACS wash. The islets were stained with 2.5 µl ki67 for 20 min at RT, in the dark before being immediately analysed using a FACS CANTO II.

2.7 ENZYME LINKED IMMUNOSORBENT ASSAY (ELISA)

2.7.1 Rat insulin ELISA

A rat insulin ELISA kit was used as per manufacturer's instructions. Briefly, all reagents and samples were bought to room temperature before use. 10 µl of calibrators and samples (diluted 1:10 with calibrator 0) were aliquoted into appropriate wells. Enzyme conjugate solution (100 µl) was added to each well. The plate was incubated on a plate shaker (700-900 rpm) for 2 h at RT. The plate was washed six times with prepared wash buffer. Substrate TMB (200 µl) was added into each well and the plate was then incubated for 15 min at RT. Stop solution (50 µl) was added to each well and the optical density was read at 450 nm within 30 min of adding the stop solution. The detection limit of the rat insulin ELISA kit was ≤0.15 µg/L.

2.7.2 Human insulin ELISA

A human insulin ELISA kit was used as per manufacturer's instructions. Briefly, all reagents and samples were bought to room temperature before use. 25 µl of calibrators and samples (diluted 1:10 with calibrator 0) were aliquoted into appropriate wells. Enzyme conjugate solution (100 µl) was added to each well. The plate was incubated on a plate shaker (700-900 rpm) for 1 h at RT. The plate was washed six times with prepared wash buffer. Substrate TMB (200 µl) was added into each well and the plate was then incubated for 15 min at RT. Stop solution (50 µl) was added to each well and the optical density was read at 450 nm within 30 min of adding the stop solution. The detection limit of the human insulin ELISA kit was 1 mU/L calculated as two standard deviations above the Calibrator 0.

2.7.3 Human IGF-II ELISA

A human IGF-II ELISA kit was used to detect human IGF-II in cell culture supernatants and cell lysates. The samples were diluted 1:10 using the provided diluent buffer. Human IGF-II standard was prepared by reconstitution of the IGF-II standard (10,000 picogram (pg)/ml) with 1 ml of sample diluent buffer. From the stock solution, dilutions of 4000, 2000, 1000, 500, 250, 125 and 62.5 pg/ml were prepared for the standard curve. In triplicate, 100 µl of each of the standards were aliquoted into the precoated 96-well plate and 100 µl of the standard diluent buffer was aliquoted for the blank well. 100 µl of each properly diluted sample was added to each empty well. The plate was incubated at 37°C for 90 min.

The plate content was discarded, and 100 µl of biotinylated anti-human IGF-II antibody working solution was aliquoted into each well. The plate was incubated at 37°C for 60 min then washed three times with 0.01M PBS. Following this, 100 uL of prepared Avidin-Biotin-Complex working solution was aliquoted into each well and the plate was incubated at 37°C for 30 min. The plate was washed five times with 0.01M PBS and then 90 µl of prepared TMB colour developing agent was added into each well and the plate was incubated at 37°C for 30 min. Stop solution (100 µl) was added into each well and then the absorbance was read at 450 nm in a plate reader within 30 min after adding the stop solution. The detection limit of the human IGF-II ELISA kit was <2 pg/ml.

2.8 GRIESS REACTION FOR NITRIC OXIDE DETERMINATION

A 100 µM nitrite solution was prepared by diluting the provided 0.1 molar (M) nitrite standard 1:1000 in the cell culture medium used for the experimental samples. 2-fold dilutions of the 100 µM nitrite solution were prepared to generate the nitrite standard reference curve (100, 50, 25, 12.5, 6.25, 3.13 and 1.56µM). The standards and experimental samples (50 µl) were added in triplicate to appropriate wells of a 96-well flat-bottom plate. Sulfanilamide Solution (50 µl) was added to all wells, which were then incubated 5-10 min at RT, protected from light. NED solution (50 ul) was added to all wells, followed by incubation for 5-10 min at RT, protected from light. The absorbance was measured within 30 min on a plate reader at 540 nm.

2.9 ANIMAL METHODS

2.9.1 Albino wistar rat islet isolation

Albino Wistar rats weighing between 250 – 350 g were anaesthetized with appropriate levels of isofluorane and oxygen delivered via nose cone. The peritoneum was opened and the liver lobes were flipped above the sternum to expose the pancreatic duct. Once identified, a small nick was made in the duct followed by cannulation with 0.96 mm sterile tubing. With the cannula in place, a syringe was attached to deliver 20 ml of cold 1x Hank's Buffered Salt Solution (HBSS) into the pancreas **(Figure 2.9.1)**. The pancreas was dissected carefully from the stomach, intestine and spleen. The portal vein was clamped prior to removal of the pancreas to minimize bleeding.

A

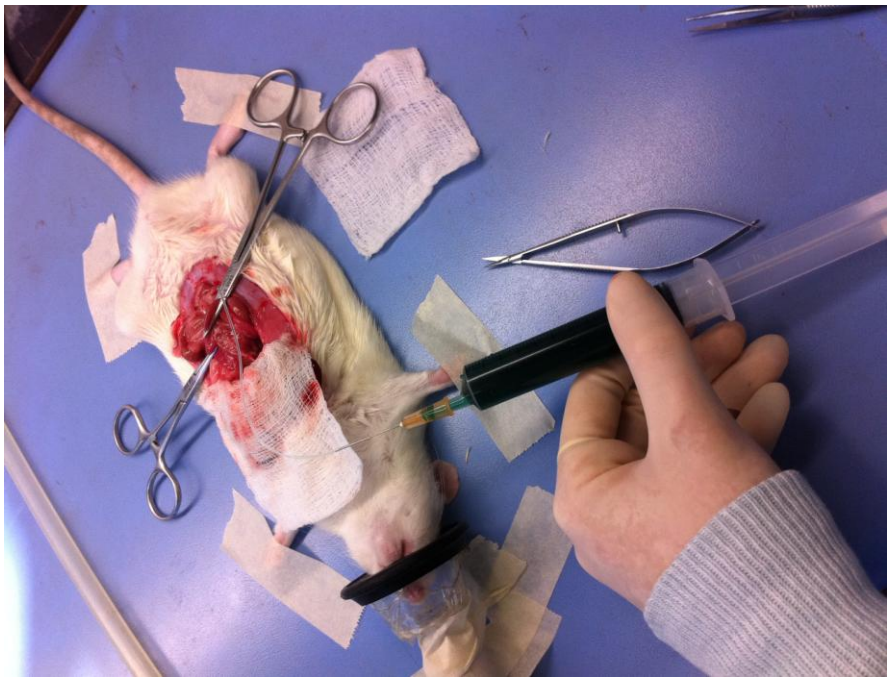

B

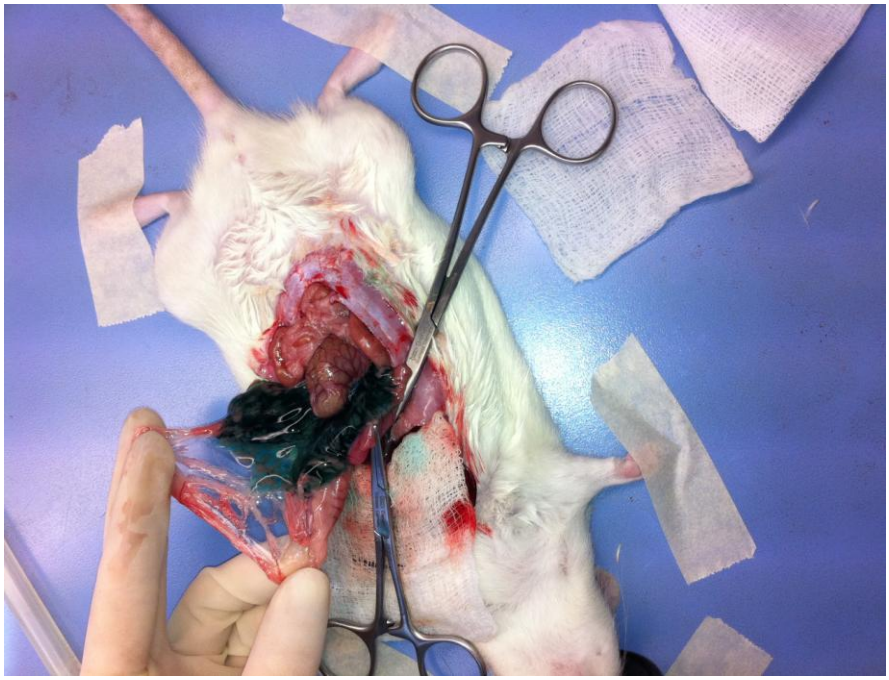

Figure 2.9.1. Surgical rat islet isolation procedure. **(A)** The rat peritoneum was opened and the liver lobes were flipped above the sternum (held in place by sterile gauze) to expose the pancreatic duct. Iris scissors were used to nick the pancreatic duct. A cannula (0.96 mm sterile tubing) was attached to a syringe filled with cold 1x HBSS. **(B)** With the cannula in place, cold 1x HBSS was infused into the pancreas via the pancreatic duct. Image shows an inflated pancreas (green).

The pancreas was minced into small pieces using sterile scissors then transferred to a 50 ml falcon tube and placed on ice. Collagenase X1 was weighed into a 5 ml polyethylene tube based on 1 mg of collagenase per 25 g rat body weight. The collagenase was reconstituted with 1 ml of 1x HBSS at RT before being transferred to the pancreas. The pancreas was digested at 37°C for approximately 15 min. The pancreas was washed twice with ice-cold 1x HBSS. The contents were filtered using a metallic filter of pore size 600 µm and transferred to a 50 ml falcon tube which was centrifuged at 200g for 2 min.

Ice-cold Histopaque-1066 (10 ml) was mixed gently with the cell pellet and 5 ml of 1x HBSS (pre-warmed to 37°C) was overlaid onto the Histopaque-1066. The cell gradient was centrifuged at 800g, for 15 min, 12°C. The islets were recovered at the interphase (middle) layer and the islets were transferred to a 100 mm low-attachment culture dish on ice. The islets were washed in the petri-dish three times using cold 1x HBSS to dilute the residual histopaque. The islets were placed in complete RPMI-1640 medium and cultured overnight in a humidified incubator at 37°C, 5% CO_2 until required. This overnight incubation allowed the islets to 'rest and recover' from the isolation process.

2.9.2 Streptozotocin diabetes induction

The 50 mg streptozotocin (STZ) vial was weighed prior to reconstitution as the exact concentration was found to vary between vials. STZ was reconstituted by aliquoting 2.5 ml of tri-sodium citrate buffer pH 4.5 to the STZ vial and mixing. The concentration of STZ was calculated by dividing the STZ weight (mg) by 2.5 ml (the volume used to reconstitute the STZ). STZ has a half life of 15 min in suspension and was used within 10 min after reconstitution. NOD-SCID mice of a minimum weight range (>20 grams) received an intra peritoneal (i.p) injection of STZ at 180 mg/kg, unless otherwise stated. Mice were monitored daily for diabetes diagnosis (blood glucose mmol/l, weight and clinical scored). Mice received hydration via 500 µl sub cutaneous injections of saline as required. Mice with two consecutive readings of high blood glucose level (BGL) (≥20 mmol/l) were treated with sub cutaneous human insulin injection (Humilin®) (1U). Mice were considered diabetic following 2 blood glucose readings ≥16.6 mmol/l (316, 317).

2.9.3 NOD-SCID kidney capsule islet transplant

Diabetic NOD-SCID mice were anaesthetised with ketamine (100 mg/kg) and xylazine (6 mg/kg) via i.p injection and kept on a heat mat for the procedure. Eye ointment (Chloromycetin) was applied to the eyes to prevent drying out of the cornea, while under anaesthesia. Under aseptic conditions and in a pathogen free environment, the left side of the cost vertebral angle was cleaned with sterile gauze. A 1 centimeter (cm) incision was made to expose the kidney.

With a sterile scalpel, a small nick was made in the kidney capsule and a glass rod was used to create a pocket for the islets. The kidney was covered with wet gauze during islet pellet preparation. Islets were prepared by gently spinning in a microcentrifuge at 100g for 1 min at RT. Islets were then collected using a sterile glass pasteur pipette and transferred to a gel-foam tip and then centrifuged at 200g for 3 min at RT. Excess media was removed and the tip was unplugged prior to insertion under the kidney capsule. Using an insulin syringe plunger, the islets were gently transferred under the kidney capsule. Islets were spread by gently rubbing them with the glass rod and the kidney was returned to its natural position and the muscle and skin was sutured. Pain relief (temgesic) (100 μg/ml) was administered via sub cutaneous injection for three days post transplantation.

2.10 IMMUNOHISTOCHEMISTRY

2.10.1 Islet cytospins

Islets were harvested and resuspended in cytospin wash buffer (50-100 IEQ) in 100-200 μl. Glass slides were fastened into cytospin clips and the cell suspension was transferred to each cytospin funnel, avoiding bubbles. The slides were centrifuged at 400 rpm in a Shandon cytospin 5 and then fixed with 4% paraformaldehyde for 20 min. Excess paraformaldehyde was removed by washing with PBS, the slides were left to air dry (in fume hood) and were then stored at -80°C until staining.

2.10.2 Paraffin embedding of human islet cell suspensions

Human islets were harvested, resuspended in 1 ml of 10% buffered formalin and incubated for 10 min, RT. The islets were then resuspended in 55 µL RPMI-1640. 300 µl of 1% agarose in PBS was then mixed with the islet preparation. The agarose islet 'plug' was set at 4°C for 30 min prior to paraffin embedding and sectioning by histopathology at the IMVS, Adelaide.

2.10.3 Terminal deoxynucleotidyl transferase dUTP nick end labeling (TUNEL)

Islet cytospins were removed from -80°C storage and left to air dry prior to staining **(see section 2.10.1)**. TUNEL staining was performed according to manufacturer's instructions. Briefly, slides were incubated in freshly prepared permeabilisation solution for 2 min on ice and then washed twice with PBS. TUNEL reaction mixture was prepared by removing 100 µl from the label solution and adding 50 µl of enzyme solution to the remaining label solution to obtain 500 µl. TUNEL reaction mixture (50 µl) was aliquoted onto each slide and the slides were incubated in a humidified atmosphere for 60 min at 37°C in the dark. The slides were washed three times with PBS and then stained with ProLong Gold Antifade reagent with DAPI nuclear stain.

2.10.4 Antigen retrieval

Paraffin slides were melted at 60°C for 2 x 15 min. The slides were deparaffinised and rehydrated as followed (xylene 3 changes 5 min each, 100% ethanol 3 changes 5 min each, 95% ethanol 5 min, 70% ethanol 5 min, 50% ethanol 5 min, PBS 5 min). Approximately 500 ml of MilliQ water was heated in a pressure cooker for 9 min on high. The slides were placed inside a staining pot filled with sodium citrate buffer and transferred to the pressure cooker and heated for 20 min. The slides were incubated at RT for a further 20 min. The slides were washed twice in PBS for 5 min.

2.10.5 Insulin staining of islets

Slides were blocked with 3% goat serum in PBS for 30 min at RT. Slides were incubated with primary guinea-pig anti insulin (1:100 dilution) for 2 h at RT prior to washing with PBS for 5 min. Primary antibody was detected with goat anti-guinea pig rhodamine IgG (1:100 dilution). Slides were incubated with secondary antibody for 1 h at RT. Slides were washed with PBS for 5 min and then stained with ProLong Gold Antifade reagent with DAPI nuclear stain.

2.10.6 Fluorescent confocal microscopy of transduced islets

Transduced islets were washed twice in PBS and then incubated with DAPI (5µg/ml) for 30 min at 37°C. Islets were washed with PBS for 5 min prior to mounting with DAKO mounting medium. The islets were mounted on superfrost plus slides with a coverslip.

2.11 STATISTICAL ANALYSIS

Values were given as data ± standard error of the mean (SEM) and compared using Student-t test or one-way analysis of variance (1way ANOVA), followed by Bonferroni's multiple comparison test, with *p≤0.05, **p≤0.01, ***p≤0.001, ****p≤0.0001, where appropriate. Log-rank (Mantel Cox) analysis was used in the marginal islet mass model. For all comparisons, $P \leq 0.05$ was considered to be statistically significant (GraphPad Prism software 5, Inc, San Diego, CA). Densitometry of western blots was performed using ImageJ software (Rasband, W.S., ImageJ, U. S. National Institutes of Health, Bethesda, Maryland, USA).

2.12 SOLUTIONS AND BUFFERS

DMEM Complete Media (500 ml)

DMEM (High Glucose)

10% FCS (50 ml)

1% Penicillin/Gentamicin (5 ml)

1% Glutamine (5 ml)

1% non-essential amino acids (5 ml)

DMEM Serum-free Media (500 ml)

DMEM (High Glucose)

1% Glutamine (5 ml)

1% Penicillin/Gentamicin (5 ml)

1% non-essential amino acids (5 ml)

RPMI Complete Media (500 ml)

RPMI-1640 450 ml

10% FCS (50 ml)

1% Glutamine (5 ml)

1% Penicillin/Gentamicin (5 ml)

RPMI Serum-free Media (500 ml)

RPMI-1640 450 ml

1% Glutamine (5 ml)

1% Penicillin/Gentamicin (5 ml)

CMRL-1066 Complete Media (500 ml)

CMRL media 450 ml

Albumex 20 (25 ml)

1% Glutamine (5 ml)

1% Penicillin/Gentamicin (5 ml)

CMRL-1066 Serum-free Media (500 ml)

CMRL media 450 ml

1% Glutamine (5 ml)

1% Penicillin/Gentamicin (5 ml)

50x TAE (100 ml)

Trizma base, 193.8 g (1.6M)

Sodium acetate, 65.6 g (800 mM)

EDTA, 14.9 g (40.27 mM)

pH to 7.2

Agarose gel (60 ml)

2% gel = 1.2g agarose

6x Loading buffer

50x TAE, 600 µl

Glycerol, 5 ml (50%)

Bromophenol blue, 2.4 ml (24%)

H_2O, 2.4 ml

Western blot lysis buffer

HEPES, 50 mM (pH 7.4)

NaCl, 150 mM

Triton-X 100, 1%

Na_3VO_4, 1 mM

NaF, 30 mM

$Na_4P_2O_7$, 10 mM

EDTA, 10 mM

Western blot blocking buffer

1x TBS

Tween-20

5% w/v nonfat dairy milk

FACS washing buffer (100 ml)

2% FCS, 5 ml

0.1% Sodium azide, 100 µl

1x PBS, to 100 ml

FACS lysing buffer (100 ml)

10% FACS lysing solution, 10 ml

Distilled H_2O, to 100 ml

Dithizone

Dithizone, 0.1 g

DMSO, 10 ml

Albumex 20, 10 ml

HEPES, 2 ml

1 x HBSS, 78 ml

Filter using 0.45 µm filter

Low glucose RPMI for rat insulin release assay (2.8 mM)

10% glucose, 250 µl

Complete RPMI (glucose free), to 50 ml

High glucose RPMI for rat insulin release assay (25 mM)

10% glucose, 2 ml

Complete RPMI (glucose free), to 50 ml

Freezing medium

FCS, 9 ml

DMSO, 1 ml

Xylazine/Ketamine injectable anestehetic

Xylazine, 250 µl

Ketamine, 500 µl

Sterile Saline, to 5 ml

Humilin®/Saline Buffer

Sterile saline, 9 ml

Humilin®, 30 units

Cytospin wash buffer (500 ml)

0.5% FCS, 2.5 ml

1 x PBS, to 500 ml

20% paraformaldehyde (to prepare 4% paraformaldehyde)

Paraformaldehyde, 4 g

1 x PBS, 20 ml

10 M NaOH, 10 µl

To prepare 4% paraformaldehyde, 2 ml of 20% paraformaldehyde was added to 8 ml 1 x PBS

1.0 M Citric Acid Buffer

Citric acid, 10.5 g

Sterile Baxter H_2O, to 50 ml

0.1 M tri-Sodium Citrate Buffer pH 4.5

Tri-Sodium Citrate, 1.47 g

Sterile Baxter H_2O, to 50 ml

Adjust to pH 4.5 using 1.0 M citric acid buffer

1 M Citrate Buffer pH 6

Tri-Sodium Citrate, 2.94 g

MilliQ H2O, to 1000 ml

Adjust to pH 6 using 1 M HCL

TUNEL permeabilisation solution

Tri-Sodium Citrate, 0.2 g

Triton-X, 200 µl

MilliQ H_2O, to 200 ml

Islet FACS wash

Albumex 20, 25 ml

1 x PBS (- calcium chloride and magnesium chloride), to 500 ml

Annexin V binding buffer

10X Annexin V Binding Buffer, 50 ml

Sterile MilliQ H_2O, to 200 ml

Propidium Iodide (PI) working stock

PI stock (1mg/ml), 2.5 ml

1 x PBS sterile, 7.5 ml

7-AAD (1mg/ml)

7-AAD powder, 1 mg

1 x PBS, 1ml

Use at 250 µg/ml

0.01M PBS

1 x PBS, 500 ml

MillQ H_2O, 500 ml

CHAPTER 3

COMPARISON OF ADENOVIRAL AND ADENO-ASSOCIATED VIRAL TRANSDUCTION OF HUMAN AND RODENT PANCREATIC ISLETS

3.1 Introduction

There are major obstacles that need to be overcome before islet transplantation can be considered the 'gold standard' treatment for type 1 diabetic (T1D) patients. For example, islets isolated from the pancreas are removed from their native vasculature and become rapidly hypoxic (318). In addition, the islet isolation process severs interactions between islets and macromolecules of the extracellular matrix (319). Biomolecular cues from the extracellular matrix are important for islet survival, proliferation and function and without these signals, isolated islets undergo apoptosis (320).

Currently, the vulnerability of pancreatic islets to peri-transplant cell death, requires transplantation of high numbers of islets and multiple infusions to achieve insulin independence (94). In this regard, there is a need for an anti-apoptotic strategy to prevent loss of functional islet mass in the early post-transplant period (321). Specifically, *ex vivo* delivery of an anti-apoptotic molecule to pancreatic islets prior to transplantation may promote islet cell survival and improve insulin independence rates. Viral vectors offer the most effective means of gene delivery, as they can efficiently infect multiple cell types and tissues to express the required therapeutic gene (322). Non-viral vectors are less immunogenic compared to their viral vector counterparts, however they have the major limitation of inefficient cell transduction *in vitro* and *in vivo* (323, 324).

Gene therapy studies performed in isolated islets utilize four common viral vector types, namely Adenovirus (Ad), Adeno-Associated Virus (AAV), Herpes Simplex Virus and Retrovirus (includes Lentivirus) based vectors (157, 202, 325-327). Retroviral transduction is restricted to dividing cells (50), however lentiviral vectors can transduce non-dividing cells, such as islets.

Despite a number of published anti-apoptotic strategies, the optimal viral vector type for use in an islet gene therapy setting is unknown. Therefore, this chapter aims to identify the most effective vector type for this purpose. The optimal vector for use against any clinical indication must be selected on the basis of a number of criteria, such as the duration of transgene expression, the immune response elicited by the vector, the ability of the vector to transduce quiescent/dividing cells, the ease of vector production and vector safety/toxicity (328).

Ad is a medium sized, icosahedral, non-enveloped virus that carries a linear, double stranded 36-kilo base (kb) DNA genome (329). Ad-based vectors can be efficiently generated to produce high titer viral stocks, stably stored and transduce both diving and non-dividing cells (330), an important property when considering the transduction of senescent islet cells. In some therapeutic applications, the Ad capsid and viral DNA elicit potent immune responses (157, 331). However, this would be limited within an *ex vivo* islet transplant setting as any remaining virus would be washed off prior to transplantation. *Ex vivo* gene therapy offers an advantage over systemic administration of viral vectors, as it circumvents the toxic side effects that the latter can confer (332).

AAV is a small virus with a non-enveloped icosahedral capsid of approximately 22 nm and a 4.5-kb genome of single stranded DNA (116). AAV-based vectors are generally considered a 'safe' vector type (333), as despite the high seroprevalence of AAV2 (80%) in the human population the virus has not been linked to any human illness (116, 334). In addition, AAV integrates into the host cell genome at a specific location on chromosome 19, significantly decreasing the likelihood of insertional mutagenesis (335).

The viral genome of both Ad and AAV based vectors is packaged within a protein coat called the capsid. The capsid contains viral proteins that enable the virus to attach to host cells and aid entry into cells. Specific viral receptors on the cell surface are involved in defining the host range and tropism of a virus (132). Secondary interactions of the viral capsid with co-receptors dictate the intracellular trafficking pathway and biological fate of the virus. It is this stage of the infectious pathway (and eventually transduction efficiency) that is most significantly influenced by the choice of vector (336).

Ad entry into host cells is mediated via attachment to Coxsackie Adenovirus Receptor (CAR) with the knob domain of the Ad viral fiber (337), followed by secondary interactions between viral capsid proteins and αv integrin internalization receptors (αvβ3, αvβ5 and αvβ1) (338). Various studies have shown the presence of CAR on human islets, porcine islets and islet endothelial cells (339-341). Regarding AAV, each serotype exhibits unique cell/tissue tropism and therefore unique transduction efficiency (342), determined by each serotypes preference for different receptors (343). This is made even more complex by the fact that not all AAV receptors are currently known for each serotype.

AAV serotypes 4 and 5 utilize sialic acid with different linkage specificities (α-2,3-O-linked and α-2,3-N-linked, respectively) for cell surface binding and transduction (344, 345). The platelet derived growth factor receptor is a coreceptor for AAV5 (346). α-2,3 and α-2,6-N-linked sialic acid facilitates binding and transduction by AAV1 and AAV6 (347). As such, AAV6 effectively transduce airway epithelial cells (348). The 37/67-kDa laminin receptor (lamR) is a cellular receptor for AAV8 and AAV9 (349, 350). AAV3 uses hepatocyte growth factor receptor as a co-receptor for viral entry (351). AAV2 utilize heparan sulphate proteoglycan (HSPG) as a primary receptor, in addition to subsequent interactions with αvβ5/α5β1 integrins and/or human fibroblast growth factor receptor 1 (132, 134, 352, 353).

Several approaches have been trialed to target AAV vectors for transduction of specific cell types or to increase the range of cells that are amenable to transduction by AAV. Some strategies include utilizing natural serotypes that target a desired cell receptor, producing pseudotyped vectors, and engineering chimeric or mosaic AAV capsids (342). This chapter investigated the use of two pseudotype AAV vectors that accommodate capsid proteins from AAV1 and AAV8 viral serotypes, termed AAV2/1 and AAV2/8, respectively.

Tyrosine to phenylalanine mutations on the surface of AAV capsids has been reported to enhance transduction efficiency *in vitro* and *in vivo* (354). Phosphorylation of tyrosine residues on AAV2 capsids following viral entry negatively affects viral intracellular trafficking and transduction efficiency *in vivo*. Tyrosine phosphorylation targets the cells for proteasomal mediated degradation (355), via a pathway likely to serve as an antiviral mechanism (356).

This chapter examines the ability of Ad and AAV based vectors expressing a green fluorescent protein (GFP) reporter gene to transduce isolated human and rat pancreatic islets with the primary aim to determine the optimal vector for islet transduction. The consequence of Ad or AAV transduction on islet viability and function was determined for each vector type and was subsequently shown to be unaffected by exposure to either virus type. Given the varied tropism reported with AAV, it was of interest to investigate the islet transduction efficiency of a panel of six AAV vector types, with specific interest placed on pseudotype AAV vectors and tyrosine mutant AAV-based vector types, which the latter, to our knowledge remain unexplored in human and rodent pancreatic islets. Ad and AAV transduced human and rat pancreatic islets with varying levels of efficiency. In this study, tyrosine mutation on the AAV capsid did not enhance AAV-mediated transduction of pancreactic islets. In addition, AAV failed to effectively transduce isolated human islets and showed a varied ability to transduce rat islets. The results in this chapter demonstrate that Ad vectors are more efficient at transducing isolated islets than AAV-based vector types.

3.2 Results

3.2.1 Ad-GFP transduction induces GFP expression in rat islets

The ability of Ad-GFP to transduce isolated rat islets was assessed using fluorescence microscopy and flow cytometry to detect GFP expression. Rat islets were transduced with Ad-GFP at multiplicity of infection (MOI) 10, 100, 200, 1000, 2000, 5000 and 10000 for 48 h. Under a fluorescent microscope, untransduced islets were used to establish the specificity of transduction and any background fluorescence. Representative images showing the pattern of GFP positive (green) islet cells following transduction are shown in **Figure 3.2.1(A)**. GFP expression was increased in islets transduced with increasing MOI.

Using flow cytometry, untransduced islet cells were used to define background (negative) and transduced cells were gated corresponding to their expression of GFP (positive). Transduction of rat islets at MOI 10, led to 17.8 ± 3.3% of cells transduced. There was no difference in the transduction efficiency of Ad-GFP at MOI 100 or MOI 200 with 36.2 ± 6.7% and 36.2 ± 8.5% of rat islet cells transduced, respectively. Transduction with MOI 1000 or MOI 2000 resulted in 47.3 ± 7.8% and 48.4 ± 10.7% rat islet cells transduced. Ad-GFP transduction with the two highest MOIs (5000 and 10000) led to 51.9 ± 4.3% and 50 ± 8.8% of rat islets transduced (**Figure 3.2.1(B**)).

3.2.2 Ad-GFP transduction does not affect rat islet viability or function

Rat pancreatic islets were transduced with Ad-GFP at MOI 10, 100, 200, 1000, 2000, 5000 and 10000 or untransduced for 48 h to investigate the effects of Ad transduction on rat islet viability and function. Rat islet viability was not adversely affected compared to untransduced control islets following Ad-GFP transduction at all tested MOI **(Figure 3.2.2(A))**.

Based on the above experiment, MOI 1000 was chosen as the optimal MOI for use in future Ad-GFP characterisation experiments. Ad-GFP transduction of rat islets (MOI 1000) did not adversely affect the insulin secretory function of Ad-GFP transduced rat islets (5.2 ± 1.5) compared to untransduced control islets (4.3 ± 1.5), as measured by stimulation index (SI) **(Figure 3.2.2(B))**. The SI of islets was measured by dividing the islets insulin response to high glucose by the islets insulin response to low glucose.

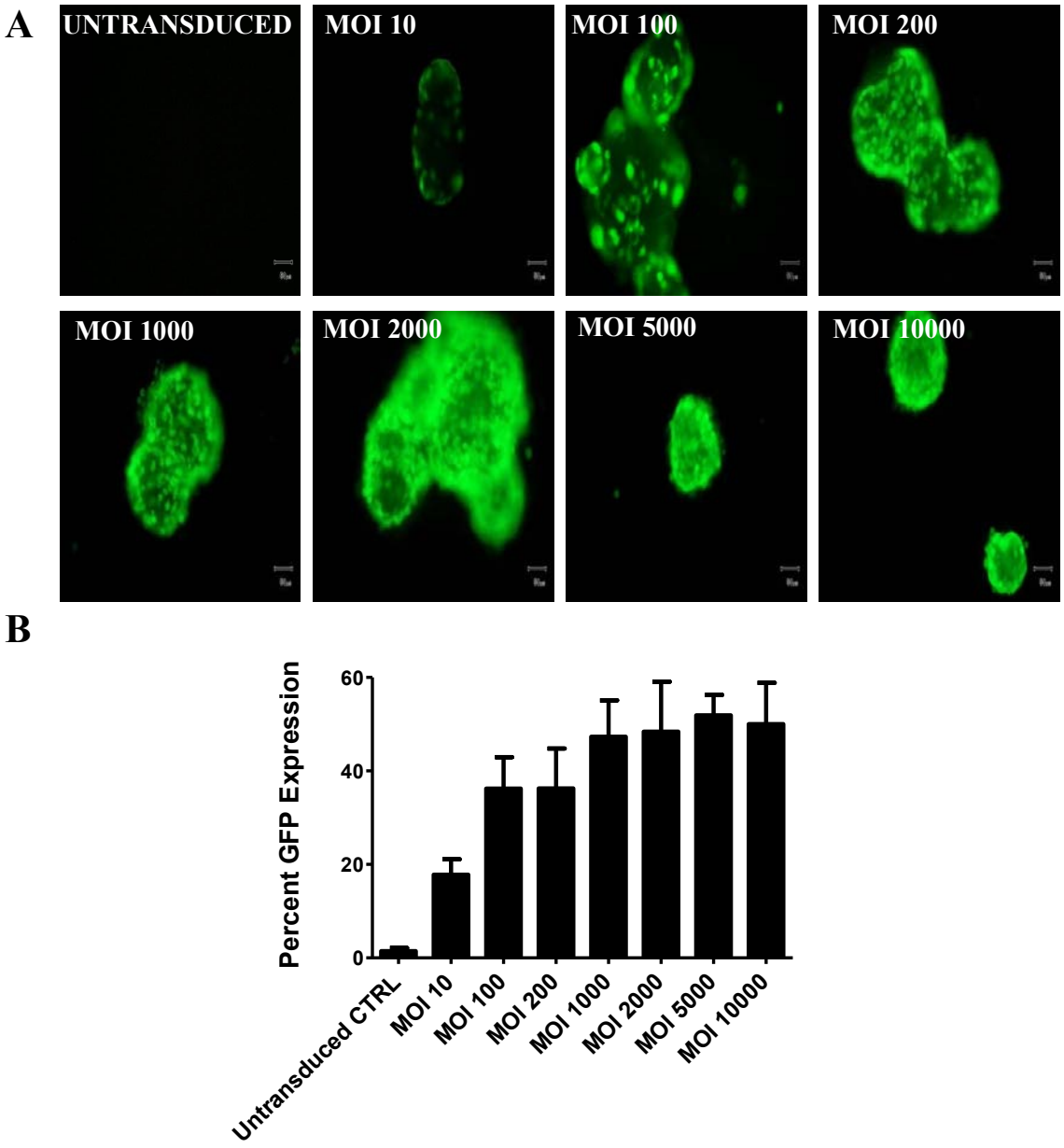

Figure 3.2.1. Ad-GFP transduction of rat islets. Rat islets were transduced with Ad-GFP at MOI 10, 100, 200, 1000, 2000, 5000 and 10000 or untransduced for 48 h. **(A)** Fluoresence microscopy was used to determine GFP positive (green) islet cells following Ad-GFP transduction. Representative images were taken at 10 x magnification, scale bar = 50 µm. **(B)** Transduced islets were dissociated and analysed for GFP expression using flow cytometry. Percent GFP expression was determined by three replicate experiments and expressed as mean ± SEM, $p \leq 0.0001$ (1way ANOVA).

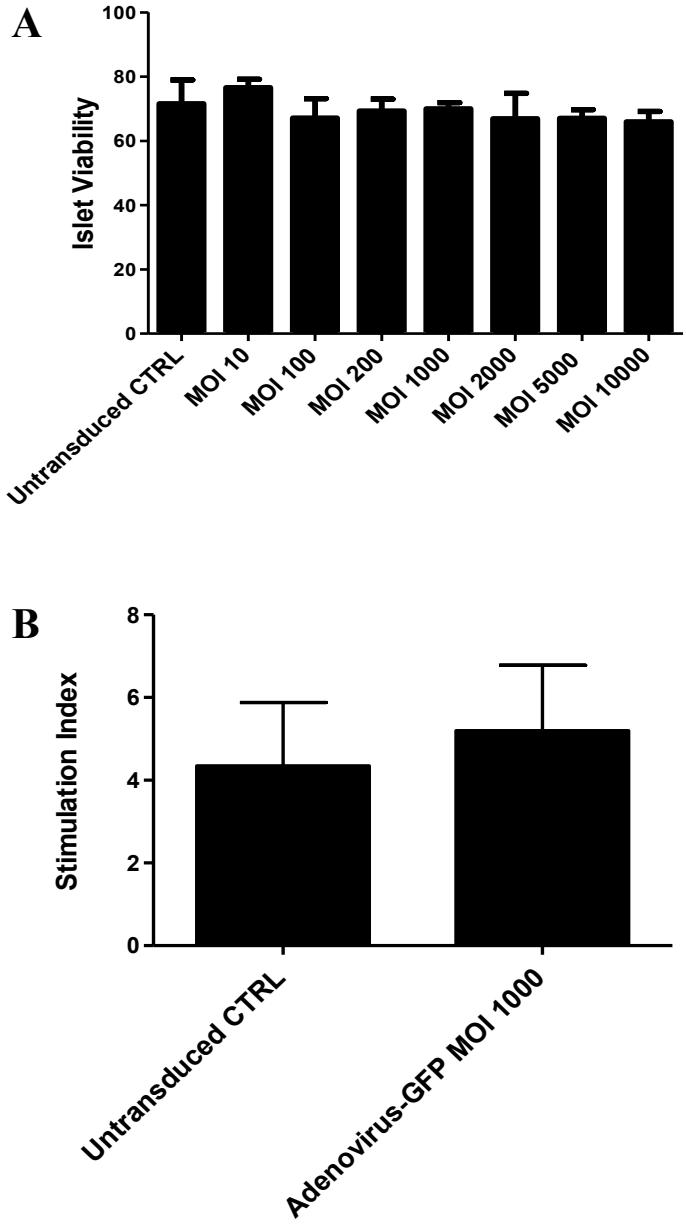

Figure 3.2.2. Characterisation of transduced rat islets *in vitro*. Rat islets were transduced with Ad-GFP at MOI 10, 100, 200, 1000, 2000, 5000, 10000 or untransduced for 48 h. **(A)** Transduced islet cells were dissociated and islet viability was assessed by 7-AAD staining using flow cytometry. Data was determined by two independent experiments and expressed as the mean ± SEM. **(B)** Rat islets were transduced with Ad-GFP (MOI 1000) for 48 h and stimulated to release insulin by exposure to high (25 mM) or low (2.8 mM) concentrations of glucose. Insulin ELISA was used to determine the SI in experimental samples. SI was determined by four replicate experiments and expressed as mean ± SEM.

3.2.3 GFP expression is localized to the perimeter in Ad-GFP transduced islets

To determine the pattern of GFP reporter gene expression in Ad-GFP transduced rat islets, isolated islets were transduced at MOI 1000 for 48 h. Using fluoresence confocal microscopy, positive GFP expression was localized to cells that were located at the islet periphery and no GFP positive cells were observed within the central core of the islet **(Figure 3.2.3)**.

3.2.4 Ad-GFP transduction induces GFP expression in human islets

The ability of Ad-GFP to transduce isolated human islets was assessed by fluorescence microscopy. Human islets were transduced with Ad-GFP at MOI 10, 100, 200, 1000, 2000, 5000 and 10000 for 48 h. Representative images showing the pattern of GFP positive (green) islet cells following transduction are shown in **Figure 3.2.4(A)**. Transduction of human islets at MOI 10 and MOI 100 led to 42.4 % ± 2.9 and 46.4 % ± 3.2 of human islet cells transduced, respectively. Transduction with either MOI 200 or MOI 1000 resulted in 52.4 ± 2.5 % and 71.5 ± 3.3 % human islet cells transduced, respectively. Ad-GFP transduction with MOI 5000 and 10000 reached a plateau of 72.2 ± 2.4 % and 70.3 ± 2.3 % human islet cells transduced, respectively **(Figure 3.2.4(B))**.

3.2.5 Ad-GFP transduction does not affect human islet viability

Human pancreatic islets were transduced with Ad-GFP at MOI 10, 100, 200, 1000, 5000 and 10000 or untransduced for 48 h to investigate the effects of Ad transduction on human islet viability. Human islet viability was not adversely affected following Ad-GFP transduction at any tested MOI **(Figure 3.2.5)**.

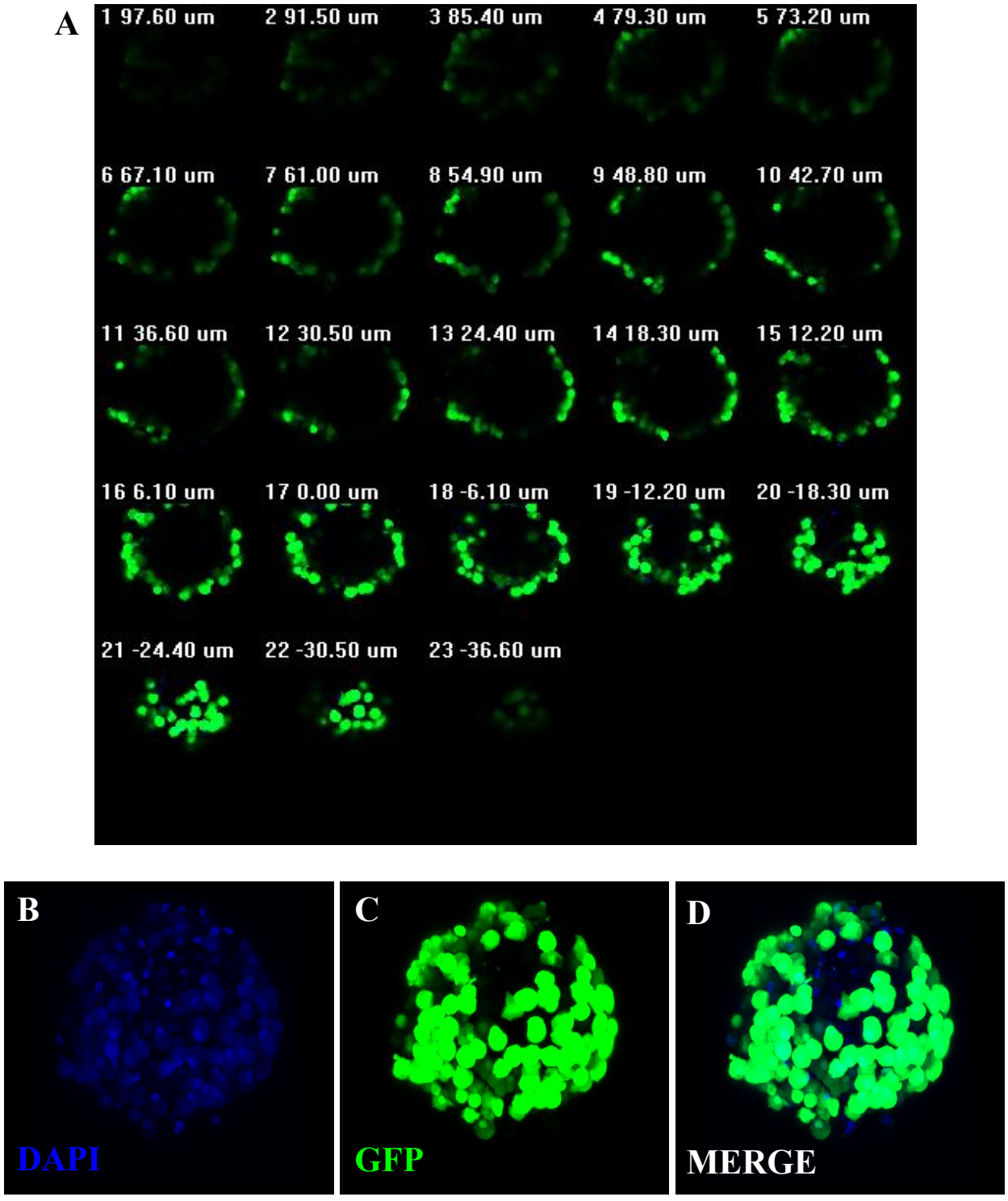

Figure 3.2.3. Pattern of Ad-GFP expression in transduced rat pancreatic islets. Rat islets were transduced with Ad-GFP at MOI 1000 for 48 h. **(A)** Fluoresence confocal image taken at fixed intervals along the z-axis of a Ad-GFP transduced islet, **(B)** Z-stack fluoresence confocal image of a DAPI (blue) stained islet, **(C)** Z-stack fluoresence confocal image showing GFP positive expression and **(D)** Z-stack fluoresence confocal image showing merge DAPI and GFP expression (23 sections). Images were taken at 60 x magnification, Scale bar = 50µm.

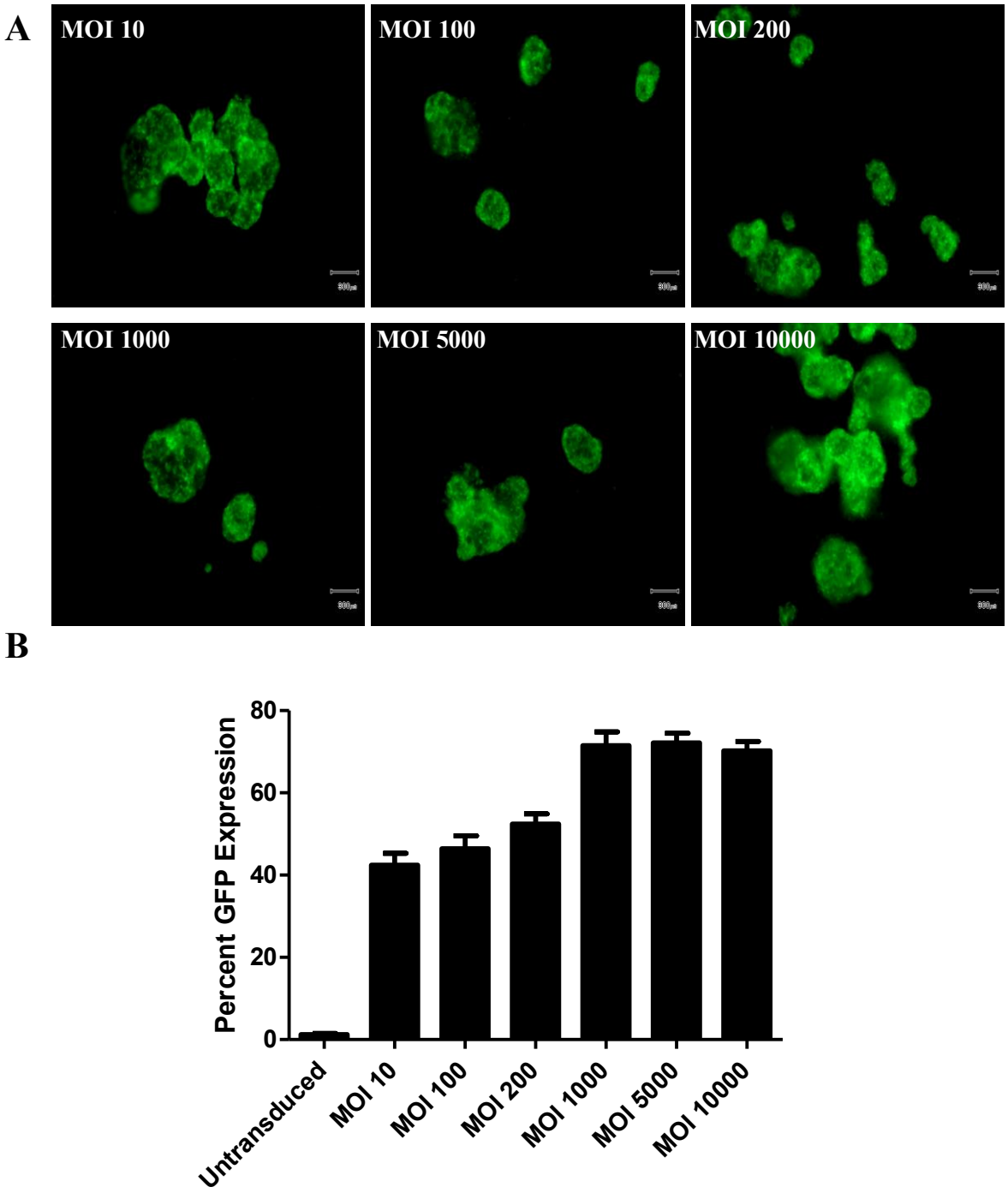

Figure 3.2.4. Ad-GFP transduction of human islets. Human islets were transduced with Ad-GFP at MOI 10, 100, 200, 1000, 2000, 5000 and 10000 or untransduced for 48 h. **(A)** Fluorescence microscopy was used to determine GFP positive (green) islet cells following Ad-GFP transduction. Representative images were taken at 4 x magnification, scale bar = 300 µm. **(B)** Transduced islets were dissociated and analysed for GFP expression using flow cytometry. Percent GFP expression was determined by two replicate experiments and expressed as mean ± SEM.

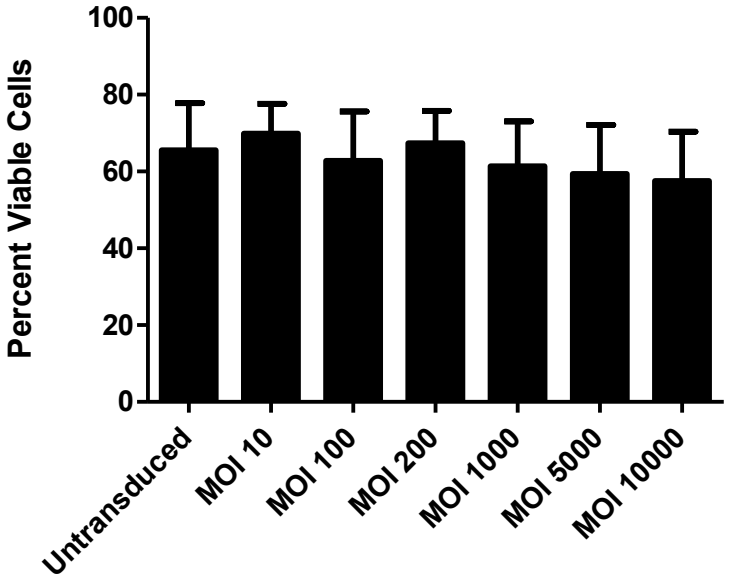

Figure 3.2.5. Viability of transduced human islets *in vitro*. Human Islets were transduced with Ad-GFP at MOI 10, 100, 200, 1000, 2000, 5000 and 10000 or untransduced for 48 h. Transduced islet cells were dissociated and islet viability was assessed by 7-AAD staining using flow cytometry. Data was determined by two independent experiments and expressed as the mean ± SEM.

3.2.6 GFP expression profile of AAV-GFP transduced rat pancreatic islets

Isolated rat islets were transduced with AAV2, AAV2/1, AAV2/8, AAV8mutY733F, AAV2muttriple or AAV2mutY444F vector types for five days. This preliminary experiment was performed to investigate the ability of AAV to transduce rat islets. Therefore, rat islets were transduced with the highest possible dose of each AAV vector (at varying titers).

Each AAV vector transduced rat islets with varying efficiencies **(Figure 3.2.6(A))**. AAV2/1, AAV2/8 and AAV8mutY733F transduced islets displayed positive GFP reporter gene expression at the earliest time point of 48 h. Subsequently, this GFP expression increased in AAV2/1, AAV2/8 and AAV8mutY733F transduced islets at 72 and 96 h. There was no positive GFP expression observed in AAV2, AAV2muttriple or AAV2mutY444F transduced islets at 48 h and GFP expression did not substantially increase over the transduction period.

At the conclusion of the experiment many of the islets in culture had become fragmented and possessed darkened, necrotic centres. This was particularly evident with AAV8mutY733F transduced islets (one of the highest titered vectors, 1.36×10^{13} vector genomes (vg)/ml) **(Figure 3.2.6(B))**, suggesting that the vectors are toxic to rat islets when used at high dosages.

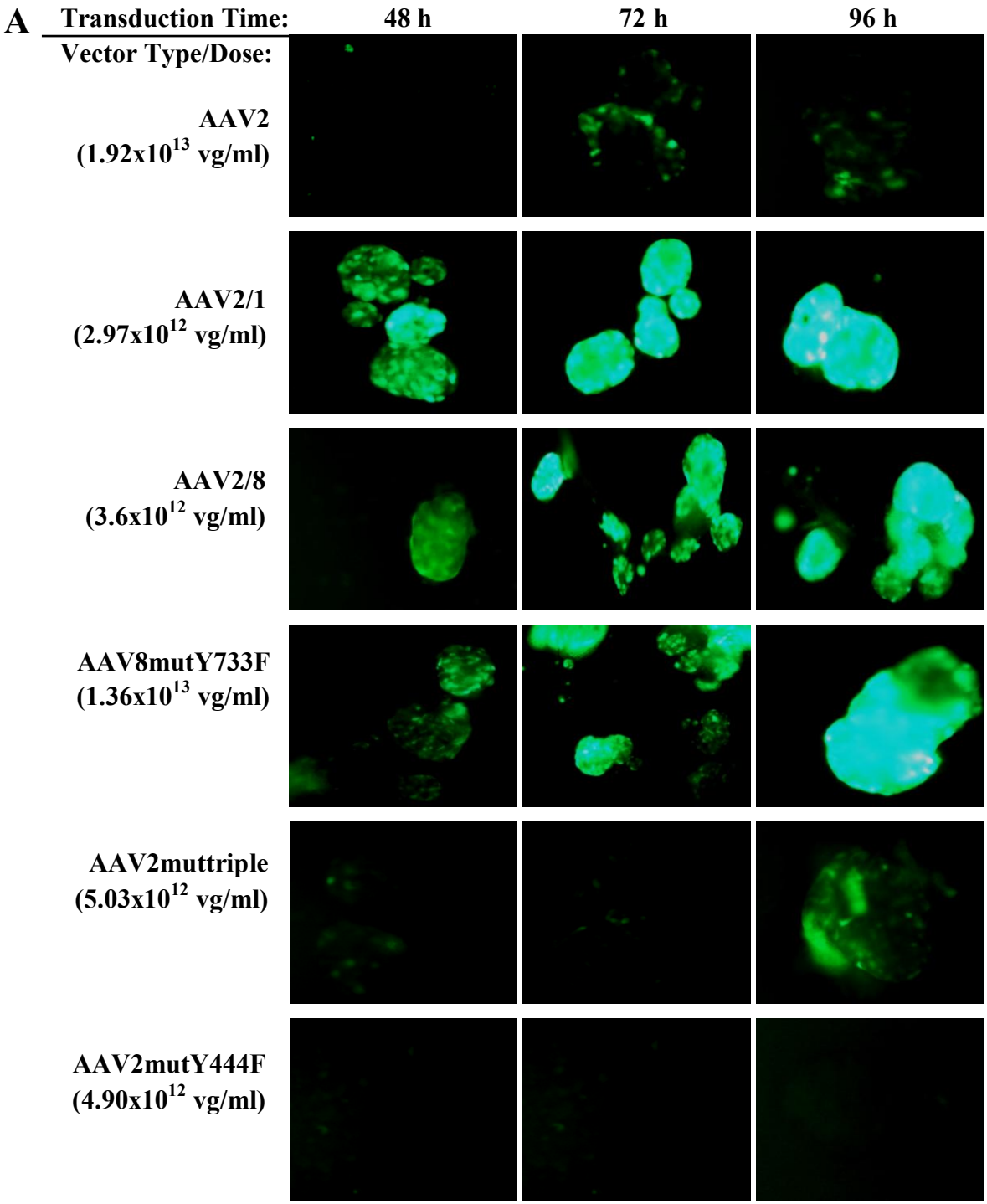
A
Transduction Time:
48 h
72 h
96 h
Vector Type/Dose:
AAV2
(1.92x10^13 vg/ml)
AAV2/1
(2.97x10^12 vg/ml)
AAV2/8
(3.6x10^12 vg/ml)
AAV8mutY733F
(1.36x10^13 vg/ml)
AAV2muttriple
(5.03x10^12 vg/ml)
AAV2mutY444F
(4.90x10^12 vg/ml)

B **AAV8mutY733F transduced rat islets**

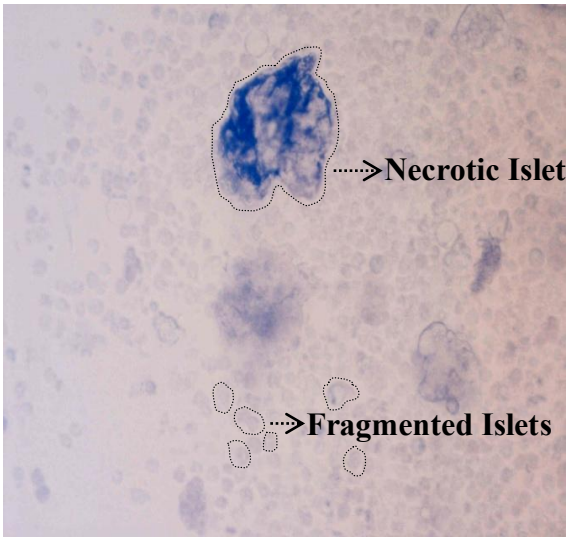

Figure 3.2.6. GFP expression and viability of AAV transduced rat pancreatic islets. Rat Islets were transduced with AAV2, AAV2/1, AAV2/8, AAV8mutY733F, AAV2muttriple and AAV2mutY444F for 96 h. **(A)** The vector type and viral dose used in transduction experiments is included on the left hand side of the fluorescent images. Representative images were taken at 10 x magnification. **(B)** Transduced islets were visualised under a light microscope to determine islet morphology following transduction. Representative image of AAV8mutY733F transduced islets was taken at 10 x magnification.

3.2.7 GFP expression profile of AAV-GFP transduced rat islets with vector dose $6.25x10^8$, $1.25x10^9$, $2.5x10^9$ and $5x10^9$ vg

Due to the varied ability of AAV2, AAV2/1, AAV2/8, AAV8mutY733F, AAV2muttriple and AAV2mutY444F vectors to transduce isolated rat islets and the adverse toxic effects to the transduced islets as a result of the high vector dose used for transduction **(see figure 3.2.6)**, rat islets were transduced with AAV vectors at four lower doses ($6.25x10^8$, $1.25x10^9$, $2.5x10^9$ and $5x10^9$ vg total/well). Vector genomes (vg) represent the total number of viral particles (live and dead combined) in a viral preparation. Therefore, the vg number does not represent the amount of active virus in the preparation. Based on this, viral dose is often described using particle forming units (pfu)/ml as it reflects the amount of working virus in the preparation. The vg:pfu ratio is often 50:1 (Vector Biolabs, www.vectorbiolabs.com/vbs/faq-product.htm) therefore based on this the four lower vector doses equate to MOI 1000, 500, 250 and 125, respectively.

Fluoresence resulting from GFP reporter gene expression in transduced rat islets was evaluated by flow cytometry to determine transduction efficiency**.** Rat islet transduction with AAV vectors resulted in dose-dependent GFP expression **(Figure 3.2.7)**. AAV2/1 was the most efficient vector at transducing rat islets as it led to 10.4 ± 1.3% of rat islet cells transduced at the highest vector dose of $5x10^9$ vg. Furthermore, AAV2/1 provided 1.6- and 3.6-fold higher transduction of rat islet cells compared to AAV2 (4.5 ± 0.4%) and AAV2/8 (3.02 ± 0.9%) at the highest vector dose of $5x10^9$ vg, respectively. Surprisingly, all AAV mutants (AAV8mutY733F, AAV2muttriple and AAV2mutY444F) displayed minimal transduction of islets (1 ± 0.4%, 0.7 ± 0.1% and 0.7 ± 0.08%, respecitvely), with 5 – 15 fold lower transduction compared to AAV2/1 even at the highest vector dose of $5x10^9$ vg.

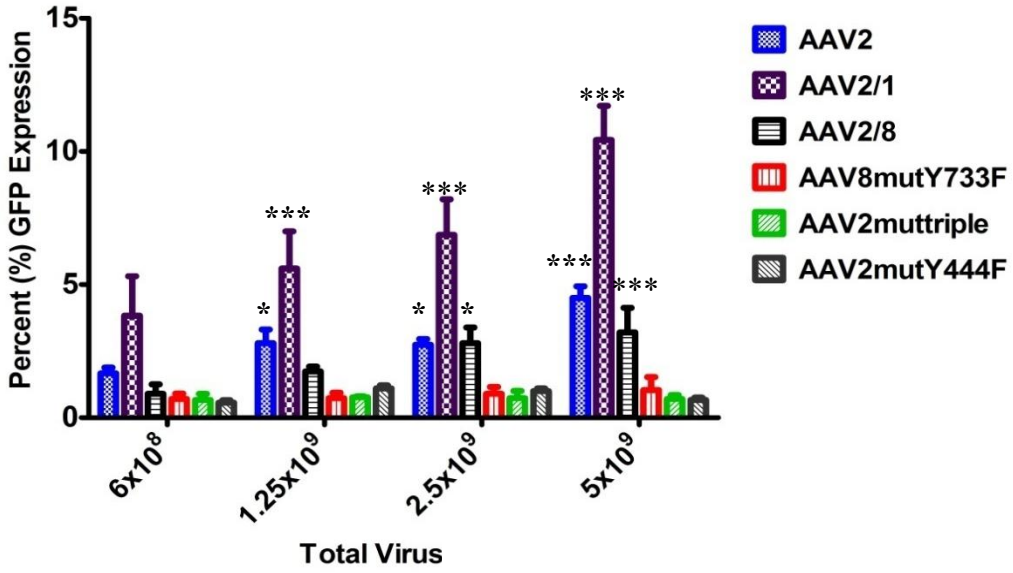

Figure 3.2.7. GFP expression following AAV-GFP transduction of rat islets. Rat islets were transduced with AAV2, AAV2/1, AAV2/8, AAV8mutY733F, AAV2muttriple and AAV2mutY444F at $6.25x10^8$, $1.25x10^9$, $2.5x10^9$ and $5x10^9$ vg or untransduced for 48 h. Specific vector types are listed in the margin on the right hand side of the graph. Transduced islets were dissociated and analysed for GFP expression using flow cytometry. Percent GFP expression was determined by three replicate experiments and expressed as mean ± SEM, $p \leq 0.0001$ (1way ANOVA). Bonferroni Post-Test: *$p \leq 0.05$ or ***$p \leq 0.001$ compared to untransduced control islets.

3.2.8 AAV-GFP based vectors transduce rat islets with various levels of efficiency

The ability of AAV-GFP based vectors to transduce isolated rat islets at $5x10^9$ vg, was determined by transducing rat islets with AAV2, AAV2/1, AAV2/8, AAV8mutY733F, AAV2muttriple or AAV2mutY444F and assessed by fluorescence microscopy. A vector dose of $5x10^9$ vg was chosen based on the fact that it correlates to a MOI of 1000 which allows it to be directly compared with the previous Ad-GFP characterisation experiments.

Representative images showing the pattern of GFP positive (green) islet cells following transduction are shown in **Figure 3.2.8**. AAV2, AAV2/1 and AAV2/8 provided the best transduction of rat islets, as all islets within the culture were transduced **(Figure 3.2.8(B-D))**. AAV8mutY733F showed minimal transduction of isolated rat islets and AAV2muttriple and AAV2mutY444F showed a very modest ability to transduce rat islets **(Figure 3.2.8(E-G))**, as reflected by the flow cytometric data **(See Figure 3.2.7)**

3.2.9 GFP expression is localized to the islet perimeter in AAV2/1 transduced rat islets

To determine the pattern of GFP reporter gene expression in AAV2/1 transduced rat islets, isolated islets were transduced at $6.25x10^8$, $1.25x10^9$, $2.5x10^9$ and $5x10^9$ vg or untransduced for 72 h. As found with Ad transduction **(See Figure 3.2.2)**, positive GFP expression was localized only to the periphery cells of the islet and no GFP positive cells were observed within the central core of the islet **(Figure 3.2.9)**.

3.2.10 AAV-GFP transduction does not affect viability or glucose stimulated insulin secretion of rat islets

Rat pancreatic islets were transduced with AAV2, AAV2/1, AAV2/8, AAV8mutY733F, AAV2muttriple and AAV2mutY444F or untransduced for 72 h to investigate the effect of AAV transduction on islet viability and function. Rat islet viability was not adversely affected following transduction with any of the AAV vector types, compared to untransduced islet controls **(Figure 3.2.10)**.

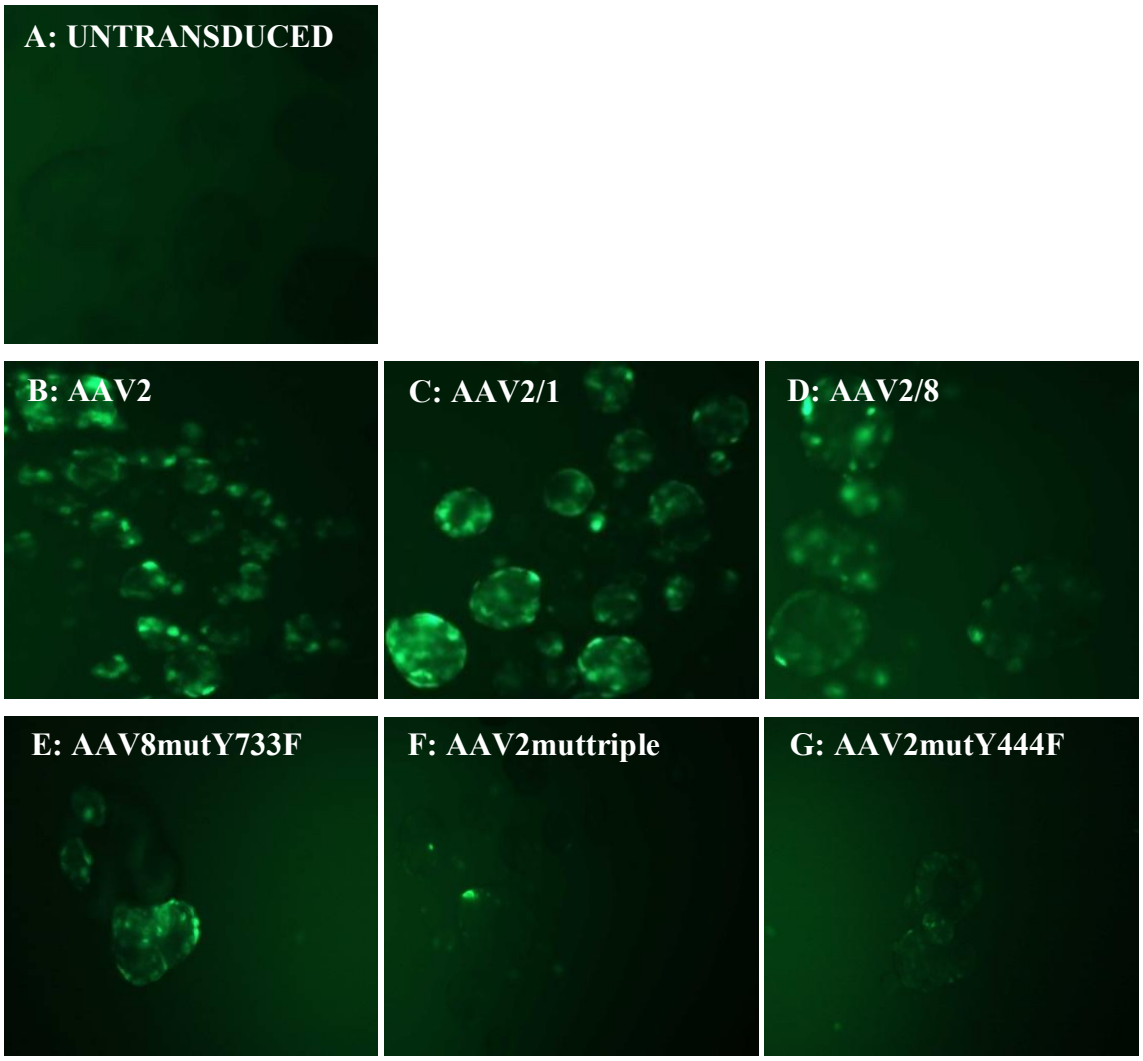

Figure 3.2.8. GFP Expression in AAV-GFP transduced rat pancreatic islets. Rat islets were **(A)** untransduced or **(B-G)** transduced with AAV2, AAV2/1, AAV2/8, AAV8mutY733F, AAV2muttriple and AAV2mutY444F at $5x10^9$ vg for 72 h. Fluorescence microscopy was used to determine GFP positive (green) islet cells following transduction. Representative images were taken at 4 x magnification.

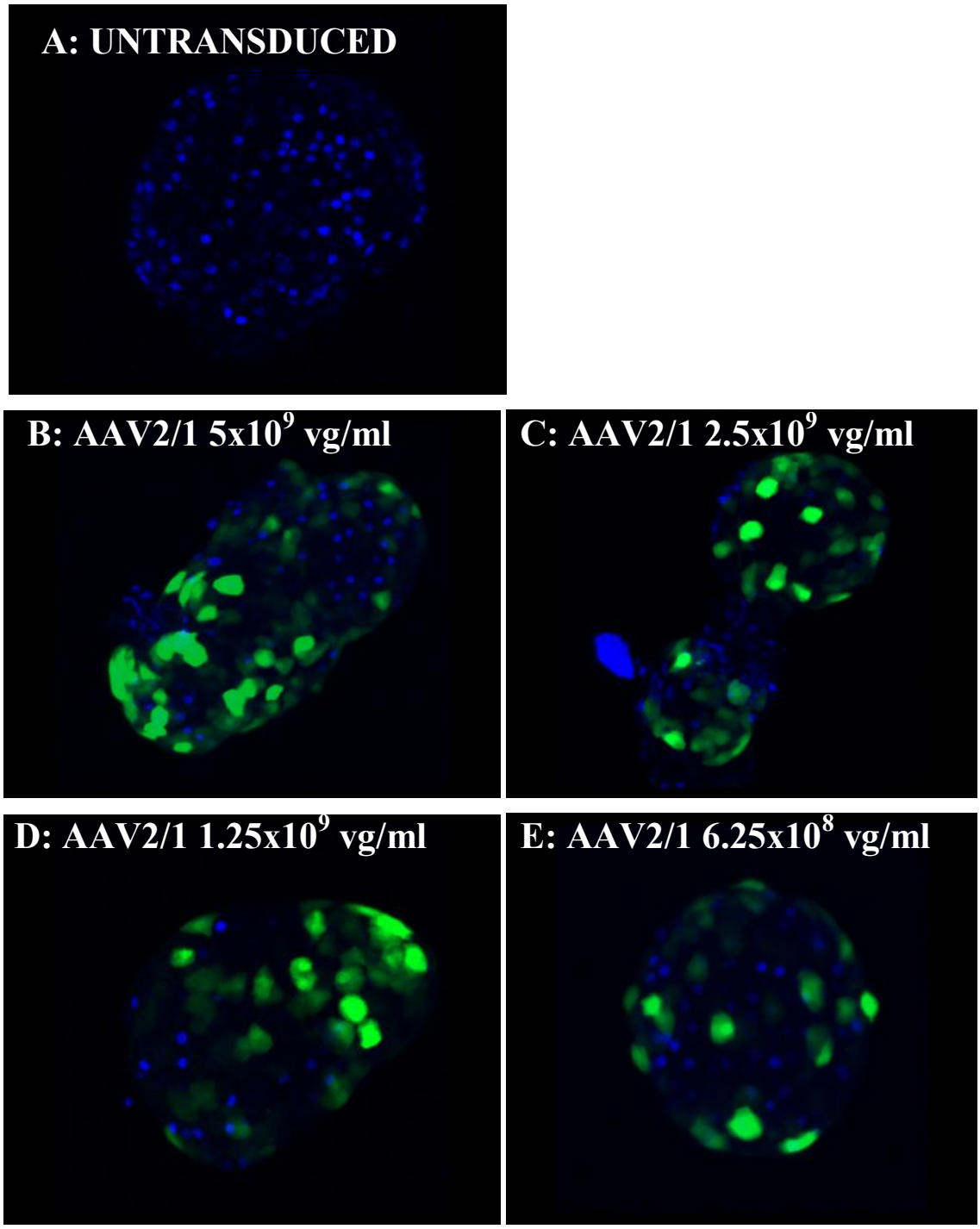

3.2.9. Pattern of AAV2/1 GFP expression in transduced rat pancreatic islets. Rat islets were **(A)** untransduced or transduced with AAV2/1 at $6.25x10^8$ (36 sections, 0-42 µm) $1.25x10^9$ (34 sections, 0-32 µm) $2.5x10^9$ (26 sections, 0-28 µm) and $5x10^9$ (32 sections 0-32 µm) vg total/well **(B-E)** for 72 h. Z-stack fluorescent confocal images show merge DAPI (blue) and GFP expression (green). Images were taken at 40 x magnification.

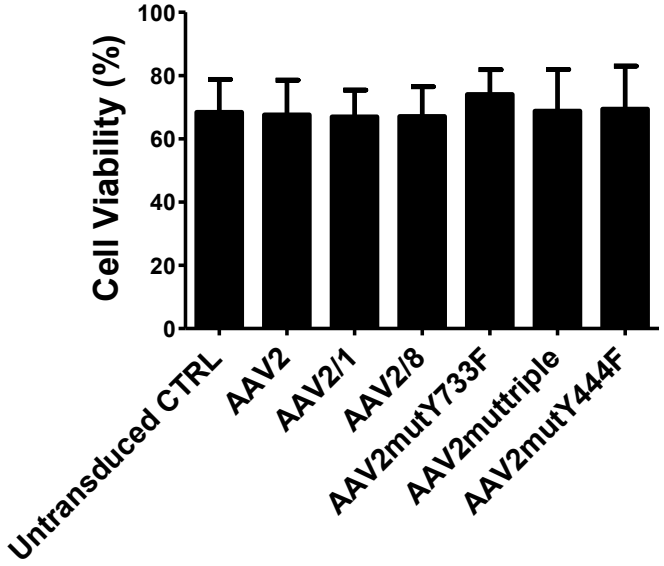

Figure 3.2.10. Characterisation of AAV transduced rat islets *in vitro*. **A.** Rat islets were transduced with AAV2, AAV2/1, AAV2/8, AAV8mutY733F, AAV2muttriple and AAV2mutY444F at $5x10^9$ vg or untransduced for 72 h. Transduced cells were dissociated and islet viability by 7-AAD staining using flow cytometry. Data was determined by three independent experiments and expressed as the mean ± SEM.

3.2.11 AAV-GFP based vectors failed to transduce isolated human islets

The ability of AAV-GFP based vectors to transduce isolated human islets at $5x10^9$ vg, was determined by transducing human islets with AAV2, AAV2/1, AAV2/8, AAV8mutY733F, AAV2muttriple and AAV2mutY444F. The transduction efficiency of each vector type was assessed by fluorescence microscopy. GFP expression was not observed in human islets transduced with any of the six AAV vector types, indicating that all vector types failed to effectively transduce human islets **(Figure 3.2.11)**.

3.2.12 GFP expression profile of AAV-GFP transduced human islets

Human islets were transduced with AAV2, AAV2/1, AAV2/8, AAV8mutY733F, AAV2muttriple or AAV2mutY444F at $5x10^9$ vg for 72 h. Fluoresence resulting from GFP reporter gene expression in transduced human islets was evaluated by flow cytometry to determine transduction efficiency **(Figure 3.2.12)**. Transduction of human islets with all AAV vector types resulted in very weak GFP expression, which was only slightly increased compared to the background GFP expression in untransduced control islets (0.4 ± 0.2%). AAV2, AAV2/1 and AAV2/8 transduction resulted in 3.3 ± 0.9%, 1.2 ± 0.2% and 0.9 ± 0.3% of GFP positive human islet cells, respectively. The three mutant vectors (AAV8mutY733F, AAV2muttriple and AAV2mutY444F) failed to transduce human pancreatic islets.

3.2.13 GFP expression profile of AAV-GFP transduced HEK 293 cells

To determine if the low transduction efficiency seen in rat and human islets with the three mutant vectors was specific to isolated islets, the transduction efficiency of AAV was investigated in another cell type. Human Embryonic Kidney (HEK) 293 cells were transduced with AAV2, AAV2mutY444F and AAV2muttriple vector types for 24 h. AAV2 transduced 10.2% of HEK 293 cells. GFP expression was markedly increased in HEK 293 cells transduced with both AAV2muttriple and AAV2mutY444F (20.5% and 97%) positive GFP expressing cells, respectively **(Figure 3.2.13)**.

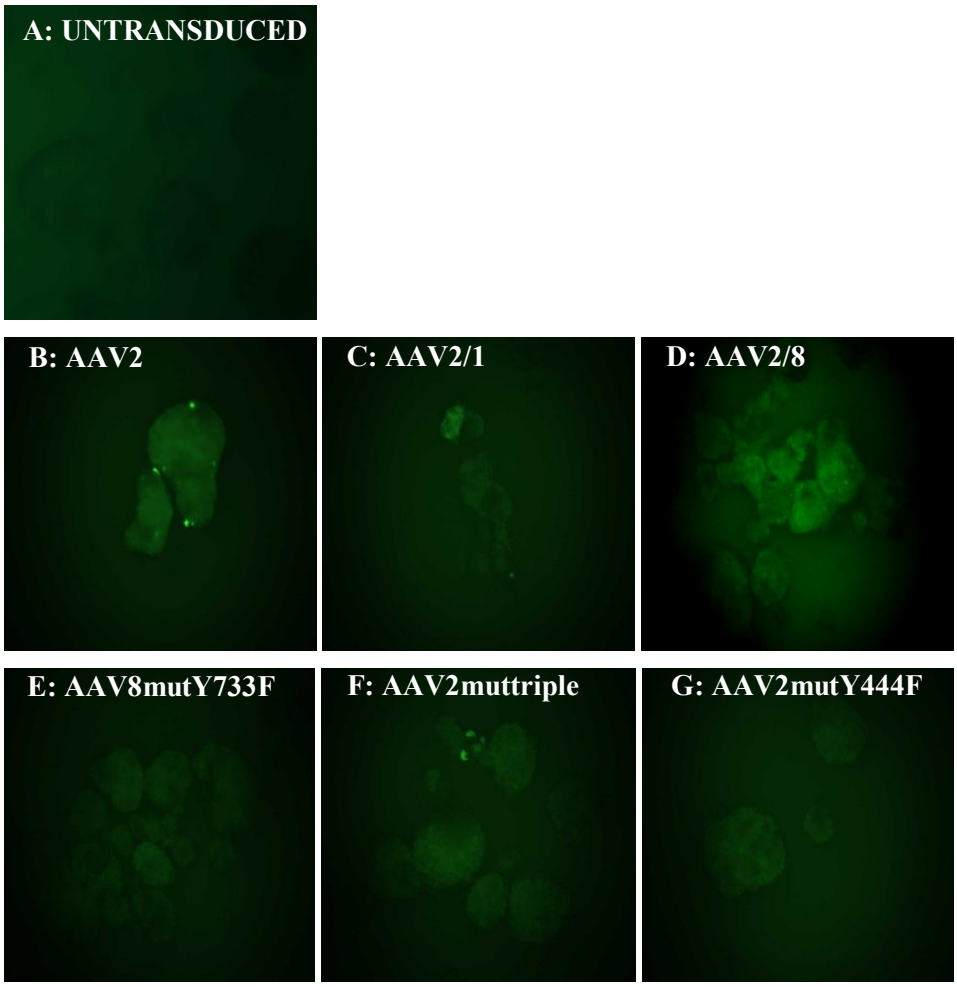

3.2.11. GFP expression in AAV-GFP transduced human pancreatic islets. Human islets were **(A)** untransduced or transduced with AAV2, AAV2/1, AAV2/8, AAV8mutY733F, AAV2muttriple and AAV2mutY444F at $5x10^9$ vg **(B-G)** 72 h. Fluorescence microscopy was used to determine GFP positive (green) islet cells following AAV transduction for 72 h. Representative images were taken at 4x magnification.

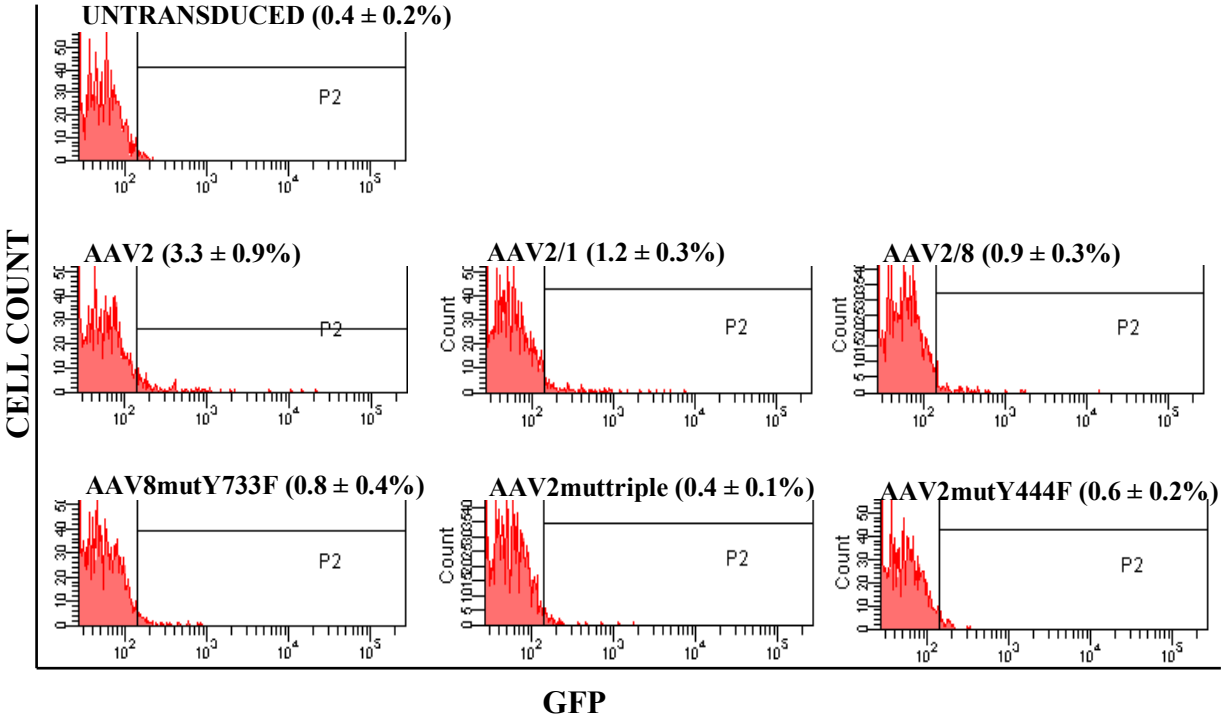

3.2.12. GFP expression following AAV-GFP transduction of human islets. Human islets were transduced with AAV2, AAV2/1, AAV2/8, AAV8mutY733F, AAV2muttriple or AAV2mutY444F at $5x10^9$ vg or untransduced for 72 h. Transduced islets were dissociated and analyzed for GFP expression using flow cytometry. Specific vector types are listed above the histograms. Histograms represent the number of cells plotted against the cellular GFP expression of transduced human islets. Data was determined by three replicate experiments and expressed as mean ± SEM.

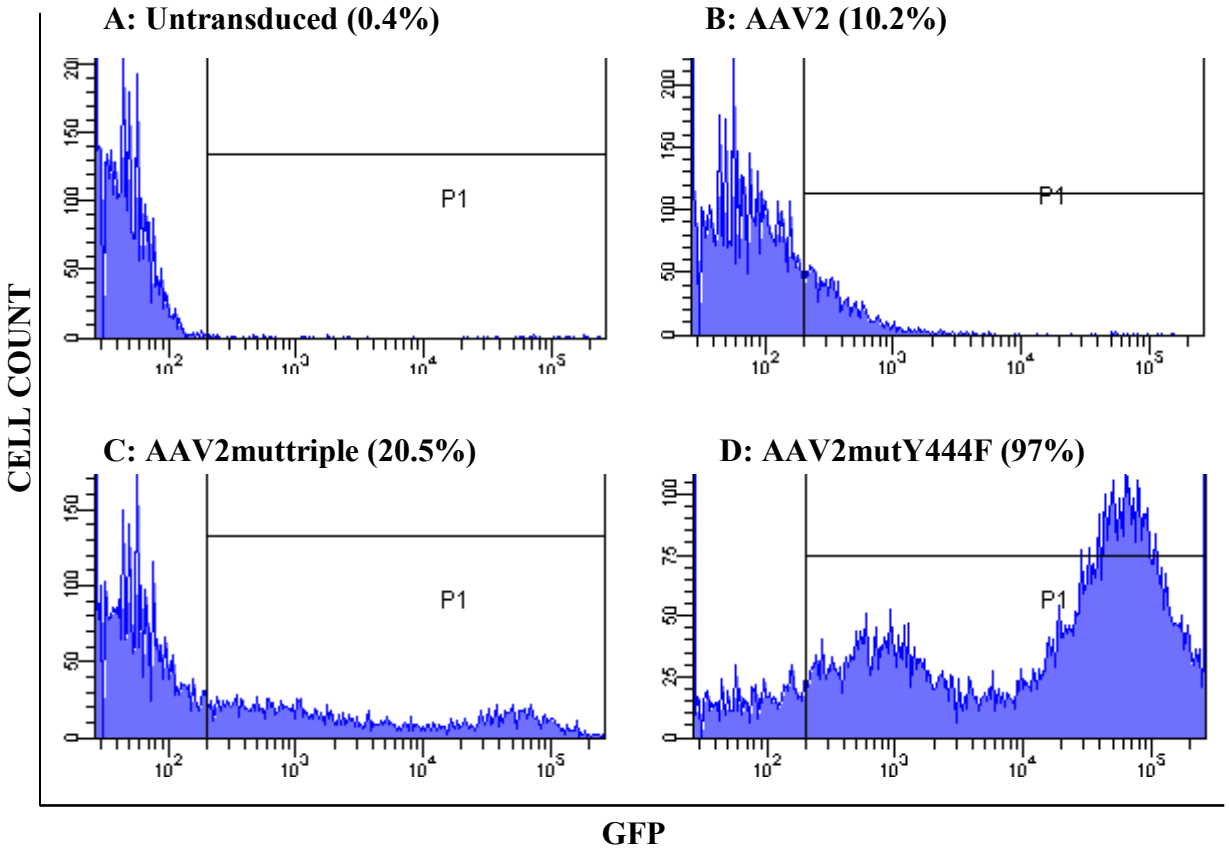

3.2.13. GFP expression following AAV-GFP transduction of HEK 293 cells. HEK 293 cells were **(A)** untransduced or transduced with AAV2, AAV2muttriple, AAV2mutY444F with $5x10^9$ vg **(B-D)** for 24 h. HEK 293 cells were harvested and analysed for GFP expression using flow cytometry. Histograms represent the number of cells plotted against the cellular GFP expression. Specific vector types are listed above the histograms. Percent GFP expression is shown in brackets above the histogram.

3.2.14 Immunohistochemical staining for heparan sulphate proteoglycan and integrin αvβ5 in human pancreatic islets

The stability of receptor compositions on human islets are not necessarily stable following the enzymatic isolation of islets. To investigate if the stripping of cellular receptors on human islets was responsible for the poor transduction efficiency of AAV, immunohistochemical staining for two AAV cellular receptors, Heparan Sulphate Proteoglycan (HSPG) and integrin αvβ5 was performed. HSPG and integrin αvβ5 were highly expressed within native pancreatic tissue. In comparison, the expression of the cellular receptors was reduced following islet isolation and did not increase during the remaining culture period **(Figure 3.2.14)**.

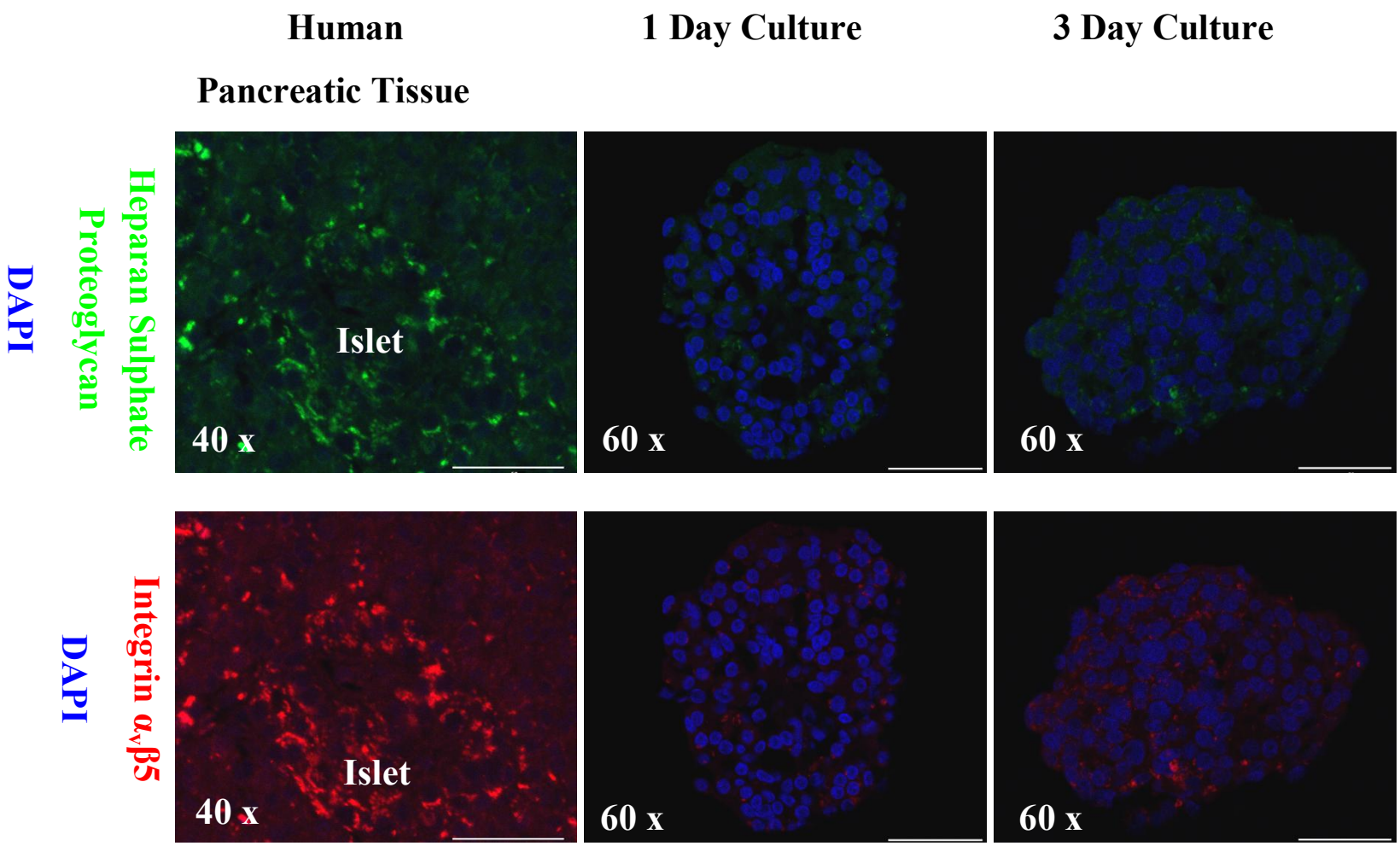
Human
Pancreatic Tissue
1 Day Culture
3 Day Culture
Heparan Sulphate
Proteoglycan
DAPI
Islet
40 x
60 x
60 x
Integrin αvβ5
DAPI
Islet
40 x
60 x
60 x

Figure 3.2.14 Heparan sulfate proteoglycan and integrin αvβ5 staining of human pancreatic islets. Native human pancreatic tissue was fixed with 10% buffered formalin prior to histochemical processing. Human pancreatic islets were cultured one or three days following isolation and then paraffin embedded prior to histochemical processing. Representative fluorescence confocal images, showing herparan sulphate proteoglycan staining, and integrin αvβ5 staining. Images were taken at 40 or 60 x magnification as indicated, scale bar = 50 μm.

3.3 Discussion

In this study, the efficiency and functional consequences of Ad- and AAV-based vector transduction of rat and human pancreatic islets was investigated *in vitro*. Firstly, Ad efficiently transduced both rat and human pancreatic islets without affecting islet viability or function, but there were slight differences in the transduction efficiency between species. For example, Ad transduced 50 ± 8.8% of rat islet cells and 70.3 ± 2.3% of human islet cells at the highest vector dose of multiplicity of infection (MOI 10000). It is also interesting to note that Ad transduction with high viral MOI (i.e. 5000 and 10000) appeared to reach a saturation threshold where all available islet cells were transduced, and there was an inability of both Ad and AAV viral vectors to transduce the inner β-cell rich core of rat islets. This finding is also supported by various other literature studies (113, 114, 117, 135, 357, 358). The three dimensional structure of intact islets (50-500 μm) in diameter and the islet basement membrane can make vector access to the islet core difficult (359).

To improve transduction of the islet core, Lefebvre and colleagues (359) briefly distended the islet membrane with Accutase. Islet distension enhanced the siRNA transduction efficiency of human and mouse islets without compromising *in vitro* function. A potential issue that exists with this method is the use of Accutase which through its enzymatic activity can strip cell surface receptors (360), including those required for viral uptake and subsequent gene expression. Another approach to improve transduction efficiency is to increase the viral MOI per cell, however increased viral load can be toxic to the islets (361). Emamaullee and colleagues (209) have shown that transduction of islets less than 1 hour after isolation (while the microcapillary network is still intact) allows for improved Ad transduction efficiency (95%) at low MOI (MOI 10).

In this study, AAV transduction efficiency was reduced in rat and human pancreatic islets, compared to Ad, and AAV exhibited a slower onset of GFP gene expression (72 hours versus 48 hours with Ad-GFP). Late onset gene expression is characteristic of single-stranded AAV vectors and is a result of the need to convert the single stranded DNA vector genome into double stranded DNA prior to transgene expression (362). Prolonged human islet culture leads to a decrease in islet function and induces islet cell death (363, 364), based on this, double stranded AAV vectors were used in this study as they provide significantly faster gene expression (3 days) versus the reported 5 – 7 days in single stranded DNA vectors (323, 365).

Zhang and colleagues (366) have shown that wild type AAV2 transduced human islets more efficiently than murine islets, while AAV2/1 transduced murine islets more efficiently than human islets. In this chapter, AAV2/1 transduced rat islets more efficiently then human islets. Others (367) have reported that rat islets can be efficiently transduced with AAV2/5 (9% transduction), but less efficiently with AAV2/2 and AAV2/8 at MOI 1500. While AAV5, which utilises α-2,3-N-linked sialic acid as a receptor was not tested in this study, it was shown that AAV2/2 did not transduce rat islets as efficiently as AAV2/1, and that AAV2/8 was even less efficient. When Rehman (368) compared AAV2 vectors pseudotyped with serotype capsids of 1, 2, 5, 6, 7, 8 in human islets, AAV 2, 6 and 8 transduced human islets more efficiently than the other serotypes. AAV2 transduced both murine and human islets (>40% GFP), although a very high MOI of 10000 was required. However the consequence of a MOI this high would have to be thoroughly investigated prior to the implementation of AAV in a clinical islet transplant setting.

An unexpected finding of this study was the limited transduction of human islets by AAV. This may be due to the loss or 'stripping' of viral receptors during the isolation process, which uses a more aggressive enzymatic digestion protocol than that required to dislodge rodent islets from their native environment. The 37/67-kDa lamR has been identified as a cellular receptor for AAV8 and AAV9 (349, 350). Laminin is present in the islet extracellular matrix (369-374), and although we did not stain for laminin, the enzyme mediated stripping of laminin during islet isolation may be a likely explanation why low transduction was seen in this study using an AAV2/8 vector. AAV2 utilize heparan sulfate proteoglycan (HSPG) as a primary receptor, in addition to subsequent interactions with αvβ5/α5β1 integrins. Summerford et al (132) have reported that the presence of HSPG on the cell surface directly correlates with the efficiency by which AAV can infect cells. The receptor composition of isolated islet cells is not necessarily stable, as integrin expression has been observed to decrease in culture (375), but integrin expression can be up regulated in the presence of certain extracellular matrix proteins (376). Human islet cells express integrins α3, α5, α6, αv, β1, β3 and β5 integrin components which co-localize closely with insulin immunoreactivity within the islet (373, 375, 377, 378). However, the expression of these integrins on islets is reduced after isolation (373, 375). It may be possible to intervene to improve the transduction efficiency of AAV by a strategy that seeks to re-establish the islet-extracellular matrix relationship and enhance the turn over rate of the stripped viral receptors (375).

It is interesting to note that unlike AAV, the Ad vector efficiently transduced human islets. The Coxsackie and Adenovirus Receptor (CAR) is a cell adhesion molecule that acts as a cellular receptor for all Ad serotypes, in addition to integrin co-receptors which are required for Ad internalization. Thus, it is possible that the internalization of Ad may have occurred via a secondary pathway, the cellular machinery for which is not removed during the islet isolation process. This is supported by Bai and colleagues (379) who have demonstrated the existence of an integrin-independent pathway of Ad internalization.

Currently, the need for large quantities of vector for clinical applications is the primary disadvantage to the utilisation of AAV. Therefore, selective mutation of AAV surface-exposed tyrosine residues is a novel strategy to enhance AAV infectivity and reduce the vector dose required (380). As discussed previously, phosphorylation of AAV capsid proteins at tyrosine residues targets the virus for ubiquitination and subsequent proteasomal-mediated degradation. This significantly affects the total amount of virus that can traffic to the nucleus and subsequently limits transgene expression. Several studies (381-385) have shown that proteasome inhibitors enhance transduction by AAV2, AAV5, AAV7, and AAV8 vectors. Higher transduction efficiency has been extensively reported in skeletal muscle, retina, lung and liver (320, 380, 386-388) when transduced with tyrosine mutant AAV compared to a wild type AAV2 vector. Moreover, Markusic et al (389) have shown 3-fold higher *in vitro* gene transfer to murine hepatocytes using an AAVmuttriple vector, compared to single-mutant vectors and 30 – 80 fold higher transduction, compared to wild type AAV2 capsids. However, in this chapter the tyrosine mutant vectors AAV8mutY733F, AAV2muttriple and AAV2mutY444F failed to effectively transduce rat or human pancreatic islets. AAV2mutY444F transduction of HEK 293 cells led to 2-fold increased transduction efficiency compared to AAV2 wild type vector. When HEK 293 cells were transduced with AAV2muttriple the percentage of transduced cells increased 9.5 fold, indicating that the inability of AAV mutant vectors in this study to transduce islets is an islet specific phenonomen, as the HEK 293 cell line was not resistant to AAV transduction.

While the enhanced transduction efficiency reported to occur with tyrosine mutant vectors is a promising step forward in the generation of clinically relvant AAV vectors, the tyrosine mutant vectors have not demonstrated enhanced efficacy in all tissue and cell types. For example, proteasome inhibitors enhanced AAV2 mediated transduction of mouse lung and liver, but did not improve transduction efficiency in skeletal or cardiac muscle (381). A more recent study has shown that proteasome inhibitors can increase AAV7 and AAV8 transduction of vascular endothelial cells, but have no effect on smooth muscle cells. In similar *in vitro* studies, proteasome inhibitors increased the transduction efficiency of AAV2 and AAV5 in human polarized airway epithelia. However, transduction by these vectors was limited on the basolateral side (385). The varied transduction efficiency of AAV mutant vectors may be linked to the differences in the intracellular milieu or viral intracellular trafficking pathways that exist in different cell and tissue types, however further studies are required to delineate the precise mechanisms controlling this phenonomen.

The results in this chapter demonstrate that Ad vectors are far more efficient at transducing rat and human pancreatic islets than AAV-based vectors. In addition, AAV vectors containing either single or triple tyrosine mutations were insufficient to enhance gene delivery to the islets. A recent study has shown that the mutation of three tyrosine residues on the AAV2 capsid to non-phosphorylated phenylalanine residues (AAV2muttriple) enhances vector transduction efficiency in ganglion cells of the eye by >30-fold, however an increase in the number of tyrosine residues (up to six) did not further enhance transduction efficiency (387). Others (354) have described an inability of single tyrosine mutant AAV8 and AAV9 vectors to enhance gene delivery to skeletal muscle and heart. A potential reason for the low transduction efficiency of AAV mutant vectors may be due to an altered receptor affinity for viral binding. This is supported by Petrs-Silva et al (387) who have shown that tyrosine residues such as 700, 704 and 730 are located close to a positively charged patch of amino acids, which comprise the heparan sulphate-binding region on the AAV2 capsid surface, and subsequently alters the ability of AAV2 to interact with its primary receptor.

The subsequent data in this chapter identified that AAV-based vectors display differing transduction efficiencies in different cell and tissue types, a finding which is in support of the previously published AAV literature. A major finding of this chapter is that the aggressive enzymation isolation of human islets may lead to stripping of the cell surface receptors required for efficient AAV vector uptake. However, this is speculative and warrants further investigation, utilizing an increased repertoire of AAV serotype and extracellular matrix markers. This information may provide clues regarding the optimal matrix proteins to re-establish the islet-matrix relationship and thereby enhance AAV transduction efficiency. Until such studies are undertaken, Ad vectors currently represent the optimal vector choice for use in an islet gene therapy setting. Therefore, an Ad vector containing the anti-apoptotic gene, Insulin-like Growth Factor-II (IGF-II) was characterised in **Chapter 4**.

CHAPTER 4

CHARACTERISATION OF AN ADENOVIRAL BASED VECTOR ENCODING HUMAN INSULIN-LIKE GROWTH FACTOR II

4.1 Introduction

The transition of islet transplantation from its experimental research beginning to current clinical practice for patients with brittle Type 1 Diabetes (T1D) and hypoglycaemia unawareness is gaining acceptance worldwide, with over 750 islet transplants performed to date. However, current limitations of islet transplantation include scarcity of donor tissue, partially effective islet isolation and purification protocols, the requirement for life-long immunosupression, inadequate transplantation sites and destruction of the transplanted islets by apoptosis. The final outcome of these processes is a reduction in the effective β-cell mass and early failure of the islet allograft (390). Therefore, inhibition of apoptosis is an imperative strategy to prevent the loss of islet mass in the immediate post-transplant period. To this end, gene transfer provides a promising approach to improve post-transplant islet survival and function for the treatment of T1D.

Various anti-apoptotic strategies have shown promise in experimental models of islet transplantation, but not all strategies have led to significant improvement in islet transplant outcomes (391-393). Recently, investigation of the anti-apoptotic molecule Insulin-like Growth Factor-II (IGF-II) has demonstrated promise in an encapsulated rodent model of engraftment (232), however this study is disadvantaged by the fact that co-encapsulated islets are unable to revascularize following transplantation, exacerbating islet hypoxia and subsequent β-cell death (183, 184). In addition, transplanted islets remain vulnerable to highly toxic chemokines, cytokines and nitric oxide (NO), which are small enough to pass through the capsule membrane (185-187).

For gene transfer, replication-deficient Adenoviral (Ad) vectors are the most efficient vectors currently available for transducing non-dividing cells such as islets (394). Ad entry is initated by binding of the Ad capsid protein to the ubiquitous Coxsackie Adenovirus Receptor (CAR), which is expressed on islet cells. The Ad particle is internalized via receptor-mediated endocytosis prior to endosome acidification, triggered when the virus trafficks through a low pH region of the cytoplasm. The capsid proteins disassemble and the Ad DNA enters the nucleus where it is transcribed. In non-replication-deficient Ad vectors, the viral proteins translocate into the nucleus and assembly of new viral products occurs here **(Figure 4.1)**.

Transduction of human islets with Ad provides effective transgene expression without affecting islet viability or function (111, 112, 118, 119), a characteristic which was confirmed in **Chapter 3** of this thesis. Once the optimal vector has been identified for a specific gene transfer strategy, this must be paired with an appropriate transgene to confer the required therapeutic benefit. IGF-II is a potent growth factor, recognised for its anti-apoptotic ability in a variety of cell types (395-397). IGF-II inhibits apoptosis via activation of the phosphoinositide-3-kinase (PI3K)/Akt signaling pathway (398), modulation of the anti-apoptotic Bcl-2 family of proteins (399) and suppression of caspase activity (400). IGF-II plays a pivotal role in mammalian cell growth, influencing fetal cell division and cell differentiation (260). Developmental β-cell apoptosis that occurs during foetal and early neonatal life is linked to IGF-II availability, whereby β-cell apoptosis is associated with a concomitant decline in islet IGF-II expression (250, 254, 397, 401). Transgenic mice over expressing IGF-II in the skin, gut and uterus suppress developmental islet apoptosis (402). These studies suggest that IGF-II is a promising candidate gene for use in islet gene therapy.

This chapter aims to investigate the ability of an Ad vector over expressing human IGF-II (Ad-IGF-II) to effectively transduce rat pancreatic islets. First, pairwise sequence alignment from a BLAST search confirmed the sequence identity of the cloned IGF-II transgene within the Ad vector. Next, Ad-IGF-II successfully transduced rat islets and IGF-II over expression did not affect islet viability or function. Moreover, IGF-II over expression did not induce uncontrolled proliferation in transduced islet cells, suggesting that Ad-IGF-II is an effective and safe vector for use in an islet gene therapy setting.

Figure 4.1. Life cycle of Ad. Ad entry into the host cell involves interaction between the Ad fiber protein binding to the CAR cell surface receptor. This is followed by a secondary interaction of Ad with internalization co-receptors, namely integrin αvβ3 or αvβ5. Ad attachment induces actin polymerization and leads to entry of the virus into the host cell within an endosome. Viral gene expression occurs in the nucleus, at this stage replication-defective Ad vectors express the proteins encoded by their DNA. This figure was adapted from Vorburger et al (403).

4.2 Results

4.2.1 Sequencing of human IGF-II from Ad based vector (Ad-IGF-II)

The Ad-IGF-II vector was sequenced to confirm the integrity of the cloned human IGF-II. Using the NCBI BLAST search (http://www.blast.ncbi.nml.nih.gov), the sequence was aligned with all highly similar sequences on the NCBI database. The alignment score (bits) is a value calculated from the number of gaps and substitutions associated with the alignment (a high score represents a good alignment). The E-value (Expect-value) provides an estimate of the statistical significance of the alignment, whereby a low E-value represents a highly significant 'hit'. This search found that the "Homo sapiens insulin-like growth factor 2 (somatomedin A) (IGF2) on chromosome 11" was the most significant alignment as shown in **Figure 4.2.1**. Each "l" symbol between the sbjct and query indicates that the base pairs at that position are identical. The identity value provides the degree of similarity between the sbjct and query, taking into account the number of gaps. Therefore, the cloned human IGF-II gene sequence was 99% similar to that of Homo sapiens insulin-like growth factor 2 (somatomedin A) (IGF2) on chromosome 11.

4.2.2 Microscopic evaluation of Ad-GFP and Ad-IGF-II transduced HEK 293 cells

Human Embryonic Kidney (HEK) 293 cells were transduced with three different vector doses ($2x10^6$ pfu/ml, $2x10^7$ pfu/ml and $2x10^8$ pfu/ml) of Ad-IGF-II or a similarly generated Ad-GFP control vector. Positive GFP reporter gene expression was detected in Ad-GFP transduced cells when viewed under the fluorescent microscope **(Figure 4.2.2(A-C))**. Morphological changes (cell rounding and detachment) were observed in Ad-GFP and Ad-IGF-II transduced HEK 293 cells, a feature that is indicative of active Ad infection and replication **(Figure 4.2.2(A-F))**.

```
>gi|209977069|ref|NG_008849.1| Homo sapiens insulin-like growth factor 2
(somatomedin A) (IGF2) on chromosome 11

Length = 27487

Score =  652 bits (329), E-value = 0.0
Identities = 338/341 (99%)
Strand = Plus / Minus

Query: 1     agctttgtgactcacacacccacaacattctcaatagctttggggaatcactggggaaat 60

              ||||||||||||||||||||||||||||||||||||||||||||||||||||||||||||

Sbjct: 11583 agctttgtgactcacacacccacaacattctcaatagctttggggaatcactggggaaat 11524

Query: 61    ccctccattttatgaaactcaggcaatcacagggcaggtcgtttatgattcacaaaagga 120

              |||||||||||||||||||||||||| |||||||||||||||||||| |||||||

Sbjct: 11523 ccctccattttatgaaactcaggcaatcagagggcaggtcgtttatgattcagaaaagga 11464

Query: 121   ttcaacatgctcggggtgtaatgaccgaatttgggggaaggtatgggaagcaattttcat 180

              |||||||||||| ||||||||||||||||||||||||||||||||||||||||||||

Sbjct: 11463 ttcaacatgctctgggtgtaatgaccgaatttgggggaaggtatgggaagcaattttcat 11404

Query: 181   actctgagggttccaaccttccagccctgctgagtgtcatgagggacttgggattcaacg 240

              ||||||||||||||||||||||||||||||||||||||||||||||||||||||||||||

Sbjct: 11403 actctgagggttccaaccttccagccctgctgagtgtcatgagggacttgggattcaacg 11344

Query: 241   tgtaaagtttagggaacccaggttagtgtgaatagatttgcgggacccaacagcaaatgt 300

              ||||||||||||||||||||||||||||||||||||||||||||||||||||||||||||

Sbjct: 11343 tgtaaagtttagggaacccaggttagtgtgaatagatttgcgggacccaacagcaaatgt 11284

Query: 301   cccatgctgaggtgaacgggaaggggcgcgggggtggggtg 341

              |||||||||||||||||||||||||||||||||||||||

Sbjct: 11283 cccatgctgaggtgaacgggaaggggcgcgggggtggggtg 11243
```

Figure 4.2.1. Pairwise sequence alignment from a BLAST report**.** HEK 293 cells ($2x10^6$) were transduced with Ad-IGF-II at $2x10^8$ pfu/ml for 48 h. Viral DNA was extracted from transduced cells and subject to PCR amplification. Using BLAST the IGF-II sequence (Query, purple text) was aligned with all highly similar sequences of human origin on the NCBI database (Sbjct, black text). The sequence was aligned with the sequence for Homo sapiens insulin-like growth factor 2 (somatomedin A) (IGF2) on chromosome 11 (grey shaded text). Gaps in the sequence alignment are highlighted in turquoise.

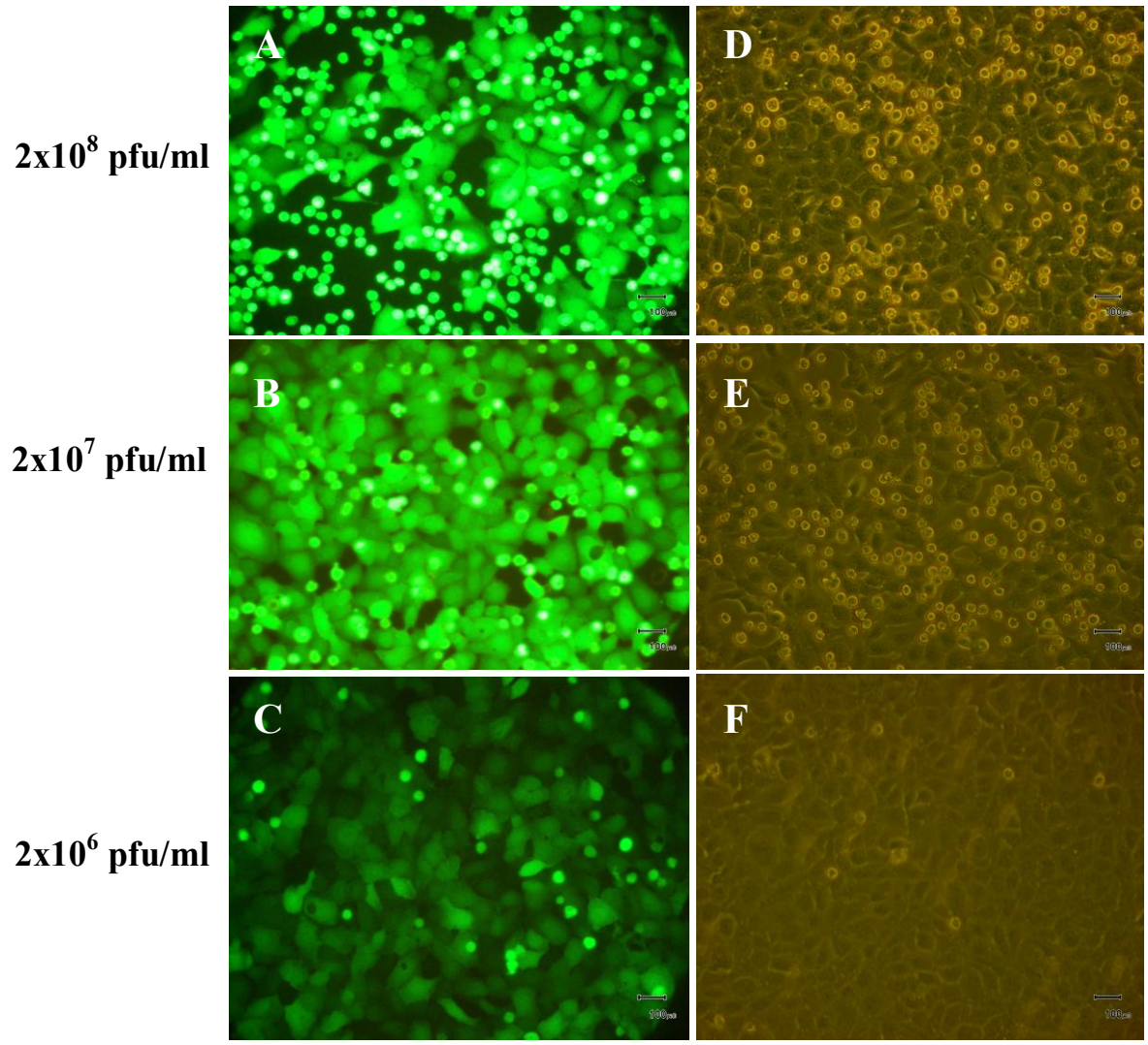

Figure 4.2.2. Fluorescent and light microscopy of Ad-GFP and Ad-IGF-II transduced HEK 293 cells**.** HEK 293 cells ($2x10^6$) were transduced with Ad-GFP or Ad-IGF-II at $2x10^8$, $2x10^7$ or $2x10^6$ pfu/ml for 48 h. **(A-C)** Ad-GFP transduced cells visualized for GFP reporter gene expression (green) under fluorescence. **(D-F)** Ad-IGF-II visualized under bright field of a light microscope. Images were taken at 4x magnification, Scale bar = 100 μm.

4.2.3 Human IGF-II transgene expression in Ad-IGF-II transduced HEK 293 cells

HEK 293 cells ($2x10^6$) were transduced with Ad-GFP ($2x10^8$ pfu/ml), Ad-IGF-II ($2x10^8$ pfu/ml, $2x10^7$ pfu/ml, $2x10^6$ pfu/ml or $2x10^5$ pfu/ml) or untransduced. RNA was extracted using an RNeasy mini kit and reverse transcribed using Omniscript®. To examine the transcription of IGF-II mRNA, quantitative TaqMan® real-time PCR (RT-PCR) was performed on Ad-IGF-II transduced HEK 293 cells with human IGF-II specific primers. For every 10-fold increase in Ad-IGF-II viral dose (i.e. $2x10^5$ pfu/ml to $2x10^6$ pfu/ml) there was an approximately 2-fold increase in IGF-II mRNA as shown in **(Figure 4.2.3(A))**. The messenger RNA (mRNA) increases were also apparent in PCR products separated by agarose gel electrophoresis **(Figure 4.2.3(B))**.

4.2.4 Secretion of human IGF-II by Ad-IGF-II transduced HEK 293 cells to examine secretion of folded protein

Ad-IGF-II transduced HEK 293 cells secreted 240 ng/ml and 300 ng/ml IGF-II within a 24 and 36 h culture period, respectively **(Figure 4.2.4(A))**. There was no IGF-II secretion detected by untransduced or Ad-GFP transduced control cells. Ad-IGF-II transduced HEK 293 cells displayed a 40-fold increase in IGF-II intracellular protein compared to untransduced control cells at 36 h **(Figure 4.2.4(B))**.

4.2.5 Transduction of isolated rat islets with Ad-GFP

Ad-GFP was used to transduce isolated rat islets *in vitro* at MOI 10, 100, 200, 500 and 1000, to assess the transduction efficiency of the Ad vector in rat islets. GFP was included in the Ad-GFP vector to function as a transduction marker. At 48 h post-transduction, GFP expression was observed in transduced islets, although at different efficiencies depending on the MOI **(Figure 4.2.5)**. At MOI 10 Ad-GFP transduced 28.2% ± 3.9 of islet cells. Transduction efficiency was increased 1.7-fold at MOI 100 (47.8% ± 8), which was increased to 54.3% ± 7.4 at MOI 200. Ad-GFP at MOI 500 and 1000 transduced a total of 59.6% ± 8 and 62.4% ± 6.3 of the islets respectively.

A

Sample	Fold-Change IGF-II Expression following 48 h Ad-IGF-II transduction
Untransduced HEK-293	1.6
Ad-GFP $2x10^8$ pfu/ml	1.1
Ad-IGF-II $2x10^5$ pfu/ml	3.3
Ad-IGF-II $2x10^6$ pfu/ml	4.5
Ad-IGF-II $2x10^7$ pfu/ml	12.4
Ad-IGF-II $2x10^8$ pfu/ml	27

B

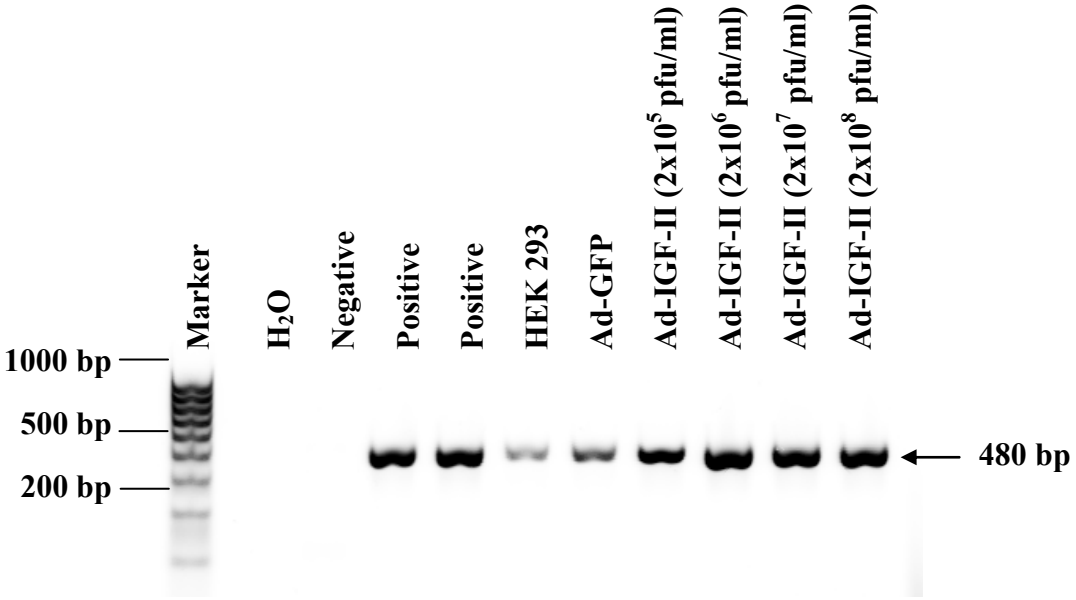

Figure 4.2.3. Determination of IGF-II expression in Ad-IGF-II transduced HEK 293 cells. **(A)** Fold-change in Human IGF-II expression was measured by real-time PCR. Untransduced islets were compared with the Ad-IGF-II samples to evaluate fold-change IGF-II gene expression. Data is representative of one experiment. **(B)** cDNA was subject to PCR amplification with human IGF-II primers (480 base pairs (bp) band size). PCR product was analysed using agarose gel electrophoresis. M= marker, Lane 1 = Nuclease free H_2O, Lane 2 = Control reaction mixture (no template), Lane 3 = Positive control HuH-7 cell line, Lane 4 = Positive control HepG2 cell line, Lane 5 = Untransduced HEK 293 cells, Lane 6 = Ad-GFP transduced HEK 293 cells, Lanes 7 – 10 = Ad-IGF-II transduced HEK 293 cells $2x10^8$ pfu/ml, $2x10^7$ pfu/ml, $2x10^6$ pfu/ml or $2x10^5$ pfu/ml, respectively.

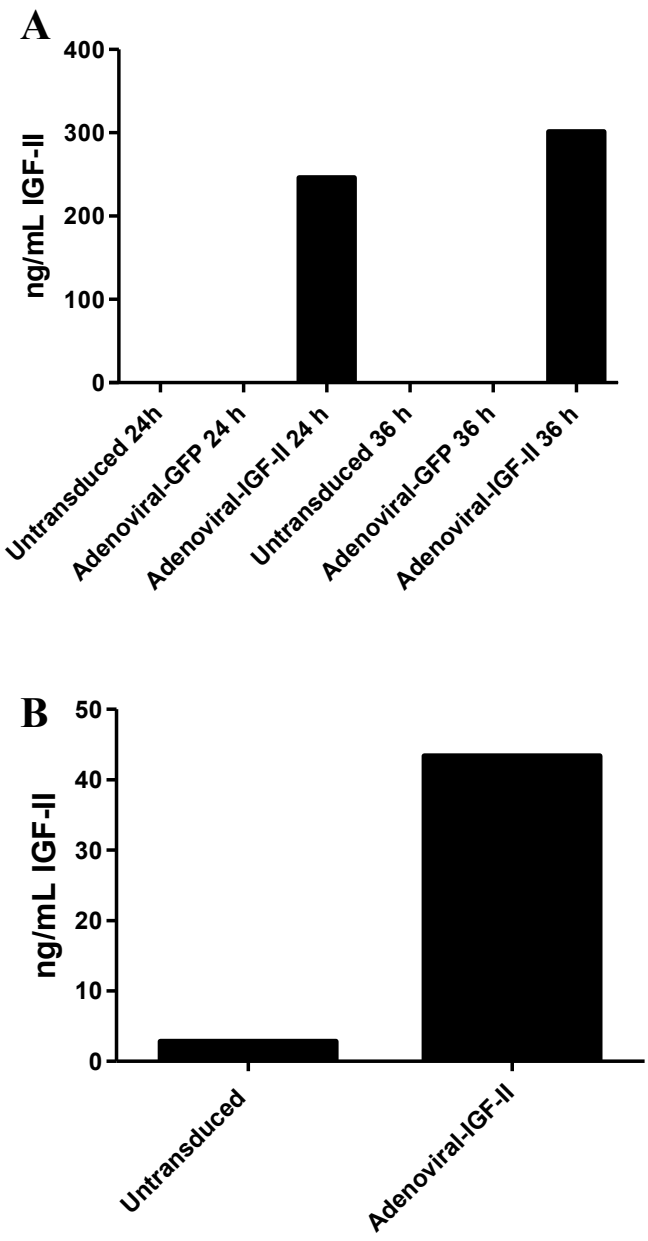

Figure 4.2.4. Human IGF-II secretion from Ad-IGF-II transduced HEK 293 cells. HEK 293 cells ($2x10^6$) were transduced with Ad-GFP, Ad-IGF-II ($2x10^8$ pfu/ml) or untransduced. **(A)** IGF-II levels in the medium or **(B)** intracellular protein at 36 h were measured using a human IGF-II ELISA. Samples were diluted 1:10. Data represents one experiment.

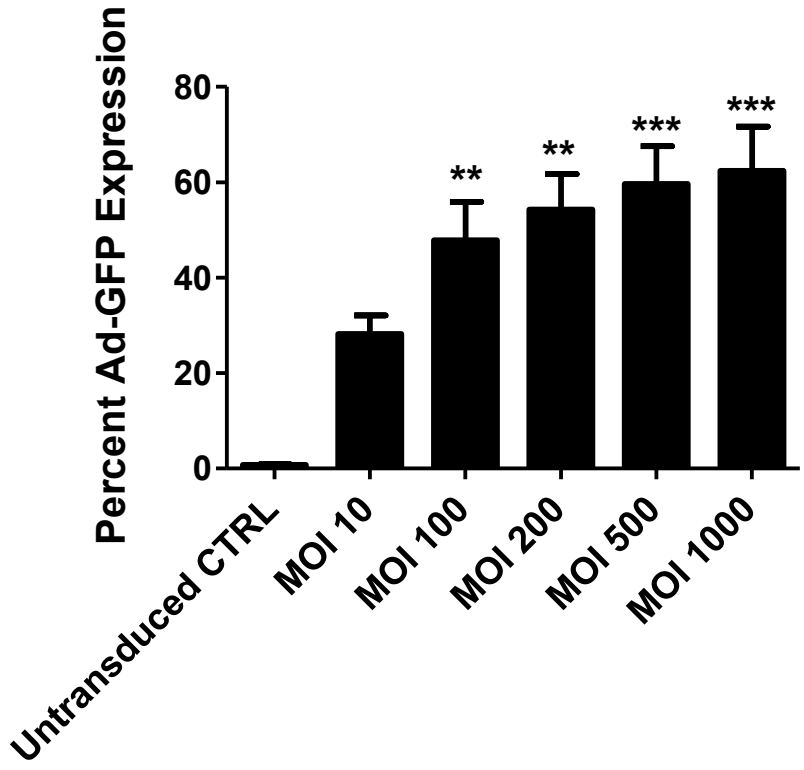

Figure 4.2.5. Evaluation of Ad Transduction on Rat Islets *In Vitro***.** Rat islets were transduced with Ad-GFP at MOI 10, 100, 200, 500 and 1000 or left untransduced. Flow cytometry was used to determine percent GFP expression in dissociated islet cells. Data are the mean ± SEM of three independent experiments, ***p≤0.001 (1way ANOVA). **p<0.01 Untransduced CTRL vs. MOI 100, 200, ***p<0.001 Untransduced CTRL vs. MOI 500, 1000 (Bonferroni Multiple Comparison Test).

4.2.6 Rat islet viability following Ad-IGF-II transduction

Isolated rat islets were transduced with Ad at MOI 100, based on the assumption that each islet cluster contains approximately 2000 cells (138, 315). Dispersed islets were examined for GFP by flow cytometry. The FACS analysis data summarises the calculated viability of islet cells 48 h post transduction **(Figure 4.2.6)**. Islet viability was not adversely affected when transduced with Ad-IGF-II at MOI 100 (74.3% ± 8.2) compared to untransduced controls (69.2% ± 4.7). However, when rat islets were transduced with Ad-GFP alone there was some cytotoxicity and as a result of this the islet cell viability was reduced to 58.2% ± 1.8.

4.2.7 Characterisation of rat islet function following Ad-IGF-II transduction

To determine whether insulin secretion was adversely affected in Ad-IGF-II, Ad-GFP or untransduced islets, *in vitro* islet function was characterised by challenging islets with glucose. Transduction of islets with Ad-GFP or Ad-IGF-II (MOI 100) did not alter the glucose stimulated insulin secretory function of islets (1.8 ± 0.4 and 2 ± 0.5 stimulation index (SI)) respectively, compared to untransduced islets (2 ± 0.5 SI) **(Figure 4.2.7)**. Based on these findings MOI 100 was accepted as the viral MOI for further experiments.

4.2.8 Evaluation of Ad-GFP β-cell transduction in isolated rat islets

Due to the sequence homology between human and rat IGF-II, it is difficult to reliably detect human IGF-II expressing rat islets without detecting a low background of endogenous IGF-II expression. Therefore, the Ad-GFP vector was used to transduce rat islets and immunohistochemical analysis was performed to determine the extent of β-cell transduction. Insulin staining revealed co-localization of insulin, GFP and DAPI nuclear stain in Ad-GFP transduced islets, indicating that Ad-GFP effectively transduced β-cells of the islet **(Figure 4.2.8)**.

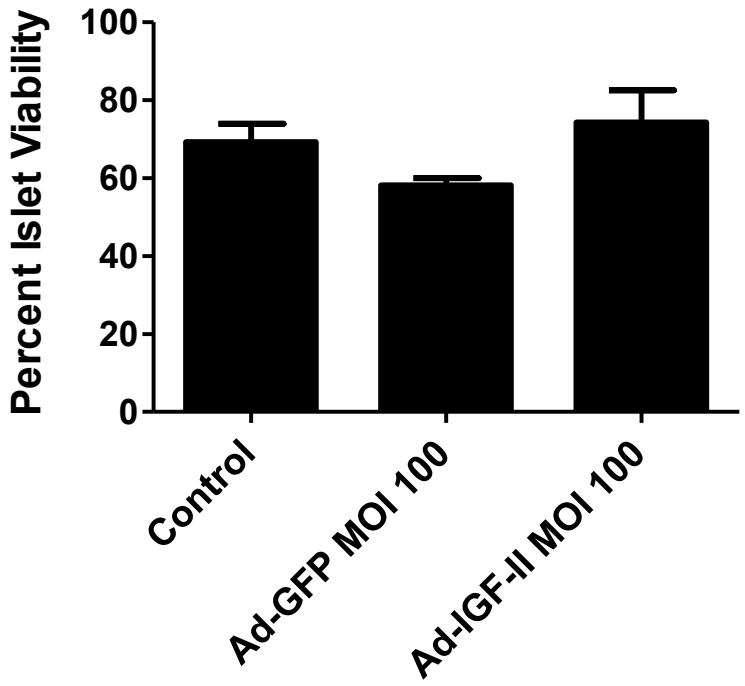

Figure 4.2.6. Evaluation of rat islet viability following Ad-IGF-II transduction**.** Rat islets were transduced with Ad-GFP, Ad-IGF-II or left untransduced. Flow cytometry 7-AAD staining was used to determine the viability in dissociated islet cells. Data are the mean ± SEM of three (Ad-IGF-II) or two (Ad-GFP) independent experiments.

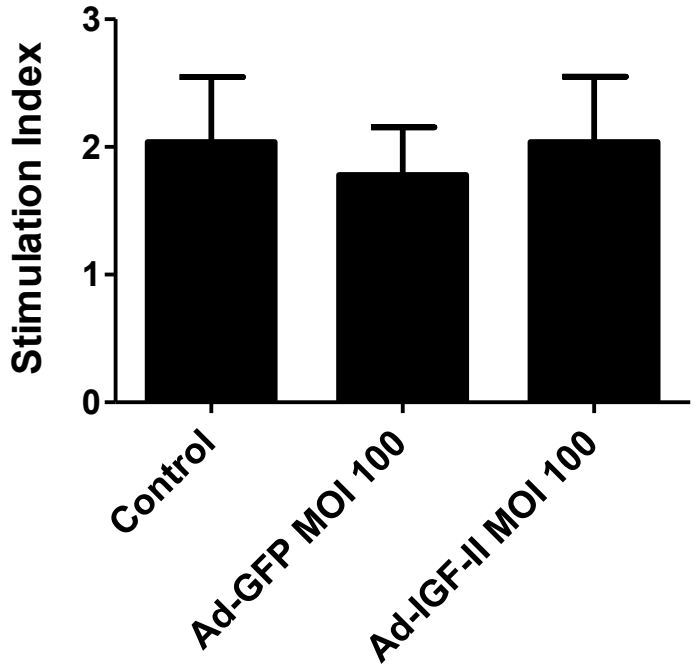

Figure 4.2.7. Evaluation of rat islet function following Ad-IGF-II transduction**.** Rat islets were transduced with Ad-GFP or Ad-IGF-II MOI 100 and then subject to a glucose stimulated insulin secretion assay. Insulin ELISA was used to determine the stimulation index in experimental samples. Samples were diluted 1:10. Data are the mean ± SEM of five independent experiments.

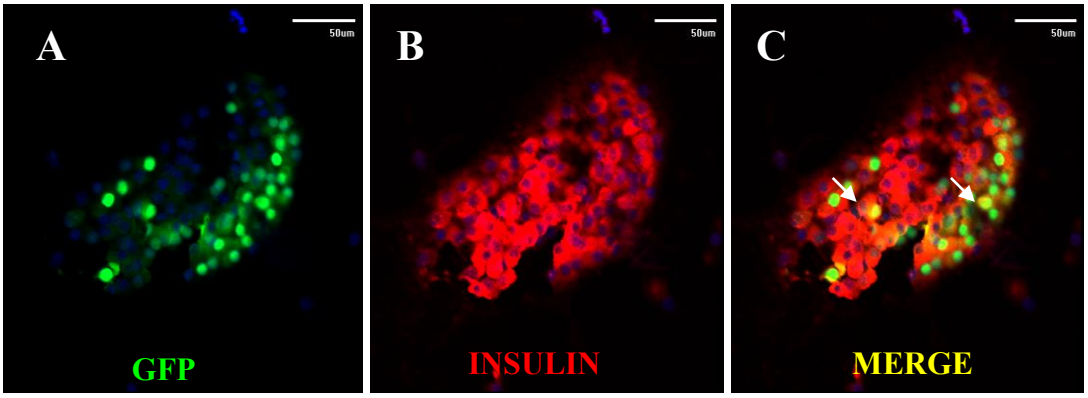

Figure. 4.2.8. Co-localisation of Ad-GFP with insulin in β-cells**.** Islets were transduced with Ad-GFP at MOI 100. Confocal image of a single slice through an intact rat pancreatic islet showing immunostaining with an anti-insulin antibody (red) and co-localisation (yellow) with GFP in β-cells (white arrows), DAPI nuclear stain (blue). Images taken at 20 x magnification, Scale bar = 50µm.

4.2.9 Determination of human IGF-II secretion in Ad-IGF-II transduced rat islets

Rat islets were transduced with Ad-IGF-II for five days and the medium was analysed each day using a human IGF-II ELISA. Ad-IGF-II transduced rat islets constitutively produced and secreted 8.9 ± 1.3 ng human IGF-II into the cell culture supernatant at 24 h, this increased to 14.3 ± 2.4 ng at 48 h. The level of secreted IGF-II reached a maximum of 24.1 ± 1 ng on day five as shown in **Figure 4.2.9**. The secretion of human IGF-II was observed only in the IGF-II transduced cells demonstrating that Ad-IGF-II mediated effective transduction and specific expression of IGF-II in transduced islet cells.

4.2.10 Determination of islet proliferation in Ad-IGF-II transduced rat islets

Due to the growth promoting effects associated with IGF-II and the increased risk of malignancy as a result of uncontrolled cell growth, the proliferation of Ad-IGF-II islets was analysed by flow cytometric analysis. Approximately, 8.9% ± 2.4 of Ad-IGF-II transduced rat islets had actively proliferating cells as determined by positive ki67 expression. However, there was no significant difference in the proliferation of Ad-IGF-II transduced islets compared to untransduced or Ad-GFP transduced islet controls (6.5% ± 3.3 and 6.1% ± 1.4, respectively) **(Figure 4.2.10)**.

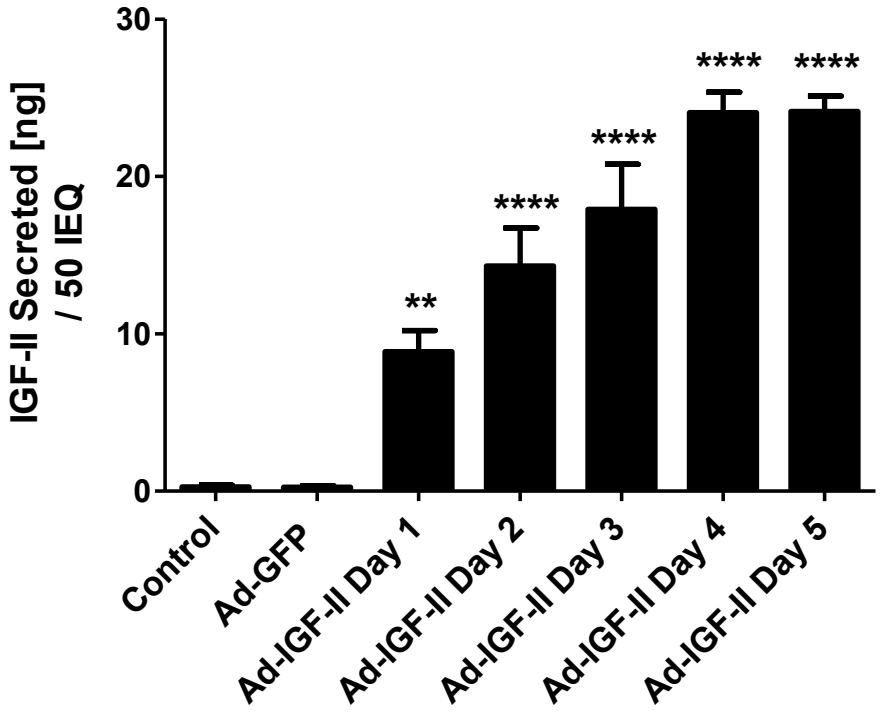

Figure. 4.2.9. Time course of human IGF-II secretion from Ad-IGF-II transduced rat islets *in vitro*. Rat islets were transduced with Ad-GFP MOI 100, Ad-IGF-II MOI 100 or untransduced. IGF-II levels in the medium were measured using a human IGF-II ELISA. Data expressed as mean ± SEM of 3 – 9 replicate experiments, ****$p<0.0001$ (1wayANOVA). **$p<0.01$ Ad-GFP transduced islets vs. Ad-IGF-II Day 1 transduced islets, ****$p<0.0001$ Ad-GFP transduced islets vs. Ad-IGF-II day 2-5 transduced islets (Bonferroni Multiple Comparison Test).

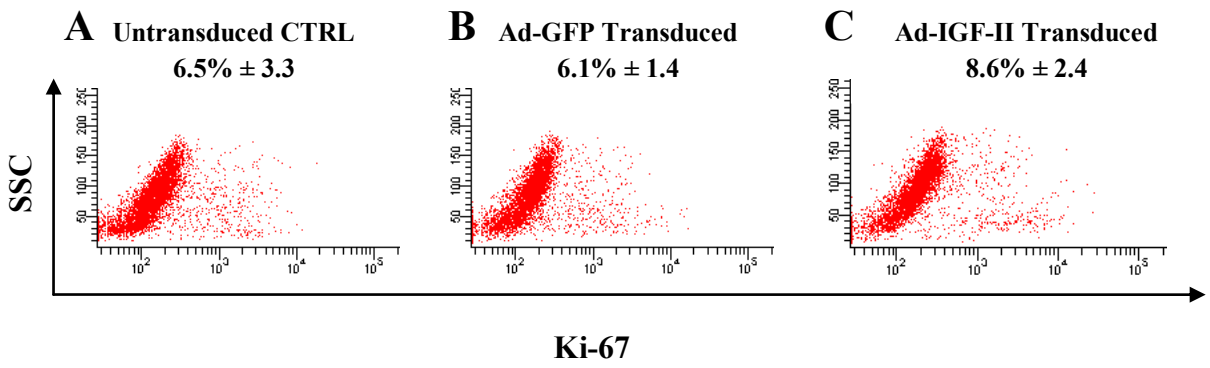

Figure 4.2.10. The effect of Ad-IGF-II transduction on islet cell proliferation. Rat pancreatic islets were **(A)** untransduced or transduced with **(B)** Ad-GFP or **(C)** Ad-IGF-II (MOI 100) for 48 h. The monoclonal antibody ki67 was used to detect proliferating cells by flow cytometric analysis. A representative histogram is shown for each sample population. Values are the mean ± SEM for three replicate experiments.

4.3 Discussion

Ex vivo gene transfer involves removing the cells of interest from the body, inserting the new DNA (that will correct the disease or provide therapeutic benefit) into the cells and then placing the cells back into the patient. The efficacy of *ex vivo* gene transfer has been demonstrated in the treatment of familial hypercholesterolaemia, the X chromosome-linked form of Alport syndrome and various types of cancer (404-406). Ad vectors possess several features that make them well suited for use in islet gene transfer. First, they infect a broad range of human cells (including islets) with very high efficiency. Second, Ad vectors can accommodate large DNA inserts (up to 7.5 kilobase pairs (kb)) and transduce these transgenes in non-proliferating cells such as islets. Third, Ad vectors exhibit low pathogenicity in humans; they often cause mild symptoms of the common cold, conjunctivitis and tonsillitis. Finally, the inserted transgene(s) are maintained without change during viral amplification (403).

Based on the promising results obtained in **Chapter 3**, regarding the ability of Ad to effectively transduce isolated human and rat pancreatic islets, **Chapter 4** aimed to characterise an Ad-based vector encoding the anti-apoptotic molecule Insulin-Like Growth Factor-II (IGF-II) (Ad-IGF-II). Firstly, the gene of interest (IGF-II) was sequenced to confirm that the IGF-II sequence used to generate the Ad-IGF-II vector was homologus to the native sequence of human IGF-II. Next, preliminary experiments were performed to appropriately characterise the Ad-IGF-II vector. For this, the Human Embryonic Kidney (HEK) 293 cell line was used as HEK 293 cells are easy to culture and transduce readily, thereby providing an optimal model system to investigate vector efficacy.

Following transduction, GFP reporter gene expression was observed in Ad-GFP transduced HEK 293 cells. HEK 293 cells grow as attatched monolayer cultures, however following Ad transduction morphological changes appeared in the cells. These morphological changes are termed cytopathic effects (CPE), which result in microscopic appearance of detached cells that are rounded in culture. Although the Ad-IGF-II vector does not contain a reporter gene, light microscope images of transduced cells revealed the same morphological features of cells undergoing active infection and subsequent CPE.

Next, molecular studies demonstrated that Ad-IGF-II transduced HEK 293 were able to efficiently transcribe the IGF-II gene and translate the IGF-II mRNA to protein. Transduction of HEK 293 cells with Ad-IGF-II resulted in specific production and secretion of IGF-II. However, no such IGF-II secretion occured in HEK 293 cells transduced with Ad-GFP, demonstrating that the increased IGF-II was not due to a HEK 293 mediated up-regulation of IGF-II as a survival response following viral exposure.

Once the functional characteristics of the Ad-IGF-II vector were confirmed in HEK 293 cells, similar experiments were performed in isolated rat pancreatic islets. Although human and rat islets were both utilised in **Chapter 3**, it was not logistically feasible to use human islets as the primary islet source in this thesis, as a consistent supply of isolated human islets are not always available for research and for this reason rat islets were chosen as the alternative primary cell type for experiments in this thesis. Another option could be the use of mouse islets however a benefit to using isolated rat islets over mouse islets is the increased islet yield per animal. For example, rat islet yields range from approximately 600 – 800 islets per animal (407) and 200 – 400 islets per mouse, with average yields of 300 islets per mouse (408, 409). Therefore, by isolating rat islets, this meant that fewer animals were utilized and an increased number of islets were obtained for experimental studies.

In the next set of experiments, Ad-IGF-II efficiently transduced rat pancreatic islets and IGF-II over expression did not affect islet viability or physiological function. The efficacy of Ad-based vectors has been demonstrated previously within islet transplant studies (197-200, 204). In this chapter, Ad-GFP transduced islets displayed decreased cell viability compared to untransduced control islets. This may be due to the potential cell toxicity associated with GFP (410-412). However, in the same set of experiments, Ad-IGF-II transduced islets displayed increased viability compared to Ad-GFP transduced and untransduced control cells. Isolated islets may be damaged during the isolation procedure leading to islet apoptosis (413, 414). Therefore, in this study the over expressed IGF-II may be exerting an anti-apoptotic effect against isolation induced apoptosis. This is supported by Ilieva and colleagues (415) who have shown that incubation of hamster islets with duct conditioned medium containing 34 ng/ml IGF-II can prevent *in vitro* apoptosis and necrosis that occur after the islet isolation procedure.

As previously discussed in **Section 1.3** of this thesis, rat pancreatic islets possess a well-defined architecture, consisting of a central core of β-cells which represent 60 – 80% of the islet. This poses an issue when considering the poor transduction capability of Ad to reach the inner mass of the islets, however in this study immunofluoresence microscopy demonstrated that the Ad vector was able to effectively transduce the β-cells of the islet. While the number of Ad transduced β-cells relative to the other endocrine islet cell types (i.e. glucagon-producing α-cells) was not quantified, there was 47.8% ± 8 total islet cells transduced at MOI 100, suggesting that the Ad vector does not specifically target β-cells. Despite this, the utility of Ad mediated IGF-II over expression is that IGF-II mediates its anti-apoptotic effect via autocrine and paracrine mechanisms, which negates the need for every islet cell to express the therapeutic gene.

While the functional characterisation experiments demonstrated that the IGF-II gene can be both transcribed and translated into functional IGF-II protein, it would have been helpful to examine whether the secreted IGF-II is bio-active. Future studies could investigate this by performing an IGF-II bioactivity assay in MCF-7 human breast cancer cells. MCF-7 cells normally grow in a monolayer however they form multilayered cellular aggregates (foci) in the presence of bio-active IGF-II. The foci retain red Rhodamine B stain better then the surrounding monolayer of cells, therefore appearing as dark red spots that can be subsequently quantified.

A very important aspect of any anti-apoptotic strategy is to minimize any vector or transgene associated effects on cell proliferation. Failure to regulate cell proliferation, ultimately leads to malignant transformation. The ki67 nuclear antigen is expressed by proliferating cells which are in the active phases of the cell cycle (late G1, S, G2 and mitosis). For this reason, ki67 was used as a marker for proliferation in Ad-IGF-II transduced islets, and it was subsequently shown that IGF-II over expression did not induce cell proliferation. This is supported by Petrik and colleagues (230) who report a five-fold increase in mean islet size in IGF-II transgenic mice but no induction of islet proliferation. Various studies suggest that IGF-II alone is not directly transforming. However, the IGF-I and IGF-II receptors have been shown to be mutated or over expressed in tumour cells, contributing to tumour formation, maintenance and progression (217). IGF-II works through the IGF-I receptor (IGF-1R) to inhibit apoptosis, whereas, the IGF-II receptor (IGF-IIR) has no intrinsic signaling transduction capability and works only to modulate IGF-II availability (416). Despite this, regular screening would be an essential requirement of any islet gene therapy strategy employed clinically.

In conclusion, in this chapter the anti-apoptotic molecule IGF-II was successfully cloned into a replication-deficient Ad (serotype 5) vector. This data demonstrates the utility of Ad-IGF-II to maintain stable *in vitro* islet viability and function in transduced islet cells. Within this chapter an efficient vector system has been characterised that will be subsequently utilized within the remaining chapters of this thesis (**Chapter(s) 5 and 6**) to assess the *in vitro* and *in vivo* survival of pancreatic islets against pro-inflammatory cytokine induced islet cell death.

CHAPTER 5

THE ANTI-APOPTOTIC ACTIVITY OF INSULIN-LIKE GROWTH FACTOR-II IN AN *IN VITRO* MODEL OF CYTOKINE INDUCED APOPTOSIS

5.1 Introduction

Islet primary non-function is defined as the loss of islet function after transplantation for reasons other than graft rejection (417). It is a major obstacle to successful and efficient islet transplantation, resulting in destruction of up to 70% of the transplanted islet mass in the early post-transplant period (77, 194, 418). Innate inflammatory responses at the transplant site, such as the instant blood mediated inflammatory reaction (IBMIR) (419) and local release of pro-inflammatory cytokines, such as TNF-α, IL-1β and IFN-γ (420-424) contribute to islet apoptosis during both the peri-transplant and early post-transplant period (425).

IL-1β alone or in combination with other pro-inflammatory cytokines such as IFN-γ, induces β-cell death in mouse, rat and human islets *in vitro* and *in vivo* (426-429). The release of pro-inflammatory cytokines by resident islet macrophages has been observed in rats following islet transplantation *in vivo* (430-432). Exposure of rat islets to IL-1β *in vitro* decreases islet insulin content, suppresses glucose stimulated insulin secretion (GSIS) and induces DNA damage in pancreatic islet cells (433, 434). Pro-inflammatory cytokines mediate their inflammatory effects largely under the control of the transcription factors nuclear factor kappa B (NF-κB) and signal transducer and activator of transcription-1 (STAT-1). Activation of these molecules, leads to the production of cytotoxic nitric oxide synthase (iNOS), and the subsequent generation of nitric oxide (NO) (29, 435) **(Figure 5.1)**.

Figure 5.1. Cell signaling pathways activated in pancreatic islets following pro-inflammatory cytokine exposure. The reasons for the decline in insulin independence rates following islet transplantation are complex, beginning before pancreas procurement (436). Brain death is associated with the endogenous production of pro-inflammatory cytokines such as TNF-α, IL-1β and IL-6 (437, 438). Release of TNF-α is associated with inflammation and is toxic to pancreatic islets (439-441). In addition, physical isolation of human islets required for transplantation triggers activation of the NF-κB and mitogen-activated kinase (MAPK) stress response pathways (442) and deprives islets of oxygen and nutrients, leading to the formation of cytotoxic NO (443). As a result, islets experience subsequent stresses including, production of free radicals, decreased β-cell and insulin function, mononuclear cell infiltration and islet apoptosis, among others. Figure was adapted from:
http://www.ucdenver.edu/academics/colleges/medicalschool/centers/BarbaraDavis/PublishingImages/Books-type1/ch5fig3.gif

One potential solution to overcome the vulnerability of β-cells to post-transplant cell death is the use of gene therapy to over express an anti-apoptotic molecule in islets prior to their transplantation (444, 445). IGF-II is a promising therapeutic gene for this purpose. IGF-II is an anti-apoptotic peptide of 7.5 kDa and is highly expressed in fetal liver tissue. IGF-II exerts a robust anti-apoptotic effect in many cell and tissue types, including cerebella granule neurons, ovarian preovulatory cells and pancreatic islets (395-397). IGF-II belongs to the insulin family of polypeptide growth factors, known for their sequence homology to insulin (219). IGF-II exerts its anti-apoptotic effects via the IGF-1 receptor (IGF-1R), while the IGF-II Receptor (IGF-IIR), also called the Mannose-6-Phosphate receptor can only bind IGF-II (219). The main role of the IGF-IIR is to clear IGF-II from the serum and target it for degradation within lysosomes.

Therefore it was hypothesized that Ad mediated over expression of anti-apoptotic human IGF-II, may act directly on isolated islet cells, to improve islet survival. Within this chapter, the influence of local human IGF-II over expression on pancreatic islet cell survival against pro-inflammatory cytokines *in vitro* was investigated. In this chapter, the transduction of rat islets with Ad-IGF-II conferred significant protection against pro-inflammatory cytokine (Interleukin-1β (IL-1β) and Interferon-γ (IFN-γ)) induced cell death. Furthermore, Ad-IGF-II transduced rat islets retained their insulin secretory function following exposure to pro-inflammatory cytokines IL-1β and IFN-γ. This chapter confirmed that IGF-II mediates its anti-apoptotic effects through binding the IGF-1R and subsequently working via the phosphoinositide-3-kinase (PI3K)/Akt signaling pathway to inhibit apoptosis.

5.2 Results

5.2.1 Pro-inflammatory cytokines Interleukin-1β and Interferon-γ induce cell death in human and rat pancreatic islets *in vitro*

Isolated human and rat islets were untreated or treated for 24 h (hours) with human or rat pro-inflammatory cytokines IL-1β and IFN-γ. A range of cytokine concentrations were tested to identify the optimal cytokine dose to induce islet cell death **(Table 5.2.1;first column)**. Following cytokine exposure, cell death was induced in human and rat islets, although at differing levels depending on the concentration of cytokines used **(Table 5.2.1;third column)**.

The lowest concentration of cytokines tested (5 ng/ml IL-1β and 10 ng/ml IFN-γ) induced cell death in 4.7% ± 0.8 and 15.4% ± 8.7 of human and rat islets, respectively. The highest concentration of cytokines (35 ng/ml IL-1β and 40 ng/ml IFN-γ) induced cell death in 8.6% ± 1.7 and 18.7% ± 1.7 of human and rat islets, respectively.

The cytokine doses of 5 ng/ml IL-1β**,** 10 ng/ml IFN-γ and 35 ng/ml IL-1β**,** 40 ng/ml IFN-γ were chosen as the optimal concentrations for further apoptosis induction experiments in human and rat islets, respectively. Although other cytokine doses induced a slightly higher level of cell death in human islets, the majority of cells in the population were necrotic rather then a population consisting of both apoptotic and necrotic cells. This was an important consideration when identifying the optimal cytokine dose in this chapter, as a previous study has shown, that pro-inflammatory cytokines induce β-cell death via a mechanism that involves both apoptosis and necrosis (426).

5.2.2 Assessment of human and rat islet morphology following IL-1β and IFN-γ pro-inflammatory cytokine exposure

Human and rat islets were untreated or treated for 24 h with 5 ng/ml IL-1β**,** 10 ng/ml IFN-γ and 35 ng/ml IL-1β**,** 40 ng/ml IFN-γ, respectively. Following cytokine exposure, the islets were visualized using a basic light microscope. Untreated islets exhibited a smooth and rounded appearance, with the presence of a well defined islet membrane border **(Figure 5.2.2(A) and Figure 5.2.2(C))**. Islets cultured in the presence of IL-1β and IFN-γ exhibited a rough islet surface and darkened (hypoxic) centre **(Figure 5.2.2(B) and Figure 5.2.2(D))**.

Table 5.2.1. Investigation of the level of cell death induced in human and rat islets following exposure to pro-inflammatory cytokines IL-1β and IFN-γ. Isolated human **(A)** and rat **(B)** islets were cultured for 24 h in the presence of pro-inflammatory cytokines IL-1β and IFN-γ. Percentage of islet cell death following cytokine exposure was assessed in dispersed islets by Annexin V and Propidium Iodide (PI) flow cytometric analysis. The data is expressed as ± SEM of experiments. Concentrations of cytokines used to treat islets are listed in the 'concentration' column in **A** and **B**.

A

Concentration	n	Percent Human Islet Cell Death Following Cytokine Exposure (24 h)
5 ng/ml IL-1β 10 ng/ml IFN-γ	4	4.7% ± 0.8
15 ng/ml IL-1β 25 ng/ml IFN-γ	1	6%
35 ng/ml IL-1β 40 ng/ml IFN-γ	4	8.6% ± 1.7

B

Concentration	n	Percent Rat Islet Cell Death Following Cytokine Exposure (24 h)
5 ng/ml IL-1β 10 ng/ml IFN-γ	4	15.4% ± 8.7
15 ng/ml IL-1β 25 ng/ml IFN-γ	1	19%
35 ng/ml IL-1β 40 ng/ml IFN-γ	2	18.7% ± 1.7

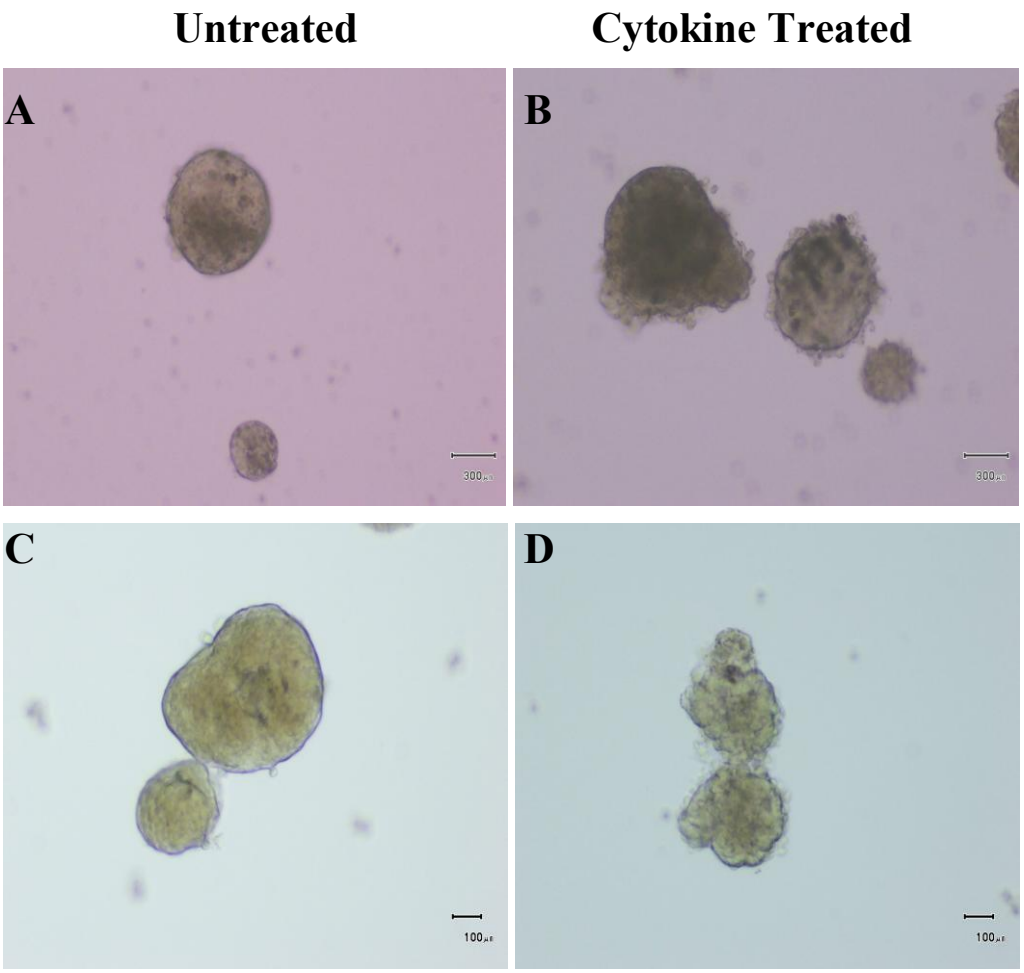

Figure 5.2.2. Pro-inflammatory cytokines induce morphological changes in human and rat islets. Human islets were **(A)** untreated or **(B)** cultured for 24 h in the presence of pro-inflammatory cytokines IL-1β (5ng/ml) and IFN-γ (10ng/ml). Isolated rat islets were **(C)** untreated or **(D)** cultured for 24 h in the presence of pro-inflammatory cytokines IL-1β (35ng/ml) and IFN-γ (40ng/ml). Morphological characteristics of islets were visualized using a light microscope. **(A – B)** Images were taken at 10 x magnification, Scale bar = 300 µm. **(C – D)** Images were taken at 20 x magnification, Scale bar = 100 µm.

5.2.3 Pro-inflammatory cytokines IL-1β and IFN-γ induce DNA damage in isolated rat islets

TUNEL staining was used to detect DNA fragmentation that occurs following activation of the apoptotic signaling cascade. Rat islets were treated for 24 h with 35 ng/ml IL-1β and 40 ng/ml IFN-γ. Untreated rat islets displayed a lower number of apoptotic (green) cells compared to rat islets exposed to pro-inflammatory cytokines **(Figure 5.2.3)**.

5.2.4 Pro-inflammatory cytokines IL-1β and IFN-γ impair the glucose stimulated insulin secretory ability of rat islets

Cytokine exposure impaired the ability of rat islets to secrete insulin in response to high glucose (Stimulation index (SI); 1 ± 0.1), compared to untreated islets which exhibited a SI of 2.9 ± 0.6 **(Figure 5.2.4)**.

5.2.5 Nitric oxide expression in rat islets following pro-inflammatory cytokine exposure

As discussed in **Section 5.1**, pro-inflammatory cytokines lead to activation of the NF-κB stress response pathway and subsequent production of NO. Therefore, accumulation of nitrite (a breakdown product of NO) was measured in rat islets following pro-inflammatory cytokine treatment. Rat islets were untreated or treated with IL-1β (35 ng/ml) and IFN-γ (40 ng/ml) for 24 h. Cytokine treated rat islets displayed an increased accumulation of nitrite (3.4 ± 0.4 μM) in assayed cell culture supernatants compared to untreated control islet cells (0.8 ± 0.08 μM) **(Figure 5.2.5)**.

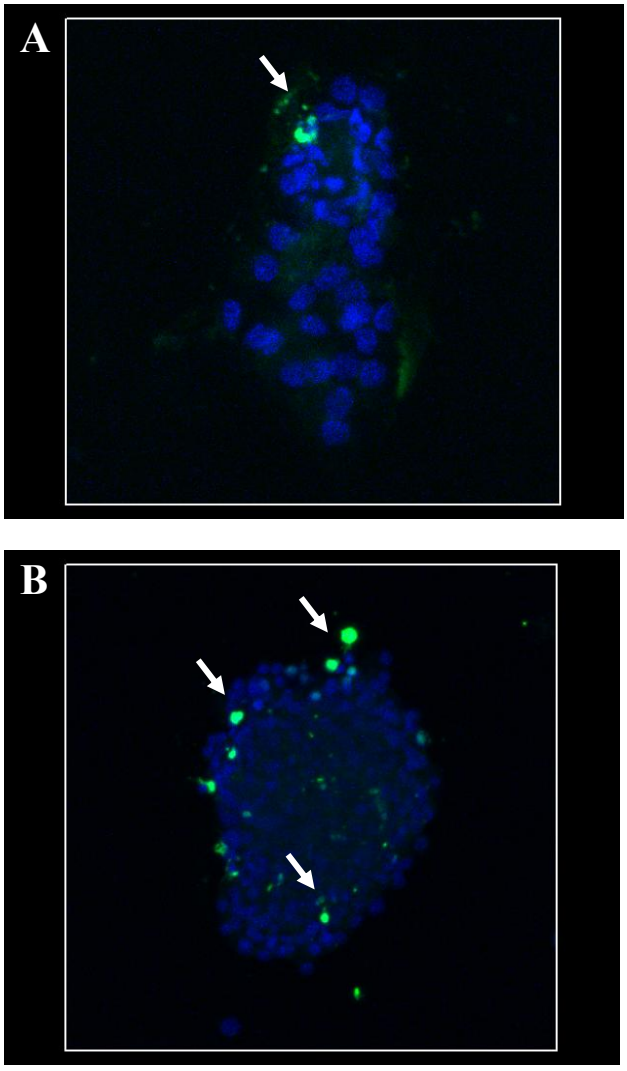

Figure 5.2.3. Pro-inflammatory cytokine treated rat islets examined for apoptosis by TUNEL staining. Isolated rat islets were **(A)** untreated or **(B)** cultured for 24 h in the presence of pro-inflammatory cytokines IL-1β (35ng/ml) and IFN-γ (40ng/ml). TUNEL staining for apoptotic cells was performed on islet cytospin preparations. TUNEL positive cells (green; white arrows) in the fluorescent images correspond to apoptotic cells. Blue = DAPI nuclear stain. Images were taken at 20 x magnification.

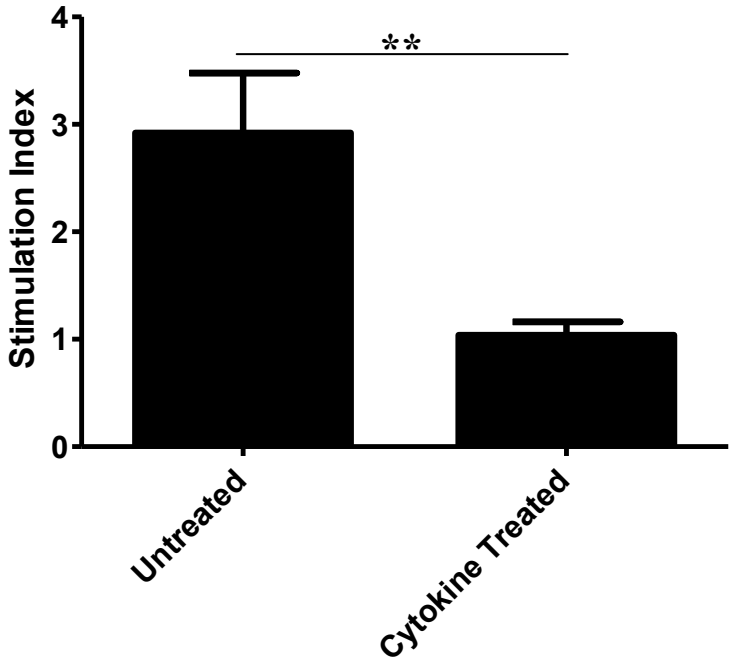

Figure 5.2.4. Investigation of rat islet function following IL-1β and IFN-γ pro-inflammatory cytokine exposure. Isolated rat islets were untreated or cultured for 24 h in the presence of pro-inflammatory cytokines IL-1β (35ng/ml) and IFN-γ (40ng/ml), and then stimulated to release insulin by exposure to high (25 mM) or low (2.8 mM) concentrations of glucose. Insulin ELISA was used to determine the stimulation index in experimental samples. Data are the mean ± SEM of five independent experiments, **$p \leq 0.01$ (student T-test).

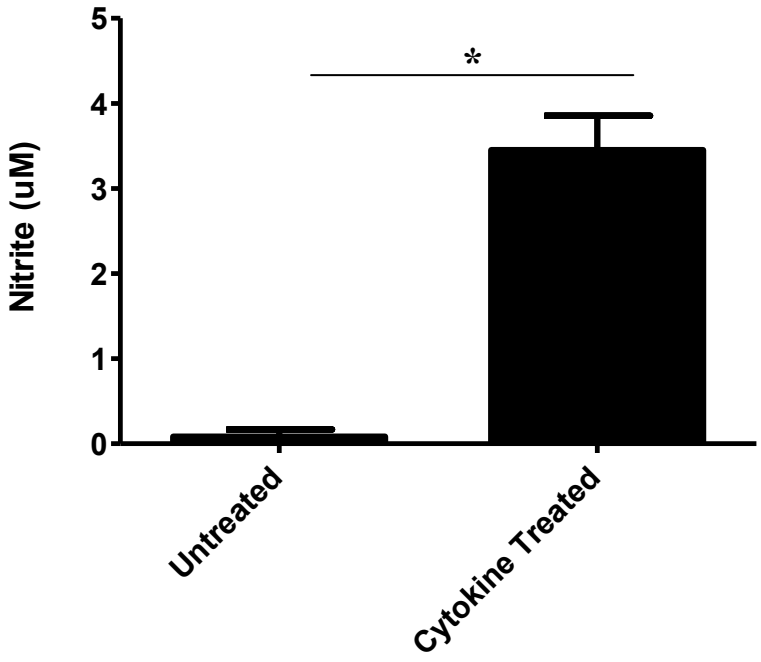

Figure 5.2.5. Detection of nitric oxide in rat islets following IL-1β and IFN-γ pro-inflammatory cytokine exposure. Isolated rat islets were untreated or cultured for 24 h in the presence of pro-inflammatory cytokines IL-1β (35ng/ml) and IFN-γ (40ng/ml). Following treatment, cell culture supernatant was collected and assayed for the presence of nitrite (NO_2^-), a breakdown product of NO using a commercial Griess reagent system. Cell culture supernatant was collected and analyzed. Data are the mean ± SEM of three replicate experiments, *$p \leq 0.05$ (Student T-test).

5.2.6 Ad-IGF-II transduction of rat islets protects against pro-inflammatory cytokine induced cell death *in vitro*

The cytoprotective effect of Ad-IGF-II on islet cell death following cytokine exposure was investigated by Annexin V and PI staining. Following cytokine exposure, Ad-IGF-II transduced islets and rIGF-II treated islets displayed a decreased level of cytokine induced cell death (39.8% ± 2.8 and 41.9% ± 3.3, respectively) when compared to control islets transduced with Ad-GFP (63.2% ± 2.5) or untransduced (53.6% ± 2.3) **(Figure 5.2.6)**, clearly demonstrating the anti-apoptotic effect of IGF-II *in vitro*.

5.2.7 Ad-IGF-II transduction of human islets does not protect against IL-1β and IFN-γ pro-inflammatory cytokine induced cell death *in vitro*

Following cytokine exposure, cell death was induced in 61.6% ± 4.1 of Ad-IGF-II transduced islets. This was not significantly different to control islets transduced with Ad-GFP (62.3% ± 2.4) or untransduced islets (59.8% ± 6.3) as shown in **Figure 5.2.7**. Human islets pre-treated with rIGF-II displayed slightly decreased cytokine induced cell death (59.8% ± 6.3) compared to Ad-IGF-II, Ad-GFP and untransduced sample groups, but this was not statistically significant. Untreated human islets displayed 51.3% ± 6.2 islet cell death.

5.2.8 Ad-IGF-II transduced rat islets display a decreased number of TUNEL positive apoptotic cells following pro-inflammatory cytokine exposure *in vitro*

Following cytokine exposure, there was a marked reduction in the number of TUNEL positive cells (apoptotic) in the Ad-IGF-II transduced rat islets compared to Ad-GFP transduced islets **(Figure 5.2.8)**. Specifically, 46.5% ± 6.2 and 41% ± 4.2 total islet cells in the untransduced and Ad-GFP transduced groups were TUNEL positive, respectively. However, when IGF-II was over expressed in islets during cytokine exposure a decrease in the number of TUNEL positive apoptotic cells was observed (8.3% ± 1.4)

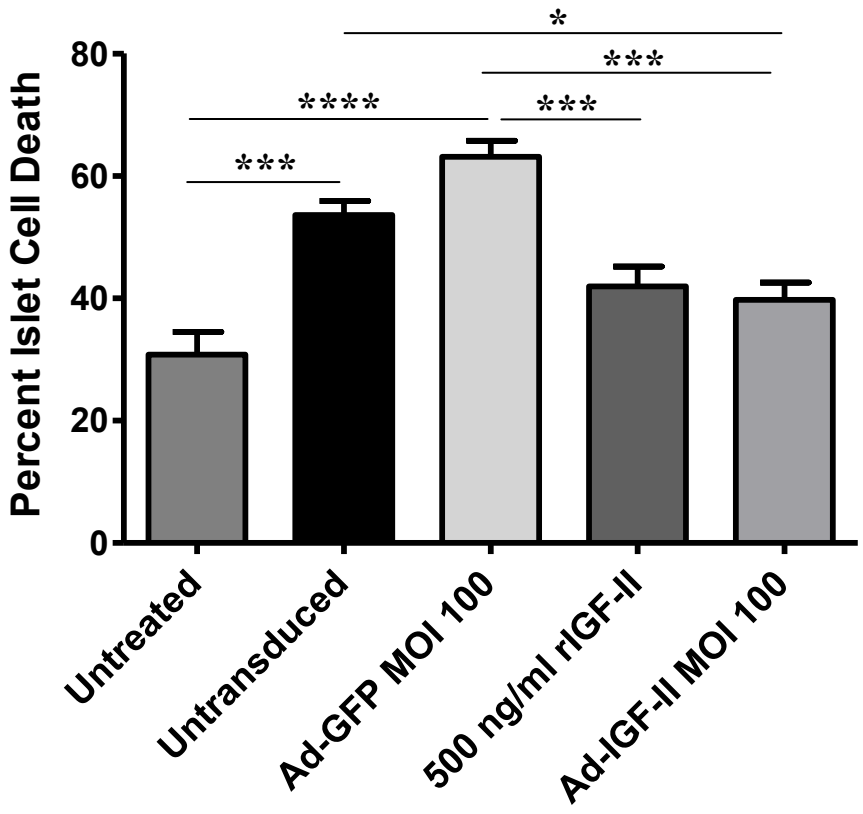

Figure. 5.2.6. Anti-apoptotic investigation of Ad-IGF-II transduced islets following pro-inflammatory cytokine exposure. Islets were left untreated or transduced at MOI 100 with Ad-GFP, Ad-IGF-II or untransduced 48 h before addition of IL-1β (35ng/ml) and IFN-γ (40 ng/ml) for an additional 24 h, or islets were pre-treated for 2 h with rIGF-II (500 ng/ml) before addition of pro-inflammatory cytokines. Flow cytometry was used to determine percent islet cell death of dispersed islet cells using Annexin V and PI staining. The data is expressed as ± SEM of five independent experiments, ***$p<0.001$ (1wayANOVA). Bonferroni Multiple Comparison Test: ***$p<0.001$ Untreated islets vs. Untransduced islets, ****$p<0.0001$ Untreated islets vs. Ad-GFP transduced islets, *$p<0.05$ Untransduced vs. Ad-IGF-II transduced islets, ***$p<0.001$ Ad-GFP transduced islets vs. 500 ng/ml rIGF-II islets, ***$p<0.001$ Ad-GFP transduced islets vs. Ad-IGF-II transduced islets.

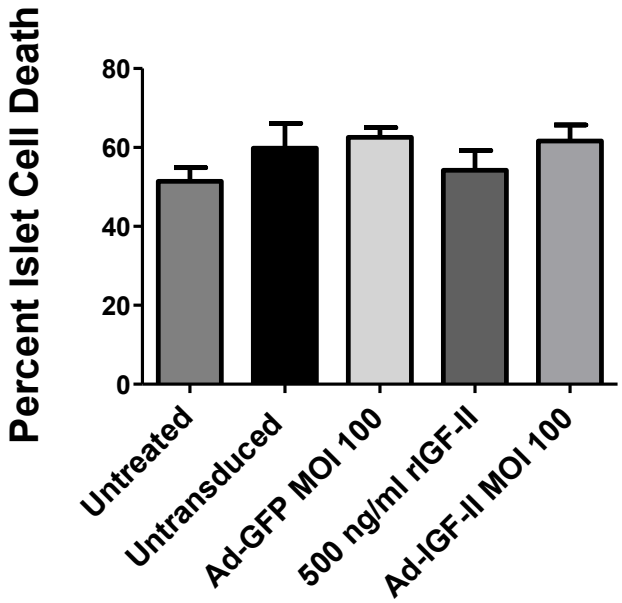

Figure. 5.2.7. Anti-apoptotic investigation of Ad-IGF-II transduced human islets following pro-inflammatory cytokine exposure. Human islets were left untreated or transduced at MOI 100 with Ad-GFP, Ad-IGF-II or untransduced 48 h before addition of IL-1β (5ng/ml) and IFN-γ (10 ng/ml) for an additional 24 h, or islets were pre-treated for 2 h with rIGF-II (500 ng/ml) before addition of pro-inflammatory cytokines. Flow cytometry was used to determine percent islet cell death of dispersed islet cells using Annexin V and PI staining. The data is expressed as ± SEM of two independent experiments.

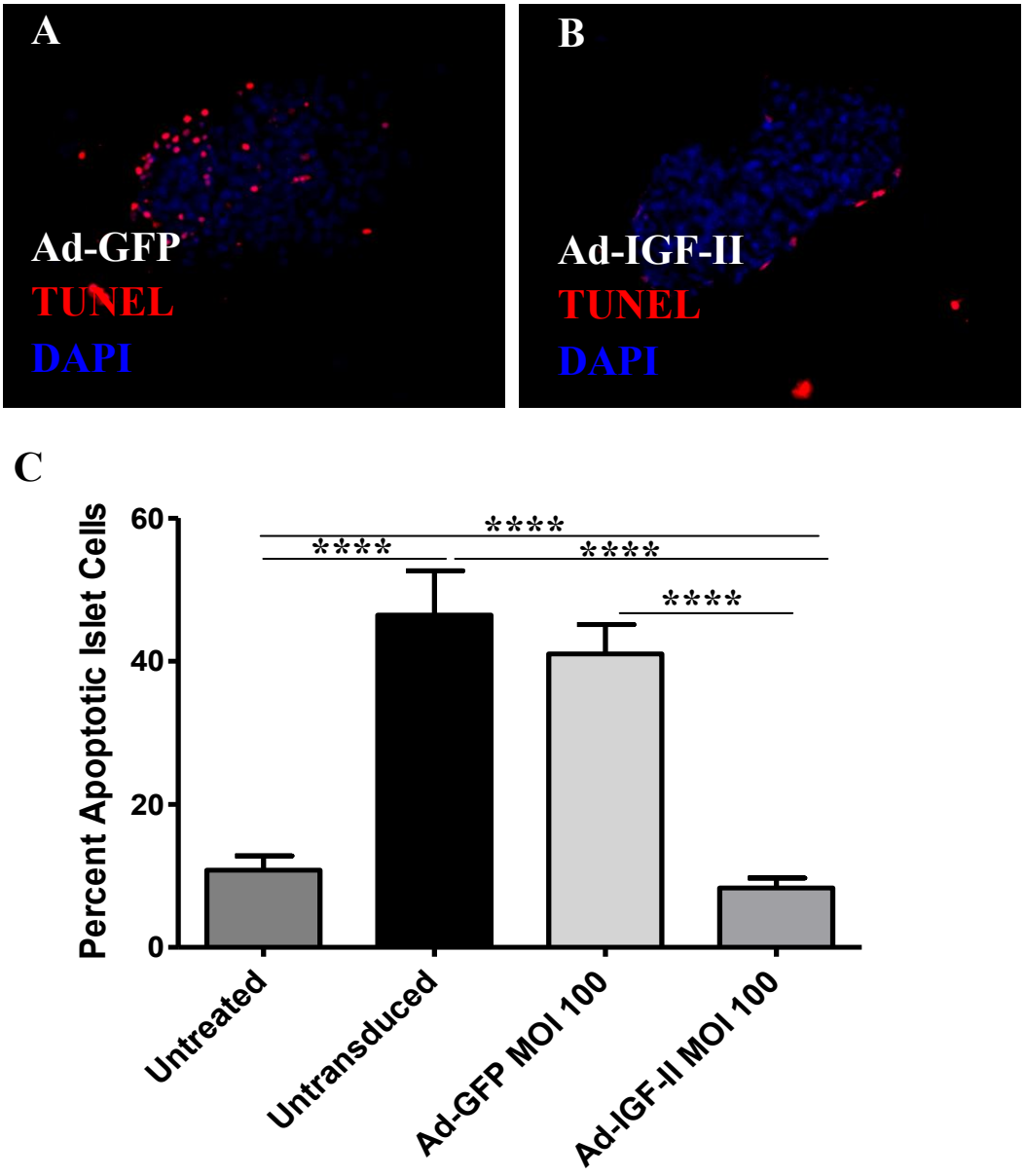

Figure. 5.2.8 Pro-inflammatory cytokine treated Ad-IGF-II transduced rat islets examined for apoptosis by TUNEL staining. Islets were left untreated or transduced at MOI 100 with Ad-GFP, Ad-IGF-II or untransduced 48 h before addition of IL-1β (35ng/ml) and IFN-γ (40 ng/ml) for an additional 24 h. TUNEL staining was used to determine islet cell apoptosis. Representative images of Ad-GFP and Ad-IGF-II TUNEL stained islets are depicted in (**A)** and (**B)** respectively. TUNEL positive cells (red) in the fluorescent images correspond to apoptotic cells. Blue = DAPI nuclear stain. Images were taken at 20 x magnification, Scale bar = 50µm. A total of 25 untreated islets, 22 untransduced islets, and 32 Ad-GFP or Ad-IGF-II transduced islets from six different rat islet preparations were counted to quantify the number of apoptotic cells **(C)**. The percentage of apoptotic islets was calculated by dividing the number of TUNEL positive islets by total islet

cells. Data are mean ± SEM, ****P<0.0001 (1way ANOVA). Bonferroni Multiple Comparison Test: ****p<0.0001 Untreated islets vs. Untransduced islets, ****p<0.0001 Untreated islets vs. Ad-IGF-II transduced islets, ****p<0.0001 Untransduced vs. Ad-IGF-II transduced islets, ****p<0.0001 Ad-GFP transduced islets vs. Ad-IGF-II transduced islets.

5.2.9 Characterisation of Ad-IGF-II transduced rat islet function following IL-1β and IFN-γ pro-inflammatory cytokine exposure

A glucose stimulated insulin secretion assay (GSIS) assay was performed to determine the glucose responsiveness of Ad-IGF-II transduced islets following 24 h cytokine exposure. The ability of untransduced and Ad-GFP transduced rat islets to secrete insulin following cytokine treatment was reduced compared to Ad-IGF-II transduced islets **(Figure 5.2.9)**.

5.2.10 The anti-apoptotic effect of IGF-II is neutralized by blocking the IGF-1R

Having characterised the anti-apoptotic function of IGF-II *in vitro,* the next step was to investigate the contribution of the IGF-1R in this effect. Blocking of the IGF-1R using an IGF-1R neutralization antibody on rat islets inhibited the ability of IGF-II to protect against cytokine induced cell death **(Figure 5.2.10)**. Specifically, following cytokine exposure Ad-IGF-II transduced islets treated with the IGF-1R antibody displayed 72.7% ± 6.5 total islet cell death, whereas Ad-IGF-II transduced islets displayed a 1.2-fold reduction in cell death (61.7% ± 4.3). Untransduced control islet cells displayed a high background of cell death (70.6% ± 4.3), as the blocking assay required the islets to be cultured in serum free culture conditions, for four days.

5.2.11 IGF-II activates the PI3K/Akt pathway to inhibit islet apoptosis

To investigate the pathway through which IGF-II works to inhibit apoptosis, rat islets were transduced with Ad-IGF-II or pre-treated with wortmannin, a potent and specific PI3K inhibitor prior to Ad-IGF-II transduction. Ad-IGF-II transduced islets demonstrated activation of both Akt and pAkt, whereas, wortmannin treatment led to a decrease in the phosphorylation of Akt **(Figure 5.2.11)**.

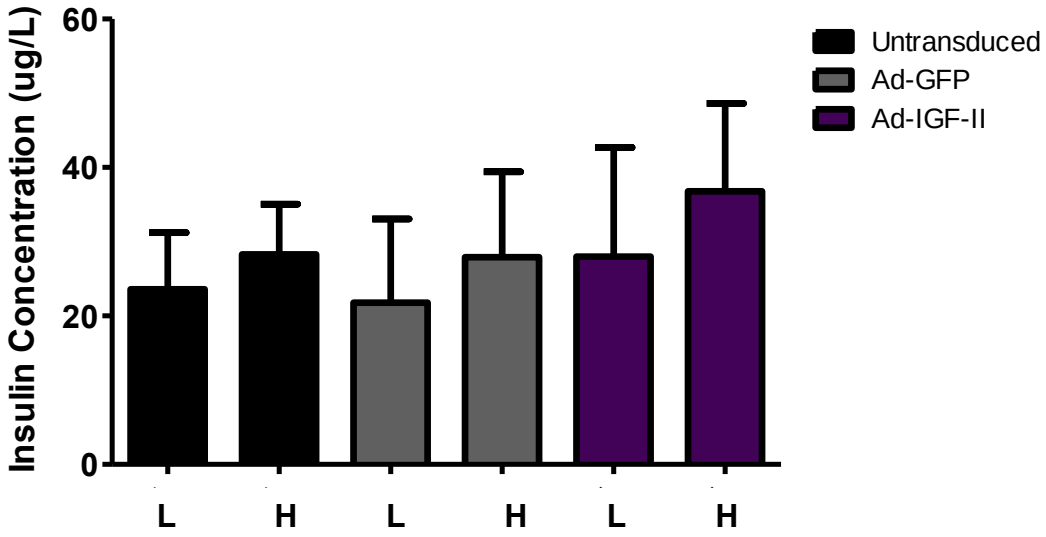

Figure 5.2.9. Evaluation of islet function of Ad-IGF-II transduced islets following cytokine exposure. Isolated rat islets were cultured for 24 h in the presence of pro-inflammatory cytokines IL-1β (35ng/ml) and IFN-γ (40ng/ml), and stimulated to release insulin by exposure to high (H) (25 mM) or low (L) (2.8 mM) concentrations of glucose. Insulin ELISA was used to determine the insulin released (µg/L) in experimental samples. Data are the mean ± SEM of three independent experiments. P= NS.

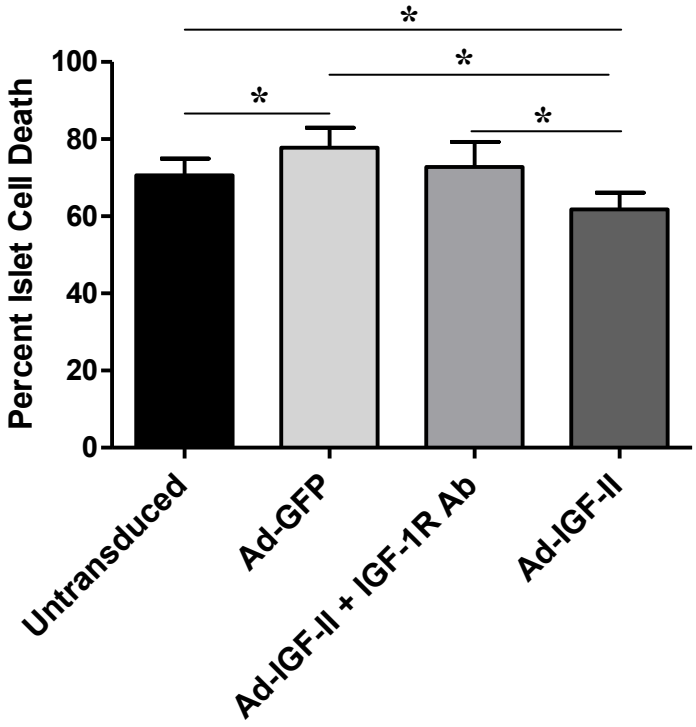

Figure. 5.2.10. Effect of IGF-1R blocking on pro-inflammatory cytokine induced Ad-IGF-II islet cell death. Islets were transduced at MOI 100 with Ad-GFP, Ad-IGF-II or untransduced 48 h before addition of IL-1β (35ng/ml) and IFN-γ (40 ng/ml) for an additional 24 h, or islets were pre-treated for 30 min with IGF-1R blocking antibody (10 µg) then transduced with Ad-IGF-II 48 h and treated for 30 min with IGF-1R blocking antibody before addition of pro-inflammatory cytokines as described above. Flow cytometry was used to determine percent islet cell death of dispersed islet cells using Annexin V and PI staining. The data is expressed as ± SEM of three independent experiments, *p=0.03 Untransduced islets vs. Ad-GFP transduced islets, *p=0.01 Untransduced islets vs. Ad-IGF-II transduced islets, *p=0.02 Ad-GFP transduced islets vs. Ad-IGF-II transduced islets, *p=0.04 Ad-IGF-II + IGF-1R Ab vs. Ad-IGF-II transduced islets (Student t-test, one-tailed).

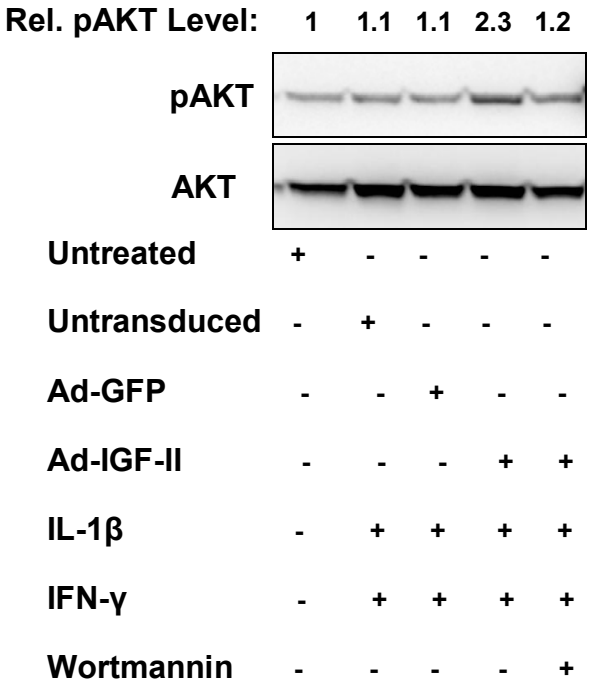

Figure. 5.2.11 IGF-II signals through the PI3K/Akt pathway to inhibit apoptosis. Western blot of islets untreated or transduced at MOI 100 with Ad-GFP, Ad-IGF-II or untransduced in serum-free RPMI for 48 h, before addition of IL-1β (35 ng/ml) and IFN-γ (40 ng/ml) for an additional 24 h. Islets were also treated with wortmannin (200 mM) for 1 h prior to Ad-IGF-II transduction and cytokine treatment. Relative phospho-Akt (pAKT) levels were determined by densitometry and corrected for total Akt levels relative to the untransduced islet control lane (above pAKT blot). Wortmannin treatment of Ad-IGF-II transduced islets reduced the phosphorylation of Akt, indicating that IGF-II activates the PI3K/Akt pathway to inhibit apoptosis.

5.3 Discussion

Apoptosis is a primary cause of islet cell death in the early post-transplant period (446). Inhibition of islet apoptosis is a very attractive and potentially effective therapeutic strategy to prevent loss of functional islet mass post-transplantation and improve clinical islet transplant outcomes. In this chapter, the effect of IGF-II over expression on human and rat pancreatic islet cell survival was investigated via an *ex vivo* gene transfer approach.

The efficacy and utility of any gene transfer strategy is influenced by the choice of transgene and by the method used to over express the chosen gene (447). When designing an anti-apoptotic strategy, there are a plethora of potential genes, drugs and growth factors that work by targeting specific intracellular molecules or cell signaling pathways to effectively inhibit apoptosis. The optimal gene must be paired with an appropriate vector type and gene promoter to firstly ensure efficient delivery of the transgene to the target cell and secondly to ensure sufficient gene expression without compromising target cell viability. The over expressed gene product can then exert its therapeutic effect in one of two ways, via a paracrine approach or by targeting specific intracellular molecules.

The anti-apoptotic strategy presented in this thesis fulfills a number of the above requirements. For example, Insulin-like Growth Factor-II (IGF-II) exerts its anti-apoptotic function in an autocrine and paracrine manner and as shown in **Chapter 4**, Ad-IGF-II efficiently transduces rat pancreatic islets without affecting islet viability or function. The fact that IGF-II works to inhibit apoptosis by exerting a paracrine influence on neighbouring cells is particularly advantageous, as it means that not every cell within the islet needs to be transduced in order to achieve the maximal therapeutic benefit. This is further supported by Ishii et al (448) who suggests that molecules which work in an autocrine and paracrine manner display a more marked biological action then those targeting intracellular molecules.

The preliminary aim of this chapter was to establish an *in vitro* model of apoptosis to mimic the *in vivo* stimulation of pro-inflammatory cytokine mediated insult occurring during the peri- and post-transplant period. A treatment time of 24 hours (h) was chosen to induce islet cell death, based on studies which have shown that β-cells have the ability to repair their metabolic and secretory function and damaged DNA following 24 h incubation with pro-inflammatory cytokines IL-1β and IFN-γ, but this damage can not be reversed following 36 h incubation (449, 450). IL-1β alone is capable of inducing apoptosis in β-cells, but TNF-α and IFN-γ act synergistically to potentiate the effects of IL-1β (451). Based on this IL-1β and IFN-γ were the

two cytokines utilised in this model. In the presence of IL-1β and IFNγ, islet cell death was induced in both human and rat islets. A final dose of 5 ng/ml IL-1β and 10 ng/ml IFN-γ and 35 ng/ml IL-1β and 40 ng/ml IFN-γ was chosen as the optimal dose to induce cell death in human and rat islets respectively. The concentrations were chosen based on their ability to induce both apoptosis and necrosis **(see section 5.2.1)** (426).

During apoptosis, phosphatidyl serine (PS) which is normally restricted to the internal surface of the plasma membrane becomes exposed on the surface of the cell. Annexin V is a 36 kDa phospholipid-binding protein that has a high affinity to PS (452) and is therefore used in studies of cell death. In most apoptotic assays, cells are stained with both Annexin V and Propidium Iodide (PI) and then analysed using flow cytometry. PI is a nucleic acid stain that binds to DNA by intercalating between the bases with little or no sequence preference (453). PI is a membrane impermeant which is excluded from viable cells and is therefore commonly used for identifying dead cells.

One caveat of anti-apoptotic studies is the transience and brevity of the apoptosis induced, which can sometimes be the culprit for the low sensitivity rate of apoptosis assays (454), this includes the Annexin V and PI assay which aims to capture specific cell populations undergoing early, mid and late stages of cell death. Therefore, this chapter utilised a combination of methods to rigorously evaluate, and confirm islet cell death following cytokine exposure. These methods include, microscopic evaluation, terminal deoxynucleotidyl-transferase mediated dUTP nick end-labelling (TUNEL) staining, Annexin V and PI flow cytometric staining and cell culture supernatant sampling for the presence of nitric oxide (NO). In addition, islet function was assessed using a glucose stimulated insulin secretion assay (GSIS).

In the mid 1950s, apoptosis was first observed in developing tissues using histological methods, and subsequently characterised via its unique morphology. For example, the morphological changes that are exhibited by apoptotic cells include cell blebbing, cell shrinkage, chromosomal condensation and chromosomal DNA fragmentation. In this chapter, changes in islet structure and morphology were evident following IL-1β and IFN-γ cytokine treatment. A similar finding has been reported by Yeung et al (455) who have described alterations in human islet morphology following pro-inflammatory cytokine exposure *in vitro*. Others (450) have shown that IL-1β induces islet cell sloughing following 48 h incubation, and within four days less than 10% of intact islets remain as many have degenerated into single cells or clusters of cells. In this

study, cytokine treated islets displayed rough and sometimes broken membrane borders, darkened hypoxic centres and cell shrinkage, the presence of which are indicative of cell death.

Hopcroft et al (456) have shown that disruption of the islet microanatomy leads to a reduction in the insulin secretory response of islets. In another study, isolated rat islets treated with IL-1β led to concentration and time dependent inhibition of insulin biosynthesis that was followed by islet destruction (457, 458). Mechanistically, *In vitro* exposure of β-cells to a combination of IL-1β and IFN-γ causes functional changes similar to those observed in pre-diabetic patients, namely a preferential loss of first-phase insulin secretion in response to glucose, caused by a decrease in the docking and fusion of insulin granules to the β-cell membrane (459). In this chapter, IL-1β and IFN-γ significantly impaired the ability of islets to secrete insulin when challenged with an exogenous glucose load. However, when islets were transduced with Ad-IGF-II prior to cytokine exposure they retained their insulin secretory capacity and fewer apoptotic cells were observed in TUNEL stained cytospin preparations. It is particularly interesting to note that Ad-IGF-II transduced islets secreted more insulin in response to an increased glucose load than relevant control islets. This is supported by Cohen et al (460) who have shown that mouse islets from transgenic animals over expressing IGF-II secrete more insulin than control mice islets, a phenomenon that may be linked to the growth promoting effects of the IGF-II peptide.

As discussed previously, islet culture should not exceed 2 – 3 days as to ensure no substantial loss of viability prior to transplantation. Based on this, rat pancreatic islets were transduced for a maximum time of 48 h prior to treatment with pro-inflammatory cytokines IL-1β and IFN-γ. In this chapter, Ad-IGF-II transduced rat islets were protected from apoptosis and cell death induced by pro-inflammatory cytokine exposure *in vitro*, confirming the anti-apoptotic action of IGF-II.

Furthermore, the anti-apoptotic effect mediated by IGF-II was effectively neutralised by a blocking antibody targeting the IGF-1R and western blot analysis confirmed that IGF-II inhibits islet apoptosis via activation of the PI3K/Akt intracellular signaling pathway. This result is further supported by the well-documented ability of IGF-II to prevent apoptosis in many cell types working via the IGF-1R to activate PI3K (461-463). In contrast to this, others (464, 465) have shown that the mitogen-activated protein kinase (MAPK) intracellular signaling pathway plays a primary role in potentiating the mitogenic and migratory actions of IGF-II.

Ilieva and colleagues (415) have shown that incubation of hamster islets with pancreatic duct conditioned medium containing 34 ng/ml IGF-II, successfully protects islets from apoptosis and necrosis that occurs following the islet isolation procedure. Furthermore, the supplementation of minimally nutritive (serum-free) medium with 500 ng/ml IGF-II improves *in vitro* islet viability (466). Our data confirms the ability of IGF-II to promote islet survival *in vitro* and this was achieved with a 40-fold lower concentration of IGF-II than that used by Robitaille (466). In addition, Ad mediated IGF-II over expression led to improved protection of islets against cytokine induced apoptosis, compared to rat islets pre-treated with 500 ng/ml recombinant IGF-II. These results suggest that there is an enhanced anti-apoptotic function when IGF-II is over expressed within the local islet microenvironment.

This concept is supported by other investigators (436) who cultured islets with zVAD-fmk, a pan caspase inhibitor, prior to transplantation and showed no improvement in islet allograft function *in vivo*, suggesting a lack of sustained local caspase inhibition. To circumvent this issue, in the same study diabetic BALB/C mice were treated with exogenous zVAD-fmk by injection, in addition to receiving an islet transplant under the kidney capsule. The outcome was an improvement in marginal mass islet function. However, this anti-apoptotic approach is dependent on systemic administration, increasing the likelihood of toxic side-effects on non-target patient organs. The *ex vivo* anti-apoptotic strategy presented in this thesis avoids the need for systemic treatment of recipients.

However, in this chapter Ad mediated IGF-II over expression did not adequately protect human islets against IL-1β and IFN-γ mediated cell death. This was likely due to the high background of apoptotic and necrotic islets in the islet preparations prior to performing the experiments. In this case, the two islet preparations utilized had less than 50% viable cells, and therefore a potential reason for the experimental result could be due to the fact that the islet cells were already necrotic or in the process of becoming necrotic prior to beginning the assay. Considering the experiment is run for a total of four days it would be expected that the already reduced islet viability would continue to decrease during the experimental culture period. This is supported by Robitaille (466) who have shown that islets with more than 50% dead cells usually do not recover and all cells eventually die.

Moreover, isolated human islet preparations are only allocated for research use when the donor family has consented and the preparation is considered unsuitable for clinical transplantation. Prior to transplantation, isolated islets must undergo viability and functionality testing. Therefore, research consent human islets have failed the strict requirements for clinical islet transplantation and may already exhibit reduced viability, making apoptosis assays difficult to perform. Subsequently, there is often a large batch to batch variability in the quality and purity of human islets, which complicates data analysis and correlation of results from one experiment to another (467). Based on this, it is suggested that future studies should adhere to a strict (>70%) viability cut off before being utilized in experiments. This would mean that a higher percentage of viable and functional islet cells would then be used, in order to obtain an accurate respresentation of the anti-apoptotic effects mediated by IGF-II. In future studies, it would be advantageous to investigate novel methods to maintain islet viability during extended islet culture. For example, in this thesis islets were maintained in culture at 37°C with 5% CO_2, however others (468) have shown that culture of islets at 4°C improves the outcome of islet transplantation compared to islets cultured at either 22°C or 37°C.

In conclusion, in this chapter an *in vitro* IL-1β and IFN-γ pro-inflammatory cytokine induced model of apoptosis was established in human and rodent pancreatic islets. The application of Ad-IGF-II transduced islets within this model confirmed the *in vitro* anti-apoptotic effect of IGF-II in rodent islets. Although the ability of IGF-II to inhibit apoptosis has been shown previously (415, 466), these studies required high doses of exogenous IGF-II (100 – 500 ng/ml) to achieve either the same anti-apoptotic effect, or a reduced effect than that conferred by Ad-IGF-II transduced islets. The major advantage of this anti-apoptotic strategy, compared to other published strategies, is the local and constitutive over expression of IGF-II, which cannot be adequately controlled or maintained in culture systems that employ only exogenous IGF-II islet treatment.

CHAPTER 6

A MARGINAL MASS ISLET TRANSPLANT MODEL TO STUDY THE ABILITY OF AD-IGF-II TRANSDUCED RAT ISLETS TO IMPROVE ISLET SURVIVAL IN DIABETIC NOD-SCID MICE

6.1 Introduction

Type 1 Diabetes (T1D) is a disease of metabolic dysregulation, most notably abnormal glucose regulation (469). The worldwide incidence of T1D has increased rapidly in recent decades, particularly in young children (470). Insulin therapy is the current treatment of choice for T1D patients, however it is associated with long-term complications including retinopathy, neuropathy, impaired kidney function and cardiovascular disease (471). Transplantation of pancreatic islets is a promising alternative treatment for T1D patients. However, it is estimated that 50–70% of islets are destroyed in the immediate post transplant period by various intrinsic and extrinsic apoptotic stresses (418, 446). Therefore, protecting β-cells against early apoptotic death may ultimately improve β-cell function and reduce the number of islets required for successful transplantation.

One way to achieve this is the use of gene transfer, to over express an anti-apoptotic molecule, such as Insulin-like Growth Factor-II (IGF-II) in pancreatic islets prior to their transplantation. IGF-II is highly expressed during early development, whilst IGF-I is characteristic of post-weaning childhood and adult tissues (472-474). While **Chapter 5** successfully demonstrated the *in vitro* anti-apoptotic function of IGF-II against pro-inflammatory cytokines IL-1β and IFN-γ, this chapter aimed to investigate the anti-apoptotic effect of Ad-IGF-II transduced islets in an *in vivo* islet transplant setting. Animal testing and clinical trials are two methods of *in vivo* testing. Animal models of T1D are often utilised to investigate the progression and genetics of T1D (475), or to test the efficacy of new therapeutic interventions, such as the over expression of IGF-II to improve islet survival post-transplantation.

The most complete way to induce diabetes *in vivo* is to remove the pancreas, either partially or totally (476). However, pancreatectomy is a major procedure, requires advanced surgical skills and it is almost impossible to restore normoglycemia in pancreatectomised animals (477). Chemically induced diabetes, using Streptozotocin (STZ) or Alloxan, offers the most rapid and cost effective alternative (478). STZ, also known as 2-deoxy-2-(3-(methyl-3-nitrosoureido)-D-glucopyranose, is a glucose moiety which contains a very reactive nitrosurea group from the mould *Streptomyces Griseus* (479). STZ is transported into the cell via the glucose transporter 2 (GLUT2) receptor, which is highly expressed on pancreatic β-cells (480). STZ is toxic to β-cells, it causes alkylation of DNA and results in the formation of cytotoxic superoxide, hydrogen peroxide and hydroxyl radicals (481) and subsequently leads to diminished insulin production (482) **(Figure 6.1)**.

There are a variety of animal models utilized in the field of diabetes research, one example is miniature swine which share similar anatomic and physiological characteristics to humans (483). The similarity of their β-cells and insulin to those of humans is well recognized, as insulin was derived from pig pancreata prior to transgenic human insulin production. The diabetic Rhesus monkey provides another useful model for pre clinical investigation of therapeutic islet transplantation strategies and new drug treatments for T1D (484). The Non-Obese Diabetic (NOD) mouse is a spontaneous mouse model of T1D, in which insulinitus presents at 4 – 5 weeks and diabetes between 12 – 30 weeks of age (476). NOD mice share many similarities to T1D in humans, including the presence of pancreas-specific autoantibodies and autoreactive $CD4^+$ and $CD8^+$ T cells (485).

The NOD-SCID mouse is an immunodeficient mouse model with impaired T and B lymphocyte development, whereby the severe combined immunodeficiency (SCID) mutation has been transferred onto the NOD background. NOD-SCID mice are autosomal recessive and are characterised by a single nucleotide polymorphism with *Prkdc* gene on chromosome 16. NOD-SCID mice provide an excellent model system for xenogeneic islet transplant studies, such as the transplantation of human or rat islets, due to the avoidance of immune-mediated rejection (486, 487). The major benefit to using rodents for *in vivo* studies is convenience. For example rodents are small, easily handled and are relatively inexpensive.

Figure 6.1. Histology of NCr athymic nude mice pancreas. Insulin staining (brown) of murine pancreata two days after mice received either an injection of Hank's buffered salt solution (HBSS) **(A)** or streptozotocin (STZ) **(B)**. Note the reduction in insulin staining intensity after STZ. Figure adapted from Deeds et al (478).

The preliminary aim of this chapter was to investigate how NOD-SCID mice respond to the administration of STZ and their subsequent tolerance to the induced diabetic state. Next, a marginal mass islet transplant model was developed in which transplantation of 50 islet equivalents (IEQ) was shown to reverse diabetes in a marginal number of diabetic NOD-SCID mice. The primary goal of the marginal mass model was to design a transplant model whereby euglycemia rates in control mice were sufficiently low as to ensure that any improvement in transplant outcomes could be clearly observed in mice receiving Ad-IGF-II transduced islets. Subsequently, diabetic NOD-SCID mice were transplanted with untransduced, Ad-GFP or Ad-IGF-II transduced islets and followed for a return to euglycemia or 'cure'. Mice receiving Ad-IGF-II transduced islets experienced significantly improved transplant outcomes *in vivo*.

6.2 Results

6.2.1 Optimization of diabetes induction in NOD-SCID mice

The ability of a single dose of Streptozotocin (STZ), delivered via intra peritoneal (i.p) injection, to induce diabetes in NOD-SCID mice was investigated using a dose range from 170 – 200 mg/kg in female mice and 180 mg/kg in male mice as shown in **Table 6.2.1**. Mice were considered diabetic following two consecutive blood glucose (BGL) readings ≥16.6 mmol/l (316, 317). NOD-SCID mice approximately 9 weeks of age and weighing at least 20 g were used for all animal studies described in this chapter. The STZ dose of 180 mg/kg was chosen for transplant experiments, as it stably induced diabetes in 54% (15/28) of NOD-SCID female mice and 77% (20/26) of male mice. In addition, 180 mg/kg resulted in a lower mortality and is a dose which has successfully been used by other researchers (488).

6.2.2 Gender differences confer susceptibility to STZ-induced diabetes weight loss in NOD-SCID mice

Weight loss is a well described symptom of T1D in humans and is an indicator of diabetes in animal models of T1D. Excessive weight loss can be detrimental to an animal's health and well being and therefore must be appropriately monitored. Based on this, fifteen female and twenty male mice received an i.p injection of 180 mg/kg STZ and the weight of each mouse was recorded daily. As shown in **Table 6.2.2** the average weight loss of female diabetic mice was 16% but this was significantly higher in male mice (25%). The extreme weight loss experienced by the diabetic male mice did not fall within the ethical guidelines of this project, that being 15% weight loss from the animals starting weight (SW), and due to this only female mice were subsequently dosed with STZ in this thesis.

6.2.3 Generation of an *in vivo* marginal mass islet transplant model

Diabetic NOD-SCID female mice were transplanted with 200, 100 or 50 IEQ to define the minimal mass of islets required to reverse or 'cure' diabetes in a marginal number of diabetic animals. Transplantation of either 100 or 200 IEQ led to a return to euglycemia, characterised by two consecutive blood glucose (BGL) readings ≤11.2mmol/l (316) in 100% of animals, however 50 IEQ led to a 43% cure rate **(Figure 6.2.3)**. Based on this, 50 IEQ was chosen as the marginal mass for further transplantation studies.

Table 6.2.1. STZ dose optimization in NOD-SCID mice to induce diabetes. Mice received an i.p injection of STZ between 160 – 200 mg/kg, and were followed for diabetes. Doses 190 – 200 mg/kg were grouped together as they caused a high degree of STZ related toxicity.

Sex	STZ Concentration (mg/kg)	n	Diabetic (n)	Not Diabetic (n)	Mortality (n)
Female	160	4	0	4	0/0 (0%)
Female	170	26	16	10	8/26 (30%)
Female	180	28	15	13	6/28 (21%)
Female	190 – 200	18	16	2	6/18 (33%)
Male	180	26	20	6	0/26 (0%)

Table 6.2.2. Analysis of NOD-SCID mice weight following STZ injection. Female **(A)** and male **(B)** mice were weighed prior to STZ injection (180 mg/kg) and then daily for a maximum period of 28 days. The total percentage weight loss for each mouse from starting weight to end of study period day was calculated and recorded in the table as 'percentage weight loss'.

A. Female

Mouse Number	Start Weight (g)	Percentage Weight Loss
1	21.0	14%
2	21.1	17%
3	20.0	27%
4	20.0	9%
5	20.0	12%
6	20.2	9%
7	22.8	13%
8	22.9	17%
9	21.7	26%
10	20.0	11%
11	20.9	23%
12	22.0	14%
13	24.2	23%
14	20.8	18%
15	22.0	14%
Average (±SEM)	21.3 ± 0.3	16% ± 1.5

B. Male

Mouse Number	Start Weight (g)	Percentage Weight Loss
1	27.6	15%
2	29.1	13%
3	25.1	25%
4	31.6	17%
5	28.7	14%
6	25.2	27%
7	24.8	30%
8	26.5	30%
9	29.1	24%
10	26.6	28%
11	27.4	23%
12	23.7	29%
13	23.8	27%
14	28.4	24%
15	26.5	24%
16	28.0	29%
17	24.8	30%
18	25.8	33%
19	29.6	27%
20	27.1	29%
Average (±SEM)	27.0 ± 0.5	25% ± 1.3

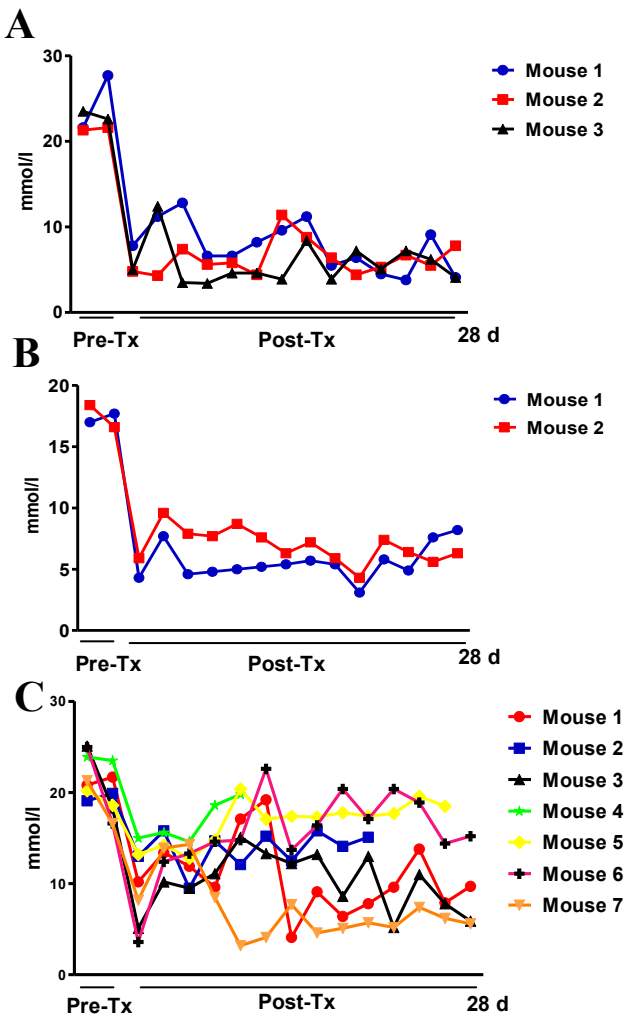

D

Number IEQ transplanted	Total Mice	Percent Euglycemia
200	3	3/3 (100%)
100	2	2/2 (100%)
50	7	3/7 (43%)

Figure 6.2.3. 50 IEQ defines the marginal mass required for diabetes reversal in an *in vivo* islet transplant model. Rat islets were isolated from Albino Wistar rats and used to transplant diabetic mice. Mice were transplanted with **(A)** 200 IEQ (n=3), **(B)** 100 IEQ (n=2) or **(C)** 50 IEQ (n=7) and were followed for a maximum of 28 days. Return to euglycemia post-transplantation was achieved in 100% of recipients receiving 200 or 100 IEQ and 43% in recipients transplanted with 50 IEQ **(D)**. Pre-tx = pre-transplant, Post-tx = Post-transplant.

6.2.4 NOD-SCID islet transplant procedure

A marginal mass of islets (50 IEQ) were transduced with Ad-GFP, Ad-IGF-II or untransduced and visualized under a light microscope prior to their transplantation under the kidney capsule of NOD-SCID STZ-induced diabetic mice **(Figure 6.2.4(A-G))**.

6.2.5 Effect of Ad-IGF-II transduced rodent islets in a marginal mass islet transplant model

To investigate the effect of Ad-IGF-II transduction in an islet transplant setting, a marginal mass of islets (50 IEQ) were transduced with Ad-GFP, Ad-IGF-II or untransduced and transplanted under the kidney capsule of female NOD-SCID STZ-induced diabetic mice. Transplantation of Ad-IGF-II islets significantly increased the rate of euglycemia to 78% (n=9), compared to 18% and 46% of Ad-GFP and untransduced islet recipients, respectively (both n=11) **(Figure 6.2.5(A))**. In addition, the mice were weighed daily following their transplant (**Figure 6.2.5(B))**. Mice receiving Ad-IGF-II transduced islets stabilized and slightly increased their weight following transplantation, while this was not the case for mice recieving untransduced or Ad-GFP transduced islet grafts.

6.2.6 Confirmation of diabetes in NOD-SCID mice following transplantation

Surgical removal of the graft bearing kidney was not performed due to ethical guidelines which prohibited a second surgical procedure to be performed on the mice following their islet transplant. Therefore, the diabetic state of NOD-SCID mice transplanted in **section 6.2.5** was confirmed by staining the transplant mice pancreata for endogenous insulin. Mice pancreata were fixed in 10% buffered formalin and paraffin-embedded prior to sectioning. Each pancreas was cut at three depths or 'levels' throughout the tissue to allow for identification of endogenous islet cells. Each pancreas section was visualized using a fluorescent confocal microscope and the mean islet area μm^2 was measured using image J software. There was no difference in the mean islet area between the transplant recipient mice and the non-diabetic control, 12108 ± 2737 and 10958 ± 982 μm^2 respectively. However, there was a 3.7-fold reduction in the number of islets per pancreas in transplant mice compared to the control **(Table 6.2.6)**. Immunohistochemical analysis of pancreas tissue demonstrated a reduction in the insulin immunoreactivity of islets from transplant mice, compared to non-diabetic control islets, which displayed strong insulin positivite staining **(Figure 6.2.6)**, thereby confirming that the transplant effect observed in **Figure 6.2.5** was mediated via the anti-apoptotic function of IGF-II in islets.

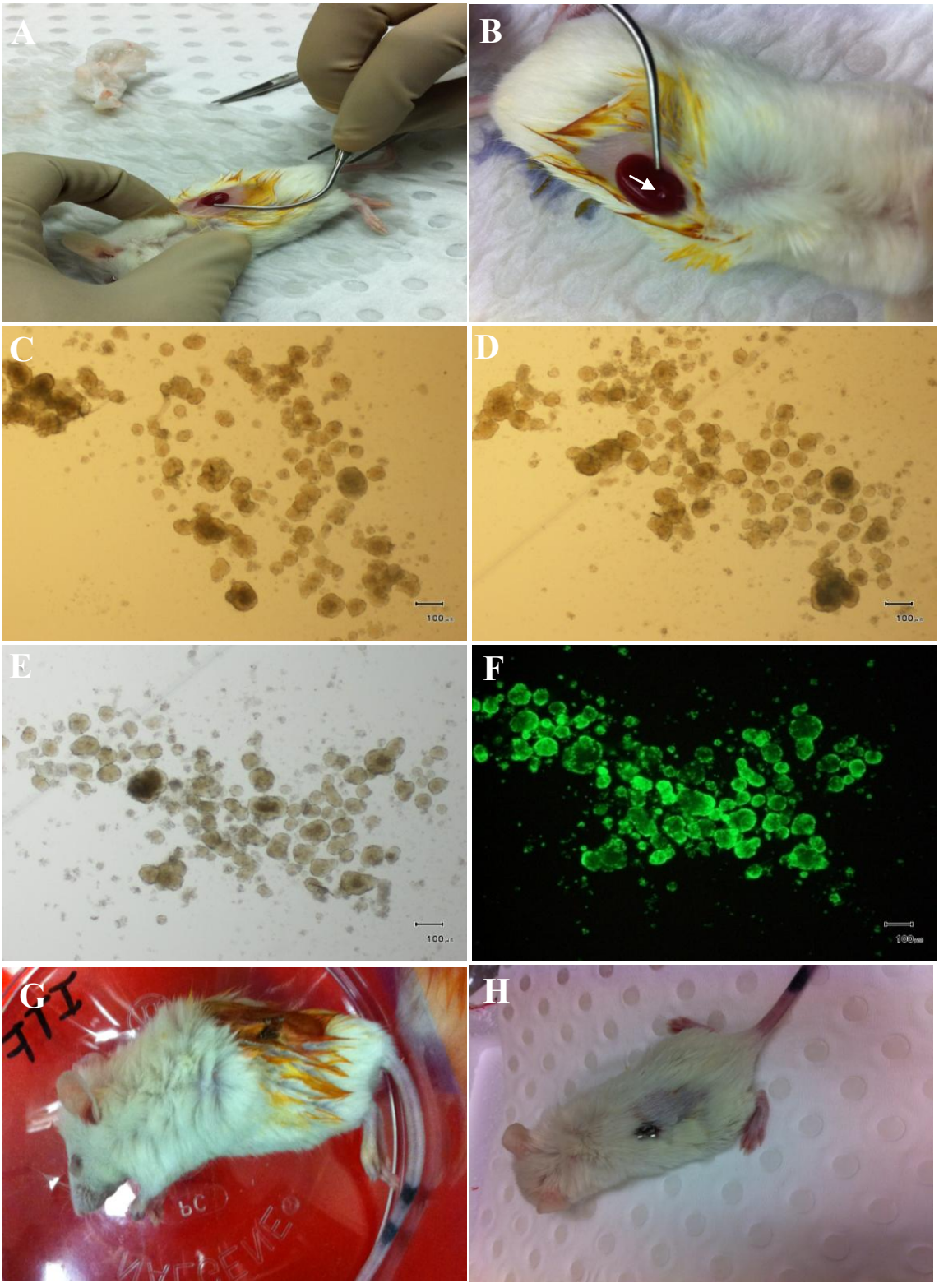
A
B
C
D
E
F
G
H

Figure 6.2.4. Rat islet transplantation procedure in NOD-SCID mice. **(A)** The mouse is anaethetised and the kidney (transplant site) is exposed. **(B)** Image of an islet graft under the kidney capsule (white arrow). Representative microscope image of **(C)** Untransduced **(D)** Ad-IGF-II and **(E-F)** Ad-GFP transduced islets in culture immediately prior to the transplant procedure. Images were taken at 4x magnification, Scale bar = 100 μm. **(G)** Immediately following the transplant procedure the animals would was sutured and antiseptic was applied to ensure sterility, the transplant site begins to heal within seven days post-transplant **(H)**.

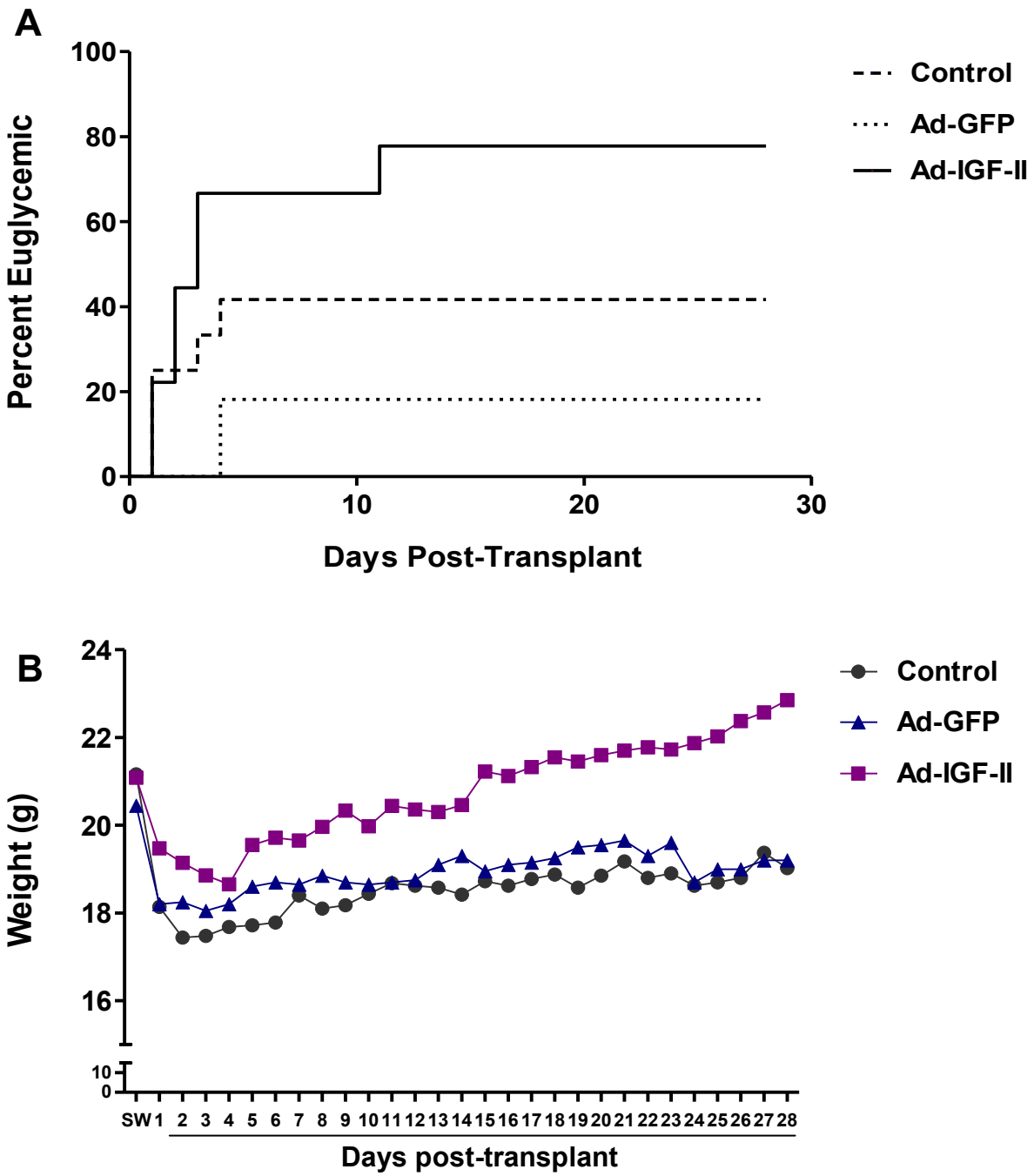

Figure. 6.2.5. STZ-induced diabetic recipients of a marginal mass islet graft. Diabetic mice were transplanted with Ad-IGF-II (n=9), Ad-GFP (n=11) or untransduced (n=11) marginal mass islet grafts and followed for a maximum of 28 days. **(A)** Return to euglycemia post-transplantation was achieved in 78% of recipients receiving Ad-IGF-II transduced islets (7/9) (solid line) compared with 18% (2/11) and 46% (5/11) of control animals receiving Ad-GFP (broken line) or untransduced islets (dotted line), respectively. $p<0.05$ (Log-rank (Mantel Cox) Test. **(B)** Mice were weighed prior to STZ injection (SW= starting weight) and then daily following their transplantation. ****P<0.0001 (1way ANOVA). Bonferroni Multiple Comparison Test: ****P<0.0001 Control vs. Ad-IGF-II, ****P<0.0001 Ad-GFP vs. Ad-IGF-II.

Table 6.2.6. Confirming native islet destruction in NOD-SCID mice. Diabetes was confirmed in NOD-SCID transplant recipients by immunohistochemical analysis for insulin staining. Mean islet number and area μm^2 ± SEM between islet transplant recipients and non-diabetic NOD-SCID mice was determined using ImageJ software.

Sample	Type of islet graft recieved	Total number of islets	Mean islet area μm^2 ± SEM
I	Nil, Non-Diabetic Control	35	10958 ± 982
II	Ad-GFP	8	12256 ± 3968
III	Ad-GFP	10	13896 ± 1675
IV	Ad-GFP	2	10220 ± 5893
V	Untransduced	4	8084 ± 1346
VI	Ad-IGF-II	14	15515 ± 3060
VII	Ad-IGF-II	7	14826 ± 2845
VIII	Ad-IGF-II	9	12118 ± 3778
IX	Ad-IGF-II	8	9996 ± 2325
X	Ad-IGF-II	18	14819 ± 3473
XI	Ad-IGF-II	15	13464 ± 2057
XII	Ad-IGF-II	9	8294 ± 623
XIII	Ad-IGF-II	10	11814 ± 1801

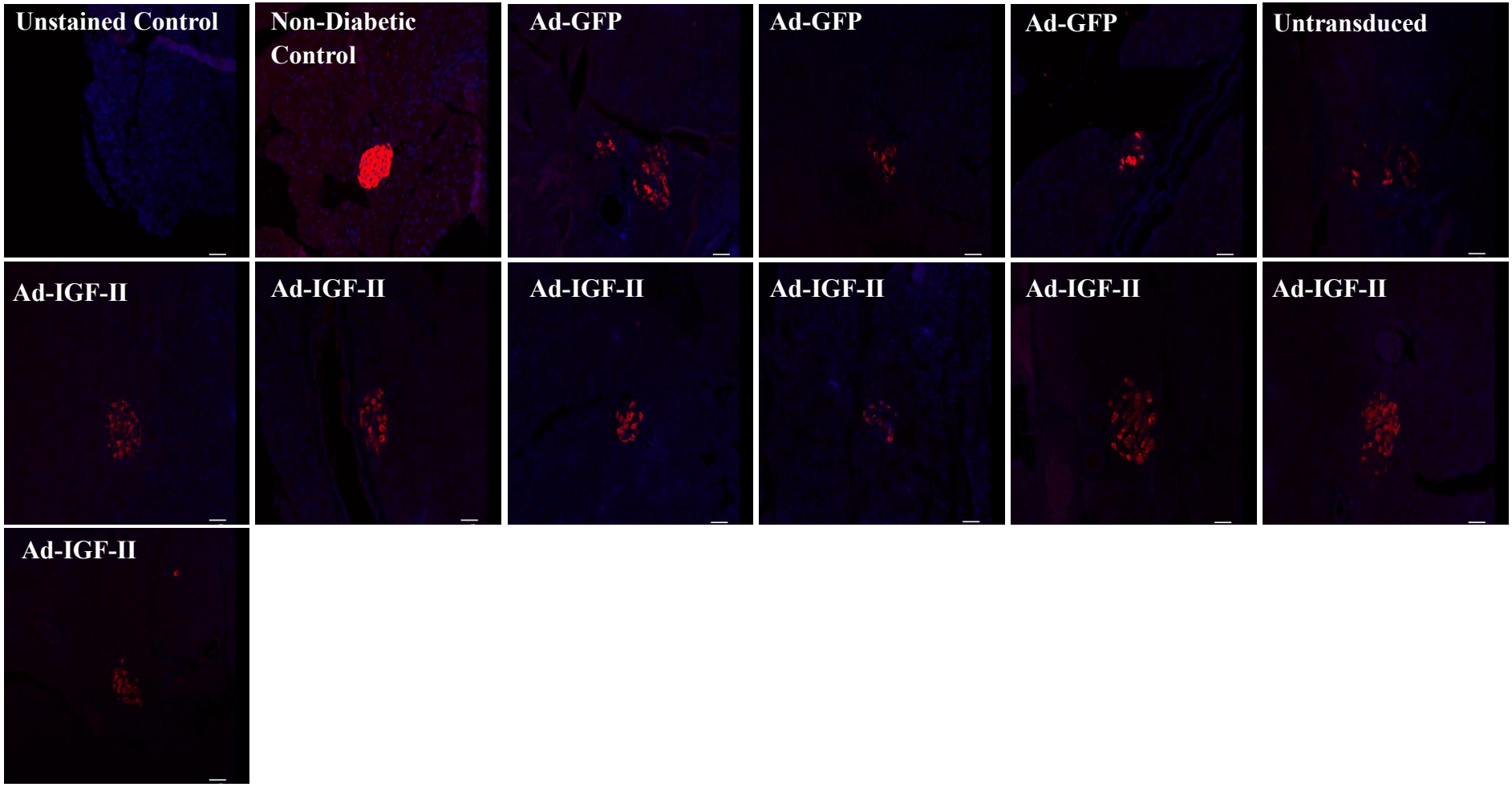
Unstained Control
Non-Diabetic Control
Ad-GFP
Ad-GFP
Ad-GFP
Untransduced
Ad-IGF-II
Ad-IGF-II
Ad-IGF-II
Ad-IGF-II
Ad-IGF-II
Ad-IGF-II
Ad-IGF-II

Figure 6.2.6. Confirming native islet destruction in NOD-SCID mice. Immunofluorescent staining of islet cells in mice pancreata, demonstrating a lack of endogenous insulin positivity in diabetic transplant recipients compared to control. Images were taken at 40 x magnification or 10 x magnification (unstained control), Scale bar = 50 μm.

6.3 Discussion

The ability of IGF-II to protect rat pancreatic islets against *in vitro* pro-inflammatory cytokine induced apoptosis was confirmed in **Chapter 5** of this thesis. Therefore, this chapter aimed to extend these promising results by investigating the effect of Ad-IGF-II transduction, in an *in vivo* islet transplant setting. Previous anti-apoptotic strategies have aimed to enhance marginal mass islet graft survival by over expressing growth factors such as hepatocyte growth factor or insulin (489, 490). However these strategies only work to improve the growth or function of islets that escape the initial apoptosis following islet transplantation. Considering that 50 – 70% of islets die due to apoptosis and necrosis in the immediate post-transplant period (188), a potential major advantage of the anti-apoptotic approach investigated in this thesis is that islets are exposed to a constitutively produced supply of anti-apoptotic IGF-II prior to transplantation and during the immediate post-transplant period. In addition, IGF-II has a number of advantages over other anti-apoptotic strategies, such as mediating cell survival by acting upstream of caspase activation. IGF-II blocks proteolytic processing of the major executioner caspases, caspase-3 and caspase-7 (491), preventing initiation of the apoptotic cascade (492).

In the human setting of T1D, β-cell destruction is ultimately induced by receptor (i.e. Fas/Fas Ligand) mediated mechanisms and/or secretion of cytotoxic molecules, such as granzymes and perforin (31). In animal models, a single high dose (180 mg/kg) of Streptozotocin (STZ) produces a diabetic state which is similar to human T1D. STZ works by inducing necrotic β-cell death so does not exactly mimic the pathogenesis of human T1D. However, STZ-induced diabetes provides a satisfactory experimental model for investigation of islet cell survival (493-495) and is the gold standard for testing the function of clinical islet transplant preparations *in vivo*.

Diabetes can be induced by STZ in one of three ways: multiple small doses over a period of several days, a single moderate sized dose or a single large dose (496, 497). A single large dose of STZ (180 mg/kg) was used for experiments in this thesis in order to rigorously evaluate improvements in islet transplant outcomes. Although a higher percentage of mice became diabetic when dosed with 190 – 200 mg/kg of STZ, the mortality rate of mice was also increased. A likely explanation for this result is due to off-target effects as STZ does not specifically target the insulin-producing β-cells for destruction (478). This is supported by Valentovic et al (498) who have shown that STZ treatment is associated with renal, cardiac and adipose tissue damage

and increased oxidative stress, inflammation and endothelial dysfunction. When considering the fact that STZ can enter any cell or tissue type expressing the glucose transporter 2 (GLUT2) receptor, such as the liver, pancreas, intestine, kidney and brain (499) it is not suprising that the reported off-target effects of STZ are numerous.

The extreme weight loss experienced by the male mice in this chapter was likely due to the administration, and subsequent toxicity of STZ. Sudden weight loss following STZ administration has been described previously (500). Specifically, Deeds and colleagues (478) suggest that weight loss approaching 20% of an animal's starting body weight within 10 days of STZ injection is not uncommon and Dekel et al (501) have reported weight loss of up to 40% within 14 days of STZ injection in a single large dose STZ model. A particularly interesting finding of this chapter, is that male NOD-SCID mice were more susceptible to STZ-induced diabetes (77% of male mice became diabetic versus 54% of female mice). This has been observed in other rodent studies (502-506) and has been subsequently attributed to the expression of oestradial, a female reproductive hormone, shown previously to protect β-cells from apoptosis (507).

As discussed in **Section 6.1** rodent models have been used to investigate both the pathogenesis of T1D and the utility of potential therapeutics for the treatment and cure of T1D (508). For example, in the NOD mouse, over 200 therapies have been shown to prevent, delay or cure diabetes (509). Despite this, these therapies have yet to be successfully translated to a clinical human setting. For experiments involving xenogeneic rat islet transplantation, the immunocompromised NOD-SCID mouse strain was used, in order to avoid immune-mediated graft rejection. As 50–70% of islets are destroyed in the immediate post transplant period by apoptosis and necrosis (188), the *in vivo* study was limited to 28 days post-transplantation to investigate the effect of Ad-IGF-II transduction on early graft survival. This study successfully highlighted the potent anti-apoptotic effects of Ad-IGF-II over expression *in vivo* as a major mechanism for enhancing islet survival post-transplantation. The improvement of islet graft survival, thus reducing the number of transplanted islets required to achieve insulin independence, is critical for improving clinical islet transplant outcomes.

The ability of IGF-II to improve *in vivo* islet transplant outcomes has been reported previously (415, 466). However, the major limitation of these studies is that islets were only subject to pre-transplant culture with exogenous IGF-II. Robitaille et al (466) have shown that pre-transplant culture of islets with IGF-II, prior to islet encapsulation and subsequent transplantation, leads to improved transplant outcomes with a reduced islet cell mass. However this transplant effect is likely to be a result of improved islet survival following isolation, resulting in a larger mass of islets being transplanted in the IGF-II treatment group. Due to the short half life of growth factors (510), it is unlikely that the residual IGF-II transplanted with the encapsulated islets would have any significant effect *in vivo*. Therefore, IGF-II supplementation as a stand-alone anti-apoptotic strategy holds limited clinical applicability, as transplanted islets are particularly vulnerable to stress induced apoptosis prior to engraftment and revascularization (418, 446). A potential major advantage of the strategy presented in this thesis is that islets are exposed to a constitutively produced supply of local anti-apoptotic IGF-II prior to transplantation and also during the immediate post-transplant period. In another study, Jourdan and colleagues (232) co-encapsulated islets with bio-engineered TM4 cells, an adherent sertoli cell line, that produces IGF-II and found *in vitro* islet survival and post-transplant outcomes to be improved. However, encapsulated islets are unable to revascularize following transplantation, exacerbating islet hypoxia and subsequent β-cell death (183, 511). Moreover, unlike in our strategy, which provides transient transgene expression, the IGF-II produced by the transfected TM4 cells raises potential concern for malignancy as the cells permanently over express IGF-II (243, 512).

In this chapter, the small number of transplanted islets (50 IEQ) prevented post-transplant examination of the islet grafts. While the transplantation of a higher IEQ number was explored within the optimization stage of the marginal mass islet model, both 200 and 100 IEQ reversed diabetes in 100% of diabetic transplant recipients, and therefore were not considered appropriate for use in a marginal mass setting. The potent euglycemic effects seen in mice receiving 200 and 100 IEQ is likely due to the robust insulin secretory response of rat islets, which is characterised by a large, rising second-phase insulin response to stimulatory glucose not present in mouse islets (513). Post-transplant examination of the islet grafts would have been particularly advantageous as IGF-II is a potent growth factor, which may confer additional survival benefits to transplanted islets, such as up-regulation of angiogenic factors. Studies have shown that IGF-II may participate in angiogenesis through its ability to up regulate vascular endothelial growth factor (VEGF) (234, 514). VEGF is an endothelial cell-specific mitogen *in vitro* and an angiogenic

inducer in a variety of *in vivo* models (515). In the context of islet transplantation, local expression of VEGF may improve the clinical outcome of islet transplantation by enhancing islet re-vascularization. One way to assess this would be to utilize molecular methods such as a PCR array to profile the expression of key genes involved in regulating new blood vessel formation, however to achieve this a larger mass of transplanted islets would be required or the islet grafts from transplant mice could be pooled to ensure an adequate RNA yield for downstream applications.

In conclusion, in this chapter an animal model of β-cell deficiency, not previously validated in our laboratory, was successfully optimized in NOD-SCID mice. While the finding that gender differences confer susceptibility to STZ-induced diabetes has been reported previously in published studies, our findings confirm this phenonomen. In addition, the transplantation of Ad-IGF-II transduced islets within this model confirmed that IGF-II over expression leads to superior diabetes reversal and stabilization of weight in immunodeficient mice receiving a marginal mass of rat islets. A significantly lower number of Ad-GFP recipient mice reached euglycemia compared to Ad-IGF-II and untransduced islet recipients. While the promising results obtained with the Ad-IGF-II recipient mice provides clear evidence regarding the efficacy of Ad-mediated gene transfer in an immunocompromised islet transplant setting, the results seen with Ad-GFP recipient mice are likely due to the toxicity associated with GFP over expression (previously described in **Section 4.3** of this thesis). When considering the results presented in this chapter, IGF-II over expression provides an effective anti-apoptotic strategy to improve islet survival post-transplantation.

CHAPTER 7

CONCLUDING REMARKS AND FUTURE DIRECTIONS

Type 1 Diabetes (T1D), formerly insulin dependent or juvenile diabetes, is a metabolic disease that results from the autoimmune destruction of β-cells in the pancreas. T1D is fatal unless treated with exogenous insulin injections, and good glycaemic control is difficult to attain with insulin therapy. As a result, life-threatening micro vascular complications such as retinopathy, nephropathy and neuropathy will present in time. Keeping blood glucose levels (BGL) within a narrow range using intensive insulin therapy, can reduce these diabetic complications (516), however patients have an increased risk of suffering severe hypoglycaemic episodes.

Islet transplantation is a promising alternative therapy for T1D patients. A landmark study published in 2000 (74), achieved insulin independence in seven out of seven T1D patients, using a steroid-free immunosuppressive regimen called the Edmonton Protocol. Since this time, over 750 transplants have been performed worldwide. However, despite this initial success, long-term follow up of islet transplant recipients reveals a marked reduction in islet graft function over time (194). As shown in the Collaborative Islet Transplant Registry (CITR) 2010 annual report, graft function can be as low as 40% at five years. The decline in islet graft function post-transplantation can be attributed to failure of islets to effectively engraft, inflammatory responses at the transplant site, allo- or auto-immune responses and immunosuppressive drug-induced β-cell toxicity (517). All of these processes result in β-cell cell death and contribute to early failure of the islet allograft (390). Thus, there is a need to develop novel therapies to adequately protect against β-cell apoptosis in the immediate post-transplant period. This need is acutely highlighted when considering that up to 70% of the transplanted β-cell mass may be destroyed following intraportal transplantation (77, 194, 418).

To this end, the main aim of this thesis was to explore an anti-apoptotic gene transfer strategy to promote islet survival following transplantation. The strategy involved the use of an Adenoviral (Ad)-based vector to over express the anti-apoptotic molecule Insulin-like Growth Factor-II (IGF-II) in islets prior to their transplantation. The main advantage of such a gene transfer strategy is its *ex vivo* nature, whereby the isolated islets are transduced outside the body and any remaining viral particles are removed prior to transplantation. This considerably limits the

likelihood of any viral vector mediated systemic response, which can be potentially life-threatening *in vivo* (123).

IGF-II is a promising candidate molecule for use in islet gene therapy. IGF-II plays an important role in prenatal growth and development and activates the phosphatidylinositol-3-kinase (PI3K)/Akt pathway and the MAPK pathway via the IGF-I receptor (IGF-1R). IGF-II is a major growth factor that regulates differentiation of most mesodermal tissues, including β-cells during embryonic life (518). Human and rat pancreatic islets express IGF-II, while exogenous IGF-II promotes increased islet cell DNA synthesis and islet survival against apoptotic stimuli (236, 415, 466, 519, 520).

Islet gene transfer requires efficient entry of the vector into isolated islet cells so that the introduced gene or 'transgene' is expressed at sufficiently high levels as to confer the required therapeutic benefit. In clinical islet transplantation there is often a delay of 2 – 3 days from the initial notification of an islet donor to completion of the transplant procedure. During this time, the islets must be isolated and may then be subject to recovery in culture. Pre-transplant assays are performed on the isolated islets to determine the proportion of β-cells and the viability of the islet preparation, using inclusion and exclusion dyes to test the integrity of the plasma membrane. This provides an excellent 'window of opportunity' whereby the isolated islets can be transduced with an appropriate viral vector to over express the desired transgene(s).

Currently the optimal vector for islet transduction is unknown. Four major viral vector types exist for use in gene transfer studies, namely Adenovirus (Ad), Adeno-Associated Virus (AAV), Herpes Simplex Virus (HSV) and Retrovirus (including Lentivirus). Regardless of the vector type utilised, the initial process of viral infection is the same, culminating with the docking and attachment of a viral particle to its cognate cell surface receptor. From this point onwards, viral transduction efficiency is influenced by the intracellular milieu and trafficking events that occur within the target cell. For example, interaction of Ad with its integrin co-receptor leads to viral internalization and packaging of Ad within an endosome (521). The internalized Ad particles will then traffic through the cell until they reach a low pH region, which causes endosomal rupture, escape and subsequently leads to trafficking of the virus to the nuclear pore (522). This is in contrast to AAV-based vectors that are internalized into the cell via clathrin coated pits, in a

process that is dependent on dynamin, a GTPase protein involved in clathrin-mediated internalization (523).

Ad transgene expression is transient whereas AAV vectors provide stable, permanent transgene expression. In immune competent hosts, Ad-mediated transgene expression has been observed for approximately 3 weeks although this can vary from 1 – 8 weeks (524-526). While the transient nature of Ad renders it less optimal for interventions that require permanent expression, it may prove advantageous in an islet gene therapy setting, that would benefit most from apoptosis inhibition in the early post-transplant period.

In **Chapter 3**, the ability of Ad- and AAV-based vectors expressing a green fluorescent protein (GFP) reporter gene to transduce isolated human and rodent pancreatic islets was investigated. The primary aim was to determine the optimal vector type for efficient islet transduction. The consequence of Ad or AAV transduction on islet viability and function was determined for each vector and found to be unaffected by exposure to either virus type. In this regard, **Chapter 3** has provided evidence that Ad- and AAV-based vectors offer efficacious transduction of human and rodent pancreatic islets.

A major limitation to the use of AAV is the high vector dose required to achieve therapeutic gene transfer in cells and tissues (including isolated islets), whereas an equivalent or lower dose of Ad leads to increased transduction efficiency and enhanced transgene expression. Recent advances in AAV vector technology and design have broadened the tropism and range of available AAV-based vectors. Phosphorylation of surface exposed tyrosine residues on the capsid of AAV2 viral vectors leads to ubiqutination and degradation of AAV viral particles (355). However, site-directed mutagenesis of tyrosine to phenylalanine capsid residues protects the viral particles from proteasome mediated degradation, and subsequently increases the transduction efficiency of AAV (388).

Therefore, **Chapter 3** aimed to provide a thorough side-by-side comparison of six AAV vector types to assess their transduction efficiency in human and rodent pancreatic islets. The AAV vector panel consisted of an AAV2 wild type vector, two pseudotype AAV vectors that accommodate capsid proteins from AAV1 and AAV8 viral serotypes (AAV2/1 and AAV2/8) and three tyrosine mutant vectors derived from the genome of AAV2 or AAV8 serotypes and contain

either single or triple tyrosine mutations on the viral capsid (AAV8mutY733F, AAV2muttriple and AAV2mutY444F). The results in **Chapter 3** demonstrate that Ad is far more efficient at transducing human and rodent pancreatic islets compared to AAV-based vectors. In addition, single or triple tyrosine mutations on the protein capsids of AAV vectors were insufficient to enhance gene delivery to the islets. This is the first study which has investigated the transduction efficiency of tyrosine-mutant vectors in human and rodent pancreatic islets, and therefore the first report describing an inability of these vector types to effectively transduce human and rat pancreatic islets.

Finally, **Chapter 3** provided preliminary experimental evidence that the human islet isolation process, which utilizes an aggressive enzyme-mediated procedure to digest the endocrine islet cells, leads to loss of the cellular receptors required for efficient AAV-mediated islet cell transduction. The receptor composition of islet cells is not necessarily stable following isolation, as integrin expression has been observed to decrease in culture (375). However integrin expression can be up regulated in the presence of certain extracellular matrix elements (376). Considering that integrin αvβ5 is a necessary co-receptor for AAV internalization, it may be possible to improve AAV transduction efficiency by promoting enhanced receptor turn over. This may be achieved via the supplementation of islet culture medium with growth factors appropriate for this purpose.

Based on the results obtained in **Chapter 3** of this thesis, a replication-deficient Ad vector (serotype 5) was chosen as the optimal gene delivery vehicle to over express human IGF-II in pancreatic islet cells. **In Chapter 4**, Ad-IGF-II successfully transduced rodent islets and IGF-II over expression did not affect islet viability or function, suggesting that Ad-IGF-II is an effective, non-toxic vector for use in an islet gene therapy setting. Molecular studies demonstrated that the IGF-II mRNA was efficiently transcribed and translated to protein. The resultant IGF-II protein expression was detected in cell culture supernant of Ad-IGF-II transduced rat islets over a five day culture period.

Pancreatic islets are subject to extensive oxidative stress during pancreas procurement and islet isolation, culture and transplantation. Multiple signaling pathways such as the nuclear factor kappa B (NF-κB) and mitogen-activated protein kinase (MAPK) stress response pathways are triggered during these processes, which leads to pro-inflammatory cytokine mediated β-cell

injury and death (527). It is well established that IL-1β alone or in combination with other pro-inflammatory cytokines, such as TNF-α and IFN-γ induce β-cell death in mouse, rat and human islets *in vitro* and *in vivo* (426-429). Therefore in **Chapter 5** an *in vitro* model of apoptosis was established to mimic the *in vivo* stimulation of pro-inflammatory cytokine mediated insult occurring during the peri- and post-transplant period.

The exposure of rat and human islets to pro-inflammatory cytokines IL-1β and IFN-γ severely diminished islet viability and function. Ad-IGF-II transduced rat islets were effectively protected against pro-inflammatory cytokine induced cell death. In other studies (232, 415, 466) it has been reported that between 34 – 500 ng/ml of IGF-II is required to effectively inhibit islet apoptosis *in vitro*. Therefore, this thesis provides the first report of rat islets expressing approximately 14.3 ± 2.4 ng IGF-II to enhance islet survival *in vitro*. Moreover, the anti-apoptotic effect mediated by IGF-II in **Chapter 5** was neutralised by a blocking antibody targeting the IGF-1R and Western blot analysis confirmed that IGF-II inhibits islet apoptosis via activation of the PI3K/Akt intracellular signaling pathway.

In **Chapter 6**, the ability of transplanted islets to normalize blood glucose levels (BGL) in diabetic NOD-SCID mice was significantly enhanced by Ad-IGF-II transduction of the islet grafts, when compared to mice receiving untransduced or Ad-GFP transduced islets. Thus, Ad-mediated over expression of anti-apoptotic IGF-II led to a significant improvement in *in vivo* transplant outcomes. Moreover, the normalization of glycemia in diabetic Ad-IGF-II recipient mice was associated with a stabilization and slight improvement, in the average weight of transplant mice.

A specific limitation of this anti-apoptotic strategy is that it targets only apoptosis as a cause of islet loss in the early post-transplant period. In addition to being protected against apoptotic insults, islets need to be able to resist alloimmunity, recurrent autoimmunity and effectively revascularize following transplantation. To this end, it is unlikely that a single gene will fulfill all the post-transplant requirements to effectively improve islet graft function post-transplantation. Advances in vector design have led to the development of multigene vectors that can successfully co-express two or three transgenes under the direction of a single promoter (528-530). Using an Ad-based vector, Narang and colleagues (467) have shown that co-expression of two genes targeting different post-transplant islet stresses, have an additive effect on islet cell survival post-transplantation, when compared to either gene alone. Others (531) have shown that co-expression of human Vascular Endothelial Growth Factor (VEGF) and human Interleukin-1 Receptor Antagonist (hIL-1Ra) decreases pro-inflammatory cytokine induced apoptosis *in vitro* and improved the outcome of islet transplantation *in vivo*. In future studies, multigene vectors may provide an excellent system to evaluate other novel genes, in combination with IGF-II for therapeutic efficacy.

The *in vivo* studies of this thesis were performed by transplanting the islets under the kidney capsule of diabetic NOD-SCID mice. However, this method does not parallel the intra portal transplantation procedure of clinical islet preparations. The kidney capsule method of transplantation was utilized in **Chapter 6** as it is a practical and reliable technique that is widely used in experimental diabetes studies (532, 533). Moreover, the kidney capsule provides a convenient location to access the transplanted islets for post-transplant assessment of the islet graft and to perform surgical nephrectomy as a method to validate islet graft function. Studies have shown that the long-term function of islets transplanted under the kidney capsule is superior compared with islets transplanted via the portal vein (534, 535). Despite this, future transplant studies, such as those aiming to investigate the utility of mutigene vectors should attempt to perform intra portal islet transplantation as a means to ensure a parallel can be drawn against the current clinical application.

After directly comparing the transduction efficiency of Ad- and AAV-based vector types, it would appear that Ad may be a more efficient vector for use in an islet transplant setting. Ad-based vectors offer the advantage of high transduction efficiency in dividing and non-dividing cells and transient gene expression, as the viral DNA does not integrate into the host cell genome.

Although the lack of pathogenicity associated with AAV vectors also makes them an attractive vector choice, they are burdened with the major disadvantage of the size of the therapeutic genes that can be packaged, which excludes many potentially useful genes or multiple transgenes. In a preclinical setting, systemic administration of Ad treatment close to reproductive organs, such as treatment for prostate cancer has been shown to be safe and no offspring have shown germline transmission (536). Moreover, data presented in this thesis suggests that Ad-IGF-II is an effective and non-toxic viral vector type for islet transduction. The major novel aspect of this work is the finding that up to a 34-fold lower concentration of human IGF-II is required to prevent *in vitro* and *in vivo* islet cell apoptosis, compared to that of previous published studies. Furthermore, the use of a transient Ad-based vector to over express IGF-II negates the need for every islet cell to be transduced, as IGF-II works to inhibit apoptosis via autocrine and paracrine mechanisms. Thus, clinically, Ad-IGF-II represents a promising candidate vector to improve islet survival in the immediate post-transplant period.

In conclusion, although the data regarding enzyme-mediated AAV receptor loss during the isolation period is preliminary, this finding may be enhanced by future studies aiming to identify the optimal molecules or extracellular matrix components that promote or enhance the rate of receptor turn over. Ad-IGF-II mediates local and specific over expression of IGF-II in transduced islet cells without affecting islet viability or function. Furthermore, IGF-II promotes islet survival against pro-inflammatory cytokine induced apoptosis *in vitro* and improves transplant outcomes *in vivo*, a process shown to be mediated via the interaction of anti-apoptotic IGF-II with the IGF-1R on the islet cell surface. Thus, the data presented in this thesis suggests that Ad-mediated over expression of IGF-II may provide a promising anti-apoptotic strategy to improve islet survival in the peri- and post-transplant period.

REFERENCES

1. Bach JF. Insulin-dependent diabetes mellitus as a beta-cell targeted disease of immunoregulation. J Autoimmun. 1995; 8: 439-63.
2. Hering BJ, Browatzki CC, Schultz A, Bretzel RG, Federlin KF. Clinical islet transplantation--registry report, accomplishments in the past and future research needs. Cell Transplant. 1993; 2: 269-82; discussion 83-305.
3. Shapiro AM, Lakey JR, Paty BW, Senior PA, Bigam DL, Ryan EA. Strategic opportunities in clinical islet transplantation. Transplantation. 2005; 79: 1304-7.
4. Edlund H. Developmental biology of the pancreas. Diabetes. 2001; 50 Suppl 1: S5-9.
5. Jorgensen MC, Ahnfelt-Ronne J, Hald J, Madsen OD, Serup P, Hecksher-Sorensen J. An illustrated review of early pancreas development in the mouse. Endocr Rev. 2007; 28: 685-705.
6. Thomas JE. The functional inervation of the pancreas. Rev Gastroenterol. 1948; 15: 813-20.
7. Slack JM. Developmental biology of the pancreas. Development. 1995; 121: 1569-80.
8. Bonner-Weir S. Morphological evidence for pancreatic polarity of beta-cell within islets of Langerhans. Diabetes. 1988; 37: 616-21.
9. Lammert E, Cleaver O, Melton D. Role of endothelial cells in early pancreas and liver development. Mech Dev. 2003; 120: 59-64.
10. Steiner DJ, Kim A, Miller K, Hara M. Pancreatic islet plasticity: interspecies comparison of islet architecture and composition. Islets. 2010; 2: 135-45.
11. Bouwens L, Rooman I. Regulation of pancreatic beta-cell mass. Physiol Rev. 2005; 85: 1255-70.
12. Kim A, Miller K, Jo J, Kilimnik G, Wojcik P, Hara M. Islet architecture: A comparative study. Islets. 2009; 1: 129-36.
13. Reddy SN, Bibby NJ, Elliott RB. Cellular distribution of insulin, glucagon, pancreatic polypeptide hormone and somatostatin in the fetal and adult pancreas of the guinea pig: a comparative immunohistochemical study. Eur J Cell Biol. 1985; 38: 301-5.
14. Baskin DG, Gorray KC, Fujimoto WY. Immunocytochemical identification of cells containing insulin, glucagon, somatostatin, and pancreatic polypeptide in the islets of Langerhans of the guinea pig pancreas with light and electron microscopy. Anat Rec. 1984; 208: 567-78.

15. Orci L, Unger RH. Functional subdivision of islets of Langerhans and possible role of D cells. Lancet. 1975; 2: 1243-4.

16. Elayat AA, el-Naggar MM, Tahir M. An immunocytochemical and morphometric study of the rat pancreatic islets. J Anat. 1995; 186 (Pt 3): 629-37.

17. Samols E, Bonner-Weir S, Weir GC. Intra-islet insulin-glucagon-somatostatin relationships. Clin Endocrinol Metab. 1986; 15: 33-58.

18. Cabrera O, Berman DM, Kenyon NS, Ricordi C, Berggren PO, Caicedo A. The unique cytoarchitecture of human pancreatic islets has implications for islet cell function. Proc Natl Acad Sci U S A. 2006; 103: 2334-9.

19. Brissova M, Fowler MJ, Nicholson WE, et al. Assessment of human pancreatic islet architecture and composition by laser scanning confocal microscopy. The journal of histochemistry and cytochemistry : official journal of the Histochemistry Society. 2005; 53: 1087-97.

20. Curry DL, Bennett LL, Grodsky GM. Dynamics of insulin secretion by the perfused rat pancreas. Endocrinology. 1968; 83: 572-84.

21. Komatsu M, Sato Y, Aizawa T, Hashizume K. KATP channel-independent glucose action: an elusive pathway in stimulus-secretion coupling of pancreatic beta-cell. Endocr J. 2001; 48: 275-88.

22. Straub SG, Sharp GW. Glucose-stimulated signaling pathways in biphasic insulin secretion. Diabetes/metabolism research and reviews. 2002; 18: 451-63.

23. Newgard CB, McGarry JD. Metabolic coupling factors in pancreatic beta-cell signal transduction. Annu Rev Biochem. 1995; 64: 689-719.

24. Cook DL, Hales CN. Intracellular ATP directly blocks K+ channels in pancreatic B-cells. Nature. 1984; 311: 271-3.

25. Tuch BE, Osgerby KJ, Turtle JR. The role of calcium in insulin release from the human fetal pancreas. Cell Calcium. 1990; 11: 1-9.

26. Porksen N, Hollingdal M, Juhl C, Butler P, Veldhuis JD, Schmitz O. Pulsatile insulin secretion: detection, regulation, and role in diabetes. Diabetes. 2002; 51 Suppl 1: S245-54.

27. Suckale J, Solimena M. Pancreas islets in metabolic signaling--focus on the beta-cell. Front Biosci. 2008; 13: 7156-71.

28. Hulme MA, Wasserfall CH, Atkinson MA, Brusko TM. Central role for interleukin-2 in type 1 diabetes. Diabetes. 2012; 61: 14-22.

29. Cnop M, Welsh N, Jonas JC, Jorns A, Lenzen S, Eizirik DL. Mechanisms of pancreatic beta-cell death in type 1 and type 2 diabetes: many differences, few similarities. Diabetes. 2005; 54 Suppl 2: S97-107.

30. Eizirik DL, Colli ML, Ortis F. The role of inflammation in insulitis and beta-cell loss in type 1 diabetes. Nat Rev Endocrinol. 2009; 5: 219-26.

31. Kawasaki E, Abiru N, Eguchi K. Prevention of type 1 diabetes: from the view point of beta cell damage. Diabetes Res Clin Pract. 2004; 66 Suppl 1: S27-32.

32. Donath MY, Storling J, Berchtold LA, Billestrup N, Mandrup-Poulsen T. Cytokines and beta-cell biology: from concept to clinical translation. Endocr Rev. 2008; 29: 334-50.

33. Yang JH, Li Y, Zhang GH, Yang QT. [Regulation of NF-kappaB signal transduction pathway on cytokines in cultured nasal epithelium]. Zhonghua Er Bi Yan Hou Tou Jing Wai Ke Za Zhi. 2010; 45: 592-6.

34. Arafat HA, Katakam AK, Chipitsyna G, et al. Osteopontin protects the islets and beta-cells from interleukin-1 beta-mediated cytotoxicity through negative feedback regulation of nitric oxide. Endocrinology. 2007; 148: 575-84.

35. Zhao Y, Krishnamurthy B, Mollah ZU, Kay TW, Thomas HE. NF-kappaB in type 1 diabetes. Inflamm Allergy Drug Targets. 2011; 10: 208-17.

36. Lernmark A, Barmeier H, Dube S, et al. Molecular analysis of the pathogenesis of beta-cell destruction in insulin-dependent diabetes mellitus. West J Med. 1990; 153: 499-502.

37. Kloppel G, Lohr M, Habich K, Oberholzer M, Heitz PU. Islet pathology and the pathogenesis of type 1 and type 2 diabetes mellitus revisited. Surv Synth Pathol Res. 1985; 4: 110-25.

38. Onkamo P, Vaananen S, Karvonen M, Tuomilehto J. Worldwide increase in incidence of Type I diabetes--the analysis of the data on published incidence trends. Diabetologia. 1999; 42: 1395-403.

39. Patterson CC, Dahlquist GG, Gyurus E, Green A, Soltesz G. Incidence trends for childhood type 1 diabetes in Europe during 1989-2003 and predicted new cases 2005-20: a multicentre prospective registration study. Lancet. 2009; 373: 2027-33.

40. Catanzariti L, Faulks K, Moon L, Waters AM, Flack J, Craig ME. Australia's national trends in the incidence of Type 1 diabetes in 0-14-year-olds, 2000-2006. Diabet Med. 2009; 26: 596-601.

41. Magliano DJ, Peeters A, Vos T, et al. Projecting the burden of diabetes in Australia--what is the size of the matter? Aust N Z J Public Health. 2009; 33: 540-3.

42. Tapp RJ, Shaw JE, Harper CA, et al. The prevalence of and factors associated with diabetic retinopathy in the Australian population. Diabetes Care. 2003; 26: 1731-7.

43. Siitonen OI, Niskanen LK, Laakso M, Siitonen JT, Pyorala K. Lower-extremity amputations in diabetic and nondiabetic patients. A population-based study in eastern Finland. Diabetes Care. 1993; 16: 16-20.

44. Yoon JW, Jun HS. Cellular and molecular pathogenic mechanisms of insulin-dependent diabetes mellitus. Ann N Y Acad Sci. 2001; 928: 200-11.

45. Morran MP, Omenn GS, Pietropaolo M. Immunology and genetics of type 1 diabetes. Mt Sinai J Med. 2008; 75: 314-27.

46. Wherrett DK, Daneman D. Prevention of type 1 diabetes. Pediatr Clin North Am. 2011; 58: 1257-70, xi.

47. Atkinson MA, Eisenbarth GS. Type 1 diabetes: new perspectives on disease pathogenesis and treatment. Lancet. 2001; 358: 221-9.

48. Achenbach P, Bonifacio E, Ziegler AG. Predicting type 1 diabetes. Curr Diab Rep. 2005; 5: 98-103.

49. Huber A, Menconi F, Corathers S, Jacobson EM, Tomer Y. Joint genetic susceptibility to type 1 diabetes and autoimmune thyroiditis: from epidemiology to mechanisms. Endocr Rev. 2008; 29: 697-725.

50. Wong MS, Hawthorne WJ, Manolios N. Gene therapy in diabetes. Self Nonself. 2010; 1: 165-75.

51. van Belle TL, Coppieters KT, von Herrath MG. Type 1 diabetes: etiology, immunology, and therapeutic strategies. Physiol Rev. 2011; 91: 79-118.

52. Bresson D, von Herrath M. Moving towards efficient therapies in type 1 diabetes: to combine or not to combine? Autoimmun Rev. 2007; 6: 315-22.

53. Notkins AL, Lernmark A. Autoimmune type 1 diabetes: resolved and unresolved issues. J Clin Invest. 2001; 108: 1247-52.

54. King H, Aubert RE, Herman WH. Global burden of diabetes, 1995-2025: prevalence, numerical estimates, and projections. Diabetes Care. 1998; 21: 1414-31.

55. Buchanan TA, Xiang AH, Peters RK, et al. Preservation of pancreatic beta-cell function and prevention of type 2 diabetes by pharmacological treatment of insulin resistance in high-risk hispanic women. Diabetes. 2002; 51: 2796-803.

56. Unger RH, Orci L. Paracrinology of islets and the paracrinopathy of diabetes. Proc Natl Acad Sci U S A. 2010; 107: 16009-12.

57. Craig ME, Femia G, Broyda V, Lloyd M, Howard NJ. Type 2 diabetes in Indigenous and non-Indigenous children and adolescents in New South Wales. The Medical journal of Australia. 2007; 186: 497-9.

58. Mokdad AH, Ford ES, Bowman BA, et al. Diabetes trends in the U.S.: 1990-1998. Diabetes Care. 2000; 23: 1278-83.

59. Gaede P, Vedel P, Larsen N, Jensen GV, Parving HH, Pedersen O. Multifactorial intervention and cardiovascular disease in patients with type 2 diabetes. The New England journal of medicine. 2003; 348: 383-93.

60. Weyer C, Bogardus C, Mott DM, Pratley RE. The natural history of insulin secretory dysfunction and insulin resistance in the pathogenesis of type 2 diabetes mellitus. J Clin Invest. 1999; 104: 787-94.

61. Bethel MA, Feinglos MN. Basal insulin therapy in type 2 diabetes. J Am Board Fam Pract. 2005; 18: 199-204.

62. Mortensen HB, Robertson KJ, Aanstoot HJ, et al. Insulin management and metabolic control of type 1 diabetes mellitus in childhood and adolescence in 18 countries. Hvidore Study Group on Childhood Diabetes. Diabet Med. 1998; 15: 752-9.

63. Johnson IS. Human insulin from recombinant DNA technology. Science. 1983; 219: 632-7.

64. Kordonouri O, Hartmann R, Danne T. Treatment of type 1 diabetes in children and adolescents using modern insulin pumps. Diabetes Res Clin Pract. 2011; 93 Suppl 1: S118-24.

65. Danne T, Battelino T, Jarosz-Chobot P, et al. Establishing glycaemic control with continuous subcutaneous insulin infusion in children and adolescents with type 1 diabetes: experience of the PedPump Study in 17 countries. Diabetologia. 2008; 51: 1594-601.

66. Danne T, Mortensen HB, Hougaard P, et al. Persistent differences among centers over 3 years in glycemic control and hypoglycemia in a study of 3,805 children and adolescents with type 1 diabetes from the Hvidore Study Group. Diabetes Care. 2001; 24: 1342-7.

67. Calne R. Cell transplantation for diabetes. Philos Trans R Soc Lond B Biol Sci. 2005; 360: 1769-74.

68. Larsen JL. Pancreas transplantation: indications and consequences. Endocr Rev. 2004; 25: 919-46.

69. Correa-Giannella ML, Raposo do Amaral AS. Pancreatic islet transplantation. Diabetology & metabolic syndrome. 2009; 1: 9.

70. Noguchi H. Pancreatic islet transplantation. World J Gastrointest Surg. 2009; 1: 16-20.

71. Lacy PE, Kostianovsky M. Method for the isolation of intact islets of Langerhans from the rat pancreas. Diabetes. 1967; 16: 35-9.

72. Kemp CB, Knight MJ, Scharp DW, Lacy PE, Ballinger WF. Transplantation of isolated pancreatic islets into the portal vein of diabetic rats. Nature. 1973; 244: 447.

73. Scharp DW, Murphy JJ, Newton WT, Ballinger WF, Lacy PE. Transplantation of islets of Langerhans in diabetic rhesus monkeys. Surgery. 1975; 77: 100-5.

74. Shapiro AM, Lakey JR, Ryan EA, et al. Islet transplantation in seven patients with type 1 diabetes mellitus using a glucocorticoid-free immunosuppressive regimen. N Engl J Med. 2000; 343: 230-8.

75. O'Connell PJ, Hawthorne WJ, Holmes-Walker DJ, et al. Clinical islet transplantation in type 1 diabetes mellitus: results of Australia's first trial. The Medical journal of Australia. 2006; 184: 221-5.

76. Merani S, Shapiro AM. Current status of pancreatic islet transplantation. Clin Sci (Lond). 2006; 110: 611-25.

77. Biarnes M, Montolio M, Nacher V, Raurell M, Soler J, Montanya E. Beta-cell death and mass in syngeneically transplanted islets exposed to short- and long-term hyperglycemia. Diabetes. 2002; 51: 66-72.

78. Berney T, Mamin A, James Shapiro AM, et al. Detection of insulin mRNA in the peripheral blood after human islet transplantion predicts deterioration of metabolic control. Am J Transplant. 2006; 6: 1704-11.

79. Eriksson O, Eich T, Sundin A, et al. Positron emission tomography in clinical islet transplantation. Am J Transplant. 2009; 9: 2816-24.

80. Olsson R, Carlsson PO. The pancreatic islet endothelial cell: emerging roles in islet function and disease. Int J Biochem Cell Biol. 2006; 38: 710-4.

81. Moberg L, Johansson H, Lukinius A, et al. Production of tissue factor by pancreatic islet cells as a trigger of detrimental thrombotic reactions in clinical islet transplantation. Lancet. 2002; 360: 2039-45.

82. Miao G, Ostrowski RP, Mace J, et al. Dynamic production of hypoxia-inducible factor-1alpha in early transplanted islets. Am J Transplant. 2006; 6: 2636-43.

83. Mahato RI. Gene expression and silencing for improved islet transplantation. J Control Release. 2009; 140: 262-7.

84. Brissova M, Powers AC. Revascularization of transplanted islets: can it be improved? Diabetes. 2008; 57: 2269-71.

85. Carlsson PO, Palm F, Andersson A, Liss P. Markedly decreased oxygen tension in transplanted rat pancreatic islets irrespective of the implantation site. Diabetes. 2001; 50: 489-95.

86. Arteel GE, Thurman RG, Yates JM, Raleigh JA. Evidence that hypoxia markers detect oxygen gradients in liver: pimonidazole and retrograde perfusion of rat liver. Br J Cancer. 1995; 72: 889-95.

87. Rabinovitch A, Sumoski W, Rajotte RV, Warnock GL. Cytotoxic effects of cytokines on human pancreatic islet cells in monolayer culture. The Journal of clinical endocrinology and metabolism. 1990; 71: 152-6.

88. Heimberg H, Heremans Y, Jobin C, et al. Inhibition of cytokine-induced NF-kappaB activation by adenovirus-mediated expression of a NF-kappaB super-repressor prevents beta-cell apoptosis. Diabetes. 2001; 50: 2219-24.

89. Corbett JA, McDaniel ML. Does nitric oxide mediate autoimmune destruction of beta-cells? Possible therapeutic interventions in IDDM. Diabetes. 1992; 41: 897-903.

90. Stadler J, Billiar TR, Curran RD, Stuehr DJ, Ochoa JB, Simmons RL. Effect of exogenous and endogenous nitric oxide on mitochondrial respiration of rat hepatocytes. Am J Physiol. 1991; 260: C910-6.

91. Harlan DM, Kenyon NS, Korsgren O, Roep BO. Current advances and travails in islet transplantation. Diabetes. 2009; 58: 2175-84.

92. Hyder A, Laue C, Schrezenmeir J. Effect of the immunosuppressive regime of Edmonton protocol on the long-term in vitro insulin secretion from islets of two different species and age categories. Toxicol In Vitro. 2005; 19: 541-6.

93. Hirshberg B, Rother KI, Digon BJ, 3rd, et al. Benefits and risks of solitary islet transplantation for type 1 diabetes using steroid-sparing immunosuppression: the National Institutes of Health experience. Diabetes Care. 2003; 26: 3288-95.

94. Contreras JL, Smyth CA, Curiel DT, Eckhoff DE. Nonhuman primate models in type 1 diabetes research. Ilar J. 2004; 45: 334-42.

95. Spirin PV, Vil'gelm AE, Prasolov VS. [Lentiviral vectors]. Mol Biol (Mosk). 2008; 42: 913-26.

96. Hughes A, Jessup C, Drogemuller C, et al. Gene therapy to improve pancreatic islet transplantation for Type 1 diabetes mellitus. Curr Diabetes Rev. 2010; 6: 274-84.

97. Van Linthout S, Madeddu P. Ex vivo gene transfer for improvement of transplanted pancreatic islet viability and function. Curr Pharm Des. 2005; 11: 2927-40.

98. Bouard D, Alazard-Dany D, Cosset FL. Viral vectors: from virology to transgene expression. Br J Pharmacol. 2009; 157: 153-65.

99. Cavazzana-Calvo M, Hacein-Bey S, de Saint Basile G, et al. Gene therapy of human severe combined immunodeficiency (SCID)-X1 disease. Science. 2000; 288: 669-72.

100. Fischer A, Hacein-Bey-Abina S, Cavazzana-Calvo M. 20 years of gene therapy for SCID. Nat Immunol. 2010; 11: 457-60.

101. LeWitt PA, Rezai AR, Leehey MA, et al. AAV2-GAD gene therapy for advanced Parkinson's disease: a double-blind, sham-surgery controlled, randomised trial. Lancet Neurol. 2011; 10: 309-19.

102. Nathwani AC, Tuddenham EG, Rangarajan S, et al. Adenovirus-associated virus vector-mediated gene transfer in hemophilia B. N Engl J Med. 2011; 365: 2357-65.

103. Rutten MJ, Lester LR, Quinlan MP, Meshul CK, Deveney CW, Rabkin JM. Prolonged survival of adult rat pancreatic islets transfected with E1A-12S adenovirus. Pancreas. 1999; 19: 183-92.

104. Gallichan WS, Kafri T, Krahl T, Verma IM, Sarvetnick N. Lentivirus-mediated transduction of islet grafts with interleukin 4 results in sustained gene expression and protection from insulitis. Hum Gene Ther. 1998; 9: 2717-26.

105. Giannoukakis N, Mi Z, Gambotto A, et al. Infection of intact human islets by a lentiviral vector. Gene Ther. 1999; 6: 1545-51.

106. Ju Q, Edelstein D, Brendel MD, et al. Transduction of non-dividing adult human pancreatic beta cells by an integrating lentiviral vector. Diabetologia. 1998; 41: 736-9.

107. Harrison SC. Mechanism of membrane fusion by viral envelope proteins. Adv Virus Res. 2005; 64: 231-61.

108. Volpers C, Kochanek S. Adenoviral vectors for gene transfer and therapy. J Gene Med. 2004; 6 Suppl 1: S164-71.

109. Becker TC, BeltrandelRio H, Noel RJ, Johnson JH, Newgard CB. Overexpression of hexokinase I in isolated islets of Langerhans via recombinant adenovirus. Enhancement of glucose metabolism and insulin secretion at basal but not stimulatory glucose levels. J Biol Chem. 1994; 269: 21234-8.

110. Becker TC, Noel RJ, Johnson JH, et al. Differential effects of overexpressed glucokinase and hexokinase I in isolated islets. Evidence for functional segregation of the high and low Km enzymes. J Biol Chem. 1996; 271: 390-4.

111. Leibowitz G, Beattie GM, Kafri T, et al. Gene transfer to human pancreatic endocrine cells using viral vectors. Diabetes. 1999; 48: 745-53.

112. Csete ME, Benhamou PY, Drazan KE, et al. Efficient gene transfer to pancreatic islets mediated by adenoviral vectors. Transplantation. 1995; 59: 263-8.

113. Sigalla J, David A, Anegon I, et al. Adenovirus-mediated gene transfer into isolated mouse adult pancreatic islets: normal beta-cell function despite induction of an anti-adenovirus immune response. Hum Gene Ther. 1997; 8: 1625-34.

114. Barbu AR, Bodin B, Welsh M, Jansson L, Welsh N. A perfusion protocol for highly efficient transduction of intact pancreatic islets of Langerhans. Diabetologia. 2006; 49: 2388-91.

115. Douglas JT. Adenoviral vectors for gene therapy. Mol Biotechnol. 2007; 36: 71-80.

116. Goncalves MA. Adeno-associated virus: from defective virus to effective vector. Virol J. 2005; 2: 43.

117. Mukai E, Fujimoto S, Sakurai F, et al. Efficient gene transfer into murine pancreatic islets using adenovirus vectors. J Control Release. 2007; 119: 136-41.

118. Weber M, Deng S, Kucher T, Shaked A, Ketchum RJ, Brayman KL. Adenoviral transfection of isolated pancreatic islets: a study of programmed cell death (apoptosis) and islet function. J Surg Res. 1997; 69: 23-32.

119. Csete ME, Afra R, Mullen Y, Drazan KE, Benhamou PY, Shaked A. Adenoviral-mediated gene transfer to pancreatic islets does not alter islet function. Transplant Proc. 1994; 26: 756-7.

120. Kay MA, Glorioso JC, Naldini L. Viral vectors for gene therapy: the art of turning infectious agents into vehicles of therapeutics. Nat Med. 2001; 7: 33-40.

121. Mitanchez D, Doiron B, Chen R, Kahn A. Glucose-stimulated genes and prospects of gene therapy for type I diabetes. Endocr Rev. 1997; 18: 520-40.

122. Muruve DA, Nicolson AG, Manfro RC, Strom TB, Sukhatme VP, Libermann TA. Adenovirus-mediated expression of Fas ligand induces hepatic apoptosis after Systemic administration and apoptosis of ex vivo-infected pancreatic islet allografts and isografts. Hum Gene Ther. 1997; 8: 955-63.

123. Raper SE, Chirmule N, Lee FS, et al. Fatal systemic inflammatory response syndrome in a ornithine transcarbamylase deficient patient following adenoviral gene transfer. Mol Genet Metab. 2003; 80: 148-58.

124. St George JA. Gene therapy progress and prospects: adenoviral vectors. Gene Ther. 2003; 10: 1135-41.

125. Worgall S, Wolff G, Falck-Pedersen E, Crystal RG. Innate immune mechanisms dominate elimination of adenoviral vectors following in vivo administration. Hum Gene Ther. 1997; 8: 37-44.

126. Zhang Y, Chirmule N, Gao GP, et al. Acute cytokine response to systemic adenoviral vectors in mice is mediated by dendritic cells and macrophages. Mol Ther. 2001; 3: 697-707.

127. Grimm D, Kleinschmidt JA. Progress in adeno-associated virus type 2 vector production: promises and prospects for clinical use. Hum Gene Ther. 1999; 10: 2445-50.

128. Conrad CK, Allen SS, Afione SA, et al. Safety of single-dose administration of an adeno-associated virus (AAV)-CFTR vector in the primate lung. Gene Ther. 1996; 3: 658-68.

129. Jimenez V, Ayuso E, Mallol C, et al. In vivo genetic engineering of murine pancreatic beta cells mediated by single-stranded adeno-associated viral vectors of serotypes 6, 8 and 9. Diabetologia. 2011; 54: 1075-86.

130. Rabinowitz JE, Rolling F, Li C, et al. Cross-packaging of a single adeno-associated virus (AAV) type 2 vector genome into multiple AAV serotypes enables transduction with broad specificity. J Virol. 2002; 76: 791-801.

131. Wu Z, Asokan A, Grieger JC, Govindasamy L, Agbandje-McKenna M, Samulski RJ. Single amino acid changes can influence titer, heparin binding, and tissue tropism in different adeno-associated virus serotypes. J Virol. 2006; 80: 11393-7.

132. Summerford C, Samulski RJ. Membrane-associated heparan sulfate proteoglycan is a receptor for adeno-associated virus type 2 virions. J Virol. 1998; 72: 1438-45.

133. Kashiwakura Y, Tamayose K, Iwabuchi K, et al. Hepatocyte growth factor receptor is a coreceptor for adeno-associated virus type 2 infection. J Virol. 2005; 79: 609-14.

134. Summerford C, Bartlett JS, Samulski RJ. AlphaVbeta5 integrin: a co-receptor for adeno-associated virus type 2 infection. Nat Med. 1999; 5: 78-82.

135. Wang Z, Zhu T, Rehman KK, et al. Widespread and stable pancreatic gene transfer by adeno-associated virus vectors via different routes. Diabetes. 2006; 55: 875-84.

136. Cheng H, Wolfe SH, Valencia V, et al. Efficient and persistent transduction of exocrine and endocrine pancreas by adeno-associated virus type 8. J Biomed Sci. 2007; 14: 585-94.

137. Wang AY, Peng PD, Ehrhardt A, Storm TA, Kay MA. Comparison of adenoviral and adeno-associated viral vectors for pancreatic gene delivery in vivo. Hum Gene Ther. 2004; 15: 405-13.

138. Flotte T, Agarwal A, Wang J, et al. Efficient ex vivo transduction of pancreatic islet cells with recombinant adeno-associated virus vectors. Diabetes. 2001; 50: 515-20.

139. Prasad KM, Yang Z, Bleich D, Nadler JL. Adeno-associated virus vector mediated gene transfer to pancreatic beta cells. Gene Ther. 2000; 7: 1553-61.

140. Aalbers CJ, Tak PP, Vervoordeldonk MJ. Advancements in adeno-associated viral gene therapy approaches: exploring a new horizon. F1000 Med Rep. 2011; 3: 17.

141. Tyler KL. Herpes simplex virus infections of the central nervous system: encephalitis and meningitis, including Mollaret's. Herpes. 2004; 11 Suppl 2: 57A-64A.

142. Ho DY, Mocarski ES, Sapolsky RM. Altering central nervous system physiology with a defective herpes simplex virus vector expressing the glucose transporter gene. Proceedings of the National Academy of Sciences of the United States of America. 1993; 90: 3655-9.

143. Mata M, Glorioso JC, Fink DJ. Targeted gene delivery to the nervous system using herpes simplex virus vectors. Physiol Behav. 2002; 77: 483-8.

144. Goss JR, Natsume A, Wolfe D, Mata M, Glorioso JC, Fink DJ. Delivery of herpes simplex virus-based vectors to the nervous system. Methods Mol Biol. 2004; 246: 309-22.

145. Ryan DA, Federoff HJ. Immune responses to herpesviral vectors. Hum Gene Ther. 2009; 20: 434-41.

146. Mellerick DM, Fraser NW. Physical state of the latent herpes simplex virus genome in a mouse model system: evidence suggesting an episomal state. Virology. 1987; 158: 265-75.

147. Liu Y, Rabinovitch A, Suarez-Pinzon W, et al. Expression of the bcl-2 gene from a defective HSV-1 amplicon vector protects pancreatic beta-cells from apoptosis. Hum Gene Ther. 1996; 7: 1719-26.

148. Rabinovitch A, Suarez-Pinzon W, Strynadka K, et al. Transfection of human pancreatic islets with an anti-apoptotic gene (bcl-2) protects beta-cells from cytokine-induced destruction. Diabetes. 1999; 48: 1223-9.

149. Blaese RM, Culver KW, Miller AD, et al. T lymphocyte-directed gene therapy for ADA-SCID: initial trial results after 4 years. Science. 1995; 270: 475-80.

150. Barquinero J, Eixarch H, Perez-Melgosa M. Retroviral vectors: new applications for an old tool. Gene Ther. 2004; 11 Suppl 1: S3-9.

151. Zufferey R, Nagy D, Mandel RJ, Naldini L, Trono D. Multiply attenuated lentiviral vector achieves efficient gene delivery in vivo. Nat Biotechnol. 1997; 15: 871-5.

152. Naldini L, Blomer U, Gage FH, Trono D, Verma IM. Efficient transfer, integration, and sustained long-term expression of the transgene in adult rat brains injected with a lentiviral vector. Proceedings of the National Academy of Sciences of the United States of America. 1996; 93: 11382-8.

153. Blomer U, Naldini L, Kafri T, Trono D, Verma IM, Gage FH. Highly efficient and sustained gene transfer in adult neurons with a lentivirus vector. J Virol. 1997; 71: 6641-9.

154. Curran MA, Ochoa MS, Molano RD, et al. Efficient transduction of pancreatic islets by feline immunodeficiency virus vectors1. Transplantation. 2002; 74: 299-306.

155. Kobinger GP, Deng S, Louboutin JP, et al. Transduction of human islets with pseudotyped lentiviral vectors. Hum Gene Ther. 2004; 15: 211-9.

156. Lu Y, Dang H, Middleton B, et al. Bioluminescent monitoring of islet graft survival after transplantation. Mol Ther. 2004; 9: 428-35.

157. Fernandes JR, Duvivier-Kali VF, Keegan M, et al. Transplantation of islets transduced with CTLA4-Ig and TGFbeta using adenovirus and lentivirus vectors. Transpl Immunol. 2004; 13: 191-200.

158. He Z, Wang F, Kumagai-Braesch M, Permert J, Holgersson J. Long-term gene expression and metabolic control exerted by lentivirus-transduced pancreatic islets. Xenotransplantation. 2006; 13: 195-203.

159. Kenmochi T, Asano T, Nakagori T, et al. Successful gene transfer into murine pancreatic islets using polyamine transfection reagents. Transplant Proc. 1998; 30: 470-2.

160. Lakey JR, Young AT, Pardue D, et al. Nonviral transfection of intact pancreatic islets. Cell Transplant. 2001; 10: 697-708.

161. Narang AS, Cheng K, Henry J, et al. Vascular endothelial growth factor gene delivery for revascularization in transplanted human islets. Pharm Res. 2004; 21: 15-25.

162. Narang AS, Thoma L, Miller DD, Mahato RI. Cationic lipids with increased DNA binding affinity for nonviral gene transfer in dividing and nondividing cells. Bioconjug Chem. 2005; 16: 156-68.

163. Saldeen J, Curiel DT, Eizirik DL, et al. Efficient gene transfer to dispersed human pancreatic islet cells in vitro using adenovirus-polylysine/DNA complexes or polycationic liposomes. Diabetes. 1996; 45: 1197-203.

164. Benhamou PY, Moriscot C, Prevost P, Rolland E, Halimi S, Chroboczek J. Standardization of procedure for efficient ex vivo gene transfer into porcine pancreatic islets with cationic liposomes. Transplantation. 1997; 63: 1798-803.

165. Noguchi H, Matsumoto S. Protein transduction technology offers a novel therapeutic approach for diabetes. J Hepatobiliary Pancreat Surg. 2006; 13: 306-13.

166. Mahato RI, Henry J, Narang AS, et al. Cationic lipid and polymer-based gene delivery to human pancreatic islets. Mol Ther. 2003; 7: 89-100.

167. Narang AS, Mahato RI. Biological and biomaterial approaches for improved islet transplantation. Pharmacological reviews. 2006; 58: 194-243.

168. Newgard CB. While tinkering with the beta-cell...metabolic regulatory mechanisms and new therapeutic strategies: American Diabetes Association Lilly Lecture, 2001. Diabetes. 2002; 51: 3141-50.

169. Levine F. Gene therapy for diabetes: strategies for beta-cell modification and replacement. Diabetes Metab Rev. 1997; 13: 209-46.

170. Mi Z, Mai J, Lu X, Robbins PD. Characterization of a class of cationic peptides able to facilitate efficient protein transduction in vitro and in vivo. Mol Ther. 2000; 2: 339-47.

171. Embury J, Klein D, Pileggi A, et al. Proteins linked to a protein transduction domain efficiently transduce pancreatic islets. Diabetes. 2001; 50: 1706-13.

172. Pileggi A, Fenjves ES, Klein D, Ricordi C, Pastori RL. Protecting pancreatic beta-cells. IUBMB Life. 2004; 56: 387-94.

173. Rehman KK, Bertera S, Bottino R, et al. Protection of islets by in situ peptide-mediated transduction of the Ikappa B kinase inhibitor Nemo-binding domain peptide. J Biol Chem. 2003; 278: 9862-8.

174. Cantarelli E, Piemonti L. Alternative transplantation sites for pancreatic islet grafts. Curr Diab Rep. 2011; 11: 364-74.

175. Yasunami Y, Lacy PE, Finke EH. A new site for islet transplantation--a peritoneal-omental pouch. Transplantation. 1983; 36: 181-2.

176. van der Windt DJ, Echeverri GJ, Ijzermans JN, Cooper DK. The choice of anatomical site for islet transplantation. Cell Transplant. 2008; 17: 1005-14.

177. Hering BJ. Achieving and maintaining insulin independence in human islet transplant recipients. Transplantation. 2005; 79: 1296-7.

178. Chhabra P, Brayman KL. Current status of immunomodulatory and cellular therapies in preclinical and clinical islet transplantation. J Transplant. 2011; 2011: 637692.

179. Meyer T, Hocht B, Ulrichs K. Xenogeneic islet transplantation of microencapsulated porcine islets for therapy of type I diabetes: long-term normoglycemia in STZ-diabetic rats without immunosuppression. Pediatr Surg Int. 2008; 24: 1375-8.

180. Dufrane D, Goebbels RM, Gianello P. Alginate macroencapsulation of pig islets allows correction of streptozotocin-induced diabetes in primates up to 6 months without immunosuppression. Transplantation. 2010; 90: 1054-62.

181. Calafiore R, Basta G, Luca G, et al. Microencapsulated pancreatic islet allografts into nonimmunosuppressed patients with type 1 diabetes: first two cases. Diabetes Care. 2006; 29: 137-8.

182. Elliott RB. Towards xenotransplantation of pig islets in the clinic. Curr Opin Organ Transplant. 2011; 16: 195-200.

183. Sakata N, Sumi S, Yoshimatsu G, Goto M, Egawa S, Unno M. Encapsulated islets transplantation: Past, present and future. World J Gastrointest Pathophysiol. 2012; 3: 19-26.

184. Siebers U, Horcher A, Bretzel RG, et al. Transplantation of free and microencapsulated islets in rats: evidence for the requirement of an increased islet mass for transplantation into the peritoneal site. Int J Artif Organs. 1993; 16: 96-9.

185. de Vos P, Spasojevic M, Faas MM. Treatment of diabetes with encapsulated islets. Adv Exp Med Biol. 2010; 670: 38-53.

186. Iwahashi H, Hanafusa T, Eguchi Y, et al. Cytokine-induced apoptotic cell death in a mouse pancreatic beta-cell line: inhibition by Bcl-2. Diabetologia. 1996; 39: 530-6.

187. Kacheva S, Lenzen S, Gurgul-Convey E. Differential effects of proinflammatory cytokines on cell death and ER stress in insulin-secreting INS1E cells and the involvement of nitric oxide. Cytokine. 2011; 55: 195-201.

188. Davalli AM, Scaglia L, Zangen DH, Hollister J, Bonner-Weir S, Weir GC. Vulnerability of islets in the immediate posttransplantation period. Dynamic changes in structure and function. Diabetes. 1996; 45: 1161-7.

189. Prowse SJ, Bellgrau D, Lafferty KJ. Islet allografts are destroyed by disease occurrence in the spontaneously diabetic BB rat. Diabetes. 1986; 35: 110-4.

190. Kaufman DB, Platt JL, Rabe FL, Dunn DL, Bach FH, Sutherland DE. Differential roles of Mac-1+ cells, and CD4+ and CD8+ T lymphocytes in primary nonfunction and classic rejection of islet allografts. J Exp Med. 1990; 172: 291-302.

191. Slover RH, Eisenbarth GS. Prevention of type I diabetes and recurrent beta-cell destruction of transplanted islets. Endocr Rev. 1997; 18: 241-58.

192. Bosi E, Braghi S, Maffi P, et al. Autoantibody response to islet transplantation in type 1 diabetes. Diabetes. 2001; 50: 2464-71.

193. Jansson L, Carlsson PO. Graft vascular function after transplantation of pancreatic islets. Diabetologia. 2002; 45: 749-63.

194. Ryan EA, Paty BW, Senior PA, et al. Five-year follow-up after clinical islet transplantation. Diabetes. 2005; 54: 2060-9.

195. Hering BJ, Kandaswamy R, Harmon JV, et al. Transplantation of cultured islets from two-layer preserved pancreases in type 1 diabetes with anti-CD3 antibody. Am J Transplant. 2004; 4: 390-401.

196. Froud T, Ricordi C, Baidal DA, et al. Islet transplantation in type 1 diabetes mellitus using cultured islets and steroid-free immunosuppression: Miami experience. Am J Transplant. 2005; 5: 2037-46.

197. Feng S, Quickel RR, Hollister-Lock J, et al. Prolonged xenograft survival of islets infected with small doses of adenovirus expressing CTLA4Ig. Transplantation. 1999; 67: 1607-13.

198. Laumonier T, Potiron N, Boeffard F, et al. CTLA4Ig adenoviral gene transfer induces long-term islet rat allograft survival, without tolerance, after systemic but not local intragraft expression. Hum Gene Ther. 2003; 14: 561-75.

199. Benda B, Ljunggren HG, Peach R, Sandberg JO, Korsgren O. Co-stimulatory molecules in islet xenotransplantation: CTLA4Ig treatment in CD40 ligand-deficient mice. Cell Transplant. 2002; 11: 715-20.

200. Potiron N, Chagneau C, Boeffard F, Soulillou JP, Anegon I, Le Mauff B. Adenovirus-mediated CTLA4Ig or CD40Ig gene transfer delays pancreatic islet rejection in a rat-to-mouse xenotransplantation model after systemic but not local expression. Cell Transplant. 2005; 14: 263-75.

201. Zhang YC, Molano RD, Pileggi A, et al. Adeno-associated virus transduction of islets with interleukin-4 results in impaired metabolic function in syngeneic marginal islet mass transplantation. Transplantation. 2002; 74: 1184-6.

202. Carter JD, Ellett JD, Chen M, et al. Viral IL-10-mediated immune regulation in pancreatic islet transplantation. Mol Ther. 2005; 12: 360-8.

203. Rehman KK, Trucco M, Wang Z, Xiao X, Robbins PD. AAV8-mediated gene transfer of interleukin-4 to endogenous beta-cells prevents the onset of diabetes in NOD mice. Mol Ther. 2008; 16: 1409-16.

204. Li ZL, Xue WJ, Tian PX, et al. Prolongation of islet allograft survival by coexpression of CTLA4Ig and CD40LIg in mice. Transplant Proc. 2007; 39: 3436-7.

205. Dupraz P, Rinsch C, Pralong WF, et al. Lentivirus-mediated Bcl-2 expression in betaTC-tet cells improves resistance to hypoxia and cytokine-induced apoptosis while preserving in vitro and in vivo control of insulin secretion. Gene Ther. 1999; 6: 1160-9.

206. Contreras JL, Bilbao G, Smyth CA, et al. Cytoprotection of pancreatic islets before and soon after transplantation by gene transfer of the anti-apoptotic Bcl-2 gene. Transplantation. 2001; 71: 1015-23.

207. Holohan C, Szegezdi E, Ritter T, O'Brien T, Samali A. Cytokine-induced beta-cell apoptosis is NO-dependent, mitochondria-mediated and inhibited by BCL-XL. J Cell Mol Med. 2008; 12: 591-606.

208. Emamaullee J, Liston P, Korneluk RG, Shapiro AM, Elliott JF. XIAP overexpression in islet beta-cells enhances engraftment and minimizes hypoxia-reperfusion injury. Am J Transplant. 2005; 5: 1297-305.

209. Emamaullee JA, Rajotte RV, Liston P, et al. XIAP overexpression in human islets prevents early posttransplant apoptosis and reduces the islet mass needed to treat diabetes. Diabetes. 2005; 54: 2541-8.

210. Plesner A, Liston P, Tan R, Korneluk RG, Verchere CB. The X-linked inhibitor of apoptosis protein enhances survival of murine islet allografts. Diabetes. 2005; 54: 2533-40.

211. Zhang N, Richter A, Suriawinata J, et al. Elevated vascular endothelial growth factor production in islets improves islet graft vascularization. Diabetes. 2004; 53: 963-70.

212. Olsson R, Maxhuni A, Carlsson PO. Revascularization of transplanted pancreatic islets following culture with stimulators of angiogenesis. Transplantation. 2006; 82: 340-7.

213. Lopez-Talavera JC, Garcia-Ocana A, Sipula I, Takane KK, Cozar-Castellano I, Stewart AF. Hepatocyte growth factor gene therapy for pancreatic islets in diabetes: reducing the minimal islet transplant mass required in a glucocorticoid-free rat model of allogeneic portal vein islet transplantation. Endocrinology. 2004; 145: 467-74.

214. Domene HM, Hwa V, Jasper HG, Rosenfeld RG. Acid-labile subunit (ALS) deficiency. Best Pract Res Clin Endocrinol Metab. 2011; 25: 101-13.

215. Salmon WD, Jr., DuVall MR. A serum fraction with "sulfation factor activity" stimulates in vitro incorporation of leucine and sulfate into protein-polysaccharide complexes, uridine into RNA, and thymidine into DNA of costal cartilage from hypophysectomized rats. Endocrinology. 1970; 86: 721-7.

216. Clemmons DR, Busby WH, Arai T, et al. Role of insulin-like growth factor binding proteins in the control of IGF actions. Prog Growth Factor Res. 1995; 6: 357-66.

217. Pavelic J, Matijevic T, Knezevic J. Biological & physiological aspects of action of insulin-like growth factor peptide family. Indian J Med Res. 2007; 125: 511-22.

218. Daughaday WH, Rotwein P. Insulin-like growth factors I and II. Peptide, messenger ribonucleic acid and gene structures, serum, and tissue concentrations. Endocr Rev. 1989; 10: 68-91.

219. van Haeften TW, Twickler TB. Insulin-like growth factors and pancreas beta cells. Eur J Clin Invest. 2004; 34: 249-55.

220. Bayes-Genis A, Conover CA, Schwartz RS. The insulin-like growth factor axis: A review of atherosclerosis and restenosis. Circ Res. 2000; 86: 125-30.

221. Kooijman R, Sarre S, Michotte Y, De Keyser J. Insulin-like growth factor I: a potential neuroprotective compound for the treatment of acute ischemic stroke? Stroke. 2009; 40: e83-8.

222. D'Ercole AJ, Ye P, O'Kusky JR. Mutant mouse models of insulin-like growth factor actions in the central nervous system. Neuropeptides. 2002; 36: 209-20.

223. Gunnell D, Miller LL, Rogers I, Holly JM. Association of insulin-like growth factor I and insulin-like growth factor-binding protein-3 with intelligence quotient among 8- to 9-year-old children in the Avon Longitudinal Study of Parents and Children. Pediatrics. 2005; 116: e681-6.

224. Russo VC, Gluckman PD, Feldman EL, Werther GA. The insulin-like growth factor system and its pleiotropic functions in brain. Endocr Rev. 2005; 26: 916-43.

225. Dempsey RJ, Sailor KA, Bowen KK, Tureyen K, Vemuganti R. Stroke-induced progenitor cell proliferation in adult spontaneously hypertensive rat brain: effect of exogenous IGF-1 and GDNF. J Neurochem. 2003; 87: 586-97.

226. Higgins MF, Russell NE, Crossey PA, Nyhan KC, Brazil DP, McAuliffe FM. Maternal and fetal placental growth hormone and IGF axis in type 1 diabetic pregnancy. PLoS One. 2012; 7: e29164.

227. Ward A. Beck-Wiedemann syndrome and Wilms' tumour. Mol Hum Reprod. 1997; 3: 157-68.

228. Singh SK, Moretta D, Almaguel F, De Leon M, De Leon DD. Precursor IGF-II (proIGF-II) and mature IGF-II (mIGF-II) induce Bcl-2 And Bcl-X L expression through different signaling pathways in breast cancer cells. Growth Factors. 2008; 26: 92-103.

229. Harris LK, Westwood M. Biology and significance of signalling pathways activated by IGF-II. Growth Factors. 2012; 30: 1-12.

230. Petrik J, Pell JM, Arany E, et al. Overexpression of insulin-like growth factor-II in transgenic mice is associated with pancreatic islet cell hyperplasia. Endocrinology. 1999; 140: 2353-63.

231. Liu JP, Baker J, Perkins AS, Robertson EJ, Efstratiadis A. Mice carrying null mutations of the genes encoding insulin-like growth factor I (Igf-1) and type 1 IGF receptor (Igf1r). Cell. 1993; 75: 59-72.

232. Jourdan G, Dusseault J, Benhamou PY, Rosenberg L, Halle JP. Co-encapsulation of bioengineered IGF-II-producing cells and pancreatic islets: effect on beta-cell survival. Gene Ther. 2011; 18: 539-45.

233. Milo-Landesman D, Efrat S. Growth factor-dependent proliferation of the pancreatic beta-cell line betaTC-tet: an assay for beta-cell mitogenic factors. Int J Exp Diabetes Res. 2002; 3: 69-74.

234. Kim KW, Bae SK, Lee OH, Bae MH, Lee MJ, Park BC. Insulin-like growth factor II induced by hypoxia may contribute to angiogenesis of human hepatocellular carcinoma. Cancer Res. 1998; 58: 348-51.

235. Bryson JM, Tuch BE, Baxter RC. Production of insulin-like growth factor-II by human fetal pancreas in culture. J Endocrinol. 1989; 121: 367-73.

236. Rabinovitch A, Quigley C, Russell T, Patel Y, Mintz DH. Insulin and multiplication stimulating activity (an insulin-like growth factor) stimulate islet (beta-cell replication in neonatal rat pancreatic monolayer cultures. Diabetes. 1982; 31: 160-4.

237. Van Schravendijk CF, Foriers A, Van den Brande JL, Pipeleers DG. Evidence for the presence of type I insulin-like growth factor receptors on rat pancreatic A and B cells. Endocrinology. 1987; 121: 1784-8.

238. Gallaher BW, Hille R, Raile K, Kiess W. Apoptosis: live or die--hard work either way! Horm Metab Res. 2001; 33: 511-9.

239. D'Ercole AJ, Ye P, Gutierrez-Ospina G. Use of transgenic mice for understanding the physiology of insulin-like growth factors. Horm Res. 1996; 45 Suppl 1: 5-7.

240. Han VK, Hill DJ, Strain AJ, et al. Identification of somatomedin/insulin-like growth factor immunoreactive cells in the human fetus. Pediatr Res. 1987; 22: 245-9.

241. Hill DJ. Relative abundance and molecular size of immunoreactive insulin-like growth factors I and II in human fetal tissues. Early Hum Dev. 1990; 21: 49-58.

242. Miettinen PJ, Otonkoski T, Voutilainen R. Insulin-like growth factor-II and transforming growth factor-alpha in developing human fetal pancreatic islets. J Endocrinol. 1993; 138: 127-36.

243. Bergmann U, Funatomi H, Kornmann M, Ishiwata T, Beger H, Korc M. Insulin-like growth factor II activates mitogenic signaling in pancreatic cancer cells via IRS-1. Int J Oncol. 1996; 9: 487-92.

244. Hoog A, Grimelius L, Falkmer S, Sara VR. A high-molecular IGF-2 immunoreactive peptide (pro-IGF-2?) in the insulin cells of the islets of Langerhans in pancreas of man and rat. Regul Pept. 1993; 47: 275-83.

245. Asfari M, De W, Noel M, Holthuizen PE, Czernichow P. Insulin-like growth factor-II gene expression in a rat insulin-producing beta-cell line (INS-1) is regulated by glucose. Diabetologia. 1995; 38: 927-35.

246. Katz LE, Bhala A, Camron E, Nunn SE, Hintz RL, Cohen P. IGF-II, IGF-binding proteins and IGF receptors in pancreatic beta-cell lines. J Endocrinol. 1997; 152: 455-64.

247. Foulstone E, Prince S, Zaccheo O, et al. Insulin-like growth factor ligands, receptors, and binding proteins in cancer. J Pathol. 2005; 205: 145-53.

248. Han VK, Lund PK, Lee DC, D'Ercole AJ. Expression of somatomedin/insulin-like growth factor messenger ribonucleic acids in the human fetus: identification, characterization, and tissue distribution. J Clin Endocrinol Metab. 1988; 66: 422-9.

249. Delhanty PJ, Han VK. The expression of insulin-like growth factor (IGF)-binding protein-2 and IGF-II genes in the tissues of the developing ovine fetus. Endocrinology. 1993; 132: 41-52.

250. Hill RA, Pell JM. Regulation of insulin-like growth factor I (IGF-I) bioactivity in vivo: further characterization of an IGF-I-enhancing antibody. Endocrinology. 1998; 139: 1278-87.

251. Sang X, Curran MS, Wood AW. Paracrine insulin-like growth factor signaling influences primordial germ cell migration: in vivo evidence from the zebrafish model. Endocrinology. 2008; 149: 5035-42.

252. Franke TF, Hornik CP, Segev L, Shostak GA, Sugimoto C. PI3K/Akt and apoptosis: size matters. Oncogene. 2003; 22: 8983-98.

253. Gajewski TF, Thompson CB. Apoptosis meets signal transduction: elimination of a BAD influence. Cell. 1996; 87: 589-92.

254. Foulstone E, Prince S, Zaccheo O, et al. Insulin-like growth factor ligands, receptors, and binding proteins in cancer. J Pathol. 2005; 205: 145-53.

255. Baserga R. The contradictions of the insulin-like growth factor 1 receptor. Oncogene. 2000; 19: 5574-81.

256. De Meyts P. [Insulin receptors and mechanism of action of insulin and of insulin-like growth factors]. Bull Mem Acad R Med Belg. 1994; 149: 181-90; discussion 90-4.

257. Amritraj A, Posse de Chaves EI, Hawkes C, Macdonald RG, Kar S. Single-Transmembrane Domain IGF-II/M6P Receptor: Potential Interaction with G Protein and Its Association with Cholesterol-Rich Membrane Domains. Endocrinology. 2012.

258. Hemberger M, Redies C, Krause R, Oswald J, Walter J, Fundele RH. H19 and Igf2 are expressed and differentially imprinted in neuroectoderm-derived cells in the mouse brain. Dev Genes Evol. 1998; 208: 393-402.

259. Khandwala HM, McCutcheon IE, Flyvbjerg A, Friend KE. The effects of insulin-like growth factors on tumorigenesis and neoplastic growth. Endocr Rev. 2000; 21: 215-44.

260. O'Dell SD, Day IN. Insulin-like growth factor II (IGF-II). Int J Biochem Cell Biol. 1998; 30: 767-71.

261. Braulke T. Type-2 IGF receptor: a multi-ligand binding protein. Horm Metab Res. 1999; 31: 242-6.

262. Fehmann HC, Jehle P, Markus U, Goke B. Functional active receptors for insulin-like growth factors-I (IGF-I) and IGF-II on insulin-, glucagon-, and somatostatin-producing cells. Metabolism: clinical and experimental. 1996; 45: 759-66.

263. Brown J, Jones EY, Forbes BE. Keeping IGF-II under control: lessons from the IGF-II-IGF2R crystal structure. Trends Biochem Sci. 2009; 34: 612-9.

264. Sia C, Hanninen A. Apoptosis in autoimmune diabetes: the fate of beta-cells in the cleft between life and death. Rev Diabet Stud. 2006; 3: 39-46.

265. Norbury CJ, Hickson ID. Cellular responses to DNA damage. Annu Rev Pharmacol Toxicol. 2001; 41: 367-401.

266. Diamantis A, Magiorkinis E, Sakorafas GH, Androutsos G. A brief history of apoptosis: from ancient to modern times. Onkologie. 2008; 31: 702-6.

267. Popper H, Keppler D. Networks of interacting mechanisms of hepatocellular degeneration and death. Prog Liver Dis. 1986; 8: 209-35.

268. McHugh P, Turina M. Apoptosis and necrosis: a review for surgeons. Surg Infect (Larchmt). 2006; 7: 53-68.

269. Bortner CD, Cidlowski JA. A necessary role for cell shrinkage in apoptosis. Biochem Pharmacol. 1998; 56: 1549-59.

270. Barros LF, Hermosilla T, Castro J. Necrotic volume increase and the early physiology of necrosis. Comp Biochem Physiol A Mol Integr Physiol. 2001; 130: 401-9.

271. Brouckaert G, Kalai M, Krysko DV, et al. Phagocytosis of necrotic cells by macrophages is phosphatidylserine dependent and does not induce inflammatory cytokine production. Mol Biol Cell. 2004; 15: 1089-100.

272. Clarke PG, Clarke S. Nineteenth century research on naturally occurring cell death and related phenomena. Anat Embryol (Berl). 1996; 193: 81-99.

273. Hacker G. The morphology of apoptosis. Cell Tissue Res. 2000; 301: 5-17.

274. Elmore S. Apoptosis: a review of programmed cell death. Toxicol Pathol. 2007; 35: 495-516.

275. Kerr JF, Wyllie AH, Currie AR. Apoptosis: a basic biological phenomenon with wide-ranging implications in tissue kinetics. Br J Cancer. 1972; 26: 239-57.

276. Reed JC. Mechanisms of apoptosis. Am J Pathol. 2000; 157: 1415-30.

277. Van Cruchten S, Van Den Broeck W. Morphological and biochemical aspects of apoptosis, oncosis and necrosis. Anat Histol Embryol. 2002; 31: 214-23.

278. Taylor RC, Cullen SP, Martin SJ. Apoptosis: controlled demolition at the cellular level. Nat Rev Mol Cell Biol. 2008; 9: 231-41.

279. Locksley RM, Killeen N, Lenardo MJ. The TNF and TNF receptor superfamilies: integrating mammalian biology. Cell. 2001; 104: 487-501.

280. Chen G, Goeddel DV. TNF-R1 signaling: a beautiful pathway. Science. 2002; 296: 1634-5.

281. Wajant H. The Fas signaling pathway: more than a paradigm. Science. 2002; 296: 1635-6.

282. Wajant H, Pfizenmaier K, Scheurich P. TNF-related apoptosis inducing ligand (TRAIL) and its receptors in tumor surveillance and cancer therapy. Apoptosis. 2002; 7: 449-59.

283. Green DR, Reed JC. Mitochondria and apoptosis. Science. 1998; 281: 1309-12.

284. Green DR. Apoptotic pathways: paper wraps stone blunts scissors. Cell. 2000; 102: 1-4.

285. Hague A, Paraskeva C. Apoptosis and disease: a matter of cell fate. Cell Death Differ. 2004; 11: 1366-72.

286. Li P, Nijhawan D, Budihardjo I, et al. Cytochrome c and dATP-dependent formation of Apaf-1/caspase-9 complex initiates an apoptotic protease cascade. Cell. 1997; 91: 479-89.

287. Trapani JA, Smyth MJ. Functional significance of the perforin/granzyme cell death pathway. Nat Rev Immunol. 2002; 2: 735-47.

288. Cullen SP, Martin SJ. Mechanisms of granule-dependent killing. Cell Death Differ. 2008; 15: 251-62.

289. Pardo J, Bosque A, Brehm R, et al. Apoptotic pathways are selectively activated by granzyme A and/or granzyme B in CTL-mediated target cell lysis. J Cell Biol. 2004; 167: 457-68.

290. Barry M, Bleackley RC. Cytotoxic T lymphocytes: all roads lead to death. Nat Rev Immunol. 2002; 2: 401-9.

291. Devadas S, Das J, Liu C, et al. Granzyme B is critical for T cell receptor-induced cell death of type 2 helper T cells. Immunity. 2006; 25: 237-47.

292. Slee EA, Adrain C, Martin SJ. Executioner caspase-3, -6, and -7 perform distinct, non-redundant roles during the demolition phase of apoptosis. J Biol Chem. 2001; 276: 7320-6.

293. Boatright KM, Salvesen GS. Mechanisms of caspase activation. Curr Opin Cell Biol. 2003; 15: 725-31.

294. Kothakota S, Azuma T, Reinhard C, et al. Caspase-3-generated fragment of gelsolin: effector of morphological change in apoptosis. Science. 1997; 278: 294-8.

295. Fadok VA, Voelker DR, Campbell PA, Cohen JJ, Bratton DL, Henson PM. Exposure of phosphatidylserine on the surface of apoptotic lymphocytes triggers specific recognition and removal by macrophages. J Immunol. 1992; 148: 2207-16.

296. Martin SJ, Reutelingsperger CP, McGahon AJ, et al. Early redistribution of plasma membrane phosphatidylserine is a general feature of apoptosis regardless of the initiating stimulus: inhibition by overexpression of Bcl-2 and Abl. J Exp Med. 1995; 182: 1545-56.

297. Koopman G, Reutelingsperger CP, Kuijten GA, Keehnen RM, Pals ST, van Oers MH. Annexin V for flow cytometric detection of phosphatidylserine expression on B cells undergoing apoptosis. Blood. 1994; 84: 1415-20.

298. Tanaka Y, Schroit AJ. Insertion of fluorescent phosphatidylserine into the plasma membrane of red blood cells. Recognition by autologous macrophages. J Biol Chem. 1983; 258: 11335-43.

299. Schroit AJ, Madsen JW, Tanaka Y. In vivo recognition and clearance of red blood cells containing phosphatidylserine in their plasma membranes. J Biol Chem. 1985; 260: 5131-8.

300. Roberts KM, Rosen A, Casciola-Rosen LA. Methods for inducing apoptosis. Methods Mol Med. 2004; 102: 115-28.

301. Stassi G, Todaro M, Richiusa P, et al. Expression of apoptosis-inducing CD95 (Fas/Apo-1) on human beta-cells sorted by flow-cytometry and cultured in vitro. Transplant Proc. 1995; 27: 3271-5.

302. Moriwaki M, Itoh N, Miyagawa J, et al. Fas and Fas ligand expression in inflamed islets in pancreas sections of patients with recent-onset Type I diabetes mellitus. Diabetologia. 1999; 42: 1332-40.

303. Stassi G, De Maria R, Trucco G, et al. Nitric oxide primes pancreatic beta cells for Fas-mediated destruction in insulin-dependent diabetes mellitus. J Exp Med. 1997; 186: 1193-200.

304. Thomas HE, McKenzie MD, Angstetra E, Campbell PD, Kay TW. Beta cell apoptosis in diabetes. Apoptosis. 2009; 14: 1389-404.

305. Thomas HE, Kay TW. Intracellular pathways of pancreatic beta-cell apoptosis in type 1 diabetes. Diabetes/metabolism research and reviews. 2011; 27: 790-6.

306. Oberholzer J, Triponez F, Mage R, et al. Human islet transplantation: lessons from 13 autologous and 13 allogeneic transplantations. Transplantation. 2000; 69: 1115-23.

307. Korsgren O, Nilsson B, Berne C, et al. Current status of clinical islet transplantation. Transplantation. 2005; 79: 1289-93.

308. Hering BJ, Kandaswamy R, Ansite JD, et al. Single-donor, marginal-dose islet transplantation in patients with type 1 diabetes. Jama. 2005; 293: 830-5.

309. Johansson H, Lukinius A, Moberg L, et al. Tissue factor produced by the endocrine cells of the islets of Langerhans is associated with a negative outcome of clinical islet transplantation. Diabetes. 2005; 54: 1755-62.

310. Sutton VR, Estella E, Li C, et al. A critical role for granzyme B, in addition to perforin and TNFalpha, in alloreactive CTL-induced mouse pancreatic beta cell death. Transplantation. 2006; 81: 146-54.

311. Noguchi H, Matsumoto S, Matsushita M, et al. Immunosuppression for islet transplantation. Acta Med Okayama. 2006; 60: 71-6.

312. Hauswirth WW, Lewin AS, Zolotukhin S, Muzyczka N. Production and purification of recombinant adeno-associated virus. Methods Enzymol. 2000; 316: 743-61.

313. Claiborn KC, Sachdeva MM, Cannon CE, Groff DN, Singer JD, Stoffers DA. Pcif1 modulates Pdx1 protein stability and pancreatic beta cell function and survival in mice. J Clin Invest. 2010; 120: 3713-21.

314. Gueret V, Negrete-Virgen JA, Lyddiatt A, Al-Rubeai M. Rapid titration of adenoviral infectivity by flow cytometry in batch culture of infected HEK293 cells. Cytotechnology. 2002; 38: 87-97.

315. Loiler SA, Conlon TJ, Song S, et al. Targeting recombinant adeno-associated virus vectors to enhance gene transfer to pancreatic islets and liver. Gene Ther. 2003; 10: 1551-8.

316. Chae HY, Kang JG, Kim CS, et al. Effect of glucagon-like peptide-1 gene expression on graft function in mouse islet transplantation. Transpl Int. 2012; 25: 242-9.
317. Rink JS, Chen X, Zhang X, Kaufman DB. Conditional and specific inhibition of NF-kappaB in mouse pancreatic beta cells prevents cytokine-induced deleterious effects and improves islet survival posttransplant. Surgery. 2012; 151: 330-9.
318. Sankar KS, Green BJ, Crocker AR, Verity JE, Altamentova SM, Rocheleau JV. Culturing pancreatic islets in microfluidic flow enhances morphology of the associated endothelial cells. PLoS One. 2011; 6: e24904.
319. Stendahl JC, Kaufman DB, Stupp SI. Extracellular matrix in pancreatic islets: relevance to scaffold design and transplantation. Cell Transplant. 2009; 18: 1-12.
320. Cheng JY, Raghunath M, Whitelock J, Poole-Warren L. Matrix components and scaffolds for sustained islet function. Tissue Eng Part B Rev. 2011; 17: 235-47.
321. Wang X, Meloche M, Verchere CB, Ou D, Mui A, Warnock GL. Improving islet engraftment by gene therapy. J Transplant. 2011; 2011: 594851.
322. Warnock JN, Daigre C, Al-Rubeai M. Introduction to viral vectors. Methods Mol Biol. 2011; 737: 1-25.
323. Zhang S, Zhao Y, Zhao B, Wang B. Hybrids of nonviral vectors for gene delivery. Bioconjug Chem. 2010; 21: 1003-9.
324. Abdallah B, Sachs L, Demeneix BA. Non-viral gene transfer: applications in developmental biology and gene therapy. Biol Cell. 1995; 85: 1-7.
325. Plesner A, Soukhatcheva G, Korneluk RG, Verchere CB. XIAP inhibition of beta-cell apoptosis reduces the number of islets required to restore euglycemia in a syngeneic islet transplantation model. Islets. 2010; 2: 18-23.
326. Xu AJ, Chen ZH, Tian F, Yan LH, Li T. [Effects of adenovirus-mediated interleukin-10 gene transfer on apoptosis and insulin secretion function of beta cell]. Zhonghua Yi Xue Za Zhi. 2010; 90: 1711-5.
327. Bindom SM, Hans CP, Xia H, Boulares AH, Lazartigues E. Angiotensin I-converting enzyme type 2 (ACE2) gene therapy improves glycemic control in diabetic mice. Diabetes. 2010; 59: 2540-8.
328. McCabe C, Samali A, O'Brien T. Cytoprotection of beta cells: rational gene transfer strategies. Diabetes Metab Res Rev. 2006; 22: 241-52.
329. Schneider MD, French BA. The advent of adenovirus. Gene therapy for cardiovascular disease. Circulation. 1993; 88: 1937-42.

330. Seregin SS, Amalfitano A. Improving adenovirus based gene transfer: strategies to accomplish immune evasion. Viruses. 2010; 2: 2013-36.

331. McCaffrey AP, Fawcett P, Nakai H, et al. The host response to adenovirus, helper-dependent adenovirus, and adeno-associated virus in mouse liver. Mol Ther. 2008; 16: 931-41.

332. Roy-Chowdhury J, Horwitz MS. Evolution of adenoviruses as gene therapy vectors. Mol Ther. 2002; 5: 340-4.

333. Conlon TJ, Flotte TR. Recombinant adeno-associated virus vectors for gene therapy. Expert Opin Biol Ther. 2004; 4: 1093-101.

334. Henckaerts E, Linden RM. Adeno-associated virus: a key to the human genome? Future Virol. 2010; 5: 555-74.

335. Buning H, Perabo L, Coutelle O, Quadt-Humme S, Hallek M. Recent developments in adeno-associated virus vector technology. J Gene Med. 2008; 10: 717-33.

336. Wu Z, Asokan A, Samulski RJ. Adeno-associated virus serotypes: vector toolkit for human gene therapy. Mol Ther. 2006; 14: 316-27.

337. Leopold PL, Crystal RG. Intracellular trafficking of adenovirus: many means to many ends. Adv Drug Deliv Rev. 2007; 59: 810-21.

338. Wickham TJ, Mathias P, Cheresh DA, Nemerow GR. Integrins alpha v beta 3 and alpha v beta 5 promote adenovirus internalization but not virus attachment. Cell. 1993; 73: 309-19.

339. Ylipaasto P, Klingel K, Lindberg AM, et al. Enterovirus infection in human pancreatic islet cells, islet tropism in vivo and receptor involvement in cultured islet beta cells. Diabetologia. 2004; 47: 225-39.

340. Myers SE, Brewer L, Shaw DP, et al. Prevalent human coxsackie B-5 virus infects porcine islet cells primarily using the coxsackie-adenovirus receptor. Xenotransplantation. 2004; 11: 536-46.

341. Zanone MM, Favaro E, Ferioli E, et al. Human pancreatic islet endothelial cells express coxsackievirus and adenovirus receptor and are activated by coxsackie B virus infection. FASEB J. 2007; 21: 3308-17.

342. Van Vliet KM, Blouin V, Brument N, Agbandje-McKenna M, Snyder RO. The role of the adeno-associated virus capsid in gene transfer. Methods Mol Biol. 2008; 437: 51-91.

343. Davidson BL, Stein CS, Heth JA, et al. Recombinant adeno-associated virus type 2, 4, and 5 vectors: transduction of variant cell types and regions in the mammalian central nervous system. Proceedings of the National Academy of Sciences of the United States of America. 2000; 97: 3428-32.

344. Walters RW, Yi SM, Keshavjee S, et al. Binding of adeno-associated virus type 5 to 2,3-linked sialic acid is required for gene transfer. J Biol Chem. 2001; 276: 20610-6.

345. Kaludov N, Brown KE, Walters RW, Zabner J, Chiorini JA. Adeno-associated virus serotype 4 (AAV4) and AAV5 both require sialic acid binding for hemagglutination and efficient transduction but differ in sialic acid linkage specificity. J Virol. 2001; 75: 6884-93.

346. Di Pasquale G, Davidson BL, Stein CS, et al. Identification of PDGFR as a receptor for AAV-5 transduction. Nat Med. 2003; 9: 1306-12.

347. Wu Z, Miller E, Agbandje-McKenna M, Samulski RJ. Alpha2,3 and alpha2,6 N-linked sialic acids facilitate efficient binding and transduction by adeno-associated virus types 1 and 6. J Virol. 2006; 80: 9093-103.

348. Seiler MP, Miller AD, Zabner J, Halbert CL. Adeno-associated virus types 5 and 6 use distinct receptors for cell entry. Hum Gene Ther. 2006; 17: 10-9.

349. Michelfelder S, Varadi K, Raupp C, et al. Peptide ligands incorporated into the threefold spike capsid domain to re-direct gene transduction of AAV8 and AAV9 in vivo. PLoS One. 2011; 6: e23101.

350. Akache B, Grimm D, Pandey K, Yant SR, Xu H, Kay MA. The 37/67-kilodalton laminin receptor is a receptor for adeno-associated virus serotypes 8, 2, 3, and 9. J Virol. 2006; 80: 9831-6.

351. Ling C, Lu Y, Kalsi JK, et al. Human hepatocyte growth factor receptor is a cellular coreceptor for adeno-associated virus serotype 3. Hum Gene Ther. 2010; 21: 1741-7.

352. Qing K, Mah C, Hansen J, Zhou S, Dwarki V, Srivastava A. Human fibroblast growth factor receptor 1 is a co-receptor for infection by adeno-associated virus 2. Nat Med. 1999; 5: 71-7.

353. Qiu J, Brown KE. Integrin alphaVbeta5 is not involved in adeno-associated virus type 2 (AAV2) infection. Virology. 1999; 264: 436-40.

354. Qiao C, Yuan Z, Li J, Tang R, Xiao X. Single tyrosine mutation in AAV8 and AAV9 capsids is insufficient to enhance gene delivery to skeletal muscle and heart. Hum Gene Ther Methods. 2012; 23: 29-37.

355. Zhong L, Li B, Jayandharan G, et al. Tyrosine-phosphorylation of AAV2 vectors and its consequences on viral intracellular trafficking and transgene expression. Virology. 2008; 381: 194-202.

356. Greber UF. Signalling in viral entry. Cell Mol Life Sci. 2002; 59: 608-26.

357. Tsukiyama S, Matsushita M, Matsumoto S, et al. Noble gene transduction into pancreatic beta-cells by singularizing islet cells with low doses of recombinant adenoviral vector. Artif Organs. 2008; 32: 188-94.

358. Narushima M, Okitsu T, Miki A, et al. Adenovirus mediated gene transduction of primarily isolated mouse islets. Asaio J. 2004; 50: 586-90.

359. Lefebvre B, Vandewalle B, Longue J, et al. Efficient gene delivery and silencing of mouse and human pancreatic islets. BMC Biotechnol. 2010; 10: 28.

360. Finbloom DS. Regulation of cell-surface receptors for human interferon-gamma on the human histiocytic lymphoma cell line U937. Biochem J. 1991; 274 (Pt 3): 775-80.

361. Imperiale MJ, Kochanek S. Adenovirus vectors: biology, design, and production. Curr Top Microbiol Immunol. 2004; 273: 335-57.

362. McCarty DM. Self-complementary AAV vectors; advances and applications. Mol Ther. 2008; 16: 1648-56.

363. Erbel S, Reers C, Nawroth PP, Ritzel RA. Prolonged culture of human islets induces ER stress. Exp Clin Endocrinol Diabetes. 2010; 118: 81-6.

364. Corbett JA, McDaniel ML. Intraislet release of interleukin 1 inhibits beta cell function by inducing beta cell expression of inducible nitric oxide synthase. J Exp Med. 1995; 181: 559-68.

365. Coura Rdos S, Nardi NB. The state of the art of adeno-associated virus-based vectors in gene therapy. Virol J. 2007; 4: 99.

366. Zhang N, Clement N, Chen D, et al. Transduction of pancreatic islets with pseudotyped adeno-associated virus: effect of viral capsid and genome conversion. Transplantation. 2005; 80: 683-90.

367. Craig AT, Gavrilova O, Dwyer NK, et al. Transduction of rat pancreatic islets with pseudotyped adeno-associated virus vectors. Virol J. 2009; 6: 61.

368. Rehman KK, Wang Z, Bottino R, et al. Efficient gene delivery to human and rodent islets with double-stranded (ds) AAV-based vectors. Gene Ther. 2005; 12: 1313-23.

369. Parnaud G, Hammar E, Rouiller DG, Armanet M, Halban PA, Bosco D. Blockade of beta1 integrin-laminin-5 interaction affects spreading and insulin secretion of rat beta-cells attached on extracellular matrix. Diabetes. 2006; 55: 1413-20.

370. van Deijnen JH, Hulstaert CE, Wolters GH, van Schilfgaarde R. Significance of the peri-insular extracellular matrix for islet isolation from the pancreas of rat, dog, pig, and man. Cell Tissue Res. 1992; 267: 139-46.

371. Meyer T, Buhler C, Czub S, et al. Selection of donor pigs for pancreatic islet transplantation may depend on the expression level of connective tissue proteins in the islet capsule. Transplant Proc. 1998; 30: 2471-3.

372. Meyer T, Chodnewska I, Czub S, et al. Extracellular matrix proteins in the porcine pancreas: a structural analysis for directed pancreatic islet isolation. Transplant Proc. 1998; 30: 354.

373. Wang RN, Rosenberg L. Maintenance of beta-cell function and survival following islet isolation requires re-establishment of the islet-matrix relationship. J Endocrinol. 1999; 163: 181-90.

374. Virtanen I, Banerjee M, Palgi J, et al. Blood vessels of human islets of Langerhans are surrounded by a double basement membrane. Diabetologia. 2008; 51: 1181-91.

375. Wang RN, Paraskevas S, Rosenberg L. Characterization of integrin expression in islets isolated from hamster, canine, porcine, and human pancreas. The journal of histochemistry and cytochemistry : official journal of the Histochemistry Society. 1999; 47: 499-506.

376. Kantengwa S, Baetens D, Sadoul K, Buck CA, Halban PA, Rouiller DG. Identification and characterization of alpha 3 beta 1 integrin on primary and transformed rat islet cells. Exp Cell Res. 1997; 237: 394-402.

377. Ris F, Hammar E, Bosco D, et al. Impact of integrin-matrix matching and inhibition of apoptosis on the survival of purified human beta-cells in vitro. Diabetologia. 2002; 45: 841-50.

378. Kaido T, Perez B, Yebra M, et al. Alphav-integrin utilization in human beta-cell adhesion, spreading, and motility. J Biol Chem. 2004; 279: 17731-7.

379. Bai M, Harfe B, Freimuth P. Mutations that alter an Arg-Gly-Asp (RGD) sequence in the adenovirus type 2 penton base protein abolish its cell-rounding activity and delay virus reproduction in flat cells. J Virol. 1993; 67: 5198-205.

380. Qiao C, Zhang W, Yuan Z, et al. Adeno-associated virus serotype 6 capsid tyrosine-to-phenylalanine mutations improve gene transfer to skeletal muscle. Hum Gene Ther. 2010; 21: 1343-8.

381. Duan D, Yue Y, Yan Z, Yang J, Engelhardt JF. Endosomal processing limits gene transfer to polarized airway epithelia by adeno-associated virus. J Clin Invest. 2000; 105: 1573-87.

382. Douar AM, Poulard K, Stockholm D, Danos O. Intracellular trafficking of adeno-associated virus vectors: routing to the late endosomal compartment and proteasome degradation. J Virol. 2001; 75: 1824-33.

383. Yan Z, Zak R, Luxton GW, Ritchie TC, Bantel-Schaal U, Engelhardt JF. Ubiquitination of both adeno-associated virus type 2 and 5 capsid proteins affects the transduction efficiency of recombinant vectors. J Virol. 2002; 76: 2043-53.

384. Ding W, Yan Z, Zak R, Saavedra M, Rodman DM, Engelhardt JF. Second-strand genome conversion of adeno-associated virus type 2 (AAV-2) and AAV-5 is not rate limiting following apical infection of polarized human airway epithelia. J Virol. 2003; 77: 7361-6.

385. Denby L, Nicklin SA, Baker AH. Adeno-associated virus (AAV)-7 and -8 poorly transduce vascular endothelial cells and are sensitive to proteasomal degradation. Gene Ther. 2005; 12: 1534-8.

386. Ryals RC, Boye SL, Dinculescu A, Hauswirth WW, Boye SE. Quantifying transduction efficiencies of unmodified and tyrosine capsid mutant AAV vectors in vitro using two ocular cell lines. Mol Vis. 2011; 17: 1090-102.

387. Petrs-Silva H, Dinculescu A, Li Q, et al. Novel properties of tyrosine-mutant AAV2 vectors in the mouse retina. Mol Ther. 2011; 19: 293-301.

388. Zhong L, Li B, Mah CS, et al. Next generation of adeno-associated virus 2 vectors: point mutations in tyrosines lead to high-efficiency transduction at lower doses. Proceedings of the National Academy of Sciences of the United States of America. 2008; 105: 7827-32.

389. Markusic DM, Herzog RW, Aslanidi GV, et al. High-efficiency transduction and correction of murine hemophilia B using AAV2 vectors devoid of multiple surface-exposed tyrosines. Mol Ther. 2010; 18: 2048-56.

390. Montana E, Bonner-Weir S, Weir GC. Beta cell mass and growth after syngeneic islet cell transplantation in normal and streptozocin diabetic C57BL/6 mice. J Clin Invest. 1993; 91: 780-7.

391. Collier JJ, Fueger PT, Hohmeier HE, Newgard CB. Pro- and antiapoptotic proteins regulate apoptosis but do not protect against cytokine-mediated cytotoxicity in rat islets and beta-cell lines. Diabetes. 2006; 55: 1398-406.

392. Mellado-Gil JM, Cobo-Vuilleumier N, Gauthier BR. Islet beta-Cell Mass Preservation and Regeneration in Diabetes Mellitus: Four Factors with Potential Therapeutic Interest. J Transplant. 2012; 2012: 230870.

393. Granata R, Settanni F, Gallo D, et al. Obestatin promotes survival of pancreatic beta-cells and human islets and induces expression of genes involved in the regulation of beta-cell mass and function. Diabetes. 2008; 57: 967-79.

394. Contreras JL, Bilbao G, Smyth CA, et al. Cytoprotection of pancreatic islets before and early after transplantation using gene therapy. Kidney Int. 2002; 61: S79-84.

395. Jung Y, Miura M, Yuan J. Suppression of interleukin-1 beta-converting enzyme-mediated cell death by insulin-like growth factor. J Biol Chem. 1996; 271: 5112-7.

396. Stewart CE, Rotwein P. Insulin-like growth factor-II is an autocrine survival factor for differentiating myoblasts. J Biol Chem. 1996; 271: 11330-8.

397. Petrik J, Arany E, McDonald TJ, Hill DJ. Apoptosis in the pancreatic islet cells of the neonatal rat is associated with a reduced expression of insulin-like growth factor II that may act as a survival factor. Endocrinology. 1998; 139: 2994-3004.

398. Conti E, Musumeci MB, Assenza GE, Quarta G, Autore C, Volpe M. Recombinant human insulin-like growth factor-1: a new cardiovascular disease treatment option? Cardiovasc Hematol Agents Med Chem. 2008; 6: 258-71.

399. Singleton JR, Dixit VM, Feldman EL. Type I insulin-like growth factor receptor activation regulates apoptotic proteins. J Biol Chem. 1996; 271: 31791-4.

400. Van Golen CM, Feldman EL. Insulin-like growth factor I is the key growth factor in serum that protects neuroblastoma cells from hyperosmotic-induced apoptosis. J Cell Physiol. 2000; 182: 24-32.

401. Hogg J, Hill DJ, Han VK. The ontogeny of insulin-like growth factor (IGF) and IGF-binding protein gene expression in the rat pancreas. J Mol Endocrinol. 1994; 13: 49-58.

402. Hill DJ, Strutt B, Arany E, Zaina S, Coukell S, Graham CF. Increased and persistent circulating insulin-like growth factor II in neonatal transgenic mice suppresses developmental apoptosis in the pancreatic islets. Endocrinology. 2000; 141: 1151-7.

403. Vorburger SA, Hunt KK. Adenoviral gene therapy. Oncologist. 2002; 7: 46-59.

404. Grossman M, Raper SE, Kozarsky K, et al. Successful ex vivo gene therapy directed to liver in a patient with familial hypercholesterolaemia. Nat Genet. 1994; 6: 335-41.

405. Heikkila P, Parpala T, Lukkarinen O, Weber M, Tryggvason K. Adenovirus-mediated gene transfer into kidney glomeruli using an ex vivo and in vivo kidney perfusion system - first steps towards gene therapy of Alport syndrome. Gene Ther. 1996; 3: 21-7.

406. Breyer B, Jiang W, Cheng H, et al. Adenoviral vector-mediated gene transfer for human gene therapy. Curr Gene Ther. 2001; 1: 149-62.

407. de Groot M, de Haan BJ, Keizer PP, Schuurs TA, van Schilfgaarde R, Leuvenink HG. Rat islet isolation yield and function are donor strain dependent. Lab Anim. 2004; 38: 200-6.

408. Gotoh M, Maki T, Kiyoizumi T, Satomi S, Monaco AP. An improved method for isolation of mouse pancreatic islets. Transplantation. 1985; 40: 437-8.

409. Shewade YM, Umrani M, Bhonde RR. Large-scale isolation of islets by tissue culture of adult mouse pancreas. Transplant Proc. 1999; 31: 1721-3.

410. Chiu W, Niwa Y, Zeng W, Hirano T, Kobayashi H, Sheen J. Engineered GFP as a vital reporter in plants. Curr Biol. 1996; 6: 325-30.

411. Liu HS, Jan MS, Chou CK, Chen PH, Ke NJ. Is green fluorescent protein toxic to the living cells? Biochem Biophys Res Commun. 1999; 260: 712-7.

412. Taghizadeh RR, Sherley JL. CFP and YFP, but not GFP, provide stable fluorescent marking of rat hepatic adult stem cells. J Biomed Biotechnol. 2008; 2008: 453590.

413. Rosenberg L, Wang R, Paraskevas S, Maysinger D. Structural and functional changes resulting from islet isolation lead to islet cell death. Surgery. 1999; 126: 393-8.

414. Paraskevas S, Duguid WP, Maysinger D, Feldman L, Agapitos D, Rosenberg L. Apoptosis occurs in freshly isolated human islets under standard culture conditions. Transplant Proc. 1997; 29: 750-2.

415. Ilieva A, Yuan S, Wang RN, Agapitos D, Hill DJ, Rosenberg L. Pancreatic islet cell survival following islet isolation: the role of cellular interactions in the pancreas. J Endocrinol. 1999; 161: 357-64.

416. Wood AW, Duan C, Bern HA. Insulin-like growth factor signaling in fish. Int Rev Cytol. 2005; 243: 215-85.

417. Wu Y, Han B, Luo H, et al. DcR3/TR6 effectively prevents islet primary nonfunction after transplantation. Diabetes. 2003; 52: 2279-86.

418. Davalli AM, Ogawa Y, Ricordi C, Scharp DW, Bonner-Weir S, Weir GC. A selective decrease in the beta cell mass of human islets transplanted into diabetic nude mice. Transplantation. 1995; 59: 817-20.

419. Bennet W, Groth CG, Larsson R, Nilsson B, Korsgren O. Isolated human islets trigger an instant blood mediated inflammatory reaction: implications for intraportal islet transplantation as a treatment for patients with type 1 diabetes. Ups J Med Sci. 2000; 105: 125-33.

420. Barshes NR, Wyllie S, Goss JA. Inflammation-mediated dysfunction and apoptosis in pancreatic islet transplantation: implications for intrahepatic grafts. J Leukoc Biol. 2005; 77: 587-97.

421. Kaufman DB, Rabe FL, Platt JL, Dunn DL, Sutherland DE. Effect of host immunomodulation on the prevention of islet allograft primary nonfunction in a murine model. Transplant Proc. 1990; 22: 857-8.

422. Nagata M, Mullen Y, Matsuo S, Herrera M, Clare-Salzler M. Destruction of islet isografts by severe nonspecific inflammation. Transplant Proc. 1990; 22: 855-6.

423. Stevens RB, Lokeh A, Ansite JD, Field MJ, Gores PF, Sutherland DE. Role of nitric oxide in the pathogenesis of early pancreatic islet dysfunction during rat and human intraportal islet transplantation. Transplant Proc. 1994; 26: 692.

424. Matsuda T, Omori K, Vuong T, et al. Inhibition of p38 pathway suppresses human islet production of pro-inflammatory cytokines and improves islet graft function. Am J Transplant. 2005; 5: 484-93.

425. Robson SC, Wu Y, Sun X, Knosalla C, Dwyer K, Enjyoji K. Ectonucleotidases of CD39 family modulate vascular inflammation and thrombosis in transplantation. Semin Thromb Hemost. 2005; 31: 217-33.

426. Saldeen J. Cytokines induce both necrosis and apoptosis via a common Bcl-2-inhibitable pathway in rat insulin-producing cells. Endocrinology. 2000; 141: 2003-10.

427. Eizirik DL, Mandrup-Poulsen T. A choice of death--the signal-transduction of immune-mediated beta-cell apoptosis. Diabetologia. 2001; 44: 2115-33.

428. Estil les E, Tellez N, Soler J, Montanya E. High sensitivity of beta-cell replication to the inhibitory effects of interleukin-1beta: modulation by adenoviral overexpression of IGF2 in rat islets. J Endocrinol. 2009; 203: 55-63.

429. Mathis D, Vence L, Benoist C. beta-Cell death during progression to diabetes. Nature. 2001; 414: 792-8.

430. Montolio M, Biarnes M, Tellez N, Escoriza J, Soler J, Montanya E. Interleukin-1beta and inducible form of nitric oxide synthase expression in early syngeneic islet transplantation. J Endocrinol. 2007; 192: 169-77.

431. Montolio M, Tellez N, Soler J, Montanya E. Role of blood glucose in cytokine gene expression in early syngeneic islet transplantation. Cell Transplant. 2007; 16: 517-25.

432. Bottino R, Fernandez LA, Ricordi C, et al. Transplantation of allogeneic islets of Langerhans in the rat liver: effects of macrophage depletion on graft survival and microenvironment activation. Diabetes. 1998; 47: 316-23.

433. Sandler S, Andersson A, Hellerstrom C. Inhibitory effects of interleukin 1 on insulin secretion, insulin biosynthesis, and oxidative metabolism of isolated rat pancreatic islets. Endocrinology. 1987; 121: 1424-31.

434. Wachlin G, Augstein P, Schroder D, et al. IL-1beta, IFN-gamma and TNF-alpha increase vulnerability of pancreatic beta cells to autoimmune destruction. J Autoimmun. 2003; 20: 303-12.

435. Eizirik DL, Flodstrom M, Karlsen AE, Welsh N. The harmony of the spheres: inducible nitric oxide synthase and related genes in pancreatic beta cells. Diabetologia. 1996; 39: 875-90.

436. Emamaullee JA, Stanton L, Schur C, Shapiro AM. Caspase inhibitor therapy enhances marginal mass islet graft survival and preserves long-term function in islet transplantation. Diabetes. 2007; 56: 1289-98.

437. Contreras JL, Eckstein C, Smyth CA, et al. Brain death significantly reduces isolated pancreatic islet yields and functionality in vitro and in vivo after transplantation in rats. Diabetes. 2003; 52: 2935-42.

438. Xiao W, Mindrinos MN, Seok J, et al. A genomic storm in critically injured humans. J Exp Med. 2011; 208: 2581-90.

439. Abramowicz D, Schandene L, Goldman M, et al. Release of tumor necrosis factor, interleukin-2, and gamma-interferon in serum after injection of OKT3 monoclonal antibody in kidney transplant recipients. Transplantation. 1989; 47: 606-8.

440. Burke GW, Alejandro R, Cirocco R, Nery J, Mintz D, Miller J. Regional cytokine changes following OKT3 induction for islet cell transplantation in humans: early increase in portal and systemic levels of interleukin-6 and tumor necrosis factors. Transplant Proc. 1992; 24: 962-4.

441. Imagawa DK, Millis JM, Olthoff KM, et al. The role of tumor necrosis factor in allograft rejection. II. Evidence that antibody therapy against tumor necrosis factor-alpha and lymphotoxin enhances cardiac allograft survival in rats. Transplantation. 1990; 50: 189-93.

442. Cowley MJ, Weinberg A, Zammit N, et al. Human Islets Express a Marked Pro-Inflammatory Molecular Signature Prior to Transplantation. Cell Transplant. 2012.

443. Campbell PD, Weinberg A, Chee J, et al. Expression of pro- and antiapoptotic molecules of the Bcl-2 family in human islets postisolation. Cell Transplant. 2012; 21: 49-60.

444. Efrat S, Fejer G, Brownlee M, Horwitz MS. Prolonged survival of pancreatic islet allografts mediated by adenovirus immunoregulatory transgenes. Proceedings of the National Academy of Sciences of the United States of America. 1995; 92: 6947-51.

445. Efrat S. Prospects for gene therapy of insulin-dependent diabetes mellitus. Diabetologia. 1998; 41: 1401-9.

446. Davalli AM, Ogawa Y, Scaglia L, et al. Function, mass, and replication of porcine and rat islets transplanted into diabetic nude mice. Diabetes. 1995; 44: 104-11.

447. Chou FC, Sytwu HK. Overexpression of thioredoxin in islets transduced by a lentiviral vector prolongs graft survival in autoimmune diabetic NOD mice. J Biomed Sci. 2009; 16: 71.

448. Ishii S, Koyama H, Miyata T, et al. Appropriate control of ex vivo gene therapy delivering basic fibroblast growth factor promotes successful and safe development of collateral vessels in rabbit model of hind limb ischemia. J Vasc Surg. 2004; 39: 629-38.

449. Scarim AL, Heitmeier MR, Corbett JA. Irreversible inhibition of metabolic function and islet destruction after a 36-hour exposure to interleukin-1beta. Endocrinology. 1997; 138: 5301-7.

450. Hughes KJ, Chambers KT, Meares GP, Corbett JA. Nitric oxides mediates a shift from early necrosis to late apoptosis in cytokine-treated beta-cells that is associated with irreversible DNA damage. Am J Physiol Endocrinol Metab. 2009; 297: E1187-96.

451. Perez-Arana G, Blandino-Rosano M, Prada-Oliveira A, Aguilar-Diosdado M, Segundo C. Decrease in {beta}-cell proliferation precedes apoptosis during diabetes development in bio-breeding/worcester rat: beneficial role of Exendin-4. Endocrinology. 2010; 151: 2538-46.

452. Mosser G, Ravanat C, Freyssinet JM, Brisson A. Sub-domain structure of lipid-bound annexin-V resolved by electron image analysis. J Mol Biol. 1991; 217: 241-5.

453. Suzuki T, Fujikura K, Higashiyama T, Takata K. DNA staining for fluorescence and laser confocal microscopy. J Histochem Cytochem. 1997; 45: 49-53.

454. Khoynezhad A. Promising aspects and caveats of studies on anti-apoptotic therapies in patients with heart failure. Eur J Heart Fail. 2007; 9: 120-3.

455. Yeung TY, Seeberger KL, Kin T, et al. Human mesenchymal stem cells protect human islets from pro-inflammatory cytokines. PLoS One. 2012; 7: e38189.

456. Hopcroft DW, Mason DR, Scott RS. Structure-function relationships in pancreatic islets: support for intraislet modulation of insulin secretion. Endocrinology. 1985; 117: 2073-80.

457. Bendtzen K, Mandrup-Poulsen T, Nerup J, Nielsen JH, Dinarello CA, Svenson M. Cytotoxicity of human pI 7 interleukin-1 for pancreatic islets of Langerhans. Science. 1986; 232: 1545-7.

458. Comens PG, Wolf BA, Unanue ER, Lacy PE, McDaniel ML. Interleukin 1 is potent modulator of insulin secretion from isolated rat islets of Langerhans. Diabetes. 1987; 36: 963-70.

459. Ohara-Imaizumi M, Cardozo AK, Kikuta T, Eizirik DL, Nagamatsu S. The cytokine interleukin-1beta reduces the docking and fusion of insulin granules in pancreatic beta-cells, preferentially decreasing the first phase of exocytosis. J Biol Chem. 2004; 279: 41271-4.

460. Cohen P, Ocrant I, Fielder PJ, et al. Insulin-like growth factors (IGFs): implications for aging. Psychoneuroendocrinology. 1992; 17: 335-42.

461. Jung Y, Miura M, Yuan J. Suppression of interleukin-1 beta-converting enzyme-mediated cell death by insulin-like growth factor. J Biol Chem. 1996; 271: 5112-7.

462. Stewart CE, Rotwein P. Insulin-like growth factor-II is an autocrine survival factor for differentiating myoblasts. J Biol Chem. 1996; 271: 11330-8.

463. Geier A, Beery R, Haimsohn M, Karasik A. Insulin-like growth factor-1 inhibits cell death induced by anticancer drugs in the MCF-7 cells: involvement of growth factors in drug resistance. Cancer Invest. 1995; 13: 480-6.

464. Groskopf JC, Syu LJ, Saltiel AR, Linzer DI. Proliferin induces endothelial cell chemotaxis through a G protein-coupled, mitogen-activated protein kinase-dependent pathway. Endocrinology. 1997; 138: 2835-40.

465. McKinnon T, Chakraborty C, Gleeson LM, Chidiac P, Lala PK. Stimulation of human extravillous trophoblast migration by IGF-II is mediated by IGF type 2 receptor involving inhibitory G protein(s) and phosphorylation of MAPK. J Clin Endocrinol Metab. 2001; 86: 3665-74.

466. Robitaille R, Dusseault J, Henley N, Rosenberg L, Halle JP. Insulin-like growth factor II allows prolonged blood glucose normalization with a reduced islet cell mass transplantation. Endocrinology. 2003; 144: 3037-45.

467. Narang AS, Sabek O, Gaber AO, Mahato RI. Co-expression of vascular endothelial growth factor and interleukin-1 receptor antagonist improves human islet survival and function. Pharm Res. 2006; 23: 1970-82.

468. Noguchi H, Naziruddin B, Jackson A, et al. Low-temperature preservation of isolated islets is superior to conventional islet culture before islet transplantation. Transplantation. 2010; 89: 47-54.

469. Nathan DM. Long-term complications of diabetes mellitus. The New England journal of medicine. 1993; 328: 1676-85.

470. Long AE, Gillespie KM, Rokni S, Bingley PJ, Williams AJ. Rising incidence of type 1 diabetes is associated with altered immunophenotype at diagnosis. Diabetes. 2012; 61: 683-6.

471. Deckert T, Poulsen JE, Larsen M. Prognosis of diabetics with diabetes onset before the age of thirty-one. I. Survival, causes of death, and complications. Diabetologia. 1978; 14: 363-70.

472. Graham DE, Rechler MM, Brown AL, et al. Coordinate developmental regulation of high and low molecular weight mRNAs for rat insulin-like growth factor II. Proceedings of the National Academy of Sciences of the United States of America. 1986; 83: 4519-23.

473. Brown AL, Graham DE, Nissley SP, Hill DJ, Strain AJ, Rechler MM. Developmental regulation of insulin-like growth factor II mRNA in different rat tissues. J Biol Chem. 1986; 261: 13144-50.

474. Beck F, Samani NJ, Penschow JD, Thorley B, Tregear GW, Coghlan JP. Histochemical localization of IGF-I and -II mRNA in the developing rat embryo. Development. 1987; 101: 175-84.

475. Brehm MA, Powers AC, Shultz LD, Greiner DL. Advancing animal models of human type 1 diabetes by engraftment of functional human tissues in immunodeficient mice. Cold Spring Harb Perspect Med. 2012; 2: a007757.

476. Rees DA, Alcolado JC. Animal models of diabetes mellitus. Diabet Med. 2005; 22: 359-70.

477. Harder T, Franke K, Fahrenkrog S, et al. Prevention by maternal pancreatic islet transplantation of hypothalamic malformation in offspring of diabetic mother rats is already detectable at weaning. Neurosci Lett. 2003; 352: 163-6.

478. Deeds MC, Anderson JM, Armstrong AS, et al. Single dose streptozotocin-induced diabetes: considerations for study design in islet transplantation models. Lab Anim. 2011; 45: 131-40.

479. Wei M, Ong L, Smith MT, et al. The streptozotocin-diabetic rat as a model of the chronic complications of human diabetes. Heart Lung Circ. 2003; 12: 44-50.

480. Wang Z, Gleichmann H. GLUT2 in pancreatic islets: crucial target molecule in diabetes induced with multiple low doses of streptozotocin in mice. Diabetes. 1998; 47: 50-6.

481. Szkudelski T. The mechanism of alloxan and streptozotocin action in B cells of the rat pancreas. Physiological research / Academia Scientiarum Bohemoslovaca. 2001; 50: 537-46.

482. West E, Simon OR, Morrison EY. Streptozotocin alters pancreatic beta-cell responsiveness to glucose within six hours of injection into rats. The West Indian medical journal. 1996; 45: 60-2.

483. Swindle MM. Swine as replacements for dogs in the surgical teaching and research laboratory. Lab Anim Sci. 1984; 34: 383-5.

484. Qiao CF, Tian BL, Mai G, et al. Induction of diabetes in rhesus monkeys and establishment of insulin administration strategy. Transplant Proc. 2009; 41: 413-7.

485. Anderson MS, Bluestone JA. The NOD mouse: a model of immune dysregulation. Annu Rev Immunol. 2005; 23: 447-85.

486. Gysemans CA, Waer M, Valckx D, et al. Early graft failure of xenogeneic islets in NOD mice is accompanied by high levels of interleukin-1 and low levels of transforming growth factor-beta mRNA in the grafts. Diabetes. 2000; 49: 1992-7.

487. Liu G, Dou S, Cheng D, et al. Human islet cell MORF/cMORF pretargeting in a xenogeneic murine transplant model. Mol Pharm. 2011; 8: 767-73.
488. Vlad G, D'Agati VD, Zhang QY, et al. Immunoglobulin-like transcript 3-Fc suppresses T-cell responses to allogeneic human islet transplants in hu-NOD/SCID mice. Diabetes. 2008; 57: 1878-86.
489. Deng S, Vatamaniuk M, Lian MM, et al. Insulin gene transfer enhances the function of human islet grafts. Diabetologia. 2003; 46: 386-93.
490. Fenjves ES, Ochoa MS, Gay-Rabinstein C, et al. Adenoviral gene transfer of erythropoietin confers cytoprotection to isolated pancreatic islets. Transplantation. 2004; 77: 13-8.
491. Chinnaiyan AM, Orth K, O'Rourke K, Duan H, Poirier GG, Dixit VM. Molecular ordering of the cell death pathway. Bcl-2 and Bcl-xL function upstream of the CED-3-like apoptotic proteases. J Biol Chem. 1996; 271: 4573-6.
492. Walsh JG, Cullen SP, Sheridan C, Luthi AU, Gerner C, Martin SJ. Executioner caspase-3 and caspase-7 are functionally distinct proteases. Proc Natl Acad Sci U S A. 2008; 105: 12815-9.
493. Shin S, Li N, Kobayashi N, Yoon JW, Jun HS. Remission of diabetes by beta-cell regeneration in diabetic mice treated with a recombinant adenovirus expressing betacellulin. Mol Ther. 2008; 16: 854-61.
494. Zhao M, Amiel SA, Ajami S, et al. Amelioration of streptozotocin-induced diabetes in mice with cells derived from human marrow stromal cells. PLoS One. 2008; 3: e2666.
495. Gerling IC, Friedman H, Greiner DL, Shultz LD, Leiter EH. Multiple low-dose streptozocin-induced diabetes in NOD-scid/scid mice in the absence of functional lymphocytes. Diabetes. 1994; 43: 433-40.
496. Hayashi K, Kojima R, Ito M. Strain differences in the diabetogenic activity of streptozotocin in mice. Biological & pharmaceutical bulletin. 2006; 29: 1110-9.
497. Ito M, Kondo Y, Nakatani A, Naruse A. New model of progressive non-insulin-dependent diabetes mellitus in mice induced by streptozotocin. Biological & pharmaceutical bulletin. 1999; 22: 988-9.
498. Valentovic MA, Alejandro N, Betts Carpenter A, Brown PI, Ramos K. Streptozotocin (STZ) diabetes enhances benzo(alpha)pyrene induced renal injury in Sprague Dawley rats. Toxicol Lett. 2006; 164: 214-20.
499. Leturque A, Brot-Laroche E, Le Gall M. GLUT2 mutations, translocation, and receptor function in diet sugar managing. Am J Physiol Endocrinol Metab. 2009; 296: E985-92.

500. Lu WT, Juang JH, Hsu BR, Huang HS. Effects of high or low dose of streptozocin on pancreatic islets in C57BL/6 and C.B17-SCID mice. Transplant Proc. 1998; 30: 609-10.

501. Dekel Y, Glucksam Y, Elron-Gross I, Margalit R. Insights into modeling streptozotocin-induced diabetes in ICR mice. Lab animal. 2009; 38: 55-60.

502. Nakamura M, Nagafuchi S, Yamaguchi K, Takaki R. The role of thymic immunity and insulitis in the development of streptozocin-induced diabetes in mice. Diabetes. 1984; 33: 894-900.

503. Szkudelski T. The mechanism of alloxan and streptozotocin action in B cells of the rat pancreas. Physiol Res. 2001; 50: 537-46.

504. Leiter EH. Differential susceptibility of BALB/c sublines to diabetes induction by multi-dose streptozotocin treatment. Curr Top Microbiol Immunol. 1985; 122: 78-85.

505. Bell RC, Khurana M, Ryan EA, Finegood DT. Gender differences in the metabolic response to graded numbers of transplanted islets of Langerhans. Endocrinology. 1994; 135: 2681-7.

506. Leiter EH. Multiple low-dose streptozotocin-induced hyperglycemia and insulitis in C57BL mice: influence of inbred background, sex, and thymus. Proc Natl Acad Sci U S A. 1982; 79: 630-4.

507. Le May C, Chu K, Hu M, et al. Estrogens protect pancreatic beta-cells from apoptosis and prevent insulin-deficient diabetes mellitus in mice. Proc Natl Acad Sci U S A. 2006; 103: 9232-7.

508. Staeva-Vieira T, Peakman M, von Herrath M. Translational mini-review series on type 1 diabetes: Immune-based therapeutic approaches for type 1 diabetes. Clinical and experimental immunology. 2007; 148: 17-31.

509. Atkinson MA, Leiter EH. The NOD mouse model of type 1 diabetes: as good as it gets? Nat Med. 1999; 5: 601-4.

510. McGeachie J, Tennant M. Growth factors and their implications for clinicians: a brief review. Aust Dent J. 1997; 42: 375-80.

511. Bloch K, Papismedov E, Yavriyants K, Vorobeychik M, Beer S, Vardi P. Immobilized microalgal cells as an oxygen supply system for encapsulated pancreatic islets: a feasibility study. Artif Organs. 2006; 30: 715-8.

512. LeRoith D, Roberts CT, Jr. The insulin-like growth factor system and cancer. Cancer Lett. 2003; 195: 127-37.

513. Zawalich WS, Zawalich KC, Tesz GJ, Sterpka JA, Philbrick WM. Insulin secretion and IP levels in two distant lineages of the genus Mus: comparisons with rat islets. Am J Physiol Endocrinol Metab. 2001; 280: E720-8.

514. Kwon YW, Kwon KS, Moon HE, et al. Insulin-like growth factor-II regulates the expression of vascular endothelial growth factor by the human keratinocyte cell line HaCaT. J Invest Dermatol. 2004; 123: 152-8.

515. Ferrara N. Vascular endothelial growth factor: basic science and clinical progress. Endocr Rev. 2004; 25: 581-611.

516. Ohkubo Y, Kishikawa H, Araki E, et al. Intensive insulin therapy prevents the progression of diabetic microvascular complications in Japanese patients with non-insulin-dependent diabetes mellitus: a randomized prospective 6-year study. Diabetes Res Clin Pract. 1995; 28: 103-17.

517. Robertson RP, Davis C, Larsen J, Stratta R, Sutherland DE. Pancreas and islet transplantation for patients with diabetes. Diabetes Care. 2000; 23: 112-6.

518. Jensen J. Gene regulatory factors in pancreatic development. Developmental dynamics : an official publication of the American Association of Anatomists. 2004; 229: 176-200.

519. Swenne I, Hill DJ, Strain AJ, Milner RD. Growth hormone regulation of somatomedin C/insulin-like growth factor I production and DNA replication in fetal rat islets in tissue culture. Diabetes. 1987; 36: 288-94.

520. Hogg J, Han VK, Clemmons DR, Hill DJ. Interactions of nutrients, insulin-like growth factors (IGFs) and IGF-binding proteins in the regulation of DNA synthesis by isolated fetal rat islets of Langerhans. J Endocrinol. 1993; 138: 401-12.

521. Nemerow GR, Stewart PL. Role of alpha(v) integrins in adenovirus cell entry and gene delivery. Microbiol Mol Biol Rev. 1999; 63: 725-34.

522. Henaff D, Salinas S, Kremer EJ. An adenovirus traffic update: from receptor engagement to the nuclear pore. Future Microbiol. 2011; 6: 179-92.

523. Duan D, Li Q, Kao AW, Yue Y, Pessin JE, Engelhardt JF. Dynamin is required for recombinant adeno-associated virus type 2 infection. J Virol. 1999; 73: 10371-6.

524. Tam BY, Wei K, Rudge JS, et al. VEGF modulates erythropoiesis through regulation of adult hepatic erythropoietin synthesis. Nat Med. 2006; 12: 793-800.

525. Kuo CJ, Farnebo F, Yu EY, et al. Comparative evaluation of the antitumor activity of antiangiogenic proteins delivered by gene transfer. Proc Natl Acad Sci U S A. 2001; 98: 4605-10.

526. Kuhnert F, Davis CR, Wang HT, et al. Essential requirement for Wnt signaling in proliferation of adult small intestine and colon revealed by adenoviral expression of Dickkopf-1. Proc Natl Acad Sci U S A. 2004; 101: 266-71.

527. Huang X, Moore DJ, Ketchum RJ, et al. Resolving the conundrum of islet transplantation by linking metabolic dysregulation, inflammation, and immune regulation. Endocr Rev. 2008; 29: 603-30.

528. Chinnasamy D, Milsom MD, Shaffer J, et al. Multicistronic lentiviral vectors containing the FMDV 2A cleavage factor demonstrate robust expression of encoded genes at limiting MOI. Virol J. 2006; 3: 14.

529. Azzouz M, Martin-Rendon E, Barber RD, et al. Multicistronic lentiviral vector-mediated striatal gene transfer of aromatic L-amino acid decarboxylase, tyrosine hydroxylase, and GTP cyclohydrolase I induces sustained transgene expression, dopamine production, and functional improvement in a rat model of Parkinson's disease. J Neurosci. 2002; 22: 10302-12.

530. Mitta B, Rimann M, Ehrengruber MU, et al. Advanced modular self-inactivating lentiviral expression vectors for multigene interventions in mammalian cells and in vivo transduction. Nucleic acids research. 2002; 30: e113.

531. Panakanti R, Mahato RI. Bipartite vector encoding hVEGF and hIL-1Ra for ex vivo transduction into human islets. Mol Pharm. 2009; 6: 274-84.

532. Matarazzo M, Giardina MG, Guardasole V, et al. Islet transplantation under the kidney capsule corrects the defects in glycogen metabolism in both liver and muscle of streptozocin-diabetic rats. Cell Transplant. 2002; 11: 103-12.

533. Napoli R, Davalli AM, Hirshman MF, Weitgasser R, Weir GC, Horton ES. Islet transplantation under the kidney capsule fully corrects the impaired skeletal muscle glucose transport system of streptozocin diabetic rats. J Clin Invest. 1996; 97: 1389-97.

534. Hiller WF, Klempnauer J, Luck R, Steiniger B. Progressive deterioration of endocrine function after intraportal but not kidney subcapsular rat islet transplantation. Diabetes. 1991; 40: 134-40.

535. Jaeger C, Wohrle M, Federlin K, Bretzel RG. Pancreatic islet xenografts at two different transplantation sites (renal subcapsular versus intraportal): comparison of graft survival and morphology. Exp Clin Endocrinol Diabetes. 1995; 103 Suppl 2: 123-8.

536. Paielli DL, Wing MS, Rogulski KR, et al. Evaluation of the biodistribution, persistence, toxicity, and potential of germ-line transmission of a replication-competent human adenovirus following intraprostatic administration in the mouse. Mol Ther. 2000; 1: 263-74.

APPENDIX

Appendix A: Morphological analysis and titering of Ad-GFP utilized in **Chapter 3**. HEK 293 cells ($2x10^6$) were transduced with Ad-GFP at various viral dilutions (10^{-1} to 10^{-6}) for 48 hours and at 48 hours the cells were **(A)** visualized under basic transmission light, **(B)** visualized for GFP expression using a fluorescent microscope and **(C)** titered to $2x10^{11}$ pfu/ml based on percent GFP expression using flow cytometry. Images were taken at 2x magnification, dilution 10^{-1}. Histograms are representative of duplicate samples. Ad-GFP transduced HEK-293 cells show positive expression of GFP reporter gene expression, indicating successful HEK 293 cell transduction.

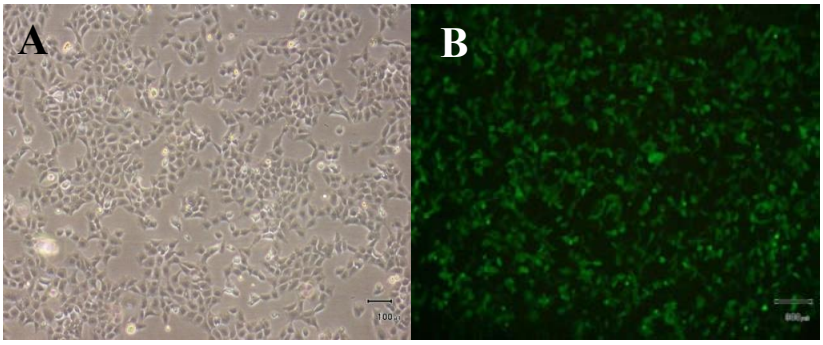

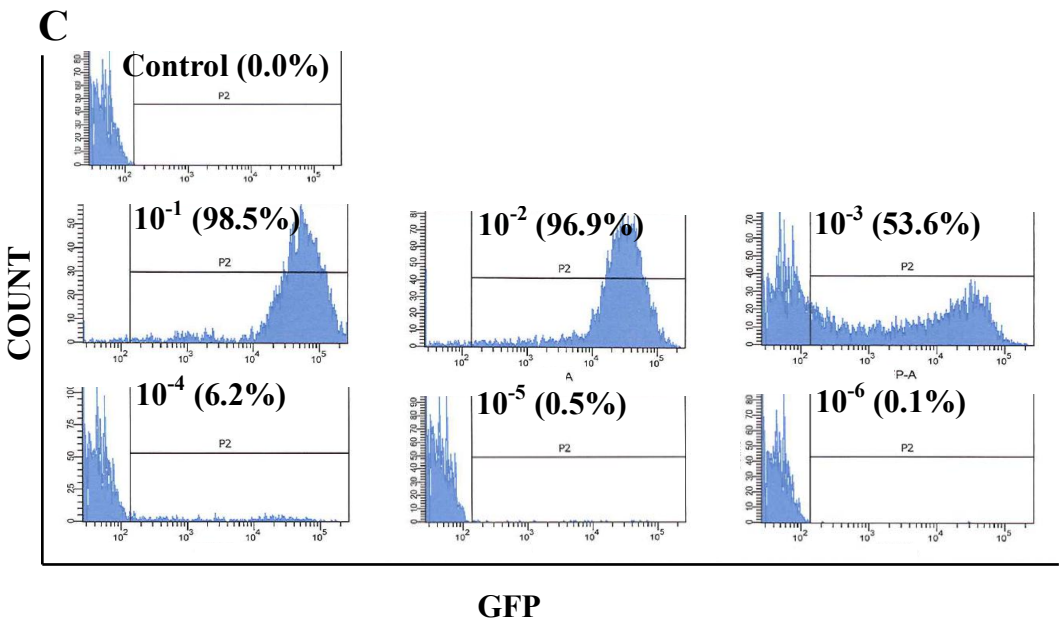

Appendix B: pENTCMV is an Adenoviral shuttle vector. It uses the cytomegalovirus (CMV) promoter for IGF-II expression. Figure provided from Welgen, Inc., USA.

Appendix C: Copy of Review Publication

Hughes A, Jessup C, Drogemuller C, Mohanasundaram D, Milner C, Rojas D, Russ GR, Coates PT. Gene therapy to improve pancreatic islet transplantation for Type 1 diabetes mellitus. *Curr Diabetes Rev*. 2010 Sep;6(5):274-84.

Hughes A., Jessup C., Drogemuller C., Mohanasundaram D., Milner C., Rojas D., Russ G.R. and Coates, P.T.H. (2010) Gene therapy to improve pancreatic islet transplantation for Type 1 diabetes mellitus.
Current Diabetes Reviews, v. 6 (5), pp. 274-84, September 2010

Appendix D: Copy of Published Manuscript

Hughes A, Mohanasundaram D, Kireta S, Jessup C, Drogemuller C, Coates PTH. Insulin-like Growth Factor-II Prevents Proinflammatory Cytokine-Induced Apoptosis and Significantly Improves Islet Survival After Transplantation. *Transplantation*. 2013;95: 00-00.

Hughes, A., Mohanasundaram, D., Kireta, S., Jessup, C., Drogemuller, C., Coates, P.T.H. (2013) Insulin-like Growth Factor-II Prevents Proinflammatory Cytokine-Induced Apoptosis and Significantly Improves Islet Survival After Transplantation. *Transplantation, v.95 (5), pp. 671-678, March 2013*